

The Boeing Company  
Santa Susana Field Laboratory  
5800 Woolsey Canyon Road  
Canoga Park, CA 91304-1148

December 14, 2009  
In reply refer to SHEA-109409

Mr. Richard Brausch  
SSFL Project Director  
Calif. Environmental Protection Agency  
Dept. of Toxic Substances Control  
1001 "I" Street  
P. O. Box 806  
Sacramento, CA 95812-0806

Subject: Draft Sitewide Groundwater Characterization Report  
Santa Susana Field Laboratory  
Ventura County, California

Dear Mr. Brausch:

On behalf of The Boeing Company, the National Aeronautics and Space Administration, and the Department of Energy, Boeing is submitting the subject report to the Department under separate cover. This submittal consists of the Draft Site-Wide Groundwater Remedial Investigation Report, Santa Susana Field Laboratory, prepared by MWH, December 2009, in one volume and appendices, and the Site Conceptual Model for the Migration and Fate of Contaminants in Groundwater at the Santa Susana Field Laboratory, prepared by the SSFL Groundwater Advisory Panel, December 2009, in four volumes. This report is submitted in accordance with the Consent Order for Corrective Action, August 2007, relevant workplans approved by DTSC, and the draft working schedule for corrective action as revised by the parties in August 2009.

Any questions regarding this submittal should be addressed to David Dassler at (818) 466-8733.

I certify that this document and all attachments were prepared under my direction or supervision in accordance with a system designed to evaluate the information submitted. I certify that the information contained in or accompanying this submittal is true, accurate, and complete. As to those identified portion(s) of this submittal for which I cannot personally verify the accuracy, I certify that this submittal and all attachments were prepared in accordance with procedures designed to assure that qualified personnel properly gathered and evaluated the information submitted. Based on my inquiry of the person or persons who manage the system, or those directly responsible for gathering the information, or the



Mr. R. Brausch, DTSC (SHEA-109409)

December 14, 2009

Page 2

immediate supervisor of such person(s), the information submitted is, to the best of my knowledge and belief, true, accurate, and complete. I am aware that there are significant penalties for submitting false information, including the possibility of fine and imprisonment for knowing violations.

Signature:   
Name: Thomas D. Gallacher  
Director, Santa Susana Field Laboratory  
Title: Environment, Health and Safety  
Date: Dec 11, 2009

DWD:bjc  
Attachment

cc: Distribution  
Ms. Cassandra Owens, RWQCB



<b>SSFL Site-wide Groundwater RI Report</b>		
<b>Review Copies</b>	<b>Internal Copies</b>	<b>Addressee</b>
0	0	Rick Brausch, SSFL Project Director, Department of Toxic Substances Control, 1001 "I" Street, 25th Floor, Post Office Box 806, Sacramento, CA 95812-0806
		<b>Distribution List</b>
0	0	Jim Pappas, Department of Toxic Substances Control, 8800 Cal Center Drive, Sacramento, CA 95826-3200, 916-255-3574
1	0	Gerard Abrams, California Environmental Protection Agency, Department of Toxic Substances Control, Region 1, 8800 Cal Center Drive, Sacramento, CA 95826-3200, 916-255-3600
1	0	Tom Seckington, Department of Toxic Substances Control, 5796 Corporate Avenue, Cypress, CA 90630, 714-484-5424
0	0	Susan Houghton, Department of Toxic Substances Control, Berkeley Regional Office, 700 Heinz Avenue, Suite 200, Berkeley, CA 94710-2721, 510-540-2122
1	0	Buck King, Department of Toxic Substances Control, Berkeley Regional Office, 700 Heinz Avenue, Suite 200, Berkeley, CA 94710-2721, 510-540-2122
0	1	Franki Burton, CH2M Hill, 155 Grand Avenue, #1000, Oakland, CA 94612, 510-251-2426
1	0	Susan Callery, Department of Toxic Substances Control, Chatsworth Office
1	0	Allen Elliott, George C. Marshall Space Flight Center, Mail Code: AS10, Marshall Space Flight Center, AL 35812, 205-544-0662
1	0	William Backous, Department of Energy, 5800 Woolsey Canyon Road, MC 055-T487, Canoga Park, CA 91304-1148, 818-466-8959

<b>SSFL Site-wide Groundwater RI Report</b>		
<b>Review Copies</b>	<b>Internal Copies</b>	<b>Addressee</b>
0	0	Rick Brausch, SSFL Project Director, Department of Toxic Substances Control, 1001 "I" Street, 25th Floor, Post Office Box 806, Sacramento, CA 95812-0806
<b>Distribution List</b>		
0	0	Patricia Berry, Department of Energy, Oakland Projects Office, 1301 Clay Street, Suite 1660N, Oakland, CA 94612-5208, 510-637-1720

**DRAFT SITE-WIDE GROUNDWATER  
REMEDIAL INVESTIGATION REPORT**

---

**SANTA SUSANA FIELD LABORATORY  
VENTURA COUNTY, CALIFORNIA**

**PREPARED FOR:**

**THE BOEING COMPANY  
NATIONAL AERONAUTICS AND SPACE ADMINISTRATION  
UNITED STATES DEPARTMENT OF ENERGY**

**December 2009**

**Contents of 3-Ring Binders Containing Full Hard Copy of  
Site-Wide Groundwater Remedial Investigation Report**

- Volume I of VII - Draft Site-Wide Groundwater RI Report: Text, Figures, and Tables, DVD of Full Copy of Draft Site-Wide Groundwater Remedial Investigation Report and Draft Site Conceptual Model Report
- Volume II of VII - Draft Site-Wide Groundwater RI Report: Plates
- Volume III of VII - Draft Site-Wide Groundwater RI Report: Appendix 2-A and Appendices 4-A and 4-B
- Volume IV of VII - Draft Site-Wide Groundwater RI Report: Appendices 4-C through 4-N
- Volume V of VII - Draft Site-Wide Groundwater RI Report: Appendices 4-O and 4-P
- Volume VI of VII - Draft Site-Wide Groundwater RI Report: Appendix 6-A
- Volume VI of VII - Draft Site-Wide Groundwater RI Report: Appendices 7-A through and 7-I and Appendix 9-A, CD of Groundwater Chemical and Radiological Data and Rock Core Sampling Results (Included in Appendix 7-A)

**Contents of 3-Ring Binders Containing  
Site-Wide Groundwater Remedial Investigation Report  
(excluding hard copies of appendices)**

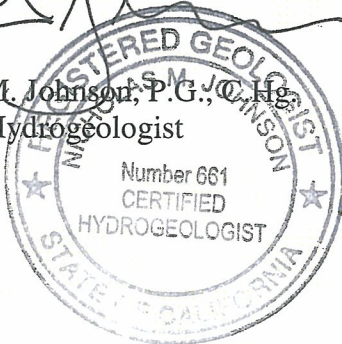
- Volume I of II - Draft Site-Wide Groundwater RI Report: Text, Figures, and Tables, DVD of Full Copy of Draft Site-Wide Groundwater Remedial Investigation Report and Draft Site Conceptual Model
- Volume II of II - Draft Site-Wide Groundwater RI Report: Plates
- Appendices provided on DVD in Volume I of II

**PROFESSIONAL CERTIFICATION**  
**Draft Site-wide Groundwater Remedial Investigation Report**  
**December 2009**  
**Santa Susana Field Laboratory**

This report has been prepared by a team of qualified professionals under the supervision of the senior staff whose seal and signature appears below. The findings, interpretations of data, specifications or professional opinions are presented within the limits of available information at the time the report was prepared, in accordance with generally-accepted professional geology, hydrogeology, and engineering practices and within the requirements of the clients. There is no other warranty, either expressed or implied.

Information included in this report is based on available data obtained from public and private sources. Additional studies may or may not disclose information that may modify the findings of this report. In the event that there are appreciable changes in the nature and/or design of the project, or if additional subsurface data are obtained, the conclusions and recommendations in the report may require further evaluation by the qualified professionals who participated in its preparation

  
Nicholas M. Johnson, P.G., C.Hg.  
Principal Hydrogeologist



  
Richard G. Andrachek, P.E.  
Principal Engineer

This page Intentionally Left Blank

## TABLE OF CONTENTS

<b>EXECUTIVE SUMMARY .....</b>	<b>ES-1</b>
<b>1.0 INTRODUCTION.....</b>	<b>1-1</b>
1.1 Operable Units at SSFL .....	1-2
1.2 Scope, Purpose, and content of Report.....	1-4
1.2.1 Scope.....	1-4
1.2.2 Purpose.....	1-4
1.2.3 Content.....	1-5
<b>2.0 BACKGROUND .....</b>	<b>2-1</b>
2.1 SSFL Ownership.....	2-1
2.2 Overview of Historic SSFL Operations.....	2-2
2.3 SSFL and Adjacent property Land Use .....	2-4
2.3.1 Surrounding Land Use .....	2-5
2.3.2 SSFL Environmental Programs .....	2-5
2.4 RCRA CORRECTIVE ACTION PROGRAM.....	2-6
2.4.1 Corrective Action Process.....	2-7
2.5 Chronological Development of Groundwater Characterization Work at SSFL .....	2-9
2.6 Overview of the Groundwater Monitoring Program .....	2-10
2.6.1 Off-Site Well Inventory .....	2-11
2.7 Groundwater Uses Designated in the LARWQCB Basin Plan .....	2-11
2.8 Groundwater Characterization Approach and Data quality objectives.....	2-12
2.9 Regulatory Requirements.....	2-13
<b>3.0 PHYSICAL CHARACTERISTICS OF SSFL.....</b>	<b>3-1</b>
3.1 Topography.....	3-1
3.2 Climate and Precipitation.....	3-2
3.3 Surface Water and Drainages.....	3-3
3.4 Surface Water Ponds.....	3-4
3.4.1 R-1 Pond .....	3-4
3.4.2 Perimeter Pond.....	3-4
3.4.3 Coca Pond .....	3-5
3.4.4 Silvernale Reservoir.....	3-5
3.4.5 R-2 Ponds.....	3-5
3.4.6 SRE Pond.....	3-6
3.4.7 Building 4056 Excavation.....	3-6
3.5 BIOLOGICAL CONDITIONS.....	3-7

<b>4.0</b>	<b>WORK PERFORMED IN SUPPORT OF GROUNDWATER REMEDIAL INVESTIGATION.....</b>	<b>4-1</b>
4.1	Installation, Purging and Sampling of Multilevel Monitoring Systems in Northeast Coreholes.....	4-2
4.2	Installation of Corehole C-15.....	4-2
4.3	Coring of Plume Transect Coreholes.....	4-4
4.4	Hydraulic Conductivity Profiling.....	4-5
4.5	Borehole Geophysical Logging.....	4-6
4.6	High-Resolution Fluid Temperature Logging.....	4-6
4.7	Analysis of Rock Core Samples for Chloride.....	4-7
4.7.1	Vadose Zone Samples.....	4-7
4.7.2	Saturated Zone Samples.....	4-7
4.8	Additional Degradation Studies on Chlorinated Ethenes.....	4-8
4.9	Collection and Analysis of Samples from Seeps.....	4-8
4.10	Collection and Analysis of Samples from Wells.....	4-9
4.11	Straddle Packer Testing.....	4-10
4.12	Additional Work Done to Fill Data Gaps Identified During Review of Available Site Data.....	4-10
4.12.1	Geologic Field Mapping.....	4-10
4.12.2	Mapping of Joints Observed in Surface Outcrops.....	4-10
4.12.3	Integration and Analysis of Fracture Data Sets.....	4-11
4.12.4	Installation of Piezometers.....	4-11
4.12.5	Additional Sampling and Analysis of Groundwater for Geochemical and Isotopic Parameters.....	4-11
4.12.6	Optimization and Uncertainty Analysis of Three-Dimensional Groundwater Flow Model.....	4-12
4.12.7	Groundwater Data Gaps Sampling for Surficial Media/ Groundwater Transport Pathway.....	4-12
4.12.8	Collection and Analysis of Rock Core from Shallow Groundwater Piezometers.....	4-12
4.12.9	Groundwater Characterization for Radionuclides.....	4-13
<b>5.0</b>	<b>GEOLOGY OF SSFL AND VICINITY.....</b>	<b>5-1</b>
5.1	Regional Geology.....	5-2
5.1.1	Geologic Units.....	5-2
5.1.2	Geologic Structure and History.....	5-3
5.2	SSFL Geology.....	5-5
5.2.1	Geologic Units.....	5-5
5.2.2	Geologic Structure.....	5-9

<b>6.0</b>	<b>HYDROGEOLOGY</b>	<b>6-1</b>
6.1	HYDROGEOLOGIC FRAMEWORK	6-1
6.1.1	Hydrogeologic Boundaries	6-1
6.1.2	Hydrogeologic Units	6-3
6.1.3	Hydrogeologic Structures	6-7
6.2	HYDROGEOLOGIC PROPERTIES	6-8
6.2.1	Porosity	6-8
6.2.2	Hydraulic Conductivity	6-12
6.2.3	Storage Coefficients	6-18
6.3	GROUNDWATER OCCURRENCE AND MOVEMENT	6-19
6.3.1	Influencing Factors	6-19
6.3.2	Perched Zones	6-23
6.3.3	Saturated Zone	6-24
6.3.4	Groundwater Movement	6-36
6.4	GROUNDWATER BUDGET	6-44
6.4.1	Recharge	6-44
6.4.2	Discharge	6-48
6.4.3	Balance of Inflows and Outflows	6-50
6.5	GROUNDWATER FLOW MODEL	6-50
6.5.1	Model Configuration	6-51
6.5.2	Model Calibration	6-52
6.5.3	Method of Evaluating Modeled Groundwater Flow	6-53
6.5.4	Estimates of SSFL Groundwater Discharge	6-54
6.5.5	Additional Flow Analysis from Modeling	6-55
6.6	DATA GAPS	6-56
<b>7.0</b>	<b>NATURE AND EXTENT OF CHEMICALS AND RADIONUCLIDES IN BEDROCK VADOSE ZONE AND GROUNDWATER</b>	<b>7-1</b>
7.1	Chemical Nature and Extent Information Contained in Surficial Media RI Reports	7-1
7.2	Nature and Extent of Chemical Contaminants In Bedrock Vadose Zone	7-2
7.2.1	Nature of Releases and Contaminant Transport in the Bedrock Vadose Zone	7-3
7.2.2	Extent of Chemical Impacts	7-4
7.2.3	Summary of Vadose Zone Characterization	7-12
7.3	Nature and Extent of Chemical Impacts to SSFL Groundwater	7-13
7.3.1	Nature of Chemical Impacts to Groundwater	7-13
7.3.2	Groundwater Data Screening	7-15
7.3.3	Groundwater Evaluation	7-17
7.3.4	Content of Maps Depicting Chemical Extent Data	7-18

7.3.5	Extent of Chemicals in Groundwater.....	7-21
7.4	Nature and Extent of Radionuclides in Bedrock and Groundwater.....	7-60
7.4.1	Potential Sources of Radionuclide Impacts .....	7-61
7.4.2	Bedrock Vadose Zone Radionuclide Characterization .....	7-62
7.4.3	Extent of Radionuclide Impacts to Groundwater.....	7-62
7.4.4	Gross Alpha Activity in Groundwater .....	7-64
7.4.5	Gross Beta Activity in Groundwater.....	7-65
7.4.6	Isotopic Radium in Groundwater.....	7-67
7.4.7	Isotopic Uranium in Groundwater .....	7-68
7.4.8	Tritium in Groundwater (Site-related).....	7-68
7.4.9	Other Radionuclides in Groundwater .....	7-70
7.4.10	Summary of Radionuclides in Bedrock and Groundwater .....	7-71
7.5	Summary.....	7-72
7.5.1	Bedrock Vadose Zone.....	7-73
7.5.2	Groundwater .....	7-74
7.6	Site characterization Data gaps.....	7-75
<b>8.0</b>	<b>TRANSPORT AND FATE.....</b>	<b>8-1</b>
8.1	Transport Routes.....	8-2
8.2	Processes Affecting Chemical Transport.....	8-2
8.3	Physical Properties of Site Chemicals Affecting Their Mobility and Persistence.....	8-7
8.3.1	Halogenated and Non-Halogenated Volatile Organic Compounds .....	8-7
8.3.2	Chemicals of Recent Interest (Perchlorate, 1,4-Dioxane, NDMA, 1,2,3-TCP and MTBE) .....	8-9
8.3.3	Gasoline Range Total Petroleum Hydrocarbons.....	8-9
8.3.4	Diesel, Kerosene, and Lubricant Oil Range Petroleum Hydrocarbons, and Semi-Volatile Organic Compounds .....	8-10
8.3.5	PCBs and PCDD/Fs .....	8-11
8.3.6	Metals.....	8-11
8.3.7	Summary .....	8-12
8.4	Transport and Fate Processes in the Vadose Zone.....	8-12
8.4.1	Volatilization to the Atmosphere Through the Vadose Zone Above Areas of Impacted Groundwater .....	8-13
8.5	Chemicals Within the Groundwater System.....	8-15
8.5.1	DNAPL Persistence .....	8-15
8.5.2	TCE Transport and Retardation in Groundwater.....	8-18
8.5.3	Linking EPM Flow Hydraulic Characteristics with DFN Hydraulics and Contaminant Transport.....	8-30
8.6	Chemical Fate .....	8-40

8.6.1	1997 Field Study .....	8-42
8.6.2	2000/2001 Field Study .....	8-42
8.6.3	2003/2004 Field Study .....	8-44
8.6.4	2008 Field Study .....	8-45
8.6.5	2003-2005 Laboratory Study .....	8-46
8.6.6	2005-2007 Laboratory Study .....	8-47
8.6.7	Integrated Assessment of Chlorinated Ethene Fate .....	8-49
8.6.8	Other Chlorinated Solvents .....	8-52
8.6.9	Perchlorate .....	8-54
8.6.10	Tritium .....	8-54
8.7	Summary of Transport and Fate .....	8-55
8.8	Transport and Fate Data Gaps .....	8-56
<b>9.0</b>	<b>GROUNDWATER IMPACT ASSESSMENT .....</b>	<b>9-1</b>
9.1	Consideration of On-Site Groundwater Contaminant Impacts .....	9-1
9.2	Groundwater Investigation Findings Concerning Potential Off-Site Impacts .....	9-2
9.3	Consideration of Off-Site Contaminant Impacts .....	9-3
<b>10.0</b>	<b>SUMMARY AND CONCLUSIONS .....</b>	<b>10-1</b>
10.1	Work Performed .....	10-1
10.2	Physical Setting .....	10-3
10.3	Geology .....	10-4
10.4	Hydrogeology .....	10-5
10.5	Chemical Nature and Extent .....	10-6
10.5.1	Bedrock Vadose Zone .....	10-7
10.5.2	Groundwater .....	10-7
10.6	Radiological Nature and extent .....	10-8
10.7	Transport and Fate .....	10-8
10.8	Impact Assessment .....	10-10
10.9	Conclusions .....	10-10
10.9.1	Decision Questions .....	10-11
10.9.2	Data Gaps .....	10-15
10.9.3	Key Conclusions .....	10-16
10.10	Acknowledgements .....	10-17
<b>11.0</b>	<b>REFERENCES .....</b>	<b>11-1</b>

## LIST OF FIGURES

(Figures in paper copies are provided at the end of each section)

- 1-1 Site Location Map
- 1-2 Regional Map
- 1-3 Cross Sectional Depiction of Operable Units
  
- 2-1 Land Acquisition History Map
- 2-2 RFI Sites, Group Reporting Areas and NPDES Outfalls
- 2-3 Historic and Current Groundwater Monitoring Wells
- 2-4 Corehole Completion Diagrams
- 2-5 Regional Groundwater Basins
  
- 3-1 SSFL Physical Setting
- 3-2 Santa Susana Field Laboratory Wind Roses
- 3-3 Annual Precipitation at SSFL, 1990-2008
- 3-4 Monthly Precipitation at SSFL, October 2000- June 2008
- 3-5 Average Monthly Precipitation at SSFL, 2000-2008
- 3-6 Historical Climate and Precipitation in Areas near SSFL, 1770-1965
  
- 4-1 Site Conceptual Model Groundwater Characterization Field Work for 2008/2009
- 4-2 Cross-section of Plume Transect
- 4-3 Seeps Sampled for VOCs (September 2007-March 2009)
- 4-4 Seeps Sampled for Geochemical and Isotopic Parameters
- 4-5 Wells Sampled for VOCs and Dissolved Gases
- 4-6 Areas of Additional Geologic Mapping
- 4-7 Piezometers Installed in 2008/2009
- 4-8 Wells Sampled for Geochemical and Isotopic Parameters
- 4-9 Wells Sampled for Surficial Media-to-Groundwater Pathway
- 4-10 Locations of Shallow Rock Core Samples
- 4-11 Locations of Radiological Characterization to Fill Data Gaps
  
- 5-1 SSFL in Relation to the Physiographic Provinces of Southern California
- 5-2 Regional Geologic Setting
- 5-3 Generalized Stratigraphy of the Simi Hills and Santa Susana Mountains
- 5-4 Geologic Map of the Simi Hills Near SSFL
- 5-5 SSFL Geologic Map
- 5-6 Stratigraphic Column of the Chatsworth Formation at SSFL
- 5-7 Conceptual Representation of the Lithology, Bedding, Fracturing, and Structure of the Chatsworth Formation
- 5-8 Distribution of Mapped Alluvium at SSFL
  
- 6-1 Hydrogeologic Boundary Conditions of the Groundwater Flow System Encompassing SSFL
- 6-2 Hydrogeologic Units of the Groundwater Flow System Encompassing SSFL

## LIST OF FIGURES (CONTINUED)

(Figures in paper copies are provided at the end of each section)

- 6-3 Geologic Structures with Potential Influence on SSFL Hydrogeology
- 6-4 Measurements of Matrix Porosity by Material Type and Method
- 6-5 Hydraulic Apertures Estimated by Application of the Cubic Law to FLUTE®  
Continuous Hydraulic Conductivity Profiling
- 6-6 Distribution of Wells with Hydraulic Conductivity Measurements
- 6-7 Core Sample Measurements of Matrix Conductivity by Hydrogeologic Unit
- 6-8 Measurements of Bulk Hydraulic Conductivity by Method and Hydrogeologic  
Unit
- 6-9 Estimated Relation Between Bulk Hydraulic Conductivity and Depth Below  
Ground Surface Derived for SSFL Sandstone and Shale Hydrogeologic Units
- 6-10 Conceptual Range of Fault Zone Permeability Structures
- 6-11 Monitored Wells, Northwestern SSFL
- 6-12 Monitored Wells, North-Central SSFL
- 6-13 Monitored Wells, Northeastern SSFL
- 6-14 Monitored Wells, South-Central SSFL
- 6-15 Cross Sections Showing Influence of Fine-Grained Units on Groundwater Levels
- 6-16 Multiport Well Profile Showing Influence of Fine-Grained Unit on Groundwater  
Levels
- 6-17 Cross Section Showing Fault Influence on Groundwater Levels
- 6-18 SSFL Groundwater Production and Water Use, 1948-2008
- 6-19 Groundwater Extraction Wells Active Before and After 1984
- 6-20 Annual Precipitation and Cumulative Departure from Average, 1950-2008
- 6-21 Selected Hydrographs Illustrating Precipitation Influence on Groundwater Levels
- 6-22 Known Areas of Shallow Perched Groundwater
- 6-23 Water-Supply Well Groundwater Level Hydrographs, 1950-2008
- 6-24 Cluster Well Groundwater Level Hydrographs, 1985-2008
- 6-25 Vertical Groundwater Gradients, 1990-2008
- 6-26 Estimated Groundwater Surface Elevation Excluding Shallow Perched Zones,  
October 2008
- 6-27 Estimated Depth to Groundwater Excluding Shallow Perched Zones, October  
2008
- 6-28 Trilinear Diagram of SSFL Water Types
- 6-29 Correlograms of WS-6 Water Levels Versus Other Area Wells During 2001-09  
Water-Level Recovery
- 6-30 Groundwater Level Hydrographs Illustrating Hydraulic Continuity Across IEL  
and Woolsey Faults
- 6-31 Groundwater Level Hydrographs Illustrating Potential Hydraulic Continuity  
Along Happy Valley Fault and Bowl Structure
- 6-32 Simulated Distribution of Groundwater Discharge Originating from On-Site  
Recharge, 1995-1998 Pumping Condition
- 6-33 Simulated Distribution of Groundwater Discharge Originating from On-Site  
Recharge, 1949 Non-Pumping Conditions

## LIST OF FIGURES (CONTINUED)

(Figures in paper copies are provided at the end of each section)

- 7-1 Rock Core Sampling Locations
- 7-2 Rock Core Locations with Vadose Zone Sampling Results
- 7-3 Cumulative Equivalent TCE Mass Plots in Rock Core
- 7-4 Excavations Conducted for Site Clean-up
- 7-5 Screening of Chemical Groundwater Data
- 7-6 Extent of TCE in Groundwater
- 7-7 Simulated Flow Paths of Particles from Known or Suspected TCE Sources, Steady-State Pumping Condition (1995-1998)
- 7-8 Simulated Flow Paths of Particles from Known or Suspected TCE Sources, Steady-State Non-Pumping Condition
- 7-9 Extent of PCE in Groundwater
- 7-10 Extent of cDCE in Groundwater
- 7-11 Extent of tDCE in Groundwater
- 7-12 Extent of Vinyl Chloride in Groundwater
- 7-13 Extent of 1,1-DCE in Groundwater
- 7-14 Extent of 1,2-DCA in Groundwater
- 7-15 Extent of 1,1-DCA in Groundwater
- 7-16 Extent of 1,4-dioxane in Groundwater
- 7-17 Extent of Carbon Tetrachloride in Groundwater
- 7-18 Extent of 1,2,3-trichloropropane in Groundwater
- 7-19 Extent of Formaldehyde in Groundwater
- 7-20 Extent of TPH (C<sub>4</sub>-C<sub>30</sub>) in Groundwater
- 7-21 Extent of n-Nitrosodimethylamine in Groundwater
- 7-22 Extent of Perchlorate in Groundwater
- 7-23 Extent of Nitrate in Groundwater
- 7-24 Extent of Fluoride in Groundwater
- 7-25 SESOIL/AT123D Boron Breakthrough Curves
- 7-26 Locations of Other Chemicals in Groundwater Exceeding Screening Levels
- 7-27 Extent of MTBE in Groundwater
- 7-28 Simulated Backward Flow Paths of Particles from Monitoring Wells, Steady-State Pumping Condition (1995-1998)
- 7-29 Simulated Backward Flow Paths of Particles from Monitoring Wells, Steady-State Non-Pumping Condition
- 7-30 Area IV Radiological Excavation Areas
- 7-31 Locations Sampled for Radiochemistry in Groundwater
- 7-32 Extent of Tritium in Groundwater
- 7-33 Summary of Areas of Impacted Groundwater
  
- 8-1 Diagram of Transport Pathways
- 8-2 Vadose Zone Transport Analysis – Scenarios 1 and 2
- 8-3 Base Case Vertical Cross Section Fracture Network
- 8-4 Fracture Length Histograms

## LIST OF FIGURES (CONTINUED)

(Figures in paper copies are provided at the end of each section)

- 8-5 Fracture Aperture Histograms
- 8-6 Hydraulic Head Contours: Base Case
- 8-7 TCE Source Position and Conditions Used in Simulations
- 8-8 TCE Transport Simulation Results for Base Case: 20, 50 and 100
- 8-9 TCE Transport Simulation Results for Base Case: 50, 100 and 150
- 8-10 TCE Transport Simulation Results for Vadose Zone Case 1: 50, 100 and 150 year Contours
- 8-11 TCE Transport Simulation Results for Vadose Zone Case 2: 50, 100 and 150 year Contours
- 8-12 TCE Transport Simulation Results, Vadose Zone Source Only
- 8-13 Perchlorate and NDMA/1,4-dioxane Source Position and Conditions Used in Simulations
- 8-14 Perchlorate Transport Simulation Results for Base Case: 20, 50 and 100 year Contours
- 8-15 NDMA/1,4-dioxane Transport Simulation Results for Base Case: 20, 50 and 100 year Contours
- 8-16 Schematic Approach of Linking EPM Flow to DFN Contaminant Transport
- 8-17 Range of Darcy Fluxes from Flow Model at RI Sites, Non-Pumping Condition
- 8-18 IEL RI Site: Hydraulic Characteristics from Flow Model
- 8-19 IEL RI Site: 2-Dimensional DFN and Hydraulic Characteristics
- 8-20 IEL RI Site: DFN Fracture Characteristics
- 8-21 IEL RI Site: DFN Transport Simulations
- 8-22 ELV RI Site: Hydraulic Characteristics from Flow Model
- 8-23 ELV RI Site: 2-Dimensional DFN and Hydraulic Characteristics
- 8-24 ELV RI Site: DFN Transport Simulations
- 8-25 Delta RI Site: Hydraulic Characteristics from Flow Model
- 8-26 Delta RI Site: 2-Dimensional DFN and Hydraulic Characteristics
- 8-27 Delta RI Site: DFN Transport Simulations
- 8-28 Co-occurrence of PCE and TCE in Groundwater
- 8-29 Co-occurrence of cDCE and TCE in Groundwater
- 8-30 Co-occurrence of tDCE and TCE in Groundwater
- 8-31 Co-occurrence of 1,1-DCE and TCE in Groundwater
- 8-32 Co-occurrence of Vinyl Chloride and cDCE in Groundwater
- 8-33 Co-occurrence of Ethene/Ethane and Vinyl Chloride in Groundwater
- 8-34 Chlorinated Ethene Fate at SSFL
- 8-35 Co-occurrence of 1,1-DCA and 1,1-DCE in Groundwater
- 8-36 Co-occurrence of 1,4-Dioxane and 1,1-DCE in Groundwater
- 8-37 Co-occurrence of 1,1-DCA and 1,4-Dioxane in Groundwater
- 9-1 Seep Locations

## LIST OF TABLES

(Tables in paper copies are provided at the end of each section)

- 2-1 Land Acquisition History
- 2-2 Summary of Operations at Remedial Investigation Sites
- 2-3 Pumping Well Construction Data
- 2-4 Regulations, Guidance and Other Documents Applicable to Groundwater RI Report
  
- 4-1 Summary of Geophysical Logging
- 4-2 Seep Sampling Results for VOCs, Fall 2007 through Spring 2009
  
- 5-1 Mapped and Named Faults, Santa Susana Field Laboratory and Vicinity
  
- 6-1 Summary of Bulk Hydraulic Conductivity Tests by Geologic Unit
- 6-2 SSFL Annual Groundwater Pumping and Water Importation, 1948-2008
- 6-3 Construction Data for Historically Active Water Supply and Remedial Extraction Wells
- 6-4 Areas of Shallow Perched Groundwater
- 6-5 Cluster Well Vertical Hydraulic Gradients, 1990-2005
- 6-6 Vertical Hydraulic Gradients Observed in Wells Installed with Multilevel Systems
- 6-7 SSFL Groundwater Quality Types
- 6-8 Pumping Rates and Monitoring Well Responses, 1996 SSFL Hydraulic Communication Study
- 6-9 Summary of WS-6 2001-09 Water-Level Correlogram Analysis
- 6-10 Hydraulic Characteristics of Faults
- 6-11 Estimated SSFL Groundwater Balance
  
- 7-1 Overview of Chemicals Used
- 7-2 Wells Assigned to RI Sites
- 7-3 Summary of RI Site Chemical Review and Groundwater Impact Assessment
- 7-4 Rock Core Sampling Summary, VOCs and EFH
- 7-5 Rock Core Sampling Summary, Perchlorate
- 7-6 EPA Method 8260 Target Analytes and Rock Core Detection Limits
- 7-7 Summary of Rock Porewater Sampling Results, Chlorinated Ethenes
- 7-8 Summary Statistics of Vadose Zone Rock Porewater Results
- 7-9 Groundwater Screening Values
- 7-10 Summary of Groundwater Sampling Results
- 7-11 Summary Results of Data Screening – July 2007 through June 2008
- 7-12 Summary of TCE Extent in Groundwater
- 7-13 Summary of PCE Extent in Groundwater
- 7-14 Summary of cDCE Extent in Groundwater
- 7-15 Summary of tDCE Extent in Groundwater
- 7-16 Summary of Vinyl Chloride Extent in Groundwater
- 7-17 Summary of 1,1-DCE Extent in Groundwater

## LIST OF TABLES (CONTINUED)

(Tables in paper copies are provided at the end of each section)

7-18	Summary of 1,2-DCA Extent in Groundwater
7-19	Summary of 1,1-DCA Extent in Groundwater
7-20	Summary of 1,4-dioxane Extent in Groundwater
7-21	Summary of Carbon Tetrachloride Extent in Groundwater
7-22	Summary of 1,2,3-trichloropropane Extent in Groundwater
7-23	Summary of Formaldehyde Extent in Groundwater
7-24	Summary of TPH in Groundwater
7-25	Summary of n-Nitrosodimethylamine Extent in Groundwater
7-26	Summary of Perchlorate Extent in Groundwater
7-27	Summary of Nitrate Extent in Groundwater
7-28	Summary of Fluoride Extent in Groundwater
7-29	Evaluation of Metals in Groundwater
7-30	Summary of Other Chemicals Exceeding Screening Levels in Recent Data Set
7-31	Chemicals Exceeding Screening Levels in at Least One Sample in Historical Data Set
7-32	Locations of Miscellaneous Chemical Exceedances in Historical Data Set
7-33	Summary Results of Data Screening – July 2008 through March 2009
7-34	Summary of MTBE Extent in Groundwater
7-35	Excavations Conducted for Radiological Clean-up in Area IV
7-36	Summary of Tritium Rock Porewater Sampling Results
7-37	Summary of Radiochemistry Groundwater Sampling Results
7-38	Summary of Adjusted Gross Alpha Results in Wells with One or More Exceedance of the Screening Level
7-39	Uranium Isotope Ratios for Wells with Total Uranium Greater Than 20 pCi/L
7-40	Summary of Lateral Extent of Impacted Groundwater
7-41	Assessment of Vertical Extent of Chemical Impacts
8-1	Summary of Chemical Properties
8-2	Equilibrium TCE Concentrations After Partitioning into Sorbed, Aqueous and Gaseous Phases in Vadose Zone
8-3	Input Parameters for Estimating TCE Vapor Flux to Ground Surface Above Area of Impacted Groundwater
8-4	DNAPL Disappearance Times for TCE in a Single Fracture Using Average SSFL Sandstone Parameters
8-5	Properties of Chemicals Selected for Groundwater Transport Simulations
8-6	Comparison of Plume Front Advance Rates for the “Base Case” TCE and Perchlorate 2D Fracture Network Simulations
8-7	Summary of SSFL Groundwater Redox Conditions
8-8	Summary of Sampling Results of Chlorinated Ethene Fate Studies
8-9	Half-life Constants, Reductive Dechlorination by Transition-Metal Coenzymes
10-1	Scientists/Engineers Contributing to Groundwater RI Report

## LIST OF PLATES

- 2-1 SSFL Well Completions
- 2-2 Well Cluster Diagrams and Locations
  
- 5-1 Regional Geologic Cross Sections
- 5-2 SSFL Geologic Cross-sections A-A' through D-D'
- 5-3 SSFL Geologic Cross-sections AA-AA' through EE-EE'
  
- 7-1 Wells Assigned to RI Sites
- 7-2 Trichloroethene Groundwater Results
- 7-3 Tetrachloroethene Groundwater Results
- 7-4 cis-1,2-Dichloroethene Groundwater Results
- 7-5 trans-1,2-Dichloroethene Groundwater Results
- 7-6 Vinyl Chloride Groundwater Results
- 7-7 1,1-Dichloroethene Groundwater Results
- 7-8 1,1,2,2-Tetrachloroethane Groundwater Results
- 7-9 1,2-Dichloroethane Groundwater Results
- 7-10 1,1-Dichloroethane Groundwater Results
- 7-11 1,4-Dioxane Groundwater Results
- 7-12 Carbon Tetrachloride Groundwater Results
- 7-13 1,2,3-Trichloropropane Groundwater Results
- 7-14 Formaldehyde Groundwater Results
- 7-15 TPH Groundwater Results
- 7-16 n-Nitrosodimethylamine Groundwater Results
- 7-17 Perchlorate Groundwater Results
- 7-18 Nitrate Groundwater Results
- 7-19 Fluoride Groundwater Results
- 7-20 Methyl tert-butyl ether Groundwater Results

## LIST OF APPENDICES

- 2-A Site Chronology
- 2-B Background Information on DOE Operational Activities in Area IV
- 2-C Monitoring Well and Piezometer Construction Data
- 2-D Groundwater Monitoring Schedule
- 2-E Off-Site Well Inventory
  
- 4-A Westbay Multilevel Installation and Sampling, C-16, C-17, RD-31, and RD-35C
  - Westbay Multilevel Sampling Technical Memorandum for Coreholes C-16, C-17, RD-31 and RD-35C
  - Technical Memorandum, Installation of Westbay Multilevel Systems in Coreholes RD-31, RD-35C, C-16 and C-17
  
- 4-B Coreholes C-12 through C-15, Installation Activities
  - Technical Memorandum, Installation of Coreholes C-12 through C-15
  - Technical Memorandum, Rock Core/Porewater Report
  - Transect Westbay Installation Technical Memorandum
- 4-C Methods and Results of Hydraulic Conductivity Profiling Using FLUTE Liners
  - Analysis of Continuous Conductivity Profiling in Fractured Rock Holes
  - Flute Profiling Results C-6, C-7 and C-15
- 4-D Borehole Geophysical Logs
- 4-E Technical Memorandum, Methods and Results of High-Resolution Fluid Temperature Logs
- 4-F Technical Memorandum, Analytical Results of Chloride in Rock Core Samples
- 4-G Methods and Results of Laboratory TCE Degradation Study
- 4-H Geochemical and Isotopic Sampling of Wells and Seeps
  - Results of Quarterly Seep Inspection and Sampling
  - Technical Memorandum, Geochemical and Isotopic Sampling of Wells and Seeps
- 4-I Technical Memorandum, Groundwater Sampling Using SNAP Samplers
- 4-J Technical Memorandum, Summary of Findings from Geologic Mapping at the SSFL in 2008
- 4-K Technical Memorandum, Characteristics of Joints Observed in Outcrop
- 4-L Technical Memorandum, Ground Truthing and Interpretation of Discrete Feature Data from Core, Optical Televiewer and Geophysical Logs
- 4-M Installation of Piezometers in Administrative Areas II, III and IV of the SSFL
  - Well Construction Activities at the Former SRE Site, Area IV of SSFL
  - Analytical Results for Surficial Media Data Gaps Sampling, Recently Installed Piezometers in Administrative Areas I, II and III
- 4-N Technical Memorandum, Summary of Groundwater Sampling Results for Surficial Media-to-Groundwater Transport Evaluation
- 4-O Report on Source Zone Characterization: Rock Core VOC Results for Shallow Groundwater Coreholes
- 4-P Report on Radiological Groundwater Characterization

**LIST OF APPENDICES  
(CONTINUED)**

- 6-A SSFL Groundwater Flow Model Updates, Optimization, and Application
- 7-A Assessment of Chemical Impacts to Groundwater at RI Sites
- 7-B Rock Porewater Plots
- 7-C Methodology and Results of Developing Risk-Based Screening Levels for Groundwater
- 7-D Well Data Booklet
- 7-E Laboratory Report on Immiscible Phase Petroleum Hydrocarbon Analysis
- 7-F Vadose Zone Transport Modeling
- 7-G Supplemental Information on Evaluation of Metals in Groundwater
- 7-H Monitoring Locations Sampled for Radioactivity and Radionuclides
- 7-I Supplemental Information on Evaluation of Radiological Impacts to Groundwater
- 9-A Groundwater Risk Assessment

## LIST OF ACRONYMS AND ABBREVIATIONS

A	area
AAL	Archived advisory levels
ABFF	Alfa/Bravo Fuel Farm
AI	Atomics International
AOC	Area of Concern
APTF	Advanced Propulsion Test Facility
AST	above ground storage tank
AT 123D	Analytical Transient 1-, 2-, 3-dimensional
Basin Plan	Basin Plan for the Coastal Watersheds of Los Angeles and Ventura Counties
BBC	Brandeis Bardin Campus
BTEX	benzene, toluene, ethylbenzene and xylene
bgs	below ground surface
Boeing	The Boeing Company
C/C <sub>0</sub>	relative concentration
Cal	California
CCR	California Code of Regulations
cDCE	cis-1,2-dichloroethene
[ <sup>14</sup> C]cDCE	carbon-14 labeled cis-1,2-dichloroethene
CDFE	Coca Delta Fuel Farm
CEQA	California Environmental Quality Act
CERCLA	Comprehensive Environmental Response Compensation and Liability Act
CFC	chlorofluorocarbon
CFOU	Chatsworth Formation Operable Unit
cm	centimeter
CMI	Corrective Measures Implementation
CMR	combinable magnetic resonance
CMS	Corrective Measures Study
cm/s	centimeters per second
CO <sub>2</sub>	carbon dioxide
<sup>14</sup> CO <sub>2</sub>	carbon-14 labeled carbon dioxide

**LIST OF ACRONYMS AND ABBREVIATIONS  
(CONTINUED)**

COC	contaminants of concern
CTL	Components Test Laboratory
De	effective diffusion coefficient
D <sub>0</sub>	free-solution diffusion coefficient
D&D	decommissioning and decontamination
DCA	dichloroethane
DCE	dichloroethene
DEM	digital elevation model
DF	dioxins and furans
DFN	discrete fracture network
DHS-RHB	Department of Health Services – Radiologic Health Branch
DNA	deoxyribonucleic acid
DNAPL	dense non-aqueous phase liquid
DO	dissolved oxygen
DOE	United States Department of Energy
DPH	Department of Public Health
DQO	Data Quality Objective
DTSC	Department of Toxic Substances Control
ECL	Engineering Chemistry Laboratory
EEL	Environmental Effects Laboratory
EFH	Extractable fuel hydrocarbon
ELV	Expendable Launch Vehicle
EM	Environmental Management
EPA	United States Environmental Protection Agency
EPM	equivalent porous media
ESADA	Empire State Atomic Development Authority
ETEC	Energy Technology Engineering Center
f <sub>oc</sub>	fraction organic carbon
°F	degrees Fahrenheit
FEFLOW	finite element flow

**LIST OF ACRONYMS AND ABBREVIATIONS  
(CONTINUED)**

FLUTe®	Flexible Liner Underground Technology
FS	Feasibility Study
FSDF	Former Sodium Disposal Facility
GIS	geographic information system
gpm	gallons per minute
gpm/ft	gallons per minute per foot of drawdown
Groundwater Panel	SSFL Groundwater Advisory Panel
GRC	Groundwater Resources Consultants, Inc.
GWCC	Groundwater Comparison Concentration
<sup>2</sup> H	deuterium
Hg	mercury
HMSA	Hazardous Materials Storage Area
HRFT	high-resolution fluid temperature
HSC	Health and Safety Code
IEL	Instrument and Equipment Laboratories
i	hydraulic gradient
ICF	ICF Kaiser Engineers
ISE	imminent and substantial endangerment
k	permeability
K	hydraulic conductivity
K <sub>b</sub>	bulk hydraulic conductivity
K <sub>m</sub>	matrix hydraulic conductivity
K <sub>d</sub>	distribution coefficient
K <sub>oc</sub>	organic carbon partition coefficient
K <sub>ow</sub>	octanol water partition coefficient
L	liter
LETf	Laser Engineering Test Facility
L/kg	liters per kilogram
Lm <sup>-2</sup> d <sup>-1</sup>	liters per square meter per day
LMEC	Liquid Metal Engineering Center

**LIST OF ACRONYMS AND ABBREVIATIONS  
(CONTINUED)**

LNAPL	light non-aqueous phase liquid
LOX	liquid oxygen
m	meter
m/d	meters per day
m/s	meters per second
m/yr	meters per year
m <sup>2</sup>	square meter
m <sup>2</sup> /sec	square meters per second
MCLs	Maximum Contaminant Levels
MDL	Method Detection Limit
ml/g	milliliters per gram
mg/kg	milligrams per kilogram
mg/L	milligrams per liter
mm	millimeter
mm Hg	millimeters of mercury
m/yr	meters per year
MRC	Mountain Recreation and Conservation Authority
MRL	method reporting limit
msl	mean sea level
MTBE	Methyl-tertiary-butyl-ether
NAA	North American Aviation
NASA	National Aeronautics and Space Administration
NCY	New Conservation Yard
NDMA	n-nitrosodimethylamine
NFA	No Further Action
NL	Notification Levels
NO <sub>3</sub> <sup>2-</sup>	nitrate
NPDES	National Pollutant Discharge Elimination System
NRC	National Research Council
NSGW	near-surface groundwater

**LIST OF ACRONYMS AND ABBREVIATIONS  
(CONTINUED)**

NSR	non-strippable residue
OCY	Old Conservation Yard
Ogden	Ogden Environmental and Energy Services Company, Inc.
OM	order-of-magnitude
ORP	oxidation-reduction potential
OU	Operable Unit
<sup>18</sup> O	Oxygen-18
PAHs	polycyclic aromatic hydrocarbons
PCA	tetrachloroethane
PCB	polychlorinated biphenyl
PCE	tetrachloroethene
PCDD/F	polychlorinated dibenzodioxin/furan
pCi/L	picocuries per liter
PCR	polymerase chain reaction
PDU	Process Development Unit
PEST	parameter estimation techniques
PLF	Propellant Loading Facility
q	Darcy Flux
Q	volumetric discharge
R	recharge
R	retardation factor
R <sub>A</sub>	apparent retardation factor
R <sub>m</sub>	matrix retardation factor
RAL	Regulatory Action Level
RBSL	Risk-Based Screening Level
RCRA	Resource Conservation and Recovery Act
RFA	RCRA Facility Assessment
RFI	RCRA Facility Investigation
RI	Remedial Investigation
RIHL	Rockwell International Hot Laboratory

**LIST OF ACRONYMS AND ABBREVIATIONS  
(CONTINUED)**

RMHF	Radioactive Materials Handling Facility
Rocketdyne	Rocketdyne Propulsion and Power
RWQCB	Regional Water Quality Control Board
S	solubility
SAIC	Science Applications International Corporation
SAP	Sampling and Analysis Plan
SCM	Site Conceptual Model
SDWA	Safe Drinking Water Act
SE	Southeast Drum
SESOIL	Seasonal Soil Compartment Theory and Model
SL	screening level
SMCLs	Secondary Maximum Contaminant Levels
SNAP	Systems for Nuclear Auxiliary Power
SO <sub>4</sub> <sup>2-</sup>	sulfate
SPA	Storable Propellant Area
SRE	Sodium Reactor Experiment
SSFL	Santa Susana Field Laboratory
STL	Systems Test Laboratory
STP	Sewage Treatment Plant
Surficial OU	Surficial Media Operable Unit
SVOC	semi-volatile organic compound
SWGW	site-wide groundwater
SWMU	solid waste management unit
TCA	trichloroethane
TCE	trichloroethene
TCP	trichloropropane
TD	total depth
TDS	total dissolved solids
tDCE	trans-1,2-dichloroethene
TEQ	toxicity equivalency quotient

**LIST OF ACRONYMS AND ABBREVIATIONS  
(CONTINUED)**

TPH	total petroleum hydrocarbons
UDMH	unsymmetrical dimethyl hydrazine
USGS	United States Geological Survey
UST	underground storage tank
VC	vinyl chloride
VCEHD	Ventura County Environmental Health Division
VOC	volatile organic compound
WCT	waste coolant tank
WDR	Waste Discharge Requirement
WS	water supply
XPS	x-ray photoelectron spectroscopy
0/00	per mil
2b	fracture aperture
2-dimensional	
	two-dimensional
3-dimensional	
	three-dimensional
$\phi_m$	matrix porosity
$\phi_f$	fracture porosity
$\mu\text{g}/\text{L}_v$	micrograms per liter vapor
$\mu\text{g}/\text{L}$	micrograms per liter
$\mu\text{g}/\text{m}/\text{yr}$	micrograms per meter per year
$\mu\text{mhos}/\text{cm}$	micromhos per centimeter
$n_e$	effective porosity
$\rho_b$	bulk density
$\tau$	tortuosity
$\bar{v}_f$	average linear groundwater velocity

**LIST OF ACRONYMS AND ABBREVIATIONS  
(CONTINUED)**

**Radioisotopes**

<sup>241</sup> Am	Americium-241
<sup>14</sup> C	Carbon-14
<sup>134</sup> Cs	Cesium-134
<sup>137</sup> Cs	Cesium-137
<sup>60</sup> Co	Cobalt-60
<sup>152</sup> Eu	Europium-152
<sup>154</sup> Eu	Europium-154
<sup>155</sup> Eu	Europium-155
<sup>3</sup> H	tritium
<sup>40</sup> K	potassium-40
<sup>238</sup> Pu	Plutonium-238
<sup>239</sup> Pu	Plutonium-239
<sup>239/240</sup> Pu	Plutonium-239/240
<sup>226</sup> Ra	Radium-226
<sup>228</sup> Ra	Radium-228
<sup>90</sup> Sr	Strontium-90
<sup>228</sup> Th	Thorium-228
<sup>230</sup> Th	Thorium-230
<sup>232</sup> Th	Thorium-232
<sup>234</sup> Th	Thorium-234
<sup>233/234</sup> U	Uranium-233/234
<sup>234</sup> U	Uranium-234
<sup>235</sup> U	Uranium-235
<sup>236</sup> U	Uranium-236
<sup>238</sup> U	Uranium-238

## **EXECUTIVE SUMMARY**

This groundwater remedial investigation (RI) report presents an assessment of the nature and extent of site-related chemicals and radionuclides in groundwater and vadose zone bedrock across Santa Susana Field Laboratory (SSFL). This groundwater RI report is being submitted pursuant to the Consent Order for Corrective Action signed by the California Environmental Protection Agency, Department of Toxic Substances Control (DTSC), The Boeing Company (Boeing), the National Aeronautic and Space Administration (NASA), and the United States Department of Energy (DOE) in August 2007. Environmental characterization and remedial activities are overseen by the DTSC. The RI is being conducted along two parallel paths: one for groundwater and vadose zone bedrock and the other for soil and related surficial media. This report presents the results of the groundwater RI, including the vadose zone bedrock. The surficial media investigation results have been and are being reported separately, although findings from these investigations are incorporated into this groundwater RI report where relevant.

A substantial body of data has been collected during the remedial investigation of groundwater at SSFL over a period exceeding more than two decades. The primary purpose of this RI report has been to review and interpret these data, as well as collect new data, with the objectives of fully describing the characterization of contaminants in groundwater and identifying data gaps related to that characterization. This report is supported and complemented by numerous prior published site documents and the Site Conceptual Model report prepared by the SSFL Groundwater Advisory Panel (Cherry, McWhorter and Parker, 2009).

A number of activities have been performed to support the groundwater RI project at SSFL as outlined in the Work Plan, Site-wide Groundwater Characterization (MWH, 2008a) that was approved by DTSC (2009). Further work beyond that described in the site-wide work plan was also performed to either fill data gaps identified during review of the available data (consistent with the approach presented in the site-wide work plan) or to further reduce uncertainties related to the characterization of groundwater at SSFL. This work, performed mostly since early 2008, supplements the body of work previously performed as described in Appendix 2-A. These data

have formed the basis of the current understanding of the hydrogeologic system, the nature and extent, and transport and fate of chemical and radiological impacts to the vadose zone bedrock and groundwater beneath SSFL.

More than 20,000 groundwater samples have been collected from over 485 groundwater monitoring locations over nearly a quarter century and have produced nearly a half-million chemical records. Over 1,400 groundwater samples have been collected and analyzed for radiological characterization. Samples collected from the monitoring network cover an area of about 11 square miles and extend to depths beyond 1,000 feet. Over 7,800 rock core samples have been collected from more than 40 locations to depths of 1,400 feet and analyzed for sorbing and non-reactive chemicals and for non-reactive radionuclides over the last 12 years to supplement the groundwater sampling results. Additional investigations of the groundwater system have been performed to characterize various hydrogeologic parameters of the fractured bedrock and the groundwater flow system influencing contaminant transport and fate.

The characterization program at SSFL has generated one of the largest data sets in the world that describe a fractured rock site. Scales of investigations conducted in support of the groundwater RI program extend from regional flow modeling that encompasses an area of about 336 square miles, to the use of electron microscopy and X-ray photospectroscopy instruments to inspect minerals on the surface of rock particles. Two broad areas of impacted groundwater, defined as that containing concentrations of chemicals exceeding screening values, have been identified in SSFL groundwater: an area encompassing about 247 acres along the eastern portion of SSFL, and a second area encompassing about 470 acres in the central and western part of SSFL. Four other areas have been identified totaling about 15 acres and ranging in size from 0.8 to 8.9 acres. One area extends off-site to the northeast of SSFL and groundwater periodically emerges at the ground surface in another area in the southwest portion of SSFL along the Burro Flats fault. The total area of impacted groundwater is about 732 acres. Fifty-two different chemicals are contained within these areas. Trichloroethene (TCE) and its principal daughter product cis-1,2,-DCE (cDCE) dominate the area of impacted groundwater at SSFL, with TCE covering about 88 percent of this area. Consistent with site operations, immiscible-phase kerosene-range

hydrocarbons were also found on the water table at two monitoring locations, one at the Alfa RI site and the other at the Canyon RI site.

A data gap analysis of potential radiological groundwater impacts was performed in 2004 and 14 groundwater monitoring wells and 2 coreholes were installed in response. The data gaps work resulted in the identification and characterization of an area of groundwater impacted with tritium at concentrations above the 20,000 pCi/L screening level that includes 4 wells (RD-88, RD-90, RD-93 and RD-95). The area of impact covers about 4.4 acres and extends about 300 feet or so from the suspected release location. No other radionuclides have been found at concentrations above screening levels in samples collected from the well network. However, detections of <sup>90</sup>Strontium have persisted at the well where it was detected (RD-98), indicating that it is present in groundwater, although at concentrations below the 8 pCi/L screening level. A review of radionuclide production and fate conducted by SAIC (2009) and the groundwater sampling history conducted for this report showed that seven site-related radionuclides have not been characterized in groundwater. Should future surficial media sample collection and analysis show them to be present in surficial media, then additional sampling of the existing well network should be conducted to evaluate their potential occurrence.

The transport of chemicals in bedrock groundwater was characterized with field data through the installation of source zone and plume transects and a longsect in an area of impacted groundwater in the northeast part of SSFL. Mean porewater concentrations of TCE in three source zone transect coreholes (C1, RD-35 and C10; mean of 2,544 µg/L; detected in 1,295 of 1,655 samples (78 percent)) are more than a factor of 100 higher than mean TCE concentrations in 2 plume transect coreholes (C13 and C14; mean of 23 µg/L; detected in 102 of 810 samples (13 percent)) over a horizontal distance of 2,140 feet. These data provide compelling and conclusive evidence of the strong attenuation effect of matrix diffusion on contaminant transport in the Chatsworth Formation at SSFL.

Field and laboratory assessments of chlorinated ethenes have been conducted at SSFL to assess their fate. Field studies have been done by Hurley (2007a, b, c), Pierce (2005) and Zimmerman (2009). Laboratory studies have been conducted by Darlington (2008) and results from some have been reported for the first time in previous sections of this report. Results from these

studies have been used to evaluate the fate of TCE and its daughter products. Site data show that microbially-mediated complete dechlorination of chlorinated ethenes is occurring at SSFL. Field and laboratory results also show the complete mineralization of TCE and cDCE due to abiotic reactions with ferric and ferrous oxides and oxyhydroxides found in the rock matrix. The redox conditions are also consistent with reductive dechlorination of other chlorinated solvents used at SSFL.

Data gaps related to groundwater characterization have been identified and will be addressed in a sampling and analysis plan scheduled for submittal to DTSC in 2010. The following data gaps have been identified:

- Potential impacts to bedrock groundwater beneath the CTL-V, Area I Burn Pit and SRE RI sites should be characterized through collection of additional data.
- Additional field characterization of the extent of VOC impacts at the ELV RI site is warranted.
- The distribution of monitoring wells and hydraulic testing are insufficient for demonstrating the effect of the Burro Flats Fault and the Happy Valley Fault (east of RD-10) on groundwater levels and flow. Furthermore, insights into the groundwater flow system gained from the 3-dimensional groundwater flow model indicate that evaluation of two faults in the northwest portion of SSFL is warranted (i.e. FSDF structures).
- Collection and analysis of samples from select wells within the groundwater monitoring network for a specified set of target analytes should also be conducted to confirm their vertical and/or lateral extent.
- Seeps around the perimeter of SSFL should be sampled and analyzed for VOCs to confirm the absence of impacts to off-site receptors.

Human health and ecological risk assessments were conducted for groundwater during preparation of surficial media RI site and group reports. Both cancer and non-cancer endpoints were characterized in the risk assessments for both indirect (i.e. exposure by inhalation of VOCs transported from groundwater) and direct exposure pathways (i.e. use and exposure to groundwater by consumption and other direct contact pathways). When using standard risk assessment protocols, calculations show that groundwater below portions of SSFL is impacted with contaminants with calculated incremental lifetime cancer risk and hazard index values that exceed regulatory guidance. It is anticipated a groundwater use prohibition will be imposed on the site to restrict access to on-site groundwater in perpetuity, thus controlling drinking water and other direct exposure pathways.

However, site data supports the following conclusions related to potential off-site exposures to site-related contaminants:

- Due to the observed concentrations in plumes, the migration distance required, the strength of attenuation and retardation in the bedrock, and the mass flux available for transport in contaminant plumes at SSFL, it is not scientifically plausible for contaminants to migrate to wells within outlying communities at concentrations causing human and ecological impacts.
- The absence of site-related contaminants at off-site seeps is consistent with what is known about the migration, attenuation, and retardation of groundwater contaminant plumes originating at SSFL. The sampling of off-site wells shows no presence of SSFL-related contaminants in wells sampled, which is consistent with the results from seeps sampling and the understanding of contaminant transport.
- Community water supply sources in the surrounding valleys are a combination of surface water from northern California (the State Water Project) and local groundwater. Water supply wells in both the Simi Valley and San Fernando Valley are more than 3 miles from SSFL, much farther than the predicted contaminant transport distances from former SSFL sources.
- The available data indicates there are no known or projected impacts to off-site human or ecological receptors from impacted groundwater originating beneath SSFL.

## CONCLUSIONS

Analysis of available site data supports the following conclusions:

- Groundwater flow paths from site sources to off-site exposure points are long (i.e. typically >1,000 meters), and contaminant transport distances are short relative to the average linear groundwater velocity.
- Chemical and radiological constituents that entered the groundwater at SSFL remain within the local groundwater and sandstone matrix, extending a few hundred to a few thousand feet from former input locations.
- Contaminant transport has been influenced by sorption to aquifer solids, diffusion from the fracture network into the nearly immobile porewater in the rock matrix, biological and abiotic transformations, and/or radioactive decay.
- Transport of chemicals and radionuclides by groundwater flow in the fracture network and diffusion into the rock matrix creates plumes that are identifiable and detectable using monitoring wells and/or seeps.
- Nearly all groundwater contaminant mass resides in the low permeability rock matrix blocks between fractures local to where the contaminants entered the ground.
- Contaminant plumes are generally stable and plume fronts are generally stationary.

- TCE is the chemical detected at the highest concentration relative to a regulatory threshold, is detected most frequently, and comprises the vast majority of impacts to groundwater beneath SSFL.
- Contaminant impacts to groundwater have been identified on-site and at one location off-site at concentrations that exceed drinking water standards, as defined in agency regulations. It is anticipated a groundwater use prohibition will be imposed on the site to restrict access to on-site groundwater in perpetuity, thus controlling drinking water and other direct exposure pathways.
- Application of standard risk assessment protocols confirms that hypothetical receptors inhaling volatiles from shallow groundwater beneath former release locations at SSFL show both cancer- and non-cancer endpoints above the acceptable risk range as defined in agency regulations.
- The preponderance of site data supports the conclusion that it is not scientifically plausible for contaminants to migrate to wells in outlying communities at concentrations that may cause human and ecological impacts.
- Groundwater characterization is sufficient for the preparation of feasibility and treatability studies.

This groundwater remedial investigation report confirms the nature and extent of contamination in groundwater beneath SSFL have been characterized at nearly all locations, the transport and fate of contaminants in groundwater are well understood, the nature of groundwater plumes are defined and monitorable, and the Site Conceptual Model (Cherry, McWhorter, and Parker, 2009) is a valid tool for guiding site risk management decisions.

## 1.0 INTRODUCTION

This remedial investigation (RI) report presents an assessment of the nature and extent of site-related chemicals and radionuclides in groundwater and the unsaturated zone across the Santa Susana Field Laboratory (SSFL). Environmental characterization and remedial activities are being overseen by the California Environmental Protection Agency, Department of Toxic Substances Control (DTSC). This groundwater RI report is being submitted pursuant to the 2007 Consent Order for Corrective Action, Docket No. P3-08/003, and DTSC's June 2, 2009 Conditional Approval of the Site-Wide Groundwater Characterization Work Plan. The RI is being conducted along two parallel paths: one for groundwater and the unsaturated bedrock and the other for soil and related surficial media. This report presents the results of the groundwater RI, including the unsaturated bedrock. The surficial media investigation results have been and are being reported separately although findings from these investigations are incorporated into this groundwater RI report.

The SSFL is located approximately 29 miles northwest of downtown Los Angeles, California, in the southeast corner of Ventura County (Figure 1-1). The SSFL occupies approximately 2,850 acres of hilly terrain, with approximately 1,100 feet of topographic relief near the crest of the Simi Hills. Figure 1-2 shows the geographic location and property boundaries of the site, as well as surrounding areas. The site is divided into four administrative areas (Areas I, II, III, and IV) and includes undeveloped land both to the north and south (Figure 1-2). Most of Area I and all of Areas III, and IV are owned by The Boeing Company (Boeing). Area II is owned by the federal government and administered by the National Aeronautics and Space Administration (NASA) along with a portion of Area I. Ninety acres of Area IV were leased to the United States Department of Energy (DOE), who also owns facilities in Area IV. The northern and southern undeveloped lands of SSFL were not used for industrial activities and are owned by Boeing.

This report has been prepared under the direction of the SSFL Groundwater Advisory Panel (Groundwater Panel) on behalf of Boeing, NASA and DOE. The Groundwater Panel is comprised of Dr. John Cherry, Distinguished Professor Emeritus, Department of Earth and Environmental Sciences, University of Waterloo, Waterloo, Ontario; Dr. David McWhorter,

Distinguished Professor Emeritus, Department of Chemical and Agricultural Engineering, Colorado State University, Fort Collins, Colorado; and Dr. Beth Parker, Professor and NSERC Industrial Research Chair in Fractured Rock Contamination Hydrology, School of Engineering, University of Guelph, Guelph, Ontario and formerly of the University of Waterloo (1996-2006). The Groundwater Panel was formed initially by Rocketdyne Propulsion and Power (Rocketdyne) in 1997 to provide advice and guidance concerning investigations of the distribution, and transport and fate of chemicals in the bedrock beneath SSFL. The Groundwater Panel has been intimately involved in the bedrock characterization program since then, and has been charged with the preparation and issuance of a complementary, stand-alone document to this Groundwater RI report, which is incorporated into this report by reference (Cherry, McWhorter, and Parker, 2009).

## **1.1 OPERABLE UNITS AT SSFL**

Since the early 1980s, SSFL site characterization has proceeded along two parallel paths: one for groundwater and the other for soil and related surficial media. In 1999, DTSC formalized this approach by identifying two operable units (OUs) (DTSC, 1999). As defined by United States Environmental Protection Agency (EPA), an OU is a discrete entity that may comprise various attributes, including characteristics of the impacted media, geographical location, vertical and aerial considerations, specific site problems, and potential exposure pathways. The OUs identified at SSFL are consistent with this definition and incorporate different geographical portions of the site, project phases, and exposure pathways. The two SSFL OUs have been identified through discussion with DTSC based on an understanding of where chemicals are present today, where they may migrate in the future, and how either human or ecological receptors may be exposed to those chemicals (DTSC, 1999). The OUs at SSFL are:

- The surficial media OU (Surficial OU) comprised of saturated and unsaturated soil, sediment, surface water, near-surface groundwater (NSGW), air, biota, and weathered bedrock. NSGW occurs within alluvium or weathered bedrock.
- The Chatsworth Formation OU (CFOU) comprised of the Chatsworth Formation groundwater, and both saturated and unsaturated unweathered (competent) bedrock.

The boundary between the Surficial OU and the CFOU occurs at the transition from weathered to unweathered bedrock, which has historically been defined (in consultation and agreement with

DTSC) as the maximum depth to which one can bore using a hollow-stem auger. Although the terms weathered and unweathered bedrock do not define distinct stratigraphic units, they distinguish regions of the subsurface that have different physical characteristics. Weathered bedrock is typically more permeable as a result of natural physical and chemical degradation processes. The OUs are depicted graphically in Figure 1-3.

The Surficial OU consists primarily of soil, sediment, and surface water, which are potentially impacted by spills. Also included in this OU are NSGW, air, biota, and the upper, weathered portion of the bedrock. These additional media have been included in the Surficial OU because chemicals released into soil, sediment, or surface water could directly contact, or potentially be transferred to, NSGW, surface seeps or springs, air, biota, and weathered bedrock. Direct exposure to surficial media by receptors is possible, although the type of exposure may vary based on location (e.g., steep terrain typically adjacent to drainages or certain bedrock outcrops versus flat upland terrain).

The CFOU consists of groundwater and associated unweathered, competent bedrock of the Chatsworth Formation, which is faulted and comprised of thickly-bedded sandstone with interbeds of siltstone and shale. This unit has been impacted by downward migration of chlorinated solvents (primarily trichloroethene (TCE) and its daughter products) from surficial spills, subsurface releases, and/or by dissolved-phase contaminants transported to and within Chatsworth Formation groundwater by recharge waters and/or vapors. The CFOU has also been impacted by releases of other chemicals to surficial media primarily through transport by recharge waters.

As stated above, one goal of the RI Program is to characterize chemical impacts in all relevant environmental media at SSFL. This goal is achieved by combining and integrating site data from the characterization programs for both OUs. Similarly, the goal of the RI risk assessment is to evaluate risks from all relevant environmental media. This goal is accomplished by combining the estimated risk associated with exposure pathways for both OUs. Several possible pathways of chemical migration across or between OUs have been identified. The potential pathways for transferring site-related chemicals between the surficial media OU and the CFOU are described and assessed in subsequent sections of this report.

## **1.2 SCOPE, PURPOSE, AND CONTENT OF REPORT**

This report presents RI findings for groundwater and unsaturated bedrock beneath all areas of SSFL. The scope, objectives, content and format of this report are presented below.

### **1.2.1 Scope**

This report includes results for both groundwater present in the Surficial OU (i.e., that present in the alluvium and/or weathered bedrock) and the Chatsworth Formation (i.e., that present within the unweathered portions of the bedrock). Groundwater present within both OUs has been combined in this report since the groundwater present within the alluvium and/or weathered bedrock flows into, or is continuous with (i.e., not separated by a vadose zone), groundwater in the unweathered bedrock. This report includes both historical results and results of data collected during 2008 and 2009 under approved work plans (DTSC, 2007b and 2007c).

The SSFL Groundwater Advisory Panel has been engaged in the groundwater project since 1997 and has developed a site conceptual model to guide site characterization and the understanding of the transport and fate of chemicals and radionuclides in groundwater. In summary, the site conceptual model for contaminant transport in groundwater and bedrock indicates that nearly all of the contaminant mass remains in the rock near where the contaminants entered the subsurface decades ago. Much data have been collected, reduced and analyzed to evaluate the validity of this conceptual model and the work is documented in a complementary deliverable to this RI report (Cherry, McWhorter and Parker, 2009).

### **1.2.2 Purpose**

The purpose of the site-wide groundwater RI report is to complete the assessment of the nature and extent of site-related chemicals and radionuclides in groundwater and the unsaturated bedrock and to forecast both their short- and long-term transport and fate in these media. The majority of the characterization work conducted at SSFL has been performed under the Resource Conservation and Recovery Act (RCRA) Corrective Action program, as implemented in the current 2007 Consent Order for Corrective Action, Docket No. P3-08/003. As of the date of DTSC's Conditional Approval on June 2, 2009, the parties agreed that the regulatory framework

for remediation would be transitioned from the RCRA Corrective Action (Chapter 6.5) process to the State superfund (Chapter 6.8) process due to the enactment of California Health and Safety Code (HSC), Division 20, Chapter 6.8., Article 5.5, Section 25359.20. Both the RCRA corrective action program and the State Superfund program identify contamination for cleanup and outline a similar process. This RI report was prepared to fulfill the requirements established in the Consent Order (DTSC, 2007a), as amended by the Conditional Approval of Site-Wide Characterization Work Plan (DTSC, 2009), and to complete the RI for groundwater and the unsaturated portions of the bedrock underlying SSFL.

### 1.2.3 Content

This report includes ten additional sections, with a summary of each provided below.

**Section 1.0 – Introduction:** This section describes the content of the report and its principal basis.

**Section 2.0 - Background Information:** This section provides general background information and describes the regulatory framework at SSFL. It also includes a chronological overview of the history of the groundwater characterization program at SSFL. This section has been included in this report, as the long history (i.e., over 20 years) of investigations and data collection at SSFL formed part of the basis for the scope of work to complete the groundwater and unsaturated zone investigation program.

**Section 3.0 - Physical Characteristics of SSFL:** This section provides a descriptive summary of SSFL physical characteristics including: topography; climate and precipitation; surface water hydrology; and land use and demographic information.

**Section 4.0 - Work Performed in Support of Groundwater Remedial Investigation:** This section describes work performed during 2008 and 2009 under DTSC-approved work plans (DTSC, 2007b and 2007c), the site-wide work plan (MWH, 2008a) and to fill data gaps identified during the preparation of this report.

**Section 5.0 – Geology of SSFL and Vicinity:** This section presents a summary of the geology of SSFL. Both regional and site-specific information are included with updated information gathered during field reconnaissance conducted in the fall of 2008.

**Section 6 – Hydrogeology:** This section presents a summary of the hydrogeology of SSFL. Both regional and site-specific information are included with updated information gathered during investigations performed in 2008 and 2009.

**Section 7 - Nature and Extent of Chemicals and Radionuclides in Bedrock Vadose Zone and Groundwater:** This section presents a summary of chemical use at SSFL, findings from the Surficial OU RI reports, and presents the assessment of the nature and extent of site-related chemical impacts to the unsaturated bedrock and groundwater beneath SSFL.

**Section 8 – Transport and Fate:** This section includes an analysis of the potential routes of migration of the site-related chemicals in the unsaturated bedrock and groundwater beneath SSFL and predictions for their movement in the subsurface.

**Section 9 – Implications of Contaminant Conditions:** This section discusses the implications of the occurrence of contaminants in the Chatsworth Formation to monitoring, restoration and exposures. Groundwater risk assessment results for human and ecological receptors are summarized and provided in an appendix.

**Section 10 - Summary and Conclusions:** This section presents a brief summary of the RI and includes a summary of the site conceptual model on the movement of chemicals and radionuclides in SSFL groundwater and unsaturated bedrock. This section also includes a discussion of the conclusions and recommendations for further work.

**Section 11 – References:** This section presents a list of the supporting documents referred to in this report.

**Appendices:** The appendices present supporting documents including: descriptions of work performed in support of the groundwater RI; analyses of existing groundwater data illustrating temporal changes in water chemistry and piezometric data; and results of groundwater risk assessments.

## 2.0 BACKGROUND

This section presents information on the location of SSFL, its ownership and operations, adjacent properties, hazardous materials that were used and waste generated from operations, and an overview of the environmental programs that have regulated site activities. Groundwater usage as defined in the Los Angeles Regional Water Quality Control Board's (RWQCB) Basin Plan for the Coastal Watersheds of Los Angeles and Ventura Counties (Basin Plan) is also briefly described in this section (RWQCB, 1994). This section also includes a chronological description of the groundwater characterization work that has been completed at SSFL and an overview of the existing groundwater monitoring program. A more detailed summary of site-wide groundwater characterization work is provided in Appendix 2-A.

### 2.1 SSFL OWNERSHIP

The SSFL is divided into four administrative areas (Areas I, II, III, and IV) and undeveloped land areas to both the north and south (Figure 1-2). Boeing owns most of Area I and all of the land in Areas III and IV. The federal government owns and NASA administers Area II and a 42 acre parcel in Area I. Ninety acres of Area IV were leased to the DOE, who also owns facilities in Area IV. The northern and southern undeveloped lands of SSFL were not used for industrial activities and are owned by Boeing.

Prior to development, the land at SSFL was used for ranching. The land acquisition history of SSFL is summarized in Table 2-1 and graphically depicted in Figure 2-1. During 1948, North American Aviation (NAA), a predecessor company to Boeing, began using (by lease) what is now known as the northeastern portion, or administrative Area I, of SSFL. The majority of SSFL was acquired with the purchase of the Silvernale property in 1954, and development of the western portion of SSFL began soon after. Undeveloped land parcels to the south of SSFL were acquired during 1968 and 1976 and to the north during 1998.

## 2.2 OVERVIEW OF HISTORIC SSFL OPERATIONS

The following section presents an overview of past operations at SSFL. The primary site activities at SSFL since 1948 have included research, development, and testing of liquid-fueled rocket engines and associated components (pumps, valves, etc.) (Science Applications International Corporation [SAIC], 1994). Predecessor companies to Boeing have included North American Aviation (NAA), whose Rocketdyne division conducted rocket engine testing. NAA later merged with Rockwell Standard Corporation to form North American Rockwell, which later became Rockwell International Corporation. In 1966, Boeing acquired the aerospace and defense assets of Rockwell International, including the Santa Susana site.

In addition to the primary facility operation of rocket engine testing, SSFL was used for research, development, and testing of water jet pumps, lasers, and liquid metal heat exchanger components; nuclear energy research; and research and development of related technologies. Nuclear energy research, testing, and support facilities were located within the 90-acre portion of Area IV that was leased to DOE or DOE's predecessor. This area was designated as the Liquid Metal Engineering Center (LMEC) until 1978, at which time it was renamed the Energy Technology Engineering Center (ETEC). Operations were conducted by Atomics International (AI), a division of NAA, and subsequently Rocketdyne on behalf of DOE, with operations primarily from the 1950s through the mid-1990s. Area IV was inactive prior to 1953, when the land was purchased by NAA. The research and energy development activities included nuclear energy operations (development, fabrication, disassembly, and examination of nuclear reactors, reactor fuel, and other radioactive materials) and large-scale liquid sodium metal experiments for testing liquid metal fast-breeder reactor components. Nuclear energy activities within Area IV ceased in 1988. Since the mid-1990s, activities in Area IV have focused on site restoration. Additional information regarding the operations conducted by and for the DOE and its predecessor in Area IV are provided in Appendix 2-B.

Major operational activities at SSFL broadly fit into the categories identified below. Facility names where these activities occurred are also identified. Activities conducted in support of these operational areas have been geographically consolidated into what are now referred to as RI sites, the locations of which are shown in Figure 2-2.

- **Large Rocket Engine Testing** – Large rocket engine and some component tests were conducted at six sites in two areas: the Canyon and Bowl test stands in Area I; and the Alfa, Bravo, Coca, and Delta test stands in Area II. These areas typically included flow-through or collection ponds for cooling water used in support of the engine or component tests.
- **Small Rocket or Other Engine Testing** – Small rocket engine testing was performed at Advanced Propulsion Test Facility (APTF). Jet engine testing was conducted at the B-1 site, and what is now referred to as the Laser Engineering Test Facility (LETF). These RI sites are located in Area I.
- **Component Testing** – Engine component or systems testing was conducted at five areas: Component Test Laboratory (CTL)-I (comprises one combined RI site combined with the LETF); CTL-III; and CTL-V in Area I; the Expendable Launch Vehicle (ELV) (formerly CTL-II) in Area II; and the Systems Test Laboratory (STL)-IV (formerly CTL-IV) in Area III.
- **Support or Testing Laboratories** – Support or testing laboratories were located at four sites: the Instrument and Equipment Laboratories (IEL) in Area I; the Environmental Effects Laboratory (EEL) and Engineering Chemistry Laboratory (ECL) in Area III; and the Building 4065 Metals Laboratory in Area IV.
- **Other Materials Testing/Production** – Various facilities either tested or produced other chemicals on-site. Flare research and igniter and solid propellant testing involving energetic materials and perchlorate were conducted at Building 359, Happy Valley North and Happy Valley South, all in Area I; fluorine testing/production was conducted at Compound A (Area III); propellant loading operations at Propellant Loading Facility (PLF, Area II); molten salt and coal gasification at Process Development Unit (PDU, Area IV); and liquid oxygen (LOX) production at (NASA parcel in Area I); pipe strength testing and zirconium hydride-covered fuel pellet testing at the Empire State Atomic Development Authority (ESADA) site in Area IV.
- **Storage Areas** – Storage areas are located throughout SSFL and include smaller areas used in support of specific site operations and larger storage areas that served multiple operations at SSFL. RI sites used primarily as storage areas include: Storable Propellant Area (SPA); Hazardous Materials Storage Area (HMSA); Old Conservation Yard (OCY); New Conservation Yard (NCY); Southeast (SE) Drum Storage Yard.
- **Landfills** – Landfills were located at three sites: Area I landfill; Area II landfill; and the Building 4056 landfill in Area IV.
- **Surface Water Ponds** – Seven surface water features are present at SSFL: four ponds comprise individual RI sites (the R-1 Pond and Perimeter Pond in Area I, the R-2 Ponds in Area II, and Silvernale Reservoir in Area III); and three are within RI sites (the Coca Pond in Area II, and the Sodium Reactor Experiment (SRE) Pond and Building 56 Excavation in Area IV). The Pond Dredge site in the Burro Flats portion of Area IV was also possibly used for disposal of pond dredge materials.

- **Fuel Farms and Storage Tanks** – Two fuel farms were used to support large engine testing in Area II [Alfa/Bravo Fuel Farm (ABFF) and Coca Delta Fuel Farm (CDFF)]. Other storage tanks include the waste coolant tank (WCT) in Area II and tanks included in other RCRA Facility Investigation (RFI) sites (e.g., OCY).
- **Leach Fields** – Leach fields were used for domestic sanitary waste from on-site facilities prior to the 1961 installation of a site-wide sewage collection and treatment system. Leach fields associated with RI sites were evaluated as part of those sites. Leach fields not associated with RFI sites were grouped and evaluated as a separate RFI site (i.e., in Area IV, DOE leach fields characterized as three RI sites and Boeing leach fields as characterized as one RI site).
- **Sewage Treatment Plants (STPs)** – Discharges from the STP (when operational) were monitored as part of the National Pollutant Discharge Elimination System (NPDES) permit. However, the RI includes investigation of areas associated with STPs at the Building 515 Area (former Area II STP clarifier and leach field area) and the former catchment pond associated with the Area III STP.
- **Maintenance/Incinerator Locations** – These sites include: the Area I Burn Pit site; SSFL facility maintenance area (Building 204) and a former document incinerator (Ash Pile site), both in Area II. Machine and maintenance areas also occur within previously mentioned RI sites (B-1 Area, and LETF/CTL-I), and small incinerators occur at others (Happy Valley, and NCY).
- **Support of Area IV Nuclear Energy Operations** – These sites were used primarily for nuclear energy research or support activities and are managed by the DOE. The DOE has or will remediate these sites for radiological impacts prior to investigation of chemical impacts during the RI. These sites include the SRE, Rockwell International Hot Laboratory (RIHL), Systems for Nuclear Auxiliary Power (SNAP) Facility, Building 100 Trench, Former Sodium Disposal Facility (FSDF), Radioactive Materials Handling Facility (RMHF), and Buildings 4029 and 4133.

Additional descriptions of operations conducted at each of the RI sites are provided in Table 2-2. Detailed descriptions regarding the past operational use at each of the RI sites can be found in individual Group RI reports (MWH, 2006b, 2007d, 2007f, 2009b and 2009c; NASA, 2008, 2009a and 2009b; CH2MHill, 2008, 2009a and 2009b).

### 2.3 SSFL AND ADJACENT PROPERTY LAND USE

Current land use at SSFL is zoned by Ventura County as rural agricultural, but modified by a special use permit to allow industrial use as described above. Buildings that formerly housed research and testing support facilities are either: inactive, undergoing or planned for demolition, or are being used to support the environmental cleanup.

### **2.3.1 Surrounding Land Use**

Land adjacent to SSFL is generally zoned open space or residential, although other uses are present. A brief description of the current land use of each of the off-site adjacent properties is presented below. Adjacent land use is shown in Figure 1-2.

Northern Adjacent Properties - The adjacent property to the northwest is occupied by the American Jewish University Brandeis Bardin Campus (BBC), formerly known as the Brandeis-Bardin Institute, is zoned as rural agricultural on Ventura County zoning maps. The adjacent property to the northeast is occupied by the Mountains Recreation and Conservation Authority (MRCA) and currently operates as Sage Ranch Park (a County of Ventura Park). Approximately 75 acres in the southern and eastern portion of the current MCRA property was formerly leased by Rockwell between 1947 and 1970 (Rockwell, 1984).

Eastern Adjacent Properties - The properties situated immediately adjacent to the east of SSFL are zoned light agricultural, with variances that permit higher-density use (i.e., mobile home parks). These properties are located in Los Angeles County.

Southern Adjacent Properties - The properties situated adjacent to the south of SSFL are used for residential purposes (Bell Canyon). Residential development begins just south of SSFL's boundary and carries into the San Fernando Valley southeast of SSFL.

Western Adjacent Properties - The majority of properties situated adjacent to the west of SSFL are designated by Ventura County as open space. This land has been and is currently used for cattle grazing.

### **2.3.2 SSFL Environmental Programs**

As of the date of this report, four environmental programs at SSFL are being conducted under the authority of the RCRA. The RCRA Program is described further in Section 2.4. In addition to RCRA, other federal, state, and county environmental programs are being conducted at SSFL, including permitting for air emissions, surface water discharge permitting, and other site investigation and closure activities. Information regarding environmental programs conducted at

SSFL is provided in the RFI Program Report (MWH, 2004b). Since these other environmental programs overlap and are relevant to some of the RI sites, they are briefly described below:

- Waste Discharge Requirements (WDR) have been issued to SSFL by the RWQCB since 1958. Currently, surface water discharge from SSFL is regulated under a NPDES permit issued by the RWQCB, which began providing oversight in 1984. Surface water discharges are regularly monitored at NPDES outfalls, the locations of which are shown in Figure 2-2.
- Historically, underground storage tanks (USTs) were regulated by the Ventura County Environmental Health Division (VCEHD). Aboveground storage tanks (ASTs) were regulated by the RWQCB. Fuel storage tanks at the site are now included in the clean-up program being overseen by the DTSC.
- Closure of nuclear testing and research facilities in Area IV is being performed under the jurisdiction of DOE. The California Department of Health Services, Radiologic Health Branch (DHS-RHB) oversees the Boeing-owned Radioactive Materials License, conducts facility verification surveys, evaluates the radioactive facility cleanup, and conducts environmental monitoring.

## 2.4 RCRA CORRECTIVE ACTION PROGRAM<sup>1</sup>

RCRA corrective action at SSFL is being conducted as required by the Consent Order on Corrective Action issued by DTSC in 2007. Specifications regarding the ongoing corrective action program were subsequently provided in three Hazardous Waste Facility Permits issued to Boeing by the DTSC. The three permits governing the RCRA corrective action program at SSFL include:

---

<sup>1</sup> The majority of the characterization work conducted at the SSFL has been performed under the RCRA Corrective Action program, as implemented in the current 2007 Consent Order for Corrective Action, Docket No. P3-08/003. As of the date of DTSC's Conditional Approval on June 2, 2009, the parties agreed that the regulatory framework for remediation would be transitioned from the RCRA Corrective Action process to the State superfund process due to the enactment of California HSC, Division 20, Chapter 6.8., Article 5, Section 25359.20. Both the RCRA corrective action program and the State Superfund program identify contamination for cleanup and outline a similar process. This Site-Wide Groundwater Remedial Investigation Report is the first report submitted under Chapter 6.8 process. As such, this section of the report recaps the work performed at the SSFL under the Chapter 6.5 RCRA corrective action program and describes the transition to Chapter 6.8.

- Areas I and III Post-Closure permit issued in 1995 (PC 94/95-3-02 Mod SC3 111904-A);
- Area II Post-Closure permit issued in 1995 (PC 94/95-3-03 Mod SC3-111904-B); and
- Area IV Hazardous Waste Management Facility Operating permit issued in 1993 (93-3-TS-002).

The RCRA-related activities at SSFL are performed as part of four major environmental programs, all directed by the DTSC. These programs include:

- RCRA corrective action;
- Closure of inactive RCRA units;
- Compliance/permitting of RCRA units; and
- Interim measures.

In some instances these programs overlap (e.g., closed RCRA units within RFI sites that are investigated as part of corrective action). Although related under RCRA, each program has separate process requirements and guidelines. Collectively, these programs represent a comprehensive program for the handling and cleanup of hazardous chemicals. The RCRA corrective action program is described below, and the reader is referred to the RFI Program Report (MWH, 2004b) for descriptions of the other RCRA Programs.

#### **2.4.1 Corrective Action Process**

The RCRA corrective action process includes four phases to achieve site cleanup and closure. These are the RCRA Facility Assessment (RFA), RFI, Corrective Measures Study (CMS), and Corrective Measures Implementation (CMI) phases. The first phase of the RFA is performed to identify Solid Waste Management Units (SWMUs) and Areas of Concern (AOCs), which are units that have used, stored, or handled various hazardous materials. The RFA was completed in 1994 (SAIC, 1994).

The SSFL RCRA Corrective Action program has been proceeding until now in the RFI phase. During the RFI, additional AOCs (beyond those listed in the RFA) have been identified and investigated at SSFL (MWH, 2004b). A total of 135 SWMUs and AOCs have been identified at SSFL, and those undergoing closure as part of the RFI Program have been grouped by location

for purposes of investigation and are called “RFI sites.” The RFI Program Report (MWH, 2004b) listed 51 RFI sites.

As a result of the change in process from Chapter 6.5 to Chapter 6.8 described above, the RFI reports will be described under analogous Chapter 6.8 terminology of Remedial Investigation Reports, and Chapter 6.8 terminology will be used throughout the rest of this report. The RI sites identified for investigation are shown in Figure 2-2. For ease of presentation on this figure, and as reported in previous documents (MWH, 2004b), Boeing and DOE leach fields not associated with an existing RI site have been grouped together (i.e., three DOE groups and a Boeing group) and listed as additional RI sites.

Based on input from DTSC, SSFL has been divided into 11 Group reporting areas as shown on Figure 2-2 for the purpose of reporting data and results for the Surficial OU. While 10 of the reporting areas consist of contiguous land, Group 7 includes two separate areas that have been reported together. The Group reporting areas have been established to accomplish the goal of providing a comprehensive, integrated description of site data from all media across large, interrelated areas of the site. As such, the Group RI Reports include evaluation of data from both OUs to determine characterization completeness, transport and fate of contaminants, and assessment of potential risks to receptors. Off-site areas are included in the RI evaluation of SSFL-related impacts. Group reporting areas were identified generally based on natural topographic constraints at SSFL, but groundwater plume extents, RI site responsibility, and operational boundaries were also considered. The Group reporting areas shown on Figure 2-2 serve to facilitate evaluation of all migration pathways and, therefore, capture all appropriate site data for risk assessment.

The RFI reports, now RI Reports, includes characterization of all relevant environmental media present at SSFL. Investigations of environmental media have been conducted following DTSC-approved work plans (ICF Kaiser Engineers [ICF], 1993a, 1993b, 1993c; Groundwater Resources Consultants, Inc. [GRC], 1995c and 1995d; Ogden Environmental and Energy Services Company, Inc. [Ogden], 1996, 2000a, and 2000b; Montgomery Watson, 2000b; MWH, 2001, 2002b, 2003a and d, and 2005a, 2005b, 2005c, 2007a, 2007c and 2008a). The scope and

extent of sampling of SSFL during the RI is described in the Program Report (MWH, 2004b) and in the Site-Wide Groundwater Characterization Work Plan (MWH, 2008a).

The objectives of the RI are to characterize the nature and extent of chemical contamination in environmental media, evaluate risks to potential receptors, gather data for the Feasibility Study (FS, formerly CMS) and identify areas for additional work (DTSC, 1995a). Site action recommendations resulting from the RI are categorized into either: (1) further evaluation in the FS; (2) no further action (NFA); or (3) interim source area stabilization measures to control contaminant migration (stabilization areas) while cleanup plans are prepared. Stabilization areas are included at or within CMS areas when warranted based on characterization findings and site conditions.

The FS phase of the Superfund program will be an evaluation of remedial alternatives for areas that are identified in the RI for further evaluation. The FS may also include further evaluation of uncertainties identified in the RI, such as risk assessment uncertainties or delineation of chemicals requiring cleanup. The FS will be prepared and findings will be published in a final FS report for DTSC approval.

During the remedy selection and implementation phases, the program moves from cleanup planning to cleanup implementation and confirmation/monitoring sampling. The complete SSFL cleanup plan will be evaluated in a California Environmental Quality Act (CEQA) analysis prior to implementation. Public review and comment will be included during several steps in this process prior to the selection and implementation of cleanup activities.

## **2.5 CHRONOLOGICAL DEVELOPMENT OF GROUNDWATER CHARACTERIZATION WORK AT SSFL**

There is a long history of groundwater characterization work at SSFL (i.e. nearly 25 years of investigations and data collection, and groundwater interim measures) that form the basis of this groundwater RI report. A description of the work conducted prior to 1984 and an annual summary of the work performed from 1985 through the much of 2009 is presented in Appendix 2-A.

## 2.6 OVERVIEW OF THE GROUNDWATER MONITORING PROGRAM

Figure 2-3 is a map of SSFL groundwater monitoring locations. Currently, more than 350 piezometers and wells are monitored within and surrounding SSFL:

Wells and Piezometers Monitored for Water Levels, 2008-2009		
Well Type	No.	Maximum Screen Depth (ft bgs)
Piezometers	77	87
Shallow wells	97	40
Chatsworth Formation wells	179	
Open hole or single screen: Investigation wells	148	798
Former water supply wells	13	2,304
Off-site private wells	3	515
Multilevel Wells: FLUTe	11	440
Westbay	4	853
Total	353	

Appendix 2-C provides construction information for the monitored wells and piezometers. Additionally, Figure 2-4 and Plates 2-1 and 2-2 present profiles showing their construction.

Specific groundwater monitoring and sampling requirements at SSFL include detection monitoring, evaluation monitoring and interim corrective action monitoring as described in the Post-Closure Permit, and the requirements of Title 22, California Code of Regulations (CCR), Sections 66264.97 through 66264.99. Periodic monitoring and sampling activities include:

- Measuring static water levels
- Collecting groundwater samples and submittal for laboratory analysis, and

- Quarterly reporting of measurements, results and interpretations.

Wells are sampled quarterly, semi-annually, or annually in accordance with the current Sampling and Analysis Plan (SAP) for the site (GRC, 1995a, 1995b). Per the groundwater monitoring program, groundwater samples are collected quarterly from both near-surface and Chatsworth Formation wells, and selected off-site wells and springs. The sampling and analysis program that was implemented in 2008 is summarized in Appendix 2-D. Samples from wells not within the currently approved SAP have also been collected over the last few years and analyzed for various constituents to fill data gaps that are identified from the Surficial OU characterization program.

Target analyte groups for samples collected from wells across SSFL include: volatile organic compounds (VOCs), fuel hydrocarbons, trace metals, cyanide, inorganic constituents, semi-volatile organic compounds (SVOCs), perchlorate, radioactivity and radionuclides. Other inorganic constituents include major cations (calcium, magnesium, potassium, and sodium), major anions (bicarbonate, carbonate, chloride, fluoride, nitrate, and sulfate), total and dissolved iron, total dissolved solids, pH, and specific conductance. As part of the CFOU groundwater investigation, a number of wells were monitored for constituents of concern, the list of which is defined in the Post-Closure Permit.

### **2.6.1 Off-Site Well Inventory**

An inventory of wells located outside of SSFL property was conducted. Results of the inventory are provided in Appendix 2-E. One hundred twenty-seven (127) wells were identified within a study area that spanned 7 miles east-to-west and 5 miles north-to-south (see Figure 1 in Appendix 2-E).

## **2.7 GROUNDWATER USES DESIGNATED IN THE LARWQCB BASIN PLAN**

Groundwater underlying SSFL is not specifically designated for any particular or specific use according to the Basin Plan (RWQCB, 1994). Regional groundwater basins are located both to the north (Simi Valley) and to the southeast (San Fernando Valley) of SSFL, as depicted on Figure 2-5. However, footnotes to the Basin Plan state that:

“Beneficial uses for ground waters outside of the major basins . . . have not been specifically listed. However, ground waters outside of the major basins are, in many cases, significant sources of water. Furthermore, ground waters outside of the major basins are either potential or existing sources of water for down gradient basins, and as such, beneficial uses on the down gradient basins shall apply to these areas.”

As noted in the Basin Plan, existing beneficial groundwater uses for the Simi Valley and San Fernando Basins include municipal, industrial service supply, industrial process supply and agriculture.

## **2.8 GROUNDWATER CHARACTERIZATION APPROACH AND DATA QUALITY OBJECTIVES**

As described in the Work Plan for Additional Field Investigations (Montgomery Watson, 2000b), the Data Quality Objective (DQO) process (EPA, 1994) was used to guide the SSFL groundwater RI. The problem statement developed for the CFOU is:

“Comply with regulatory requirements by developing an accurate site conceptual model that describes and predicts the transport and fate of chemicals of concern in the Chatsworth Formation Operable Unit. Substantiate the conceptual site model and determine actions for the site.”

Eight decision questions were identified during DQO development and have been used to guide the data collection and evaluation process for the site-wide groundwater RFI. These eight questions are:

- 1) Is the subsurface mass of chemicals present consistent with the estimated mass of TCE that may have been released and consistent with the site conceptual model (i.e. highest concentrations adjacent to the input locations)?
- 2) Has the maximum depth of penetration of contaminants of concern (COCs) been characterized?
- 3) Does the presence of COCs in the unsaturated portion of the Chatsworth Formation contribute to the further migration of the plume front?
- 4) Has the three dimensional flow of groundwater been defined such that the direction of COC solute transport can be predicted?

- 5) Has the migration of COC solute at the plume front become effectively stable relative to a concentration threshold?
- 6) Does the current groundwater monitoring program adequately characterize the temporal and spatial variability of COC solute?
- 7) Have the attenuation effects of dispersion and biodegradation been considered and quantified?
- 8) Is restoration of the Chatsworth Formation groundwater technically practicable?

Four supplemental work plans were subsequently prepared and submitted to DTSC for review and approval. Three of the work plans proposed work to collect additional field data needed to answer these decision questions (MWH, 2005b, 2007a and c) and were subsequently approved by DTSC (2005, 2007b and 2007c). The fourth work plan (MWH, 2008a) proposed that this report be prepared and submitted that integrates all of the data collected from the site and that data gaps be identified during the preparation of the report.

## **2.9 REGULATORY REQUIREMENTS**

The RCRA corrective action regulatory framework (as modified by California HSC Section 25359.20), was reviewed to evaluate the requirements needed to complete the groundwater characterization program. Five different documents were reviewed and the characterization requirements were identified and are listed in Table 2-3. This table identifies each of the documents that were reviewed, the applicable characterization requirement and the section of this report where the requirement is addressed. Three of the five regulatory documents reviewed are from the RCRA permit and corrective action programs (Division 4.5 of Title 22 of the CCR, and two attachments from the 1995 post-closure permits for Areas I, II and III). The fourth document is DTSC's Conditional Approval of the Site-Wide Groundwater Characterization Work Plan and the fifth is the Guidance for Conducting Remedial Investigations and Feasibility Studies Under CERCLA, Interim Final (EPA, 1988). The latter was reviewed to assess requirements associated with SSFL transitioning to clean-up under Chapter 6.8.

This report has been designed to answer both, these decision questions presented in Section 2.8 and the regulatory requirements described in Section 2.9 in a comprehensive, integrated manner

for the site. Another objective of the site-wide groundwater RI report is to provide DTSC sufficient information so that remedial action alternatives can be identified and evaluated in the FS.

### **3.0 PHYSICAL CHARACTERISTICS OF SSFL**

This section presents information on the topography, climate, surface water features and biological conditions. Information on the geology and groundwater at SSFL, including the occurrence of springs/seeps, are described in later sections of this report (Sections 5.0 and 6.0, respectively).

#### **3.1 TOPOGRAPHY**

SSFL occupies approximately 2,850 acres of hilly terrain that expresses approximately 1,100 feet of topographic relief near the crest of the Simi Hills. A shaded-relief topographic map depicting site topography is provided as Figure 3-1. The highest surface elevation at SSFL occurs near the center of the site at an approximate elevation of 2,245 feet above mean sea level (msl). The highest surface elevations at SSFL occur along two general ridges that trend northeast-southwest, consistent with the geology of the Chatsworth Formation.

The lowest elevation within SSFL occurs at the eastern property boundary in Dayton Canyon, which has an elevation of approximately 1,175 feet above msl. The lower elevations at SSFL occur primarily along the eastern, southern and north-central to northwestern perimeters of the property. A broad, relatively flat area of topography exists within the northwestern portion of SSFL, which is referred to as the Burro Flats area.

SSFL lies within the Simi Hills, a northeast/southwest trending sub-range of the Santa Monica Mountains. The Simi Hills extend to the Santa Susana Mountains northeast of the site and to the Santa Monica Mountains to the south. To the north, the Simi Hills form the south wall of the Simi Valley, which is a relatively flat valley that slopes gently toward the west-southwest. To the east, the Simi Hills form the western boundary of the San Fernando Valley, which slopes gently to the southeast. Both of these valleys are encountered approximately 1¼ to 2 miles from SSFL property boundary.

### 3.2 CLIMATE AND PRECIPITATION

Climate at SSFL and surrounding area falls within the Mediterranean sub-classification, and monthly mean temperatures range from 50 degrees Fahrenheit (°F) during winter months to 70°F during summer months (SAIC 1994). During the summer months (April through October), a landward wind pattern occurs due to the site's proximity to the Pacific Ocean; during the winter months this is interrupted by weather fronts (SAIC, 1994). Based on wind measurements collected at SSFL in Area IV from 1994 through 1997, the prevailing wind pattern is northwest-southeast (Figure 3-2). The pattern is consistent with historical data collected in both the 1960s and 1990s.

Precipitation has been measured at SSFL daily at two on-site stations since 1960. Precipitation at SSFL is normally in the form of rain, although snow has occasionally fallen during winter months. Precipitation at the site has averaged approximately 18.5 inches per year between 1960 and 2008 (Figure 3-3). The annual precipitation has ranged from a low of 6.15 inches in 2007 to a maximum of 41.24 inches in 1998. The majority of annual precipitation at SSFL and surrounding area occurs between the months of November and March, consistent with the regional precipitation pattern of southern California. Figure 3-4 presents a graph of the actual monthly SSFL precipitation data and Figure 3-5 presents the average precipitation data by month from 2000 to 2008.

Historical information on the climate in the vicinity of SSFL was found in a report by the United States Geological Survey (USGS, 2003). The report presented a graph of tree ring indices in Southern California dating back to 1770 and precipitation at Port Hueneme starting in about 1890. For reference, Port Hueneme is about 29 miles west-southwest of SSFL along the Ventura County coastline. A graph of the estimated precipitation at Santa Paula from about 1760 to 1872 and measured precipitation from 1872 to 1965 is also presented in the report. For reference, Santa Paula is about 23 miles west-northwest of SSFL at an elevation of about 450 feet msl and both Santa Paula and SSFL are about 13 miles inland from the Pacific Ocean. These graphs are reproduced here as Figure 3-6. The figure shows episodes of both wetter than normal and drier than normal periods that last for decades and also shows both accumulations and depletions of rainfall that depart based on annual rainfall events. The period most germane to SSFL and data

that are utilized in subsequent sections of this report are from the latest timeframes presented in this figure. As shown in the figure, the wettest period recorded over the 200 year timeframe presented on the graph ended a few years prior to the purchase of land in 1949 to support SSFL operations (then referred to as the Propulsion Field Laboratory). A dry period was then experienced through 1965.

### **3.3 SURFACE WATER AND DRAINAGES**

Figure 3-1 depicts the surface water drainages at and surrounding SSFL. Most surface water that collects and drains at SSFL is intermittent and is conveyed off-site via one of four drainages: the Northwestern Drainage, the Northern Drainage, the Happy Valley Drainage, and the Bell Creek Drainage. Operational discharges of water, associated with extracted groundwater after treatment to discharge standards, have historically occurred within the central portion of SSFL in the Bell Creek Drainage. These discharges have now stopped due to cessation of rocket engine testing and groundwater extraction. As described in Section 2.3.2, surface water discharges from SSFL are monitored as part of the NPDES program. A more detailed view of SSFL drainages, surface water divides, ponds, and NPDES outfall locations is provided in Figure 3-1.

The majority of the surface water (estimated at greater than 60 percent) exits SSFL administrative areas I–IV through the southern property boundary into Bell Creek, which subsequently discharges into the Los Angeles River. NPDES Outfalls 011 and 001, and 018 and 002 (Figure 3-1), monitor these surface water discharges from the site. Most of the eastern portion of the facility drains through Dayton Canyon into Dayton Creek and combines with Bell Creek downstream before joining the Los Angeles River. Surface water discharges from this portion of the site are monitored at the Happy Valley monitoring location (NPDES Outfall 008).

The northwestern perimeter of the site drains northward into Meier Canyon, which subsequently discharges into Arroyo Simi. Surface water discharges from the northwestern portion of the site are monitored at NPDES Outfalls 003, 004, 005, 006, 007, and 010 (Figure 3-1). Surface water from the northeastern and north-central portions of SSFL drain into the Northern Drainage and is monitored at NPDES Outfall 009. The Northern Drainage connects to the Meier Canyon Drainage north of SSFL on Brandeis-Bardin property.

Three other small parcels of SSFL that have had no operations convey storm water runoff through three other drainages (i.e., Runkle Canyon, Woolsey Canyon, and Eastern Drainages) (Figure 3-1).

### **3.4 SURFACE WATER PONDS**

There are seven surface water features within SSFL, as shown on Figure 3-1. Their purpose was to retain and store water from adjacent or upstream operations. Boeing currently manages some of these features to reduce peak flows and subsequent erosion in downstream drainages. As described in Section 2.2, these features are either themselves RI sites (R-1 Pond [Solid Waste Management Unit (SWMU) 4.16], Perimeter Pond [SWMU 4.17], R-2 Ponds [SWMU 5.26], and Silvernale Reservoir [SWMU 6.8]), or they occur within an RI site (Coca Pond [SWMU 5.19]). The two other surface water features are the SRE Pond and the Building 56 Excavation. The SRE Pond was associated with the SRE site in Area IV (Area IV AOC). Surface water exists in the Building 56 Excavation (SWMU 7.1, part of the Building 56 Landfill RI site), which contains a mixture of surface water and groundwater. Similar to the Coca Pond, both of these features also are located within RI sites (SRE and Building 56 Landfill sites, respectively). Each of these seven water features is briefly described below.

#### **3.4.1 R-1 Pond**

The R-1 Pond is an approximately 3 million gallon capacity reservoir (SAIC 1994) located along the Area I Road (Figure 3-1). It collects storm water runoff from the eastern tributary of the Bell Creek Drainage and formerly treated groundwater (primarily from extraction at former water supply well Water Supply (WS)-5, no longer operating).

#### **3.4.2 Perimeter Pond**

The Perimeter Pond is an approximately 2 million gallon capacity reservoir (SAIC 1994) located near the southernmost portion of the Area I Road, north of a large area of undeveloped land (Figure 3-1). It is located downstream of the R-1 Pond. The Perimeter Pond is typically dry but temporarily stores surface water during heavy and/or long-term precipitation events. Discharge from this pond leads to the Bell Creek Drainage and is monitored at the NPDES Outfall 001.

### **3.4.3 Coca Pond**

The Coca Pond is an approximately 300,000 gallon capacity reservoir (SAIC 1994) located in Area II along the Coca Drainage west-northwest of the Coca test stands (Figure 3-1). This collection of surface water in this pond is now ephemeral. During the late 1990s and early 2000s, the pond continuously stored water that appeared to be the result of leaks in the test stand water supply piping system. These leaks were observed starting about 1999 (MWH, 2003b) but have since been repaired. Discharge from this pond leads to the R-2A Pond.

### **3.4.4 Silvernale Reservoir**

The Silvernale Reservoir is an approximately 6 million-gallon capacity reservoir located in Area III (Figure 3-1) and represents the largest surface water body at SSFL. The Silvernale Reservoir collects storm water runoff from the central portion of SSFL, former operational water discharges that occurred at the Alfa and Bravo test stands, and former treated groundwater primarily from former water supply wells WS-6 and WS-9, neither of which is active as of the date of this report. It should be noted that groundwater extraction from WS-9 has been proposed as part of the groundwater interim measure (MWH, 2009a), but the extracted groundwater will be conveyed by pipeline to a new groundwater treatment plant to be constructed between the R-1 and Perimeter Ponds. Treated groundwater from this new plant is anticipated to be discharged downstream of the Perimeter Pond at a new NPDES outfall location (019).

### **3.4.5 R-2 Ponds**

The R-2 Ponds include two surface water collection features: the larger R-2A Pond (approximately 2.5 million gallon capacity); and the smaller R-2B Pond (500,000 gallon capacity). The R-2B Pond receives flow from the Silvernale Reservoir and surface water runoff from the Burro Flats area of SSFL. The R-2A Pond also collects runoff from the Coca and Delta test stand areas (no current operational discharges) and treated groundwater, primarily from

former water supply well WS-9A, although this well was not active as of the date of this report<sup>2</sup>. The R-2B Pond drains to the R-2A Pond via a subsurface culvert. Discharge from the R-2A Pond leads to the Bell Creek Drainage and is monitored at the NPDES Outfalls 018 and 002.

### **3.4.6 SRE Pond**

The SRE Pond is an approximately 250,000 gallon capacity surface water body, located in the north-central portion of Area IV (Figure 3-1). This pond historically collected storm water runoff from SRE site activities (site now inactive, with all facilities demolished and removed) and is typically dry except in wet winter months. Discharge from this pond was pumped to a drainage leading to Silvernale Pond, although there is a controlled overflow discharge pipe that can be used to discharge water to a drainage north of SSFL that flows into the Meier Canyon Drainage.

### **3.4.7 Building 4056 Excavation**

The Building 4056 excavation is an approximately 100-foot diameter circular feature that extends approximately 65 feet deep into bedrock (about 0.2 acres in size) in Area IV (GRC, 1999) (Figure 3-1). The excavation was performed in anticipation of the installation of Building 4056; however the building was never constructed. The excavation collects both surface water runoff from the surrounding area, as well as groundwater. Because of surrounding bedrock exposures, surface water drainage into this feature is localized; water levels in the excavation are quite variable and depend on the amount of pumping from wells nearby and the amount of runoff generated by rainfall intensity. Depth to water in this excavation ranges between 5 and 50 feet.

---

<sup>2</sup> Groundwater extraction from WS-9A has been proposed as part of the groundwater interim measure (MWH, 2009a). The extracted groundwater will be conveyed by pipeline to a new groundwater treatment plant to be constructed between the R-1 and Perimeter Ponds.

### 3.5 BIOLOGICAL CONDITIONS

A broad range of wildlife and vegetative habitats occur at SSFL. Site-wide biological mapping was conducted in 1997 and published in a Biological Conditions Report (Ogden, 1998a). This report was updated in the Addendum to the Biological Conditions Report, which was prepared in 2003 (AMEC, 2003a). As part of group RI report preparation, ongoing detailed biological inspections of the plant communities at each RI site have also been conducted. In addition, detailed biological surveys were required for some RI field investigations or interim measures. Site-specific biological conditions are presented in individual RI site reports, group reports and/or work plans.

There are 16 different vegetation habitat types at SSFL: freshwater marsh, open water, unvegetated drainage channels, coast live oak woodland, southern coast live oak riparian forest, southern willow scrub, mulefat scrub, baccharis scrub, Venturan coastal sage scrub, chaparral, native grassland, nonnative grassland, ruderal, rock outcrop, eucalyptus woodland, and developed. Rock outcrops occur throughout the site and may be found in any of the habitat types (Ogden 1998a).

Four sensitive plant species have been observed at SSFL: Santa Susana tarplant, southern California black walnut, Mariposa lily, and Braunton's milk vetch. The Santa Susana tarplant is located on rocky outcrop areas throughout the facility. The southern California black walnut has been observed primarily in the Burro Flats area and the western side of SSFL, with solitary individual plants sparsely located across the facility. Mariposa lily has been observed in the Happy Valley Drainage, and Braunton's milk vetch is present in the far western portions of the site (Ogden, 1998a; AMEC, 2003a).

Sixty-nine bird species were observed during surveys at SSFL. The scrub jay, yellow-rumped warbler, turkey vulture, red-shouldered hawk, northern flicker, California quail, and red-winged blackbird were the most frequently observed bird species. Three sensitive bird species have been observed at SSFL: the great blue heron, loggerhead shrike, and southern California rufous-crowned sparrow. Five raptor species have been observed at SSFL, sharp-shinned hawk,

Cooper's hawk, red-shouldered hawk, red-tailed hawk, and great horned owl (Ogden, 1998a), along with the turkey vulture, a scavenger.

Thirteen mammal species were observed during surveys. Three sensitive mammal species have been observed: bobcat, mule deer, and San Diego black-tailed jackrabbit.

Ten reptile species have been observed at SSFL, including western whiptail and side-blotched lizards. Two species are considered sensitive: the two-striped garter snake and the Coast horned lizard (Ogden, 1998a; AMEC, 2003b).

Three amphibian species and two fish species have been observed during surveys: California slender salamander, Pacific tree frog, California toad, catfish, and goldfish (Ogden, 1998a).

#### **4.0 WORK PERFORMED IN SUPPORT OF GROUNDWATER REMEDIAL INVESTIGATION**

A number of activities have been performed to support the groundwater remedial investigation project at SSFL as outlined in the Work Plan, Site-wide Groundwater Characterization (MWH, 2008a) that was approved by DTSC (2009). Consistent with the site-wide work plan, the following work has been performed:

- Installation, purging, monitoring and sampling of Westbay multilevel systems in northeast area coreholes RD-31, RD-35C, C-16 and C-17,
- Installation of deep corehole C-15 (to a depth of 1,400 feet below ground surface [bgs]) that is a vertical extension of corehole C-6 located at the Delta RI site,
- Coring of plume transect coreholes C-12 through C-14 off the northeast perimeter of SSFL, including the installation of Westbay multilevel systems,
- Hydraulic conductivity profiling,
- Borehole geophysical logging,
- High-resolution fluid temperature logging,
- Analysis of additional rock core samples for chloride,
- Laboratory TCE degradation studies,
- Springs and seeps sampling and analysis,
- Collection of samples from wells using Snap samplers and analysis for dissolved gases, and

Further work beyond that described in the site-wide work plan was also performed to either fill data gaps identified during review of the available data (consistent with the approach presented in the site-wide work plan) or to further reduce uncertainties related to the characterization of the groundwater at SSFL. This additional work included:

- Field mapping of the geology in the southern undeveloped land area of SSFL and in off-site areas to the east,
- Mapping of joints observed in surface outcrops,
- Evaluation of fracture information obtained using borehole geophysical and corehole logging methods,
- Installation of 34 piezometers to evaluate the occurrence of groundwater within Areas I, II, III and IV of SSFL,

- Collection and analysis of samples from on-and off-site monitoring wells for additional geochemical characterization,
- Optimization and uncertainty evaluation of the three-dimensional groundwater flow model using parameter estimation techniques ([PEST], Doherty, 2009),
- Collection of groundwater samples to complete the characterization of the transport pathway from surficial media to groundwater,
- Collection and analysis of rock core from shallow groundwater piezometers (performed in 2000), and
- Characterization of groundwater for potential radionuclide impacts.

Additional descriptions of the work performed and references to appendices describing details and presenting results are provided below.

#### **4.1 INSTALLATION, PURGING AND SAMPLING OF MULTILEVEL MONITORING SYSTEMS IN NORTHEAST COREHOLES**

Westbay multilevel monitoring systems were installed at four locations within and outside of the northeast portion of SSFL as shown in Figure 4-1. These systems were designed and installed to evaluate variations in hydraulic head and to characterize VOC and other constituent concentrations in targeted depth intervals. Installation of the systems at RD-35C and C-16 occurred in late 2007 and has previously been reported (Parker, Cherry and McWhorter, 2008). Purging of these systems occurred in January 2008. Installation of the multilevel systems at RD-31 and C-17 was completed in May of 2008 and purging of both systems was completed in June 2008. Samples from the multilevel systems in C-16 and C-17 were collected in December 2008 while samples from the systems in RD-31 and RD-35C were collected in January of 2009. All samples were submitted to the environmental laboratory at the University of Guelph for analysis of VOCs by gas chromatography techniques. Additional details of the installation, monitoring and sampling of these systems, including as-built details, analytical results and hydraulic head profiles, are provided in Appendix 4-A.

#### **4.2 INSTALLATION OF COREHOLE C-15**

C-15 was installed as a new corehole in lieu of deepening corehole C-6 (completed to a depth of 898 feet) due to concerns related to the potential for (1) catastrophic caving, damage to, and/or

loss of the existing corehole; (2) vertical transport of contamination from the upper 900 feet to deeper portions of the hole during drilling and/or following the installation/removal of packers; and (3) rupture of a blank liner due to anticipated head differentials within the corehole. Data that were obtained from the installation of C-15 were used to: characterize the vertical distribution of VOCs in bedrock at the Delta RI site, evaluate variations in the salinity of the water contained in the rock, and evaluate the reduction in the bulk hydraulic conductivity with depth. The latter two activities were completed by analyzing rock core for chloride content, and using transmissivity, fluid temperature and borehole geophysical results (all further discussed in subsequent sections).

C-15 was planned to be drilled to a depth of approximately 900 feet for the placement of a conductor casing, followed by continuous coring to its target total depth of 1,400 feet. Drilling for the installation of corehole C-15 was initiated in November 2008 and the pilot hole was initially completed to a depth of 890 feet in early January 2009. Geophysical logging of this portion of the pilot hole on January 8, 2009 provided information that the deviation of the pilot hole from true vertical exceeded the project specification even though periodic measurements collected during its installation using field instruments indicated that the hole was within specification. Drilling and coring activities at C-15 were deferred until the latter part of February to allow time for an adequate corrective action plan to be prepared, reviewed and approved by the necessary parties, including DTSC. Activities at this location were re-started on February 23, 2009 and included grouting the lower portion of the pilot hole to a depth of 226 feet, which was completed on March 6, 2009. The pilot hole was then re-drilled to a depth of 890 feet and a conductor casing was set to this depth, which was completed on April 21, 2009. Coring commenced on April 23, 2009 and was completed on June 1, 2009 at a total depth of 1,400 feet. Nearly 500 rock core samples were collected and submitted for VOC analysis. Additional details of the work performed and analytical results of the rock core samples are presented in Appendix 4-B.

### 4.3 CORING OF PLUME TRANSECT COREHOLES

The Phase 2 Site Conceptual Model (SCM) work plan (MWH, 2007a) described work to be performed to evaluate the magnitude of contaminant attenuation within a groundwater plume due to various physical and chemical processes. The work plan prescribed the installation of four coreholes drilled to various depths across the width of an expected contaminant plume off the northeast portion of SSFL. Coreholes C-12, C-13 and C-14 were drilled in the later part of 2008 and early part of 2009 to fulfill this objective. Three coreholes were installed instead of four because of access restrictions imparted on the project by the owner of the off-site property that prevented the installation of one of the coreholes. The property owner deemed that the physical damage to the native environment that would have been required to achieve access to the desired fourth location was not acceptable. Hence, this drilling location was abandoned and the remaining three corehole locations were re-numbered. DTSC was informed of this constraint, and provided with figures showing how the locations and target depths of the remaining three coreholes were adjusted to still achieve the work plan objectives (Boeing, 2008).

Coreholes C-12, C-13 and C-14 were drilled to depths of 410, 725 and 625 feet, respectively. The targeted completion depths were designed to intercept certain stratigraphic intervals to aid in verifying the local distribution of VOCs in the groundwater. A cross-section showing the stratigraphic intervals intercepted by these three coreholes is shown in Figure 4-2. Rock core samples numbering nearly 300 in C-12, over 600 in C-13, and nearly 500 in C-14 were collected and analyzed for a select set of nine VOCs. The nine VOCs that were analyzed in the rock core samples include tetrachloroethene (PCE), TCE, cis-1,2-dichloroethene (cDCE), trans-1,2-dichloroethene (tDCE), 1,1-DCE, 1,1,1-trichloroethane (1,1,1-TCA), carbon tetrachloride, chloroform and CFC-113. Additional details regarding the drilling and completion of these three coreholes, as well as the rock core sample analytical results, are provided in Appendix 4-B. Westbay multilevel monitoring systems were designed and installed in coreholes C-12, C-13 and C-14 consistent with the requirements of DTSC's conditional approval of the Phase 2 SCM work plan (DTSC, 2007b). The multilevel system design basis and process, installation methods, as-built details, and head profiles are further discussed in Appendix 4-B.

#### 4.4 HYDRAULIC CONDUCTIVITY PROFILING

Blank FLUTE<sup>®</sup> liners have been used at SSFL to seal coreholes after drilling since 2000. During that time, FLUTE<sup>®</sup> developed measurement and data recording technologies for use during blank liner installation to provide data that can be analyzed to yield a continuous hydraulic conductivity profile for the corehole. Conductivity profiling was performed or attempted within four coreholes to provide further estimates of hydraulic conductivity that were used to:

- 1) Calculate additional hydraulic aperture values,
- 2) Evaluate the number of hydraulically-active fractures,
- 3) Assess the reduction in bulk hydraulic conductivity with depth, and
- 4) Evaluate the base of the active groundwater flow system.

In September 2008, conductivity profiling was performed at corehole C-7 (total depth [TD] of 419 feet bgs) and was attempted at corehole C-8 (TD of 400 feet bgs). These locations are shown on Figure 4-1, and were selected for conductivity profiling to help evaluate variability in transmissivity across SSFL. Before profiling at C-8 was attempted, the existing FLUTE<sup>®</sup> multi-level monitoring system was removed from the corehole. The profiling at C-8 was unsuccessful because the transmissivity of the corehole was too low for the blank liner to descend at an appreciable rate.

Conductivity profiling was also performed in coreholes C-6 and C-15, located in Area II of SSFL near the former Delta test stands (Figure 4-1). This work was performed in October 2009. Conductivity profiling was performed at corehole C-15 to collect measurements such that a decreasing trend in the bulk hydraulic conductivity of the Chatsworth Formation with depth could be evaluated. In total, conductivity profiling provided data throughout the entire saturated length of the collocated coreholes (C-6 and C-15) over an estimated interval of approximately 1,280 feet. The conductivity profiling methods and results are further described in Appendix 4-C.

#### **4.5 BOREHOLE GEOPHYSICAL LOGGING**

Borehole geophysical logs were collected from coreholes C-2, C-7, C-12, C-13, C-14 and from both the initial C-15 pilot hole (50 feet -881 feet, subsequently grouted and re-drilled) and the cored section of C-15 (890 feet – 14005 feet). The string of packers or blank liner was removed from each corehole prior to geophysical logging. Borehole geophysical logging included the collection of one or more of the following logs: caliper, natural gamma, electrical resistivity, video, and optical or acoustic televiewer. The initial pilot hole at C-15, which was subsequently grouted because of the excess deviation from vertical, was also logged with a gyroscope/magnetometer tool to obtain more precise information about the orientation of the deviation. A summary of the logs collected at each location is provided in Table 4-1 and copies of the logs are provided in Appendix 4-D.

#### **4.6 HIGH-RESOLUTION FLUID TEMPERATURE LOGGING**

High-resolution fluid temperature (HRFT) logging was performed at coreholes C-6, C-7, C-8, and C-15. These logs were used to provide information on hydraulically active fractures. At corehole C-15, these data also provide additional information on the base of the active groundwater flow system beneath SSFL. The fluid temperature logging activities were led by Peeter Pehme of Waterloo Geophysics Inc., who has performed this type of logging previously at SSFL.

Multiple logging runs were made in each corehole. Each corehole was first logged open-hole. The corehole was then sealed by a blank liner before further testing. Following the installation of each blank liner, each corehole was allowed to stabilize for a minimum of 48 hours before fluid temperature logging was initiated. During both the open-hole and lined-hole logging, the sequence of logging runs was:

- Background passive temperature (collected before heating the hole)
- Active temperature (collected near the end of the heating time)
- Passive thermal recovery (collected after the end of heating)

Active temperature logs were not collected at C-6 or C-15 because the hole diameters were too small to simultaneously accommodate the temperature probe and the double heat cable required to heat these two longer holes. Two to three passive thermal recovery logging runs were performed at each corehole to provide thermal decay data at multiple times after the heater was turned off. Additional descriptions of the methods applied and the results obtained for the fluid temperature logging work are provided in Appendix 4-E.

#### **4.7 ANALYSIS OF ROCK CORE SAMPLES FOR CHLORIDE**

Rock core samples from both the vadose zone and the saturated zone were analyzed for chloride. Vadose zone rock core samples were analyzed to provide information on groundwater recharge, while rock core samples from the saturated zone were analyzed to provide information regarding the base of the active groundwater flow system. Each of these sampling activities is further described below.

##### **4.7.1 Vadose Zone Samples**

Vadose zone rock core samples were analyzed for chloride at University of Guelph using an ion specific electrode method to allow further evaluation of the nature of groundwater recharge. Samples of archived vadose-zone rock core from coreholes C-1, C-3, C-6, and C-8 were collected at approximately 5-foot intervals starting at the depth where core was first collected to the approximate depth of groundwater at each corehole. Seventeen samples were collected from C-1, 16 samples were collected from C-3, 15 samples were collected from C-6, and 33 samples were collected from C-8. Details of the sample collection and preparation procedures, which were used previously at SSFL for vadose-zone core samples from C-4 that were analyzed for chloride, as well as details of the laboratory equipment, analyses and techniques are presented in Appendix 4-F.

##### **4.7.2 Saturated Zone Samples**

Rock core samples from the saturated zone below 894 feet at corehole C-15 were collected and analyzed for chloride. The chloride analytical results from these rock core samples were used to evaluate the position of the freshwater/saltwater interface within the Chatsworth Formation to

help evaluate the base of the active groundwater flow system. Core samples were collected at approximately 5-foot intervals between depths of 900 and 1,400 feet for a total of 111 samples. The core sample collection, preparation, and analysis were as described above for the vadose zone samples, and as detailed in Appendix 4-F.

#### **4.8 ADDITIONAL DEGRADATION STUDIES ON CHLORINATED ETHENES**

Additional laboratory studies were performed using rock core to further evaluate and enhance the understanding of the occurrence and rate of TCE and daughter product transformation in Chatsworth Formation groundwater. Work was performed to establish a degradation rate for cDCE, identify the organism responsible for the transformation of TCE to cDCE, and to identify transformation pathways for assessing the sustainability of the degradation mechanisms. These studies were performed at Clemson University. Additional descriptions and results are presented in Appendix 4-G.

#### **4.9 COLLECTION AND ANALYSIS OF SAMPLES FROM SEEPS**

Samples of seep water were collected in late 2007, late 2008 and in 2009 to fulfill three primary purposes. One purpose was to analyze seep samples for VOCs at several seeps not previously analyzed for VOCs to evaluate their potential presence and aid in characterizing their nature and extent. A second purpose was to collect seep samples for VOC analysis using more robust quality assurance measures to allow further evaluation of prior suspect VOC detections. A third purpose was to analyze seep samples for various geochemical and isotopic parameters that would provide insight into the origin of the groundwater emanating from the seep.

Thirteen seeps were sampled and analyzed for VOCs in late-September through mid-November of 2007. Results are summarized in Table 4-2 and sample locations are shown in Figure 4-3.

Twelve seeps were inspected for three consecutive calendar quarters starting in the fourth quarter of 2008 and continuing through the second quarter of 2009, and were sampled and analyzed for VOCs if water was present. The ten seeps that were sampled on at least one of these three occasions are shown in Figure 4-3. Four of these seeps were also sampled and analyzed for

VOCs in July and September of 2008 to support the preparation of the report for RI Group 5 (CH2MHill, 2008). Results are summarized in Table 4-2, and are further discussed in Appendix 4-H.

Seeps characterized for their geochemistry and isotopic composition were sampled and analyzed for the following:

- Major ions: sodium, potassium, calcium, magnesium, sulfate, chloride, bicarbonate,
- Select metals: barium, boron, copper, iron, lithium, manganese, strontium, and zinc,
- pH, conductance, and total dissolved solids,
- ammonia, fluoride,
- Stable isotopes of sulfur, carbon, chlorine and strontium,
- Carbon-14 ( $^{14}\text{C}$ ), and
- Oxygen-18 ( $^{18}\text{O}$ ), deuterium ( $^2\text{H}$ ), and tritium ( $^3\text{H}$ )

Ninety-three seep locations were sampled for this characterization effort and their locations are shown in Figure 4-4. Additional descriptions of the seep sampling program including a summary of the sampling results are presented in Appendix 4-H.

#### **4.10 COLLECTION AND ANALYSIS OF SAMPLES FROM WELLS**

In addition to the typical quarterly groundwater sampling and analysis that is conducted at SSFL for characterizing impacts to the groundwater, additional samples were collected from 14 on-site wells to evaluate the TCE transformation pathway. Downhole sample collection devices (i.e., Snap samplers) were used to collect samples from below the water table at specified depth intervals at each of these 14 wells for analysis of VOCs, dissolved gases, compound-specific isotope analysis and major ions. The locations of the wells sampled are shown in Figure 4-5. Three distinct sampling events were conducted over a period of five months starting in June 2008 and extending into November 2008. The wells selected for this program and details of the sampling equipment, methodology and results are presented in Appendix 4-I.

#### **4.11 STRADDLE PACKER TESTING**

Hydraulic tests using straddle-packers were planned to be performed at a target interval within existing corehole C-2 in which groundwater had been observed spraying from a fracture into the open hole above the static water level in the hole. However, downhole video logging of corehole C-2 conducted in September 2009 during preparation for the straddle packer testing showed that this fracture had dewatered. An alternate spraying fracture location in corehole C-13 was subsequently selected for this work, but video logging of C-13 in early October 2009 showed that the spraying fracture in C-13 had also dewatered. In the absence of a spraying fracture interval to test, the straddle-packer testing exercise was cancelled.

#### **4.12 ADDITIONAL WORK DONE TO FILL DATA GAPS IDENTIFIED DURING REVIEW OF AVAILABLE SITE DATA**

##### **4.12.1 Geologic Field Mapping**

Additional field mapping of the geology was conducted in the fall of 2008 in the southern undeveloped land area of SSFL and in off-site areas to the east of SSFL. The purpose of this mapping exercise was to reduce uncertainty related to the occurrence and position of the stratigraphic sections and faults. Limited field mapping was also conducted off-site north of SSFL to evaluate the suspected presence of a fault. The general boundaries of the areas mapped during this exercise are shown in Figure 4-6. This mapping supplemented earlier field mapping of the geology beneath SSFL as described in MWH, 2007e. A technical memorandum describing the results of the mapping is provided in Appendix 4-J. Updates to the site geologic map and the inclusion of this additional information into the three-dimensional groundwater flow model for the site are described in Sections 5.0 and 6.0 of this report.

##### **4.12.2 Mapping of Joints Observed in Surface Outcrops**

A mapping exercise of joints observed in surface outcrops during geologic mapping and through the inspection and analysis of aerial photos and satellite images was conducted during the early part of 2009. The purpose of this exercise was to develop additional detailed information regarding the spacing, length and orientation of joints in surface outcrops in the Chatsworth

Formation within and around SSFL. Results of the joint mapping exercise are presented in Appendix 4-K.

#### **4.12.3 Integration and Analysis of Fracture Data Sets**

Computation tools were selected and applied to integrate the subsurface data collected on joints and bedding planes from borehole geophysical logging and rock core logging as described in MWH (2002c and 2002f). PETREL was the tool selected to achieve this integration and the results of the fracture network analysis of the Chatsworth Formation beneath SSFL is described in Appendix 4-L.

#### **4.12.4 Installation of Piezometers**

Thirty-four piezometers were installed in Administrative Areas I, II, III and IV of SSFL during 2008 and 2009 to characterize the potential presence of the first occurrence of groundwater. Most have been dry since their installation. The work was performed in support of the surficial media operable unit characterization programs for RI groups 2, 3, 6 and 9. Locations of the piezometers that were installed are shown in Figure 4-7. Details regarding the installation of these piezometers are provided in the reports for RI groups 2, 3, 6 and 9 (NASA, 2008, 2009a and 2009b; MWH, 2006b). Technical memoranda summarizing the groundwater occurrence and sampling results are provided in Appendix 4-M.

#### **4.12.5 Additional Sampling and Analysis of Groundwater for Geochemical and Isotopic Parameters**

Samples were collected from both on- and off-site wells for a similar set of geochemical and isotopic parameters as that collected from seeps to allow for a comparison of the groundwater beneath SSFL to the seep water. Forty-three wells were sampled in late 2007 and in 2008 for a similar set of geochemical and isotopic parameters as that listed in Section 4.9. Locations sampled are shown in Figure 4-8 and sampling results are presented in Appendix 4-H.

#### **4.12.6 Optimization and Uncertainty Analysis of Three-Dimensional Groundwater Flow Model**

As reported in AquaResource/MWH (2007), a three-dimensional groundwater flow model has been developed for SSFL. Initial calibration of the model was achieved through manual modification of the hydraulic conductivities and other parameters as discussed in the aforementioned report. The model calibration was further optimized using PEST (Doherty, 2009). Prior to optimizing the calibration, the model structure was modified to incorporate the updated geologic mapping information described in Section 4.12. Additional work was also conducted using PEST to quantitatively assess how changes within defined ranges of parameters affect the variation in the groundwater flow field. This analysis is referred to as a null-space Monte Carlo simulation. Additional descriptions of the work performed on the three-dimensional groundwater flow model are discussed in Section 6.0 of this report and its corresponding appendices.

#### **4.12.7 Groundwater Data Gaps Sampling for Surficial Media/ Groundwater Transport Pathway**

Starting in 2006, samples were collected from various groundwater monitoring wells and analyzed for specific chemicals to complete the characterization of the potential transport of chemicals encountered in surficial media to the groundwater beneath SSFL. This sampling was initiated in response to the preparation and subsequent issuance of surficial media RI group and site reports. Results have been reported in the quarterly and annual groundwater monitoring and sampling reports (e.g. Haley & Aldrich, 2009a and 2009b). This work has resulted in the collection and analysis of 534 samples from 91 groundwater monitoring locations across SSFL. Sampling and analysis conducted at each well is provided in Appendix 4-N. Locations sampled are shown in Figure 4-9.

#### **4.12.8 Collection and Analysis of Rock Core from Shallow Groundwater Piezometers**

In November 2000, 198 rock core samples were collected and analyzed for 6 targeted VOCs from 11 shallow groundwater coreholes that were subsequently converted to piezometers. Eight samples (about 5 percent) were also analyzed for the full suite of EPA Method 8260 target

analytes. The depth of the coreholes that were drilled ranged from 26 to 72 feet bgs. Physical property measurements were also made on select samples. This work was performed as a supplement to the Shallow Groundwater Investigation Work Plan (Ogden, 2000b) and results have not been previously reported. A full report describing the work is provided in Appendix 4-O. Cored locations are shown in Figure 4-10.

#### **4.12.9 Groundwater Characterization for Radionuclides**

In support of DOE Environmental Management (EM) closure activities in Area IV of SSFL, Haley & Aldrich conducted a groundwater data gap evaluation to identify potential data gaps for radiological constituents. Investigations were initiated in 2004 and continued into 2006. The objectives of the investigations were to determine if there were radiological impacts associated with suspected sources and to further characterize identified impacts. Thirteen bedrock groundwater monitoring wells were installed in Area IV to complete this evaluation. Groundwater samples were collected and analyzed from these wells for both radiological and chemical constituents. Rock core samples were also collected and analyzed for tritium from select locations. This work was further supplemented in 2007 with the installation of two coreholes from which rock core samples were collected and analyzed for tritium and in 2008 with the installation of an additional well (RD-98). Reports describing the work and results are provided in Appendix 4-P. Locations drilled for the data gaps evaluation program are shown in Figure 4-11.

This Page Intentionally Left Blank

## 5.0 GEOLOGY OF SSFL AND VICINITY

This section of the groundwater RI Report describes the geologic setting of SSFL and vicinity at regional, local, and site-specific scales. These multiple scales of description provide the context and information needed to support subsequent discussions of the area hydrogeology (Section 6) and the nature, extent, transport, and fate of contaminants (Sections 7 and 8).

The following table provides a summary of the geologic time scale. As discussed below, geologic formations relevant to SSFL are of Late Cretaceous age and younger.

Era	Period	Epoch	Millions of Years Before Present		
Cenozoic	Quaternary	Holocene	0.011		
		Pleistocene			
	Tertiary	Neogene	Pliocene	2.6	
			Miocene	5.3	
		Paleogene	Oligocene	23	
			Eocene	34	
			Paleocene	56	
				65	
		Mesozoic	Cretaceous	Late	100
				Early	146
Jurassic	202				
Triassic	251				
Paleozoic			542		
Precambrian					

## 5.1 REGIONAL GEOLOGY

SSFL is located in the Western Transverse Ranges physiographic province of southern California (Figure 5-1). The geology and physiographic expression of the Western Transverse Ranges reflects at least 70 million years of geologic history. Within this province, the region encompassing SSFL includes the Simi and Thousand Oaks valleys, the western San Fernando Valley, the Simi Hills, and portions of the Santa Susana and Santa Monica mountains.

The regional geologic map presented in Figure 5-2 is a mosaic of 1:24,000-scale maps prepared by Dibblee (1992a-1). A regional geologic map also has been compiled by the United States Geological Survey (USGS) (Yerkes and Campbell, 2005). This work is augmented by detailed geologic mapping conducted by SSFL project geologist (MWH, 2007e; Appendix 4-K). AquaResource/MWH (2007) evaluated the regional geology in support of a regional, three-dimensional groundwater flow model. The regional geologic cross-sections provided in Plate 5-1 (A-A' through F-F') are based on the work of Dibblee (1992a-1) and include enhancements and supplemental cross-sections prepared by SSFL project geologist.

### 5.1.1 Geologic Units

Basement rocks exposed in the Santa Susana Mountains and Simi Hills are primarily of sedimentary and volcanic origin and range in age from Late Cretaceous to Late Pliocene. These units are well exposed except where overlain by alluvium in some valleys and canyons. The sedimentary rocks in the region encompassing SSFL range from coarse-grained conglomerate and sandstone to fine-grained siltstone and shale.

Figure 5-3 is a generalized stratigraphic column of the region. At the base of this column is the Chatsworth Formation, a sequence of marine turbidite that underlies much of the Western Transverse Ranges and SSFL. Deposited about 70 to 65 million years ago, the Chatsworth Formation is at least 6,000 feet thick (Yerkes and Campbell, 2005) and currently extends more than 2,000 feet below sea level in the vicinity of SSFL (section F-F', Plate 5-1). It is the primary rock unit exposed at SSFL.

Overlying the Chatsworth Formation is a sequence of younger (i.e., Tertiary, about 65 to 5 million years before present) sedimentary and volcanic marine and non-marine formations. From oldest to youngest, the overlying sedimentary formations are the Simi Conglomerate and the Las Virgenes, Santa Susana, Llajas, Sespe, Vaqueros, Topanga, Calabasas, and Modelo/Monterey Formations (Figure 5-3). The Simi, Las Virgenes, and Sespe Formations were deposited primarily in fluvial and alluvial environments, whereas the other Tertiary formations were deposited primarily in marine environments. The total aggregate thickness of these sedimentary units is greater than 40,000 feet (Yerkes and Campbell, 2005). However, the entire sequence does not occur at any given location due to various local and regional unconformities (Figure 5-3 and Plate 5-1).

The most extensive non-sedimentary rock unit within the regional study area is the Early to Middle Miocene Conejo Volcanics (Figure 5-2). These rocks interfinger with the Topanga Formation and are exposed in outcrops south and southwest of SSFL. Likely associated with these volcanics are diabase dikes and similar intrusive igneous rocks that cross-cut sedimentary units in the region and locally intrude faults that probably originated or were active in the Early Miocene.

The region's youngest geologic units consist of Quaternary alluvium within the Simi, San Fernando, and other area valleys. These largely consist of stratified but unconsolidated sands, silts, and clays formed by the erosion and re-deposition of adjacent, uplifted rocks.

### **5.1.2 Geologic Structure and History**

The geologic evolution of the Western Transverse Ranges is complex and reflects several distinct episodes of deformation that include tectonic extension, rotation, compression, and shearing (Nicholson et al., 1994; Ingersoll and Rumelhart, 1999). Named faults in the region encompassing SSFL include the Simi, Santa Susana, Chatsworth Reservoir, and Burro Flats Faults (Figure 5-4). Major faults relative to SSFL include the Malibu Coast Fault approximately 14 miles to the south and the San Gabriel and San Andreas Faults more than 15 and 30 miles, respectively, to the north and northeast (Figure 5-1).

Beginning in the Early Miocene, the tectonic environment in the vicinity of SSFL evolved from east-directed subduction, to right-lateral shear, to west-directed extension, and finally to strike-slip faulting (Nicholson et al., 1994). In the vicinity of SSFL, this transition caused the Western Transverse Ranges to rotate more than 90 degrees clockwise, followed closely by (or synchronous with) a period of tectonic extension. An animated depiction of this complex structural history can be viewed at:

<http://emvc.geol.ucsb.edu/downloads.php#RegionalTectGeolHist>.

Since the Early Miocene, at least two major episodes of faulting have resulted in the folding of the Chatsworth-to-Sespe Formation sequence locally into a west-plunging syncline, the axis of which is beneath Simi Valley (Figure 5-4). Along the northern edge of the Simi Hills, the Chatsworth Formation and overlying Paleogene rock units dip moderately to the northwest, forming the southern limb of the Simi Valley syncline. Along the northern margin of Simi Valley, the syncline is cut by the Simi Fault, a steeply north-dipping reverse fault (Figure 5-4; Plate 5-1, section F-F').

During the Miocene, stratigraphic units deposited prior to and during the early Tertiary underwent uplift, tilting, and significant erosion. Many of the faults that cut these early Tertiary rocks probably first developed during this time. Erosion probably had exposed much of the early Tertiary and Late Cretaceous rock units by the Middle Miocene (approximately 14 million years before present). During the Late Miocene, the marine detrital sediments of Lindero Canyon and other units of the Modelo/Monterey Formation were deposited unconformably across the older Late Cretaceous and Paleogene rocks. These upper Miocene sediments are exposed to the south and southeast of SSFL and north of the Simi Fault (Figure 5-2).

The geologic history of the Western Transverse Ranges post-Late Miocene (less than 6 million years before present) is characterized by: 1) the superposition of roughly east-west trending antiform and synform folds across the entire geologic sequence of pre-Late Miocene basement rocks and 2) multiple tectonic periods of significant displacement along reverse and right-lateral faults.

Since the Late Pliocene or early Pleistocene (about 2.6 million years ago), the area surrounding SSFL has been subjected to intense deformation and the activation of many east-west striking structures (e.g., faults and folds) due to transpression related to the evolution of the modern San Andreas Fault system (Atwater, 1998). An animated depiction of this faulting and deformation can be viewed at: <http://emvc.geol.ucsb.edu/downloads.php#TransverseRanges>.

The Western Transverse Ranges province is currently in north-south compression as a result of its oblique east-west orientation with respect to the regional dextral motion of north-northwest striking faults related to the San Andreas Fault system. This compression is expressed by tectonic activity along numerous regional and local east-west trending faults and folds that effect rock units in the vicinity of SSFL. Northeast-southwest and northwest-southeast trending faults and folds also are mapped within and near SSFL, reflecting either the complex nature of the current stress field or older, pre-compression tectonic activity.

## **5.2 SSFL GEOLOGY**

Figure 5-4 is a geologic map of the Simi Hills near SSFL by Dibblee (1992b) and Figure 5-5 is a more detailed geologic map of SSFL that incorporates additional geologic characterization by SSFL project geologist (MWH, 2007e; Appendix 4-K). Plates 5-2 and 5-3 present a set of nine geologic cross-sections through SSFL, also prepared by the project geologist.

### **5.2.1 Geologic Units**

Mappable geologic units within the boundaries of SSFL include the Chatsworth, Simi Conglomerate, Santa Susana, Los Virgenes, and Calabasas Formations and Quaternary alluvium (Figure 5-4). Greater than 75 percent of the basement rock exposures within the boundaries of SSFL belong to the Chatsworth Formation, including all sites with documented subsurface contamination.

#### **5.2.1.1 Chatsworth Formation**

The Late Cretaceous Chatsworth Formation consists primarily of sandstone with lesser amounts of interbedded shale, siltstone, and conglomerate. Link et al. (1981) interpreted that its

deposition occurred on the surface of a sand-rich submarine fan at water depths between 600 and 3,000 feet. Beneath most of SSFL, they interpreted that the Chatsworth Formation originated from turbidites in a mid-fan environment. Data produced from the geologic characterization of SSFL and adjacent areas show a decrease in both grain-size and bedding thickness along strike from the south-central part of SSFL toward the northeast (MWH, 2007e). This suggests that the rocks in the south-central part of SSFL were deposited closer to an inner-fan environment than those further to the northeast.

The Chatsworth Formation in the vicinity of SSFL is subdivided informally into upper and lower units (Montgomery Watson, 2000a). The lower Chatsworth Formation is exposed in southeastern SSFL and dips northwest beneath the remainder of SSFL. The top of the lower Chatsworth Formation contains a higher proportion of fine-grained beds than the overlying upper Chatsworth Formation. Where exposed, the remainder of the lower Chatsworth Formation appears generally similar to the upper formation (MWH, 2007e).

The stratigraphy of the upper Chatsworth Formation in the immediate vicinity of SSFL is defined by a sequence of coarser- and finer-grained members. The coarser-grained members consist primarily of medium- to fine-grained sandstone beds with features typical of turbidite deposition. These features include thick sediment sequences, soft-sediment deformation, graded and cross bedding, variations in bedding dip and grain size, poor sorting, bioturbation, and scour at the base of beds. Individual sandstone beds range in thickness from roughly an inch to 30 feet or more, but are typically 1 to 5 feet thick. Intervals of stacked sandstone beds with few or no fine-grained interbeds typically reach tens of feet thick and may extend laterally for several thousand feet. Coarse-grained beds also include thinner and less extensive lenses of conglomerate that generally are less than several feet thick.

The finer-grained members of the upper Chatsworth Formation typically consist of 50 percent or more siltstone and shale interbedded with lesser amounts of sandstone. Individual fine-grained beds are generally less than 3 feet thick and usually less than 1 foot thick. Sandstone beds within the fine-grained members may be laterally extensive and more than 10 feet thick.

Figure 5-7 provides a conceptual representation of the characteristic lithology, structure, and fracturing of sandstone, siltstone, and conglomerate bedding within the Chatsworth Formation. The characteristic aspects of fracturing are discussed in Section 5.2.2.2.

A mineralogical analysis of 29 petrographic thin sections obtained from core samples indicates that the arkosic sandstone of the Chatsworth Formation has an average composition of 33 percent quartz, 33 percent plagioclase, 20 percent feldspar, and 10 percent phyllosilicate minerals, with about 5 percent lithic fragments. The average composition of analyzed siltstone samples is 23 percent quartz, 30 percent plagioclase, 22 percent feldspar, and 18 percent phyllosilicate minerals, with rare lithic fragments. The predominant phyllosilicate minerals are biotite and chlorite (Loomer et al., 2009). The predominant cementing agents within all bedding types are calcite (calcium carbonate), dolomite (magnesium carbonate), and clay.

As a result of field mapping and the interpretation of aerial photographs and borehole logs and cores in the immediate vicinity of SSFL, the upper Chatsworth Formation is subdivided into upper and lower stratigraphic packages—referred to as Sandstones 1 and 2, respectively. These packages are separated and bounded above and below by fine-grained units referred to as Shales 1, 2, and 3 (where Shale 1 refers to the zone of fine-grained interbeds near the top of the lower Chatsworth Formation; MWH, 2007e). Each package is subdivided into three predominantly coarse-grained members separated by predominantly fine-grained members. From oldest to youngest, Sandstone 1 consists of the Bowl, Canyon, and Sage coarse-grained members separated by the generally fine-grained Happy Valley and Woolsey members. Additionally, the coarse-grained Sage member at the top of Sandstone 1 contains four relatively thin fine-grained interbeds referred to as the upper and lower Line and Bravo beds. Sandstone 2 consists of the Silvernale and upper and lower Burro Flats coarse-grained members separated by the SPA and ELV fine-grained members. This sequence of 12 laterally-extensive members within the upper Chatsworth Formation is summarized in the following table and illustrated in the stratigraphic column presented in Figure 5-6.

Member		Relative Texture		SSFL Approximate Thickness (ft)		
		Coarse	Fine	Member	Sum	
Upper Chatsworth Formation	Shale 3			X	75 - 125	
	Sandstone 2	Upper Burro Flats <sup>a</sup>	X		500	900 - 1,100
		ELV		X	15 - 40	
		Lower Burro Flats	X		300 - 370	
		SPA		X	15 - 30	
		Silvernale	X		110 - 160	
	Shale 2			X	150 - 175	
	Sandstone 1	Sage <sup>b</sup>	X		700	1,800 - 2,300
		Woolsey		X	100 - 300	
		Canyon	X		500 - 600	
Happy Valley			X	70 - 110		
Bowl		X		400 - 600		
	Shale 1			X		
top of lower Chatsworth Formation	interbedded sandstone, siltstone, and shale	X		~1,000		

<sup>a</sup>Contains the fine-grained Lot Bed.

<sup>b</sup>Contains the fine-grained upper and lower Line and Bravo Beds.

The coarse-grained members are significantly thicker than most of the fine-grained members by a factor ranging locally from about 3 to 50. Faulting has off-set the stratigraphic sequence in portions of SSFL, as evident from the lateral off-set of shale units shown in Figure 5-5 and Plates 5-2 and 5-3.

The fine-grained members and the coarse-grained members of the upper Chatsworth Formation each share lithologic and bedding similarities such that their correlation across faults and over long distances is often difficult. Nevertheless, heterogeneities among these units do exist. For example, the Sage member sandstone is thicker and coarser grained in the south-central portion of SSFL than along strike to the northeast. Similarly, conglomerates are relatively common in the central part of SSFL but become nearly absent east of the Shear Zone (a fault discussed in Section 5.2.2.1). Conversely, fine-grained units that are relatively thick and laterally continuous east of this fault are thinner and less continuous or absent to the west. As another example, the Lower Burro Flats member contains more fine-grained interbeds than the overlying Upper Burro

Flats member or the underlying Silvernale member (MWH, 2007e). In some cases these differences are reflected in the topography. Whereas resistant and massive upturned sandstone beds of the Sage and Canyon members form ridges on either side of the Shear Zone, the more erodible Lower Burro Flats member coincides with relatively broad and flat topographic lows.

The Chatsworth Formation is conformably and/or disconformably overlain by the Paleocene Simi Conglomerate north of SSFL. Along the western part of SSFL, the Chatsworth Formation is faulted against the Simi Conglomerate and the Eocene to Paleocene Santa Susana and Las Virgenes Formations. South of SSFL, the Chatsworth Formation is unconformably overlain by south-dipping late Tertiary rocks (i.e., the Calabasas/Lindero Canyon and Modelo/Monterey Formations).

#### **5.2.1.2 Unconsolidated Deposits**

Unconsolidated deposits at SSFL include alluvium, artificial fill, and thin soils over shallow bedrock. The alluvium generally consists of silty sand and occurs in topographic lows and along ephemeral drainages. Deposits are typically 1 to 15 feet thick but range to more than 30 feet thick within small areas along the northern and northeastern portions of the site. Figure 5-8 shows the distribution of mapped alluvial deposits greater than 5 feet thick. Artificial fill derived from on-site disturbed soils have been placed in developed portions of SSFL.

#### **5.2.2 Geologic Structure**

Exposures of the Chatsworth Formation across the Simi Hills and Santa Susana Mountains indicate that it is synclinally folded about an east-west-striking axis that is located roughly at the latitude of State Route 118 at Santa Susana Pass and plunges west under Simi Valley. The exact age of folding is unknown, but is likely related to post-Middle Miocene transpression. SSFL is located on the south limb of this west-plunging syncline. Bedding orientations at SSFL are locally variable, but typically strike approximately N70°E and dip 25°- 35° to the northwest. As such, the exposed stratigraphy generally becomes younger toward the northwest.

As discussed above, the Chatsworth Formation has undergone a complex history of regional tectonic stresses, exposing it to multiple orientations of compressional, extensional, and shear

forces. In the vicinity of SSFL, the maximum compressive stress is currently oriented north-northeast, consistent with its orientation within the Simi Valley syncline. Additionally, the site has been subjected to local stresses, including faulting and erosional unloading. Given this complex and locally variable stress history, a comprehensive accounting of the orientation and magnitude of past stresses affecting SSFL is not practical.

#### **5.2.2.1 Faults**

SSFL and vicinity are traversed by numerous, steeply dipping to near-vertical displacement structures of various orientation, length, displacement, and type. Mappable structures include minor and major faults and deformation bands (MWH, 2007e; Appendix 4-K). These features laterally and/or vertically off-set pre-existing geologic features. Additionally, potential displacement structures are inferred along several lineaments observed from aerial photographs. The SSFL geologic map (Figure 5-5) identifies 20 named displacement structures and lineaments in addition to several unnamed fault traces. Table 5-1 provides a list of the named features, their mapped lengths, general orientations, and characteristics. Based on length, approximately half of the mapped fault traces are oriented roughly east-west and nearly a third are oriented roughly northeast-southwest, with various orientations among the remainder.

Named SSFL faults and fault zones consist of mappable traces with displacement measureable in feet along one or more distinct failure surfaces. In contrast, named deformation bands occur as single to multiple, thin (~0.1-inch wide) cataclastic zones with displacements generally measurable in inches or less. Several lineaments have been identified by aerial photographs in cases where outcrops are insufficient to determine whether there is appreciable displacement. Named lineaments are referred to as “Structures” and are flanked by at least one field-observed deformation band striking approximately parallel to the lineament.

The main traces of mapped, named faults have a cumulative length of more than 25 miles within SSFL and immediately adjacent areas. The generally east-west trending faults are the Woolsey, North, IEL, Happy Valley, Coca, Burro Flats, and Bell Canyon faults (listed from north to south). Faults oriented generally northeast to southwest are the Skyline, CTL, Shear Zone, Box Canyon, and Dayton faults (listed from west to east). The “Shear Zone” is a pre-existing fault

name adopted by SSFL project team; however, this fault represents a brittle stress response similar to other area faults, and is not representative of the more plastic, ductile deformation typically associated with a shear zone. In their current geometries most faults at SSFL appear to be oblique slip faults displaying primarily lateral separation. Apparent strike-slip displacement along east-west faults is generally right-lateral east of the Shear Zone and left-lateral west of the Shear Zone. Northeast trending faults lack evidence of general displacement trends (MWH, 2007e; Appendix 4-K).

The named on-site deformation bands are the Alfa Deformation Band and the North, Middle, and South Bravo deformation bands. These have a cumulative mapped length of nearly 1 mile. The named on-site lineaments are the FSDF Structure, Delta Structure, Ridge Structure, Tank Structure, and Bowl Structure. These have a cumulative mapped length of 2.6 miles (Figure 5-5; Table 5-1).

DTSC has commented that all SSFL displacement structures should be referred to simply as faults (DTSC, 2008a, b). Therefore, the features described in this report as deformation bands can also be considered as faults, and features described as structures (i.e., lineaments) can also be described as inferred or suspected faults, consistent with DTSC's request. Additionally, DTSC has proposed three other possible faults. Attempts by SSFL project geologist to field-verify the existence of these three faults have been unsuccessful (Appendix 4-K). These possible faults were considered in the optimization of SSFL groundwater flow model (Appendix 6-A).

In lithified bedrock, the structure of a fault zone typically consists of a fault-plane core and adjacent damage zones. Controls on the development, nature, and scale of these structures include the nature and magnitude of deformation, the lithologic and mechanical properties of the rock, fault-zone geometries, and fluid-rock interactions. Clay-rich *gouge*, breccias, and cataclasite typically form within the fault core. Damage zones consist of a network of subsidiary structures including minor faults, fracture sets, cataclastic deformation bands, mineralized veins, cleavage, and folds. Damage zones may be effectively absent where strain is highly localized along the fault core (Caine et al., 1996).

At SSFL, some fault-zone segments are hundreds of feet wide and contain multiple fault traces and/or deformation bands (e.g., western Woolsey Fault, western North Fault, portions of Burro Flats Fault). Other fault-zone widths are tens of feet wide (e.g., portions of the Coca, Skyline, and CTL faults and Shear Zone) or less (e.g., portions of the eastern and central North Fault, and Happy Valley and IEL faults). Fault-core gouge has been observed at one or more locations along nearly all of the named faults, ranging from 0.5 to 18 inches thick (Table 5-1; MWH, 2007e; Appendix 4-K). Broken rock and rubble zones are noted in some cores and borehole geophysical logs collected from SSFL fault zones.

An intensely fractured 25- to 50-foot wide damage zone occurs along the Shear Zone near its intersection with the Coca Fault (Figure 5-5). Fractures within this zone are typically parallel to the Shear Zone. Other described damage zones include a 5-foot-wide zone of subsidiary faults within a 30-foot-wide zone of deformation bands along a portion of the Coca Fault, and fractured zones up to 10 feet wide along portions of the Woolsey Fault. Subsidiary structures are less common along some fault segments (e.g., Happy Valley Fault and eastern end of Woolsey Fault). Some fault zone segments consist predominantly of closely spaced deformation bands (e.g., western North and Burro Flats faults), whereas deformation bands are notably lacking along other faults (e.g., CTL fault and Shear Zone). Fractured fault zones are also indicated by their alignment with linear topographic depressions and drainages (e.g., IEL and Happy Valley faults; Bravo deformation bands; Delta, Ridge, Tank, and Bowl structures) (Table 5-1; MWH, 2007e; Appendix 4-K).

Among the named faults, intersections with other mapped displacement structures average about 1 per 1,000 feet, and attain a maximum frequency of nearly 2 per 1,000 feet along the on-site portion of the Shear Zone (Table 5-1).

#### **5.2.2.2 Fractures**

Fractures are brittle mechanical breaks in rocks that can be categorized as dilational or shearing. Faults are shearing fractures with appreciable off-set, and are addressed in the previous subsection on mappable SSFL faults. This subsection pertains to dilational fractures, or joints. At SSFL, joints are subdivided between bedding-parallel fractures and bedding-perpendicular (or

interbed) fractures, with the term “joint” most commonly referring to the latter. Joints are generally high angle fractures associated with structural deformation and displacement. Relatively minor shearing may occur along some of the fracture types discussed in this subsection, such as bedding-plane slip and fracture sets associated with mapped faults.

Fractures initiate when externally applied stresses equal or exceed the mechanical strength of unfractured rock. Forces capable of creating such stresses include lithostatic and fluid pressures, tectonism (i.e., folding and faulting), thermal effects, volcanism, igneous intrusion, and impacts (National Research Council, 1996). As noted earlier in Section 5, the Chatsworth Formation has experienced a number of these mechanisms during its greater than 65-million-year geologic history. As a result, the Chatsworth Formation contains a pervasive fracture network that consists of a systematic arrangement of bedding-parallel fractures and steeply dipping joints (i.e., bedding-perpendicular fractures) with highly variable orientations, densities, and apertures.<sup>3</sup>

Four lines of evidence support the characterization of SSFL fractures: 1) lineaments observed from aerial photographs, 2) rock outcrops observed in the field, 3) rock cores collected from coreholes, and 4) borehole geophysical profiles. Aerial and field observations tend to preferentially identify near-vertical fractures such as joints, whereas downhole observations tend to identify near-horizontal features such as bedding-parallel fractures.

Variations in the mechanical properties of the rock as a function of composition, compaction, and cementation result in local variations in fracture character and density. For example, the mechanical response of individual rock layers is highly dependent on the cementing agent, which at SSFL includes calcite (calcium carbonate), dolomite (magnesium carbonate), and clay minerals. Field observations indicate that rocks cemented with calcite are typically strong and most likely to fracture, whereas rocks cemented with dolomite, clays, or some combination thereof are more likely to absorb stress through internal grain displacement and/or repacking

---

<sup>3</sup> Fracture apertures, and other aspects of both primary and secondary porosity, are evaluated more extensively in Section 6.

without generating fractures. Within the Chatsworth Formation at SSFL, beds of breccia/conglomerate often appear unfractured, probably because they are weakly cemented, predominantly with clay. Rocks cemented with silica, halite, or gypsum appear to be rare to absent at SSFL.

Figure 5-7 provides a conceptual representation of the characteristic fracturing of the Chatsworth Formation in relation to its lithology, bedding, and structure.

#### **5.2.2.2.1 Joints Observed from Field Mapping and Aerial Photographs**

The joint characteristics of layered sedimentary rocks vary as a function of the stress history, lithology, bedding thickness, and mechanical properties of the rock. At SSFL, these and other factors result in complex patterns of joint characteristics (Appendix 4-L). Joint characteristics include orientation, spacing, and aperture.

Two systematic joint sets are generally recognizable in sandstone members of the Chatsworth Formation, a dominant northwest striking set and a more secondary northeast striking set. The northwest set tends to dip steeply westward whereas the northeast set tends to dip steeply eastward. For each joint set, the relative abundance and mean trend of the joints are variable. The northwest joint set is dominant in the northwest area of SSFL, whereas the northeast joint set increases in relative abundance from west to east across the site.

Unimodal joint patterns (i.e., joints with a single trend) are characteristic of thick sandstone beds within the upper Chatsworth Formation where it is exposed along SSFL northern perimeter. Here the thick sandstone beds have a well-developed set of north-northwest trending joints. The sandstone here forms a dip slope (i.e., parallel to the bedding dip) with joints trending down-dip and only a few oriented east-northeast across this trend.

Orthogonal joint patterns are more common at SSFL. For example, these occur in thick bedded sandstone outcrops to the northeast of SSFL, where joints trend both east-northeast parallel to bedding strike and north-northwest in the down-dip direction. Similar orthogonal joint patterns occur along SSFL southern perimeter, with one joint set trending north-northeast parallel to

bedding and the second set trending west-northwest in the dip direction. Less uniform joint patterns also are common, including radiating, curvilinear, and random patterns.

Aerial photographs and field observations indicate that sandstone joint spacings are typically measurable in tens of feet and tend to be two to four times greater in Sandstone 2 than in Sandstone 1. Joint densities vary from less than 1 per 200 feet to greater than 1 per 25 feet. The lowest joint densities occur in the western and northern SSFL, whereas the highest joint densities are in the eastern SSFL. High joint densities also occur along the southern SSFL boundary, where joints range from 1 per 25 feet to 1 per 10 feet. The spacing of joints appears to be roughly proportional to the thickness of the bed or beds they intersect, i.e., thicker layers commonly have lower joint densities. Such a linear relationship between joint spacing and bed thickness is common in layered sedimentary rocks (e.g., Ladeira and Price, 1981).

Measured sandstone joint lengths range up to 1,000 feet, with nearly 90 percent ranging between 100 to 400 feet. Joint heights (i.e., normal to bedding) may be short (i.e., do not cross the full bed thickness) but more commonly cross the full thickness of one or several sandstone beds. Some joints terminate at the contact between sandstone and shale members.

The occurrence of alternating rock layers with distinctive joint densities reflects the variable mechanical properties of SSFL rocks as a function of composition, compaction, and cementation. Joints extending fully across thick shale units are relatively rare and widely spaced. Furthermore, joints within predominantly siltstone or shale units are most common within their sandstone interbeds.

#### **5.2.2.2.2 Bedding-Parallel Fractures**

Low-angle fractures tend to form parallel to bedding or stratigraphic layering as a result of the inherent weakness typical of bedding planes and vertical stress relief as a result of erosional unloading. Where bedding dips moderately or more, such as at SSFL, such fracturing may include some component of slip. However, fractures coincident with bedding planes are more difficult to distinguish and characterize than joints orthogonal to bedding. Bedding parallel fractures are difficult to distinguish from lamination, especially in fine-grained rock. Additionally, bedding-parallel fractures are more likely to “heal” under lithostatic loading in the

absence of an effective component of extension. The relative smoothness of bedding planes, especially in fine-grained rock, allows bedding-parallel fractures to fit more closely back together after fracturing. Because they are generally narrow relative to joints, bedding-parallel fractures also have a greater likelihood of filling from subsequent mineralization. Bedding-parallel fractures in relatively unjointed, fine-grained beds may extend from—and connect—joints perpendicular to bedding in over- and underlying sandstone beds.

#### **5.2.2.2.3 Fractures Observed in Rock Cores**

SSFL corehole samples and geophysical logs indicate that the vertical spacing between fractures is typically about 1 to 2 feet, although highly variable, with intervals often greater than 20 feet. This higher intensity than seen in aerial photographs or field mapping suggests that downhole observations include bedding-parallel fractures.

#### Fractures Observed in Borehole Geophysical Logs

Kennel et al. (SCM Element 4 in Cherry, McWhorter and Parker, 2009) evaluated fracture density and orientation based on visual inspection of continuous rock core and geophysical imaging logs obtained from 8 SSFL boreholes. They determined that fracture density is generally greater than one fracture per meter and commonly ranges up to 10 to 12 fractures per meter. Additionally, they found frequent occurrences of bedding-parallel fractures dipping approximately 25° to 30° and two other fracture sets generally orthogonal to the bedding plane.

Schlumberger Water Services (Appendix 4-M) conducted a statistical analysis of fracture orientation and intensity to refine the understanding of the subsurface fracture network beneath SSFL. Borehole geophysical imaging logs and rock core logs were combined into a single dataset for integration into PETREL geological modeling software to perform a site-wide spatial analysis of fracture sets.

After fracture attributes were reconciled among the various data types and appropriate filters developed, a statistical discrimination of fracture sets and computation of unique intensity and orientation attributes for each set was conducted. Stereonet and histogram analysis provided an overview of the general distribution of discrete fracture feature orientation. Fracture intensities

were then computed from discrete fracture data. A broad range of dip angles were identified, from nearly horizontal to vertical, suggesting several strongly overlapping fracture populations. Discernable relationships concerning fracture orientation and intensity within the context of the entire site were more difficult to determine as compared to those performed on a more limited sector basis. As a result, four model sectors were created: Northwest, Middle, Northeast, and South.

In the Northwest sector of SSFL the analysis found:

- Bedding plane features were noted with a mean dip angle of 31.8° and an azimuth of 319.1°. Fracture intensity was difficult to determine because only one data point is available.
- A fracture set was identified oriented approximately 180° from the bedding plane features with a mean dip angle of 47° and an azimuth of 141°. A mean fracture intensity of 1.3 fractures per meter was calculated for this fracture set.

In the Middle sector of SSFL the analysis found:

- Bedding plane features were noted with a mean dip angle of 26° and an azimuth of 321.2°. A mean fracture intensity of 1 fracture per meter was calculated for this fracture set.
- Two fracture sets were identified oriented approximately 180° to one another and nearly orthogonal to the bedding plane dip azimuth.
- One fracture set was identified with a mean dip angle of 57.9° and an azimuth of 94.2°. A mean fracture intensity of 0.4 fractures per meter was calculated for this fracture set.
- The other fracture set was observed to display a mean dip angle of 22.3° and an azimuth of 217.6°. A mean fracture intensity of 0.6 fractures per meter was calculated for this fracture set.

In the Northeast Sector of SSFL the analysis found:

- Bedding plane features were noted with a mean dip angle of 26.3° and an azimuth of 318.6°. A mean fracture intensity of 0.7 fractures per meter was calculated for this fracture set.
- Two fracture sets were identified oriented at azimuths separated by approximately 80° to one another, positioned nearly orthogonal to each other.
- One fracture set was identified oriented approximately 180° from the bedding plane features with a mean dip angle of 61.4° and an azimuth of 119.1°. A mean fracture intensity of 0.4 fractures per meter was calculated for this fracture set.

- The other fracture set was observed to display a mean dip angle of 59.9° and an azimuth of 199.8°. A mean fracture intensity of 0.3 fractures per meter was calculated for this fracture set.

In the South Sector of SSFL the analysis found:

- Bedding plane features were noted with a mean dip angle of 27.7° and an azimuth of 319.6°. Fracture intensity was difficult to determine because only one data point is available.
- Two fracture sets were identified oriented at azimuths separated by approximately 70° to one another, suggesting a conjugate set.
- One fracture set was identified oriented approximately 180° from the bedding plane features with a mean dip angle of 50° and an azimuth of 143.6°. A mean fracture intensity of 1.4 fractures per meter was calculated for this fracture set.
- The other fracture set was observed to display a mean dip angle of 41.8° and an azimuth of 199.8°. A mean fracture intensity of 1.3 fractures per meter was calculated for this fracture set.

## 6.0 HYDROGEOLOGY

This section presents an interpretation of the mountain-scale groundwater system encompassing SSFL. The basic conceptual elements of this system include:

- The framework and properties of the hydrogeologic units
- The occurrence and movement of groundwater within these units, and
- The groundwater inflows and outflows that drive this movement.

The section concludes with a summary of the equivalent porous media groundwater flow model developed for SSFL and insights to the hydrogeologic conceptual model that it provides.

This section refers to many groundwater wells within and surrounding SSFL. Their location and construction details are presented in figures, plates, and tables provided in Section 2.6.

### 6.1 HYDROGEOLOGIC FRAMEWORK

The hydrogeologic framework of the mountain groundwater system encompassing SSFL consists of its hydrogeologic boundaries, units, and structure.

#### 6.1.1 Hydrogeologic Boundaries

The mountain groundwater system encompassing SSFL lies within an area of the Simi Hills bounded by Simi Valley to the north, Box Canyon to the northeast, San Fernando Valley to the east, Bell and Las Virgenes canyons to the south, and Runkle Canyon to the west. As shown in Figure 6-1, the selected boundaries of this area are (a) where the Simi Hills meet the floor of Simi and San Fernando valleys, (b) where groundwater tends to discharge to seeps and phreatophytes along portions of Bell, Las Virgenes, and Box Canyons, and (c) over the watershed divide from Las Virgenes Canyon and down Runkle Canyon, along which seeps are absent. The potential for subsurface groundwater outflow exists along the entire boundary except due west of SSFL where the boundary is approximately parallel to inferred directions of groundwater flow. These boundaries encompass an area of 20 square miles, of which SSFL occupies approximately 22 percent. These boundaries are sufficiently distant from SSFL so as

to encompass conditions and processes potentially relevant to the hydrogeologic interpretation of SSFL. Additionally, these boundaries coincide with the area selected for groundwater modeling (Appendix 6-A).

Conceptually, the base of the active groundwater flow system occurs at the boundary between fresh and connate groundwater, where relatively fresh groundwater is defined by a total dissolved solids (TDS) concentration of less than 2,500 milligrams per liter (mg/L). The deepest SSFL well (WS-5) reaches 400 feet below mean sea level (i.e., -400 feet msl) but is currently blocked at 950 feet msl and cannot be sampled. Depth-dependent samples collected under non-pumping conditions from another deep well (WS-12) indicate TDS concentrations of less than 700 mg/L to approximately -50 feet msl, and no downward trend (Williams and Knutson, 2009). Pore-water samples collected from corehole C-15 to a minimum elevation of 317 feet msl showed no increase in chloride or other major ion concentrations with increasing depth, indicating that (a) soluble marine salts have been flushed from the rock and (b) groundwater derives solely from precipitation recharge to at least 317 feet msl (SCM Element 12 in Cherry, McWhorter, and Parker, 2009). Exploratory oil and gas wells in the region indicate a variable depth to connate water, ranging between -300 and 900 feet msl (AquaResource/MWH, 2007). For the purposes of this study, the base of fresh groundwater is assumed to occur at approximately sea level.

The upper boundary of the groundwater flow system is the regional water table and localized perched water tables. At the mountain scale, the water table is essentially a recharge mound that mimics the topography. At the site scale, however, the monitoring of more than 350 vicinity wells and piezometers indicates that the water table varies from as little as a few feet below ground surface in some flat-lying areas to several hundred feet below ground surface beneath topographic highs and areas with residual drawdown from past pumping. The maximum recorded groundwater elevation is approximately 1,910 feet msl at well RD-42 in the south-central portion of SSFL (Figure 2-3).

Hydrogeologic boundaries internal to the mountain groundwater flow system encompassing SSFL include areas of groundwater discharge to seeps and phreatophytes, pumped wells, and

various potential boundary effects along faults and geologic contacts. These internal boundaries are evaluated in greater detail in Sections 6.1.3 and 6.3.1.

### **6.1.2 Hydrogeologic Units**

As described in Section 5, geologic members of the upper Chatsworth Formation are defined by lithologic texture. Furthermore, fracture properties tend to characteristically differ between fine- and coarse-grained members. As such, these members correlate conceptually with the hydrogeologic units of SSFL groundwater flow system. Figure 6-2 shows the spatial distribution of these units within the defined boundaries of the mountain groundwater flow system encompassing SSFL.

Detailed profiles of hydraulic head with depth provided by multilevel monitoring systems installed in 33 SSFL wells typically exhibit sharp inflections of roughly 10 to 100 feet at or near the depth of lithologic contacts. However, such inflections do not always coincide with the inferred boundaries of the conceptual hydrogeologic units (SCM Element 5 in Cherry, McWhorter and Parker, 2009). Similarly, high-resolution temperature profiling reveals the frequency of hydraulically active fractures that in several but not all cases coincide with lithologic layers. Furthermore, the various data sets of measured porosity and hydraulic conductivity do not fully support the inferred distinction among the conceptual hydrogeologic units (in part because the fine-grained units tend to be under-sampled due to testing limitations). Despite these caveats, the conceptualization of hydrogeologic units based on the geologic stratigraphy presented in Section 5 provides a representative framework of the observed layered heterogeneities. A more robust definition of SSFL hydrogeologic units may evolve from the continued analysis of data.

Relatively thin deposits of surficial alluvium comprise an additional SSFL hydrogeologic unit. Areas where these deposits are at least 5 feet thick occur over approximately 315 acres (11 percent) of SSFL (Figure 5-8). Other formations exposed near and beyond SSFL boundaries comprise hydrogeologic units most relevant toward the margins of the mountain groundwater system surrounding SSFL. These include the Simi Conglomerate, Las Virgenes, Santa Susana,

and Llajas formations to the north and west, and the Calabasas/Lindero Formation to the southeast.

The upper Chatsworth Formation at SSFL is subdivided into two stratigraphic packages, Sandstones 1 and 2, each of which consists of fine- and coarse-grained members. These packages are separated and bounded above and below by Shales 1, 2, and 3. The coarse-grained (i.e., sandstone) members store and transmit locally beneficial quantities of groundwater, and thus may be considered as aquifer hydrogeologic units. Alternatively, the fine-grained members (i.e., mudstone, siltstone, and shale) tend to impede groundwater flow, and thus may be considered aquitards. Each type of unit contains interbeds of the other type.

The following table summarizes the sequence of alternating aquifer and aquitard units that comprise the mountain groundwater flow system encompassing SSFL:

Hydrogeologic Unit		Unit Type			
		Aquifer	Aquitard		
Alluvium		X			
Calabasas Formation/Detrital Sediments of Lindero Canyon (primarily sandstone/conglomerate)		X			
Llajas Formation	(primarily siltstone/shale)		X		
Santa Susana Formation			X		
Las Virgenes Formation			X		
Simi Formation (primarily sandstone/conglomerate)		X			
upper Chatsworth Formation	Shale 3			X	
	Sand-stone package 2	Upper Burro Flats member		X	
		ELV member			X
		Lower Burro Flats member		X	
		SPA member			X
		Silvernale member		X	
	Shale 2			X	
	Sand-stone package 1	Upper Sage member		X	
		Upper and Lower Bravo beds			X
		Middle Sage member		X	
		Upper and Lower Line beds			X
		Lower Sage member		X	
		Woolsey member			X
		Canyon member		X	
Happy Valley member			X		
Bowl member		X			
Upper and Lower Bowl beds			X		
lower Chatsworth Formation	Interbedded sandstone units		X		
	Shale 1 and other interbedded shale units			X	

### 6.1.2.1 Aquifer Units

Historical and ongoing groundwater production from SSFL wells demonstrates that portions of the Chatsworth Formation comprise locally productive aquifer units, although of significantly limited production and storage capacities. These units generally consist of the fractured sandstone members of the upper Chatsworth Formation, many of which are up to several

hundred feet thick (cf. Section 5.2.1). From oldest to youngest, these include the Bowl, Canyon, and Sage members that comprise most of Sandstone 1, and the Silvernale and upper and lower Burro Flats members that comprise most of Sandstone 2. Additional units of interbedded sandstone occur in the lower Chatsworth Formation.

Properties relevant to the aquifer characteristics of the sandstone members include lithologic heterogeneity (e.g., sandstone texture and sorting; inclusion of fine-grained interbeds); thickness and lateral continuity of bedding; type and degree of cementation; structure (e.g., folding and faulting); matrix porosity; and the effective porosity and interconnection of fractures. Section 5 discusses the lithology and fracture characteristics of the Chatsworth Formation. Section 6.1.3 discusses the structural aspects of these units; Section 6.2 addresses their matrix and fracture porosity and permeability and fracture interconnectivity.

Alluvial deposits comprise an additional aquifer unit given their role in (a) capturing and conveying recharge, (b) containing perched and shallow water tables, and (c) interfacing groundwater-surface water interactions.

The Simi Conglomerate and Detrital Sediments of Lindero Canyon (Calabasas Formation) are coarse-grained units mostly adjacent to SSFL that likely transmit groundwater from the Chatsworth Formation into areas surrounding SSFL.

#### **6.1.2.2 Aquitard Units**

Separating the major sandstone units of the Chatsworth Formation are a series of relatively thin shale and siltstone members that typically behave as aquitards (as further evaluated in Section 6.3.1). Shale 1 occurs below the Bowl member near the top of the lower Chatsworth Formation, Shale 2 separates the Sandstone 1 and Sandstone 2 stratigraphic packages, and Shale 3 occurs near the eroded top of the upper Chatsworth Formation. From oldest to youngest, the aquitard units within the sandstone packages are the upper and lower Bowl beds; Happy Valley and Woolsey members; upper and lower Line beds; upper and lower Bravo beds of Sandstone 1; and SPA and ELV members of Sandstone 2.

Properties relevant to the aquitard characteristics of the siltstone and shale members of the Chatsworth Formation include their lithologic heterogeneity; thickness and lateral continuity; type and degree of cementation; structure (e.g., folding and faulting); matrix porosity; and the effective porosity and interconnection of fractures. Section 5 discusses the geologic aspects of these aquitard characteristics and subsequent subsections of Section 6 address various hydrogeologic aspects.

Other potential aquitard units include the predominantly fine-grained Las Virgenes, Santa Susana, and Llajas formations, which may retard groundwater flow north of SSFL toward Simi Valley.

Fine-grained and unconsolidated basin deposits may be associated with alluviated and other flat-lying areas, and may contribute to the occurrence of shallow perched groundwater.

### **6.1.3 Hydrogeologic Structures**

The arrangement and geometry of the hydrogeologic units are controlled by the geologic contacts, folding, and faulting described in Section 5. As shown in Figure 6-2 and the geologic cross sections presented in Plates 5-2 and 5-3, these structures result in a complex three-dimensional distribution of the hydrogeologic units, permeability boundaries, and anisotropic permeability.

Contacts between aquifer and aquitard units, as well as layering within these units, result in anisotropic permeability structures that influence directions and rates of groundwater flow when unaligned with the hydraulic gradient. These influences are accentuated by the typical 25° to 35° northwest dip of the Chatsworth Formation stratigraphy. A following section on groundwater occurrence presents examples of groundwater-head differentials across aquifer-aquitard boundaries at SSFL (Section 6.3.1.1).

Faults influence hydrogeologic structure in several potential ways: the off-set or truncation of permeable zones and fractures; the juxtaposition of relatively low and high permeability units; the juxtaposition of different fold orientations; the occurrence of low-permeability boundaries from the formation of gouge, breccias, and cataclasite along fault planes (as described in Section

5.2.2.1); and potential but likely discontinuous zones of enhanced permeability from fracturing along the fault core and within adjacent damage zones (also described in Section 5.2.2.1). Though lacking appreciable off-set, cataclastic deformation bands also may form low-permeability boundaries, similar to instances reported in the literature (e.g., Edwards et al., 1993; Antonelli and Aydin, 1994; Ogilvie et al., 2001, Sternlof et al., 2006).

Figure 6-3 is a map showing the distribution of faults, deformation bands, and shale beds with the potential to influence SSFL groundwater flow. Major faults subdivide SSFL into roughly ten large blocks. These are further subdivided by shale beds. The following section on groundwater occurrence, subsection 6.3.1.1, presents examples of groundwater-head differentials across faults at SSFL.

In addition to the shearing fractures associated with faulting, the Chatsworth Formation contains ubiquitous dilational fractures. As described in Section 5, these form systematic networks of bedding-parallel and bedding-perpendicular fractures (with the latter typically referred to as joints). Section 6.2.1.2 describes fracture apertures and porosity and Section 6.5 summarizes the various lines of evidence indicating that SSFL sandstone units contain an interconnected fracture network.

## **6.2 HYDROGEOLOGIC PROPERTIES**

The physics of groundwater occurrence, storage, and movement are controlled by hydrogeologic properties that include porosity, hydraulic conductivity, and storage coefficients.

### **6.2.1 Porosity**

The porosity of the Chatsworth Formation occurs within its rock matrix (i.e., primary porosity) and as a result of fracturing and weathering (i.e., secondary porosity). As such, its saturated zone consists of a dual-porosity groundwater system. The effective porosity of the rock matrix provided by interconnected pores is relatively large (~14 percent), whereas the bulk fracture porosity is smaller by several orders of magnitude (~0.01 percent). Each type of porosity has particular significance with regard to groundwater storage, movement, hydrochemistry, and solute fate and transport, as discussed further in the remainder of this report.

### 6.2.1.1 Matrix Porosity

The matrix porosity of geologic materials at SSFL has been measured by the following direct and indirect methods: gravimetric, thin section, backscatter electron microscope, specific gravity, mercury intrusion, and down-hole geophysical logging (SCM Element 2 in Cherry, McWhorter and Parker, 2009). The gravimetric method provides direct measurements representative of effective porosity. Figure 6-4 summarizes more than 200 gravimetric measurements of rock core and unconsolidated sediment samples from SSFL. The majority of samples are rock cores of unweathered Chatsworth Formation sandstone. These range in porosity between 4 and 20 percent, and have an average porosity of about 14 percent.

Gravimetric measurements of the matrix porosity of Chatsworth Formation unweathered hard sandstone, banded sandstone, and breccia are limited to less than 10 rock cores each. Among these, hard sandstone samples have the lowest average porosity (3 percent) whereas banded sandstone and breccia have averages and ranges relatively similar to those reported for the sandstone. Thirteen gravimetric measurements of unweathered Chatsworth Formation siltstone and shale have an average matrix porosity of about 7 percent and range from 2 to 14 percent; the relatively low number of these samples reflects recovery and testing limitations associated with these rocks. Gravimetric measurements of matrix porosity for shallow and weathered samples of Chatsworth Formation range from 8 to 42 percent, indicating significant porosity enhancements compared to unweathered rock. Porosity measurements of SSFL unconsolidated deposits (e.g., alluvium and colluvium) average 38 percent and range up to 47 percent (Figure 6-4).

Figure 6-4 also shows average matrix porosity estimates derived from the thin sections of 28 Chatsworth Formation rock cores of sandstone, hard sandstone, banded sandstone, and siltstone. The variation of porosity among material types estimated by thin section is similar to that of the gravimetric measurements; however, the actual values are generally 5 to 7 percent lower. This is attributed to limitations of the thin section method (SCM Element 2 in Cherry, McWhorter and Parker, 2009).

Estimates of total porosity derived from analysis using a backscatter electron microscope are similar to gravimetric measurements of effective porosity, indicating that essentially the entire pore space of Chatsworth Formation sandstone is interconnected. Estimates of matrix porosity

by the specific gravity method are consistently lower than gravimetric measurements for the same samples. Estimates by the mercury intrusion method also are generally lower than the gravimetric measurements. Borehole geophysical methods conducted on six holes provide matrix porosity estimates averaging about 14 percent and ranging between 4 and 20 percent. Over a depth range of about 1,000 feet, none of the matrix porosity data demonstrate a significant trend with depth (SCM Element 2 in Cherry, McWhorter and Parker, 2009).

#### **6.2.1.2 Fracture Porosity, Hydraulic Aperture, and Interconnectivity**

Geologic mapping, rock cores, geophysical logs, and borehole imaging reveal the ubiquity of fracturing throughout the Chatsworth Formation at SSFL (Section 5.2.2.2). Several additional methods have been employed at SSFL for the purpose of evaluating the nature, occurrence, spacing, aperture, interconnectivity, and bulk porosity of fractures through which groundwater flow actually occurs (i.e., hydraulically active fractures). The bulk fracture porosity of the Chatsworth Formation is small (~0.01 percent; Montgomery Watson, 2000a) and contributes little to total porosity (~14 percent). Nevertheless, interconnected fractures result in a bulk hydraulic conductivity that is generally one to several orders of magnitude greater than the hydraulic conductivity of the sandstone matrix alone, as discussed in Section 6.2.2.

Hydraulic apertures are highly dependent on small local apertures that present constrictions to groundwater flow. Hydraulic aperture estimates for the Chatsworth Formation at SSFL have been derived from straddle packer tests, transmissivity profiling during FLUTE<sup>®</sup> liner installations, and other aquifer testing. The results of straddle-packer testing on two wells indicated hydraulic apertures with arithmetic means of approximately 90 to 125 microns (Sterling, 2000). FLUTE<sup>®</sup>-liner transmissivity profiling conducted in five SSFL boreholes indicates fracture hydraulic apertures ranging from approximately 15 to 800 microns, with an overall mean hydraulic aperture of about 90 microns (Figure 6-5; SCM Element 8 in Cherry, McWhorter and Parker, 2009). These estimates are corroborated by calculations based on other hydraulic tests and site-wide mean fracture spacing from core data and formation micro imager (FMI) and televiewer logs (SCM Element 8 in Cherry, McWhorter and Parker, 2009).

Several lines of evidence indicate a high degree of fracture interconnectivity within the sandstone and shale interbeds that comprise the Chatsworth Formation at SSFL (SCM Element 5 in Cherry, McWhorter and Parker, 2009).

- Geologic and geophysical logs of hundreds of SSFL boreholes indicate the presence of ubiquitous, closely spaced fractures (SCM Element 4 in Cherry, McWhorter and Parker, 2009). The observed high degree of fracture frequency strongly suggests a high degree of hydraulic connectivity.
- Water-level responses observed in multiple monitoring wells during historical groundwater production and several long-term SSFL pumping tests demonstrate highly correlated drawdown and recovery over large-scale volumes of the Chatsworth Formation. For example, production from water-supply wells completed in the Sage member influences groundwater levels more than 5,000 feet from the pumping wells (Halley & Aldrich, 2000). Such responses would not occur if the fracture network were poorly connected.
- Vertical interconnectivity was demonstrated in 10 northeastern SSFL wells equipped with FLUTE multilevel systems by pumping each port and observing the responses in ports above and below (MWH, 2004a).
- Detailed vertical profiles of hydraulic head from 33 SSFL wells equipped with multilevel monitoring systems reveal long intervals of sandstone with minimal changes in head separated by sharp changes in head associated with aquitards (SCM Element 5 in Cherry, McWhorter and Parker, 2009). Furthermore, these profiles maintain stable shapes over time (an example is provided in Section 6.3.1). These long intervals with minimal vertical hydraulic gradient indicate a well interconnected fracture network, whereas poorly interconnected fractures would exhibit more erratic head profiles.
- High-resolution temperature profiling conducted in five SSFL boreholes under ambient head conditions indicates numerous hydraulically active discrete fractures to depths in excess of 500 feet (SCM Element 5 in Cherry, McWhorter and Parker, 2009). The frequency of inferred active fractures is typically 1.5 to 3 per foot, ranging up to 4.5 to 6 fractures per foot over short intervals. Fractures with the highest apparent flow capacity occur more sporadically, about 0.5 per foot on average, ranging up to 1.5 per foot over short intervals. No consistent or significant vertical trend in fracture frequency was apparent within 500 feet depth. Variations in inferred fracture frequency tend to coincide with lithologic layers.
- Boreholes drilled at or near 18 SSFL locations where DNPL was released decades ago produce VOC detections in closely spaced rock cores (i.e., every 1 to 2 feet) throughout their upper 500 to 1,000 feet of depth, indicating a high degree of vertical interconnectivity within the fracture network (SCM Element 5 and 14 in Cherry, McWhorter and Parker, 2009). Core analyses also reveal the significant vertical migration of released tritium (to more than 220 feet deep) and perchlorate (to 165 feet),

which likely entered the Chatsworth Formation in dissolved phase, without the density-enhanced transport of DNPL.

- Detectable atmospheric tritium occurs in nearly all shallow monitoring wells, many of intermediate depth, and a few deep ones. This distribution requires an interconnected fracture network (SCM Element 9 in Cherry, McWhorter and Parker, 2009).
- Exceptionally little variation in ionic hydrochemistry is observed to depths of 1,500 feet within the Chatsworth Formation. The absence of a relic marine influence at such depths indicates a high degree of recharge flushing through an interconnected fracture network (SCM Element 12 in Cherry, McWhorter and Parker, 2009).

### 6.2.1.3 Dual Porosity

The dual (i.e., matrix and fracture) porosity of the Chatsworth Formation sandstone creates a distinct subsurface environment with regard to groundwater flow, solute transport, and various hydrogeochemical processes. Groundwater storage occurs primarily within the sandstone matrix porosity, which comprises most of the total porosity (~14 percent). Groundwater flow occurs predominantly through fractures, despite their small contribution to total porosity (~0.01 percent). This dual porosity provides for a potential disequilibrium between fracture and matrix pore-water chemistries. Stable carbon isotope ratios of dissolved inorganic carbon indicate the occurrence of both open- and closed-system calcite dissolution, consistent with dual-porosity conditions (SCM Element 12 in Cherry, McWhorter and Parker, 2009). Whereas oxygen and carbon dioxide diffuse rapidly in shallow groundwater through the fracture porosity, the interiors of sandstone matrix blocks occur under spatially variable anaerobic redox conditions. These aspects of dual porosity are critical to the diffusion-driven mass transfer of contaminants (SCM Element 19 in Cherry, McWhorter and Parker, 2009), as discussed in Section 8.

### 6.2.2 Hydraulic Conductivity

Hydraulic conductivity is the proportionality constant relating the rate of laminar groundwater flow to the hydraulic gradient. Among saturated geologic materials, values of hydraulic conductivity range over many orders of magnitude (e.g.,  $1 \times 10^{-11}$  to  $1 \times 10^2$  centimeters per second [cm/s]). Furthermore, effective values of hydraulic conductivity are generally dependent on the scale and direction of groundwater flow.

Figure 6-6 shows the distribution of matrix and bulk hydraulic conductivity measurements across SSFL. Matrix hydraulic conductivity refers to values representative of unfractured rock (e.g., core samples), for which permeability relies on the connected open pore space between cemented grains. Bulk hydraulic conductivity represents the added influence of fractures, lithologic heterogeneities, and other permeability structures within the volume of rock considered.

### 6.2.2.1 Matrix Hydraulic Conductivity

Matrix hydraulic conductivity typically is estimated from intrinsic permeability measurements performed in the laboratory on unfractured core samples. Using this approach, several studies have evaluated the matrix hydraulic conductivity of SSFL core samples. A total of 216 rock-core samples collected from 51 SSFL coreholes have been tested (Figure 6-6; SCM Element 2 in Cherry, McWhorter and Parker, 2009). Approximately 85 percent of these samples are classified generically as sandstone, whereas 5 percent or less was assigned to each of the following bedrock types: hard sandstone, banded sandstone, interbedded (i.e., sandstone and shale), and breccia. Among all samples, the estimated matrix hydraulic conductivities ranged from  $1 \times 10^{-11}$  to  $>1 \times 10^{-3}$  cm/s, and had a geometric mean of approximately  $3 \times 10^{-7}$  cm/s. The distribution of measured matrix hydraulic conductivity does not exhibit any significant trend at SSFL across 600 feet of depth.

Figure 6-7 provides a box-and-whisker plot of matrix hydraulic conductivity measured for cores representative of individual SSFL hydrogeologic units. The geometric mean of matrix hydraulic conductivities for sandstone members of the upper Chatsworth Formation ranges from  $1 \times 10^{-7}$  to  $1 \times 10^{-6}$  cm/s. Measured values for Shale 2 are generally less than  $1 \times 10^{-7}$  cm/s and are as low as  $1 \times 10^{-10}$  cm/s.

Geophysical logging of several SSFL boreholes using combinable magnetic resonance (CMR) provides continuous downhole estimates of intrinsic permeability representative of the matrix hydraulic conductivity (MWH, 2002c and d). Visual inspection of these logs indicates that point estimates range between  $1 \times 10^{-9}$  and  $1 \times 10^{-1}$  millidarcies, which correspond approximately to hydraulic conductivities of  $1 \times 10^{-7}$  cm/s or less.

### 6.2.2.2 Bulk Hydraulic Conductivity

Bulk hydraulic conductivity results from the net effect of geologic heterogeneity and structure. Higher values of bulk hydraulic conductivity relative to matrix hydraulic conductivity reflect the fracture-enhanced permeability of the Chatsworth Formation sandstone. The contribution of fractures to bulk hydraulic conductivity is a function of several factors, including fracture interconnectedness, density, and hydraulic aperture. Because of the typically directional influences of bedding, weathering, and fracturing, hydraulic conductivity tends to be strongly anisotropic. Methods used to estimate bulk hydraulic conductivity have included discrete-interval testing (e.g., packer and well-port tests), single-well slug and pumping tests, and multiple-well pumping tests. Figure 6-6 shows the locations of these tests.

As indicated by the box-and-whisker plot provided in Figure 6-8a, the total range in bulk hydraulic conductivity estimated by these methods ranges from less than  $1 \times 10^{-7}$  to greater than  $1 \times 10^{-2}$  cm/s. The geometric means of bulk hydraulic conductivity estimated by these methods range from  $8 \times 10^{-6}$  to  $7 \times 10^{-4}$  cm/s, about one to three orders of magnitude greater than the geometric mean of estimated matrix hydraulic conductivity. No simple trend is apparent relative to measurement scale. Although considerable variability exists among the various methods, these estimates of bulk hydraulic conductivity group distinctly apart from those of matrix hydraulic conductivity (SCM Element 6 in Cherry, McWhorter and Parker, 2009). The site-wide bulk hydraulic conductivity estimated by recharge-mound analysis ( $\sim 1 \times 10^{-5}$  cm/s; McWhorter, as cited by Haley & Aldrich, 2000) is near the lower end of the geometric means estimated by other methods, reflecting the cumulative influence of site-wide lithologic heterogeneities and structural boundaries (e.g., low-permeability structures associated with faults).

Figure 6-8b provides a box-and-whisker plot of estimated bulk hydraulic conductivity grouped by hydrogeologic unit. Table 6-1 indicates the testing methods used for each unit. The ranges and geometric means of estimates for Chatsworth Formation members other than the Burro Flats member are generally similar (geometric mean  $\sim 5 \times 10^{-5}$  cm/s; 50 percent of estimates ranging between about  $6 \times 10^{-6}$  and  $5 \times 10^{-4}$  cm/s). As discussed in Section 6.3.3.1, estimates of bulk hydraulic conductivity derived from the long-term specific capacities of SSFL water supply

wells are consistent with the estimates for SSFL sandstone summarized in Table 6-1 and Figure 6-8.

Estimates of the bulk hydraulic conductivity of the Burro Flats member are lower, consistent with local observations of lower fracture density (Section 5.2.2.2; geometric mean  $\sim 4 \times 10^{-6}$  cm/s; 50 percent of estimates between  $1 \times 10^{-6}$  and  $2 \times 10^{-5}$  cm/s). Additional indications of lower bulk hydraulic conductivity in this unit include areas of relatively steep hydraulic gradient and fewer significant contaminant detections at depth (e.g., in corehole C-8; Wagner, 2009, written communication).

Because of limitations in sample quantity, recovery, and testing, fine-grained units are not as well represented by the bulk hydraulic conductivity data set. To the extent that permeability enhancement by fracturing is less pronounced in the fine-grained units, measured values of matrix hydraulic conductivity may provide a reasonable lower bound for the bulk hydraulic conductivity of the fine-grained units (i.e.,  $\leq 1 \times 10^{-7}$  cm/s).

Evidence of hydrogeologic heterogeneity in terms of SSFL bulk hydraulic conductivity includes the following:

- Measured and estimated values of bulk hydraulic conductivity range over seven orders of magnitude ( $\sim 1 \times 10^{-8}$  to  $2 \times 10^{-2}$  cm/s).
- The bulk hydraulic conductivity of intervals within and among closely spaced wells commonly ranges over several orders of magnitude.
- The maximum average annual yield of some water supply wells exceeds 100 gallons per minute (gpm) (Table 6-2), whereas the majority of wells have little appreciable yield.

Estimates of SSFL bulk hydraulic conductivity appear to peak at relatively local scales, i.e., smaller than the zone of influence of SSFL pumping tests. This suggests that SSFL bulk hydraulic conductivity is ultimately limited by the cumulative influence of lithologic heterogeneities and other permeability structures. Conversely, bulk hydraulic conductivity is not enhanced at larger scales by the cumulative influence of fracturing. Compared to “textbook” ranges of bulk hydraulic conductivity for indurated sandstones ( $\sim 1 \times 10^{-8}$  to  $1 \times 10^{-3}$  cm/s), and estimates reported in the literature for other sandstones ( $\sim 4 \times 10^{-7}$  to  $4 \times 10^{-1}$  cm/s), the range of

bulk hydraulic conductivity estimated for SSFL ( $\sim 1 \times 10^{-5}$  to  $7 \times 10^{-4}$  cm/s) may be described as low to moderate (SCM Element 6 in Cherry, McWhorter and Parker, 2009).

### **6.2.2.3 Horizontal to Vertical Anisotropy**

High ratios of horizontal to vertical anisotropy are evidenced by sharp inflections in vertical hydraulic head at or near the elevation of lithologic contacts in wells equipped with multi-level monitoring systems. This anisotropy results in strong upward and downward hydraulic gradients. Within relatively homogeneous units, much lower anisotropy ratios are indicated by long intervals with little hydraulic gradient (SCM Element 5 in Cherry, McWhorter and Parker, 2009).

The horizontal to vertical anisotropy of hydraulic conductivity within the Chatsworth Formation can be inferred from the following:

- The contrast between minimum values of hydraulic conductivity (e.g., representative of shale beds,  $\leq 1 \times 10^{-7}$  cm/s) and the geometric means for sandstone units (e.g.,  $\sim 5 \times 10^{-6}$  to  $1 \times 10^{-4}$  cm/s; Figure 6-8b).
- The several orders of magnitude range among hydraulic conductivities measured in nearby wells completed at varying depths (e.g., cluster wells) and multiport wells (SCM Element 6 in Cherry, McWhorter and Parker, 2009).

These data suggest that the ratio of horizontal to vertical hydraulic conductivity could range from 50:1 to nearly 1,000:1. However, groundwater flow in three dimensions may diminish the significance of localized low-permeability beds, such that effective anisotropy ratios could range to as low as 10:1.

### **6.2.2.4 Variation of Hydraulic Conductivity with Depth**

Fracture apertures may be assumed to narrow and close as a result of increased overburden pressures with depth. As such, fracture-enhanced bulk hydraulic conductivity is expected to diminish with depth. Figure 6-9 presents a relation between bulk hydraulic conductivity and depth estimated using the Barton-Bandis method and assumed input values representative of the Chatsworth Formation (SCM Element 6 in Cherry, McWhorter and Parker, 2009). According to this relation, bulk hydraulic conductivity decreases and approaches the matrix hydraulic conductivity at depths of about 2,000 feet or less. This relation is not yet confirmed by available

SSFL hydraulic conductivity data, which generally represent depths considerably shallower than 2,000 feet. However, the relation is considered reasonable in light of indirect evidence and studies elsewhere (SCM Element 6 in Cherry, McWhorter and Parker, 2009).

#### **6.2.2.5 Fault Zone Hydraulic Conductivity**

Faults in lithified bedrock may manifest hydrogeologically as (a) zones of enhanced permeability due to increased fracturing, (b) zones of diminished permeability due to the formation of low-permeability materials, or (c) some combination thereof as a function of fault-zone permeability structures. The permeability structures of fault zones in lithified bedrock consist of three generally recognized types (e.g., Forster et al., 1994; Caine et al., 1996): (1) the fault-plane core, (2) damage zones along either side of the fault core, and (3) the surrounding protolith of host rock undeformed by faulting. Controls on the nature, scale, continuity, and relative significance of these structures include the lithologic, cementation, and mechanical properties of the protolith; fluid-rock interactions; fault-zone geometry; the nature and magnitude of deformation and subsidiary structures; and various expressions of spatial and temporal variability (Caine et al., 1996).

The permeability of the fault core is typically diminished by the formation of clay-rich gouge, breccias, and cataclasite. However, fracturing from renewed deformation may result in an ensuing period of permeability enhancement. The network of subsidiary structures comprising the damage zone includes minor faults, fracture sets, cataclastic deformation bands, mineralized veins, cleavage, and folds (Caine et al., 1996). The net effect of these subsidiary structures may be to enhance or diminish the permeability of the damage zone. Also, the damage zone may be effectively absent where strain is highly localized along the fault core. As such, there exists a conceptual suite of potential fault-zone permeability structures, as illustrated schematically in Figure 6-10.

Based on groundwater-level off-sets, Haley & Aldrich (2000) estimated a hydraulic conductivity of  $1 \times 10^{-7}$  cm/sec for the low permeability boundary that occurs along SSFL “Shear Zone” fault. Analysis of the C-1 pumping test estimated a Shear Zone hydraulic conductivity of  $1 \times 10^{-8}$  cm/sec (MWH, 2004a).

Inspection of SSFL hydraulic conductivity estimates in relation to their proximity to SSFL faults suggests that exceptionally high values of hydraulic conductivity do not occur preferentially near faults. The variability of the data is consistent with the highly variable nature expected for such fault-related structures, given the site's complex structural history and geologic variability. Such structures are likely discontinuous given their small dimension of width relative to fault length, and the influence of other local geologic processes and heterogeneities. The faults are intersected often by other faults and shale beds, illustrating that geologic processes and heterogeneities influence hydrogeologic conditions at scales relevant to individual fault segments and their permeability structures. It is reasonable to infer that fault-related permeability structures at SSFL are more likely to be irregular and discontinuous than consistent and continuous (SCM Element 7 in Cherry, McWhorter and Parker, 2009).

### 6.2.3 Storage Coefficients

Initial multi-well pumping tests of the Chatsworth Formation sandstone indicated storage coefficients in the range of  $1 \times 10^{-4}$  to  $5 \times 10^{-3}$  (Montgomery Watson, 2000a). Analysis of a pumping test performed on corehole C-1 in northeastern SSFL indicated storage coefficients of  $1 \times 10^{-5}$  to  $1 \times 10^{-2}$  for the fractured system and about  $1 \times 10^{-6}$  for the bedrock matrix (MWH, 2004a). Analysis of a pumping test performed on well RD-54B in the FSDF Area indicated storage coefficients ranging more than an order of magnitude lower than  $1 \times 10^{-5}$  (MWH, 2006a). Analysis of slug tests performed on other northeastern SSFL wells indicated storage coefficients ranging from  $1 \times 10^{-6}$  to  $1 \times 10^{-1}$ , with the larger values representative of specific yield measured under relatively shallow, water-table conditions (MWH, 2004a).

Whereas the lower range of the above-reported storage coefficients typically represent confined to semi-confined conditions, the low values estimated for the Chatsworth Formation are largely attributable to the nature of the fractured sandstone's dual porosity. The relatively large saturated porosity of the sandstone matrix is essentially confined by the low hydraulic conductivity of the matrix itself. As such, the low porosity but high conductivity of the sandstone's fractures is largely responsible for the sandstone's response to hydraulic stress.

Thus, apparent confined responses to pumping reflect the rapid draining of fractures with low overall porosity, in addition to the release of water pressurized beneath aquitards.

### **6.3 GROUNDWATER OCCURRENCE AND MOVEMENT**

The mountain groundwater system is essentially a large groundwater mound maintained predominantly by precipitation recharge. The results of monitoring nearly 500 piezometers and wells in the immediate vicinity of SSFL during the past approximately 20 years indicate the occurrence of both shallow and deep groundwater zones.

Early water-level records for SSFL water-supply wells are provided by Killingsworth (1958) and GRC (2000). More recent records, including those for monitoring and remedial-extraction wells, are provided by MWH (2008) and Haley & Aldrich (2009a). Nearly 100 of the monitored deep wells are open or partially open boreholes that potentially cross and interconnect multiple hydrogeologic units and fracture zones with distinct groundwater heads. Thus, these wells provide hydraulically averaged, or blended, heads. Depth-specific data are available from approximately 200 piezometers (up to 87 ft deep), 100 shallow wells (up to 40 ft deep), 60 wells with relatively discrete open intervals (e.g., cluster wells), and 33 wells equipped at one time or another with multilevel systems. Figures 6-11, 6-12, 6-13, and 6-14 are well-location maps for the northwestern, north-central, northeastern, and south-central areas of SSFL, respectively.

For regulatory purposes, near-surface groundwater is defined to occur within the site's unconsolidated deposits (e.g., alluvium) and shallow weathered bedrock, whereas deep groundwater occurs in the unweathered bedrock. The near-surface groundwater may be perched or vertically continuous with deeper groundwater.

#### **6.3.1 Influencing Factors**

Factors influencing the horizontal and vertical distribution of groundwater zones at SSFL include geologic influences (e.g., fine-grained units and faults), groundwater pumping, and recharge. The nature of these influences is described below before describing the details of groundwater occurrence across SSFL.

### **6.3.1.1 Geologic Influences**

Geologic influences on the occurrence and movement of groundwater include low-permeability boundaries presented by fine-grained units and both low and enhanced permeability structures associated with faults. Multiple lines of evidence demonstrating the influence of the interconnected fracture network on groundwater occurrence and movement are summarized above in Section 6.2.1.2.

### **6.3.1.2 Fine-Grained Units**

Abrupt differences in groundwater head typically occur across SSFL fine-grained units. Figure 6-15 illustrates two large-scale examples: (a) more than 200 feet of water-level off-set across Shale 2 and (b) groundwater confinement by Shale 3, as indicated by springs and flowing wells. Another example is the Woolsey member aquitard where it occurs at depth west of the Shear Zone. In this case, groundwater zones above and below the aquitard exhibit water-level differences up to 150 feet; distinctly different responses to area pumping; and zones of high versus no contaminant detection (MWH, 2002a). Similar although somewhat less pronounced effects are observed in association with the other SSFL fine-grained units, including the Bowl Bed, Happy Valley member, Line Beds, Bravo Beds, and SPA and ELV members.

Pronounced water-level differentials also are observed at smaller scales, such as the detailed vertical profiles of hydraulic head provided by the multilevel monitoring systems installed in 33 SSFL wells. Figure 6-16 presents one such profile that shows an approximately 80-foot change in head occurring in two abrupt steps across the relatively fine-grained Happy Valley member encountered by monitoring well RD-31. Sharp inflections in hydraulic head also occur within SSFL sandstone units, which probably reflect differences in sandstone cementation, induration, and fracturing (SCM Element 5 in Cherry, McWhorter and Parker, 2009).

#### **6.3.1.2.1 Faults**

Groundwater occurrence and movement also is influenced significantly by some of the faults traversing SSFL. As illustrated in Figure 6-17, groundwater levels are off-set by as much as 250 feet across the Shear Zone. Despite this strong gradient, contaminant migration is significantly restricted from east to west across the Shear Zone (SCM Element 7 in Cherry, McWhorter and

Parker, 2009). Low-permeability boundaries presented by both faults and fine-grained units serve to compartmentalize groundwater within portions of SSFL.

Conversely, evidence exists of enhanced hydraulic communication along some faults. As analyzed in greater detail below in Section 6.3.4, portions of the North Fault Zone appear to hydraulically connect sandstone units otherwise separated by Shale 2. Pumping influences also appear to have been transmitted along portions of the IEL and Happy Valley faults (SCM Element 7 in Cherry, McWhorter and Parker, 2009).

### **6.3.1.3 Pumping Influences**

Figure 6-18 and Table 6-2 summarize the record of annual groundwater extractions at SSFL since 1949. Groundwater production has occurred from 12 of the 17 deep water-supply wells installed between 1948 and 1963, and 34 shallow and deep remedial wells and sumps installed since the 1980s. The pair of well-location maps in Figure 6-19 shows the distribution of extraction wells active before and after 1984. Construction information for these wells is provided in Table 6-3. Groundwater-level responses to pumping are documented and discussed in Section 6.3.3.1. Section 6.4.2 discusses groundwater extractions in the context of the study area groundwater budget.

The water-supply wells range from 500 to 2,300 feet deep and are generally open, uncased holes below the upper several hundred feet of casing. Total groundwater production from these wells peaked between 1957 and 1964 at 70 to 170 million gallons per year, equivalent to continuous rates of 70 to 330 gpm (Figure 6-18). By the late 1950s groundwater levels had been drawn down as much as 500 feet in the most heavily pumped, north-central portion of SSFL, creating a large depression in the groundwater surface extending laterally as much as 5,000 feet. By the early 1960s, production was discontinued from all but five of the water-supply wells due to insufficient yield. Water importation from the Calleguas Water District began in 1964, replacing most groundwater use. Little to no water production or use data is available for 1964-1983 (Montgomery Watson, 2000a).

Groundwater extraction for mostly remedial purposes began in 1984 using a combination of existing water-supply wells and newly constructed shallow and deep remedial wells (Table 6-2).

The shallow remedial wells are less than 40 feet deep and are screened over much of their length. The deep remedial wells range from 80 to 500 feet deep and are completed as open boreholes below relatively shallow depths (Table 6-3). The spatial distribution of pumping changed with the onset of remediation (Figure 6- 19), although the majority of production continued to be from five deep water-supply wells. Total pumping peaked between 1989 and 2000 at approximately 70 to 150 million gallons per year, equivalent to continuous rates of 140 to 290 gpm (Figure 6-18). Pumping has decreased since 2000 for several reasons, including: (1) accommodation of subsurface characterization activities begun in 2000, (2) post-closure permit modification in 2001 for some areas, and (3) damage to extraction well pipelines as a result of the Topanga Fire in late 2005 (MWH, 2008b; Haley & Aldrich, 2008; CH2M HILL, 2008). Equivalent rates of continuous annual pumping have ranged from 2 to 17 gpm since 2003.

A 2007 inventory of residential and agricultural properties within the study area surrounding SSFL identified 127 off-site wells, of which 73 are considered active, 30 are of unknown status, and the remainder abandoned or destroyed (Appendix 2-E).

#### **6.3.1.4 Recharge Influences**

Groundwater recharge is water that enters the subsurface and reaches the saturated zone. Sources of recharge include precipitation and applied water. This subsection addresses broad aspects of the spatial and temporal variability of recharge in relation to understanding groundwater occurrence. Section 6.5 provides detailed estimates of groundwater recharge in the context of the study area groundwater budget.

Factors contributing to the variability of recharge in the study area include the spatial and temporal variability of: precipitation, runoff, ponding, infiltration capacity, evapotranspiration, and water use and disposal. Analysis of stable oxygen isotopes indicate that precipitation is the primary source of groundwater recharge and that water imported from the Calleguas Water District has contributed negligibly to recharge. The isotope results also indicate that a portion of recharge derives from the infiltration of precipitation runoff collected and partially evaporated in ponds (SCM Element 12 in Cherry, McWhorter and Parker, 2009).

Figure 6-20 provides plots of annual precipitation at SSFL and Los Angeles International Airport and their cumulative departure from average. The longer Airport record indicates a long period of below average precipitation from 1950 to 1977. Both records indicate wet periods from 1978-1986 and from 1993 until recently, separated by the 1987-1992 drought.

Figure 6-21 presents water-level hydrographs for four wells located across SSFL that illustrate responses to the temporal variability of annual precipitation. Groundwater levels in these wells rise as much as 75 feet in response to wet years, indicating rapid saturation of the low fracture porosity. Conversely, water levels tend to exhibit sustained declines throughout periods of average to below average precipitation when recharge is minimal. Water-level variability in deep wells sealed against shallow zones tends to correlate poorly with annual precipitation, as illustrated by the cluster-well hydrographs discussed in Section 6.3.3.3.

## **6.3.2 Perched Zones**

In cases where less than fully saturated conditions exist between two saturated zones, the condition of the upper zone is referred to as perched. Areas of shallow perched groundwater are documented across SSFL. The potential for deep perched zones is inferred from the steep vertical gradients documented by cluster wells and wells equipped with multilevel systems.

### **6.3.2.1 Shallow Perched Zones**

Figure 6-22 shows locations of shallow perched groundwater identified by SSFL near-surface groundwater characterization study (MWH, 2003b), various remedial investigation reports of SSFL surficial media, and additional information summarized in Table 6-4. The dataset used to identify areas of shallow perched groundwater extends from 2001 to 2009. An effort was made to omit false indications of perching, such as when small amounts of recharge or condensation collect at the bottom of a well under otherwise unsaturated conditions.

Factors contributing to the occurrence of shallow perched groundwater include:

- The topographic concentration of surface-water drainage
- Proximity to discharge:
  - At the ground surface by facility operations and the disposal of treated groundwater

- In the subsurface from leach fields and leaking water lines and sumps
- Subsurface zones of low hydraulic conductivity
- Drawdown of the saturated zone below perching layers
- Periods of elevated recharge related to storms, wet periods, or other discharge events.

Indications of perched groundwater include (a) the observation or extrapolation of unsaturated conditions beneath perched zones and (b) significant differences in water-level elevation and variability among nearby monitoring wells and piezometers completed at different depths (i.e., where the groundwater surface elevation in shallower wells is substantially greater than in deeper wells). Other areas of shallow perched groundwater may occur in areas not monitored by existing SSFL wells and piezometers (Figure 6-22).

Shallow perched groundwater is apparent in 54 shallow wells and piezometers beneath nearly 50 acres of Area I, and in 49 wells beneath nearly 60 acres of Areas II, III, and IV. As summarized in Table 6-4, typical depths to shallow perched groundwater in these areas range from 10 to 50 feet bgs.

### **6.3.2.2 Deep Perched Zones**

Given the steep downward vertical gradients observed in several well clusters and wells equipped with multilevel systems (see Section 6.3.3.1), there is a potential for semi-saturated zones to occur at depth, especially under heavy-pumping conditions and when downward gradients exceed 1 feet/foot (ft/ft). Relatively deep perched zones associated with such conditions are currently not evident.

### **6.3.3 Saturated Zone**

Saturated groundwater conditions occur primarily within the Chatsworth Formation beneath SSFL. The upper saturated zone is generally unconfined, whereas semi-confined to confined conditions may occur below aquitards and with increasing depth as a result of the cumulative influence of low-permeability zones. As illustrated in Figure 6-15, flowing artesian conditions occur where the Chatsworth Formation becomes confined beneath Shale 3 just beyond SSFL northwestern boundary. Across much of SSFL, however, the groundwater hydraulic gradient is downward regardless of the degree of confinement.

The following subsections present groundwater level hydrographs and correlograms, groundwater surface contour maps, and groundwater quality data in describing the spatial and temporal occurrence, pattern, hydraulic gradients, and variability of groundwater in the saturated zone.

### **6.3.3.1 Groundwater Level Hydrographs**

Groundwater level hydrographs provide important information regarding the groundwater system's response to hydraulic stress (e.g., pumping, recharge), both in general and in terms of historical conditions. This section presents hydrographs for 12 SSFL water-supply wells with long-term records, and 21 well clusters. Four hydrographs illustrating the response of shallow groundwater to precipitation recharge were presented above in Figure 6-21, and additional hydrographs are presented in Section 6.3.4.

#### **6.3.3.1.1 Water-Supply Well Long-Term Hydrographs**

Figures 6-23a through 6-23c present long-term groundwater level hydrographs for 12 SSFL water-supply wells in relation to annual pumping and precipitation. The plotted water level data are a compilation of static water-level measurements tabulated by Killingsworth (1958), Rocketdyne (1963), GRC (2000), and Haley & Aldrich (2007-2009a). These plots exclude water-level measurements taken during well operation. However, the duration of non-pumping prior to each static measurement is uncertain. Records are unavailable from the mid-1950s to the mid-1980s. Approximate water-level trends have been inferred for periods of missing data based on the available pumping record, proximity to other pumping wells, and water levels recorded under similar conditions.

The long-term water-level records reflect two main periods of production: (1) pumping for water supply during 1950-1965 and (2) pumping for remediation and water supply during 1984-2002 (Table 6-2). Groundwater level responses during these alternating pumping and non-pumping periods are revealing with regard to the system's response to hydraulic stress. During the earlier period of heavy pumping, the primary producing wells were WS-5, -6, -12, and -13, with minor to moderate production from WS-3, WS-4, WS-4A, and -9A. Water levels were not recorded at the time peak declines were likely to have occurred during this earlier production period. During

the latter period the primary producers were WS-5, -6, and -9A, with minor to moderate production from WS-9, WS-13 and RD-1, -2, and -4.

The water supply wells may be grouped broadly as follows, consistent with their hydrogeologic setting:

- **WS-3, -4, -4A, -5, -6, -9, and -14 (located in Figure 6-12):** These wells are completed within the Sage sandstone member aquifer unit of the upper Chatsworth Formation's Sandstone 1 hydrostratigraphic package. Production from wells WS-5 and WS-6 account for more than 50 percent of all recorded SSFL extraction, whereas the other wells have been pumped moderate to minimal amounts. Historically minimum depths to water range from 100 to 300 feet. Groundwater levels exhibited up to 100 feet of apparent residual drawdown nearly 20 years after the 1950-1965 pumping period ended. Similar residual drawdown is currently evident following the 1984-2002 pumping period.
- **WS-12 and -13 (located in Figure 6-12):** These wells (along with WS-3, -4, and -4A) align with the North Fault Zone, which cuts through Shale 2 between Sandstones 1 and 2. Minimum depths to water during non-pumping periods range from approximately 100 to 150 feet. WS-12 and WS-13 are completed in relatively productive zones within the North Fault Zone and the lower Burro Flats member (Sandstone 2) north of the North Fault. Their past production accounts for nearly 20 percent of all groundwater pumped from SSFL.
- **WS-7, -8, -9B, and -11 (located in Figures 6-11 and 6-12):** Production from each of these wells has been relatively little or none. Minimum depths to water among these wells range from 30 to 100 feet. In the case of two of these wells (WS-7 and -9B), the relatively shallow depths to water coincide with their completion in relatively low-permeability Sandstone 2. WS-8 is near the western fringe of the area influenced by pumping from the Sage member. WS-11 lies within the surface exposure of Shale 2 and exhibits a low-permeability response to pumping (i.e., significant drawdown from relatively low pumping). In addition to being relatively shallow, water levels in these wells are generally stable in the absence of nearby pumping. This suggests that their water levels are mounded as a result of low permeability; recover quickly from recharge into low-porosity fractures; are limited from rising higher by their relatively shallow depths to groundwater; and are little affected by pumping from relatively distant, productive wells.
- **WS-9A (located in Figure 6-14):** Located within the Sage member between the Coca and Burro Flats faults, this well has accounted for the majority of SSFL groundwater production since 2001, and approximately 15 percent of total SSFL groundwater production to date. It nevertheless exhibits relatively stable and shallow water levels, which appears to reflect the availability of channel recharge, as discussed in more detail below.

Further observations and interpretations based on the water-supply well long-term hydrographs presented in Figures 6-23a through 6-23c includes the following:

- Significant drawdown has occurred in four of the water-supply wells with the capacity to produce from 65 to more than 100 gpm on an average annual basis:
  - **WS-5** is a 2,300-foot deep well in which the net decline in static water levels between the early 1950s and the mid-1990s was nearly 500 feet (Figure 6-23a). The wellhead is mapped immediately east of the Shear Zone, however the well bore is interpreted to cross the fault at depth, such that its hydraulic influence is limited to the Sage member and other hydrogeologic units west of the Shear Zone (MWH, 2004a). Drawdown is probably enhanced by the low-permeability boundary associated with the Shear Zone. Additionally, water levels are probably influenced by distant wells that also produce from the Sage member. The long-term specific capacity of WS-5 during 1986-1995 was 0.26 gallons per minute per foot of drawdown (gpm/ft), given an average pumping rate of approximately 86 gpm and net drawdown of 328 feet. This specific capacity and an assumed saturated thickness of 2,000 feet and storativity of  $1 \times 10^{-5}$  provides an estimated bulk hydraulic conductivity of  $2 \times 10^{-5}$  cm/s (SCM Element 6 in Cherry, McWhorter and Parker, 2009). This may be an under estimate as a result of enhanced drawdown caused by the Shear Zone low-permeability boundary. Nevertheless, it is consistent with the central range of other bulk hydraulic conductivity estimates for the Sage member (Figure 6-8).
  - **WS-6** is a 1,440-foot deep well located approximately 3,100 feet west of WS-5. The net decline in WS-6 static groundwater levels was approximately 250 feet between the mid-1950s and the mid-1990s (Figure 6-23a). The Sage member aquifer unit from which both WS-5 and WS-6 draw is bound by the Shear Zone to the southeast, Shale 2 to the northwest, and to some degree by the North and Coca faults to the north and south. Production from these two wells accounts for greater than 50 percent of the total volume of SSFL groundwater pumped since 1950. Periods of heavy pumping influenced water levels across this entire aquifer unit, as demonstrated by the response of other, fairly distant wells described below. As a result, the groundwater surface typically forms a flat-bottomed trough across this area, whether from active pumping or residual drawdown. The long term specific capacity of WS-6 during 1989-1995 was 0.68 gpm/ft, given an average pumping rate of approximately 100 gpm and net drawdown of nearly 150 feet. Assuming a saturated thickness of 1,000 feet and storativity of  $5 \times 10^{-5}$ , this specific capacity suggests a bulk hydraulic conductivity of approximately  $1 \times 10^{-4}$  cm/s (SCM Element 6 in Cherry, McWhorter and Parker, 2009), which is consistent with the central range of other bulk hydrologic conductivity estimates for the Sage member (Figure 6-8).
  - **WS-12** is a nearly 1,800-foot deep well that lies in the North Fault Zone within Sandstone 2, but is deep enough to penetrate into the top 200 feet or more of the Sage member in Sandstone 1 below Shale 2. Production from this well occurred during 1956-1963 at an average annual rate of about 100 gpm, accounting for about one third

- of all groundwater pumped during that time. WS-12 was not pumped during 1984-2002 when other SSFL water supply and remedial wells operated. Nevertheless, water levels in WS-12 responded to the 1984-2002 pumping period, demonstrating the well's continuity with the Sage member at depth (Figure 6-23c). Most of this drawdown appears related to production from WS-6, 2,000 feet to the south.
- **WS-13** is located within the Burro Flats member just north of the North Fault and 1,300 ft west of WS-12. This 940-foot deep well pumped at average rates of about 65 gpm during 1959-1962 and at nearly 30 gpm during 1984-86. Maximum drawdown was not monitored during either period. Similar to WS-12, water levels in WS-13 clearly responded to production by other wells (Figure 6-23c), e.g., WS-6, located 2,300 feet to the southeast. However, unlike WS-12, WS-13 does not extend into the Sage member by penetrating Shale 2. This suggests that the North Fault Zone has good hydraulic continuity with the Sage member by cutting through Shale 2 at depth and in plan view between WS-4A and WS-12, and extends this hydraulic communication into the Burro Flats member north of the North Fault.
  - **WS-9A** is a 540-foot deep well completed in the Sage member between the Coca and Burro Flats faults in southwestern SSFL. Its annual average rate of production has exceeded 100 gpm and net drawdown has exceeded 300 feet at times during pumping periods. Maximum drawdown appears to occur during dry periods, recovering quickly afterward (Figure 6-23b). Haley & Aldrich (2000) attributed this to variable recharge via fractures crossing a nearby stream channel. The upstream discharge of treated groundwater has contributed to the flow of this channel since approximately 1987. During times when pumping from WS-9A coincided with streamflow, Haley & Aldrich observed the channel to go dry in the vicinity of the well. They interpreted that a large fracture observed during the logging of WS-9A intersects the channel bed at the general location where the stream goes dry. WS-9A does not exhibit water-level interactions with the other water-supply wells.
  - Water-level changes in generally unpumped wells as a result of other, relatively distant pumping wells include the following:
    - **WS-4A** is a 500-foot deep well located immediately south of the North Fault along the northern boundary of the Sage member aquifer unit. It is approximately 1,900 and 2,900 feet to the southeast and southwest of WS-5 and WS-6, respectively. WS-4A experienced nearly 120 feet of maximum water-level decline during the 1984-2000 period when the other two wells were pumping (Figure 6-23a).
    - **WS-8** and **WS-9** are respectively 700 and 1,800 feet deep and about 3,300 and 2,100 feet west of WS-6 within the Sage member aquifer unit. These wells experienced approximately 120 feet of drawdown when WS-6 operated during the late 1980s and 1990s (Figure 6-23b).
    - **WS-14** (1,270 feet deep) is within the Sage member immediately southwest of the intersection of the Shear Zone and North Fault. WS-5 is 2,300 feet to the southwest and WS-6 is 4,800 feet to the west-southwest. WS-14 experienced a maximum

- 70 feet of drawdown when these other wells were pumping during 1984-2000 (Figure 6-23c).
- Generally non-pumped water-supply wells that exhibit relatively little water-level response to distant pumping include the following:
    - **WS-7** (700 feet deep) is located in Sandstone 2 northeast of the ELV member aquitard outcrop, 3,500 feet northwest of WS-6 and respectively 2,700 and 3,900 feet east-southeast of WS-12 and WS-13. It experienced more than 200 feet of drawdown when it was pumped at an average annual rate of 8 gpm or less between 1955 and 1959 (Figure 6-23a). However, it exhibited no water-level response when other wells pumped after 1984. This response is consistent with the relatively low hydraulic conductivity of Sandstone 2 and the low-permeability, fine-grained members that separate it from Sandstone 1. The specific capacity of WS-7 during the years that it pumped was about 0.02 gpm/ft, given an average pumping rate of 4.5 gpm and net drawdown of 212 feet. This specific capacity and an assumed saturated thickness of 650 feet and storativity of  $1 \times 10^{-5}$  suggest an estimated bulk hydraulic conductivity of  $4 \times 10^{-6}$  cm/s (SCM Element 6 in Cherry, McWhorter and Parker, 2009), consistent with the central range of other bulk hydrologic conductivity estimates for Sandstone 2 (Figure 6-8).
    - **WS-9B** (220 feet deep) is located in Sandstone 2 between the aquitard outcrops of Shale 2 and the SPA member. It is approximately 900 feet from WS-12 and WS-13 to the north, and 1,500 feet from WS-6 to the south. This well never has been pumped and exhibits little apparent water-level influence from surrounding pumping wells (Figure 6-23b) for reasons most likely similar to those for WS-7.
    - **WS-11** (677 feet deep) is located within the outcrop of Shale 2 near the far western corner of the Sage member aquifer unit discussed above, and is more than 5,000 feet west of WS-6. This well experienced more than 200 feet of drawdown when pumped at average annual rates of 7 gpm or less between 1956 and 1959 (Figure 6-23c). Water levels subsequently recovered and have demonstrated little if any response to other pumping wells. Similar to WS-7, the specific capacity of WS-11 during the years that it pumped was about 0.02 gpm/ft, given an average pumping rate of 4.7 gpm and net drawdown of 212 feet. This specific capacity, and an assumed saturated thickness of 625 feet and storativity of  $1 \times 10^{-5}$ , suggests an estimated bulk hydraulic conductivity of about  $5 \times 10^{-6}$  cm/s (SCM Element 6 in Cherry, McWhorter and Parker, 2009), consistent with the central range of other bulk hydraulic conductivity estimates for Sandstone 2 (Figure 6-8).
  - Residual drawdown of 50 to 100 feet appears to have persisted in WS-4A, WS-5, WS-6, and WS-9 toward the end of the 1983. These wells produce from the productive Sage member aquifer unit between Shale 2 and the Shear Zone. This apparent long-term loss of groundwater storage suggests that groundwater extraction from this portion of SSFL during the 1950s and early 1960s exceeded recharge and the potential for groundwater inflow from adjacent areas. Some uncertainty exists regarding the exact occurrence and amount of residual drawdown due to gaps in the pumping and water-level records.

Areas of residual groundwater-level drawdown appear to persist across portions of SSFL as a result of high rates of pumping prior to 2002; low average annual recharge; low bulk hydraulic conductivity; and the finite areal extent of aquifer units bounded by shale units, fault boundaries, and the mountain topography.

- Fluctuations in annual precipitation during seasonal to multi-year segments of the climatic cycle appear responsible for some degree of the observed short-term variability of water levels. This influence is evident in non-productive wells relatively uninfluenced by pumping (e.g., WS-7 and WS-9B), for which water-level increases in response to wet periods appears to range up to 50 feet. Among all SSFL water-supply wells, long term climatic trends are generally not apparent in the water-level records, either because water-levels are consistently mounded within low-permeability zones or because of the more dominant influence of pumping wells.

#### 6.3.3.1.2 Cluster-Well Hydrographs

Clusters of two to four wells completed at varying depths have been constructed at 21 locations across SSFL and the immediately adjacent area. Plate 2-2 provides their construction profiles and general location map. Figures 6-24a through 6-24g present hydrographs for each of the 21 clusters and illustrate the vertical hydraulic gradients at each location. Table 6-5 provides the average, minimum, and maximum vertical gradients for each cluster calculated as the difference in head divided by the vertical distance between open-interval (i.e., screened or uncased) mid-points. Figure 6-25 is a map illustrating the distribution of downward, upward, and relatively neutral vertical gradients among the well clusters.

The cluster-well hydrographs are discussed below grouped by hydrogeologic unit and local area, beginning in northwestern SSFL and continuing clockwise around the site. Within each cluster, the wells are labeled alphabetically by depth, where “A” designates the shallowest monitored zone. The hydrographs of wells equipped at one time or another with multilevel systems are discussed in Section 6.3.3.1.3.

- **Upper Burro Flats Member, Northwestern SSFL, Cluster Wells RD-33ABC, RD-34ABC, and RD-54ABC (Figures 6-24a and f):** These three well clusters are located at the top of the northwest-sloping escarpment that forms the border of the Burro Flats plateau (Figures 6-11 and 6-25). Groundwater flow from the mountain in response to this topography results in fairly strong downward gradients from the A to B zones, with head drops of up to 100 feet and gradients ranging from -0.1 to -0.8 ft/ft (Table 6-5). At the depth of the C zones, however, groundwater draining from the mountain results upward gradients ranging up to +0.3 ft/ft.

- **Shale 3, Northwest of SSFL, Cluster Wells RD-59ABC and RD-68AB (Figure 6-24g):** These two well clusters are located just beyond SSFL northwestern boundary down the escarpment described above (Figures 6-11 and 6-25). Groundwater flow from the mountain results in generally upward gradients of as much as 0.5 ft/ft. The heads of B and C zone wells are above ground surface, resulting in flowing artesian conditions.
- **Burro Flats Member and North Fault Zone, North-Central SSFL, Cluster Wells RD-51ABC, RD-52ABC, and RD-56AB (Figures 6-24d, f, and g):** These well clusters are aligned with the North Fault Zone where it cuts through the Burro Flats member between Shale 2 and the ELV member (Figures 6-12 and 6-25). Similar to WS-12 and WS-13, the B and C zone wells of these clusters exhibit a strong response to groundwater production in the Sage Member. Since production from WS-5 and WS-6 ended in 2001, these wells have experienced a relatively smooth and continuing water-level recovery of as much as 120 ft to date. As stated above in the case of WS-13, this response suggests that the North Fault Zone has good hydraulic continuity with the Sage member by cutting through Shale 2 at depth and in plan view between WS-4A and WS-12, and extends this hydraulic communication into the Burro Flats member north of the North Fault. The A-zone wells of these clusters exhibit little trend, suggesting that head variability is constrained below by confining layers and above by points of groundwater discharge. During the water-level recovery of the B and C zones, a strong downward gradient occurred from the A zone at RD-51 and RD-52 (ranging to -1.5 ft/ft), suggesting that leakage from shallow zones contributed to the water-level recovery of deep zones.
- **Sage Member, North-Central SSFL, Cluster Wells RD-45ABC and RD-49ABC (Figure 6-24e):** Well cluster RD-45ABC is located immediately west of the Shear Zone approximately 500 feet from WS-5, whereas RD-49ABC is located approximately 1,000 feet west of WS-6 (Figures 6-12 and 6-25). Since production from WS-5 and WS-6 ended in 2001, water levels have recovered several hundred feet in all zones of RD-45 and as much as 100 feet in the B and C zones of RD-49. The occurrence of exceptionally low water levels in RD-45C accompanied by strong downward gradients from the B zone (-0.9 ft/ft) reflect the well cluster's proximity to 2,300-foot deep WS-5 and drawdown enhancement as a result of the low-permeability boundary associated with the Shear Zone. Consistent with where RD-49 is located within the outcrop of Shale 2, its A-zone well appears isolated from the Sage member with water levels more than 200 feet above those of the B zone, a downward gradient of as much as -1.2 ft/ft. This A-zone well exhibits little trend, suggesting that head variability is constrained by confining layers below and potential points of groundwater discharge above.
- **Canyon and Bowl Members, Northeast SSFL, Well Clusters RD-35ABC, RD-36ABC, RD-38AB, RD-39AB, and RD-43ABC (Figures 6-24a, b, c, d):** These well clusters are located east of the Shear Zone and from the IEL Fault northward (Figures 6-13 and 6-25). Other than at RD-35, the vertical hydraulic gradients at these clusters is strongly downward at up to -1.1 ft/ft. Heads in the upper zones of these clusters are significantly higher than water levels west of the Shear Zone, and none of the hydrographs exhibit a definitive response to past pumping from the Sage member west of the Shear Zone. Rather, the downward gradients appear to reflect groundwater drainage from the

mountain east toward the San Fernando Valley. The steep, short-term dip in RD-35B water levels reflects the influence of the 5-month C-1 pumping test performed from August 2003 through January 2004.

- Bowl and Sage Members and Lower Chatsworth Formation, South-Central SSFL, RD-5ABC, RD-46AB, RD-48ABC, RD-55AB, RD-58ABC (Figures 6-24a, d, f, and g): These well clusters are distributed throughout the area lying between the Coca and Burro Flats faults across the south-central portion of SSFL (Figures 6-14 and 6-25). With the exception of the RD-5 cluster, the vertical hydraulic gradients exhibited by these clusters is generally downward, ranging to -0.6 ft/ft, indicative of groundwater drainage from the mountain south toward Bell Canyon. These hydrographs do not exhibit any clear response to past pumping from the Sage member north of the Coca Fault. RD-5B and -5C respond distinctly to wet years, suggesting the upward gradient is caused by pressurization from recharge into somewhat distant fractures, whereas RD-5A responds to pumping by WS-9A approximately 2,000 feet away. The shallow upward gradient between RD-46B and -46A is probably related to confinement by Shale 1, whereas a multilevel system installed in RD-46B has exhibited a downward gradient (Table 6-6).

#### **6.3.3.1.3 Multilevel Well System Hydrographs**

Detailed vertical profiles of hydraulic head are provided by 33 SSFL wells equipped at one time or another with multilevel monitoring systems. These profiles typically (a) consist of long intervals with minimal vertical gradient, indicative of interconnected fractures, which (b) are separated by sharp inflections coinciding with certain lithologic contacts, and (c) maintain stable shapes over time (SCM Element 5 in Cherry, McWhorter and Parker, 2009). An example is provided in Figure 6-16. Poorly interconnected fractures would be expected to exhibit more erratic multilevel head profiles.

The vertical gradients observed in wells equipped with multilevel monitoring systems are summarized in Table 6-6 and mapped in Figure 6-25. The majority of these wells exhibit downward gradients consistent with most of the cluster well hydrographs discussed above. Because of the greater resolution of the multilevel profiles, however, the head drops are observed to occur over short intervals with generally steeper gradients, ranging up to 10 ft/ft.

#### **6.3.3.2 Groundwater Surface**

Figure 6-26 presents a hand-contoured map of the estimated October 2008 groundwater surface, exclusive of shallow-perched and deep-confined zones. For wells lacking October 2008 data, water levels from before and after months were considered, followed by data from other years, as

needed. Interpreted elevations were constrained by the bottom elevations of wells recorded as dry in October 2008. Data from wells identified in Section 6.3.2.1 as representative of shallow, perched zones were not considered. Water-level values from deep wells potentially representative of piezometric surfaces other than the regional water table were considered in areas of sparse data. The resulting data set consists of water-level elevations for 216 wells and the bottom elevations of 66 dry wells, as summarized below:

Well Type	No. Wells	
	Values	Dry
Piezometers (PZ)	58	36
Shallow wells (ES, HAR, RS, SH)	39	29
Off-site wells (OS)	11	
RD wells	95	1
Water-supply wells (WS)	13	
Total	216	66

These data locations are posted on Figure 6-26. Similar maps have been prepared by others (e.g., Haley & Aldrich, 2007, 2008, 2009a and b).

The dominant features of this map include the residual drawdown trough between Shale 2 and Shear Zone, surrounded by various groundwater mounds. Areas of relative groundwater mounding include Burro Flats, the portion of SSFL east of the Shear Zone, an area near the intersection of Coca and Skyline faults, and high terrain toward and beyond the northeast and west-southwest boundaries of SSFL. Steep hydraulic gradients occur down the flanks of the mountain to the north and south. As has been interpreted by others (e.g., Haley & Aldrich, 2009a and b), sharp lines exhibiting as much as 200 feet of water-level discontinuity bound the residual drawdown trough along the Shear Zone to the east and Shale 2 to the west.

The residual drawdown trough appears to have a notably extensive, flat surface that lay just below 1,600 ft msl in October 2008. This surface extends across the North Fault just west of the Shear Zone, and follows the North Fault Zone where it cuts through Shale 2 and the SPA and ELV fine-grained members along the top of the east branch of Meier Canyon. This suggests that the groundwater surface may be controlled in part by points of groundwater discharge (i.e., seeps

and phreatophytes) along the canyon near and to the north of SSFL boundary. The potential topographic control of the canyon on water levels can be visualized in Figure 6-12, on which the 1,600-foot topographic contour is highlighted. The water-level trough within the Sage member appears to extend beneath the ridge northeast of SSFL, as evidenced by well OS-25, but appears to be overlain by mounded groundwater within shallower zones as evidenced by RD-69 and OS-26. The southern boundary of the trough to the west of the Shear Zone is poorly delineated by the existing configuration of wells in this area, but is interpreted to occur approximately along the Ridge and Skyline faults.

Monitoring data for WS-14 and nearby RD-37 and RD-78 appear to delineate a small water-level depression centered on WS-14. Although WS-14 has never been pumped, its 1,270-foot depth may facilitate groundwater drainage in response to downward vertical gradients exhibited among the several well clusters within eastern SSFL. Several of the other water-supply wells exhibit static groundwater elevations slightly lower than surrounding, shallower wells, however WS-14 is the only one of these wells that appears to extend its influence to other nearby wells.

The groundwater-level contours appear to be inflected up Bell Canyon in southwestern SSFL and may reflect the influence of groundwater production from WS-9A that continued through 2007.

### **6.3.3.3 Depth to Groundwater**

Figure 6-27 is a map of October 2008 estimated depths to groundwater generated directly by subtracting the groundwater surface elevation map in Figure 6-26 from a digital elevation model (DEM) ground-surface elevation grid. Consistent with the methodology described above, this map does not reflect water levels from wells identified in Figure 6-22 to be representative of shallow perched zones.

This map clearly shows the boundary effects of the Shear Zone and Shales 2 and 3 with regard to groundwater levels, as discussed previously in Section 6.3.3.1 and illustrated with cross sections in Figures 6-15 and 6-17. These boundaries of relatively low permeability significantly influence the distribution of shallow and deep groundwater areas. Although not apparent from

this analysis, similar but probably less pronounced boundary effects may occur elsewhere within and near SSFL.

The mapped depths to groundwater range from 0 to more than 500 feet. The largest area of shallow groundwater occurs beneath Burro Flats, the 2,000-foot wide mountain plateau northwest of the Shear Zone. This area is underlain by the Burro Flats member of the Chatsworth Formation, which is characterized by relatively low permeability and fracture frequency south of the North Fault, and by banded outcrops of the SPA and ELV fine-grained members and the fine-grained Lot bed. Shallow groundwater also occurs along a band several hundred feet wide immediately east of the ground-surface trace of the Shear Zone; along alluviated valley floors and canyon bottoms; and along the outcrop of Shale 3, where underlying groundwater zones occur under artesian conditions.

The largest area of deep groundwater occurs in central SSFL between the Shear Zone and the outcrop of Shale 2. This results from the high, mountainous topography and residual groundwater-level drawdown trough in the underlying Sage member. Other areas of deep groundwater occur along mountain-top margins underlain by steep hydraulic gradients toward the surrounding lowlands.

#### **6.3.3.4 Major-Ion Groundwater Quality**

The major-ion hydrochemistry of the fractured sandstone aquifer is largely homogeneous, both laterally and vertically (SCM Element 12 in Cherry, McWhorter and Parker, 2009). Table 6-5 summarizes the major-ion chemistry for groundwater samples collected from 40 SSFL wells during 2003-08. As shown in Figure 6-28, these data plot in a fairly tight cluster on trilinear diagrams. Samples from most wells are of a mixed-calcium-bicarbonate type. Other types include calcium sulfate, calcium chloride, mixed magnesium, and mixed sodium. Strong spatial trends among these types are not apparent, and sampling indicates that the major-ion groundwater chemistry is well mixed with depth. Electrical conductivity and concentrations of bicarbonate, sulfate, and chloride do not trend higher with increasing sample depth. Among all samples, the sum of major ions ranges from approximately 300 to 1,300 mg/L.

In order of relative abundance, the major-ion composition of SSFL groundwater is bicarbonate, sulfate, and chloride as the dominant anions, and calcium, sodium, and magnesium as the dominant cations. The bicarbonate derives from calcite dissolution driven by carbon dioxide produced in the soil zone, and to a lesser degree by acid from sulfate reduction. The sulfate derives from pyrite oxidation, as limited by sulfate reduction. Chloride derives solely from precipitation and dry fallout. Relatively high sulfate and/or sodium are characteristic of samples from shale units, consistent with the geochemistry of silts and clays. Samples from the lower Chatsworth Formation tend to be relatively high in magnesium and sulfate. Samples from the major sandstone units of the upper Chatsworth Formation have similar ranges in composition.

Trends in the variability of groundwater quality with depth are not evident, indicating that the groundwater's characteristic ionic signature is inherited from dominant hydrochemical processes occurring in the vadose zone and shallowest groundwater (SCM Element 12 in Cherry, McWhorter and Parker, 2009). The rapid diffusion of oxygen and carbon dioxide through the vadose zone needed to drive these processes is evidence of the vadose zone fracture porosity. Stable isotope ratios of dissolved inorganic carbon indicate the occurrence of both open- and closed-system calcite dissolution, consistent with the dual-porosity (i.e., fracture and matrix) model (SCM Element 12 in Cherry, McWhorter and Parker, 2009).

The absence of general groundwater quality trends with depth, distance of travel, and among the hydrogeologic units indicates that connate water has been flushed from the rock by groundwater derived primarily from precipitation recharge to depths near sea level. Vertically well-mixed groundwater is also indicated by the lack of notable trends in stable oxygen isotope ratios with depth, although some degree of mixing is probably attributable to sampling (e.g., from well with long open intervals; SCM Element 12 in Cherry, McWhorter and Parker, 2009).

#### **6.3.4 Groundwater Movement**

Groundwater mounded by recharge across SSFL and adjacent uplands moves toward pumping wells, hill-slope and canyon-floor seeps, and the subsurface of surrounding lowlands. Groundwater has both lateral and vertical components of flow. Lines of evidence indicative of the pattern of groundwater flow, a hydraulic continuum between shallow and deep zones, and an

interconnected fracture network include the distribution of water quality, hydraulic head, seeps, and phreatophytes, and the response of the groundwater system to major changes in hydraulic stress.

#### **6.3.4.1 Indicated by the Distribution of Hydraulic Heads and Water Quality**

Maps presented above of the estimated groundwater surface and direction of vertical hydraulic gradients at well clusters (Figures 6-26 and 6-25, respectively) indicate the pattern and range of hydraulic gradients that drive lateral and vertical groundwater flow in the vicinity of SSFL. The magnitude and direction of three-dimensional groundwater flow results complexly from the combination of these gradients and the distribution of hydraulic conductivity. The pattern of flow is generally divergent from areas of groundwater mounding toward surrounding lowlands, except where convergent toward residual pumping depressions.

As indicated by the majority of cluster-well and multilevel hydrographs presented earlier the potential for vertical flow is largely downward across the site. The occurrence of downward flow is supported by the geochemistry (SCM Element 12 in Cherry, McWhorter and Parker, 2009 and see Section 6.3.3.4), which indicates that a significant portion of recharged groundwater penetrates deep into the groundwater system before flowing consistent with the horizontal head distribution.

Upward groundwater gradients and the potential for upward groundwater flow occur along the mountain flanks, consistent with groundwater flow lines arcing outward and upward after descending into the mountain. At some locations the potential exists for groundwater flow to converge at mid-depths as a result of both shallow downward and deep upward gradients (e.g., at well clusters RD-34 and RD-54; Figures 6-24a and 6-24f).

More than 200 feet of water-level off-set across the Shear Zone indicates that it serves as a significant, albeit partial, barrier to groundwater flow. This interpretation is further supported by areas of contaminated groundwater largely restricted to the eastern side of the Shear Zone, despite the strong westward hydraulic gradient (e.g., see Figure 7-7).

The large groundwater-level off-set that occurs along the outcrop of Shale 2 indicates that lateral groundwater flow is restricted from the Burro Flats member southeast into the Sage member. However, small rates of downward leakage through Shale 2 beneath the Burro Flats area may comprise significant groundwater flux into the underlying Sage member, and thus be partially responsible for the ongoing recovery of groundwater levels within the Sage member's residual drawdown trough.

#### **6.3.4.2 Indicated by the Distribution of Seeps and Phreatophytes**

The locations of some seeps and phreatophytes may be influenced by geologic features such as faults and shale beds. However, the occurrence of topographic lows appears to exert the dominant influence on seep and phreatophyte distribution. Nearly all seeps and phreatophytes occur along the thalwegs of canyons surrounding SSFL (SCM Element 13 in Cherry, McWhorter and Parker, 2009).

Evidence derived from the analysis of hydrogeochemical, hydrochemical, and isotopic data indicates that seep discharge originates largely from recharge on the mountain plateau. Nevertheless, water quality differences between many of the seeps and much of the mountain's groundwater suggest that local, shallow groundwater flow paths in the general vicinity of seeps also contribute to seep discharge. For example, seep water quality tends to exhibit higher concentrations of sulfate and/or sodium, probably as a result of enhanced pyrite oxidation and the weathering of mafic minerals where oxygen is relatively available along local, shallow flow paths. Such seeps may represent a convergence of both mountain-scale and local groundwater flow paths. Additionally, the ionic signature of seep discharge from groundwater flow paths that pass through younger geologic formations exhibits the influence of secondary gypsum (SCM Element 12 in Cherry, McWhorter and Parker, 2009).

#### **6.3.4.3 Indicated by the Response to Major Changes in Hydraulic Stress**

The SSFL groundwater monitoring period includes the following major changes in hydraulic stress: (1) the initiation of groundwater production around 1950, (2) the mid-1960s cessation of most groundwater production, (3) the resumption of groundwater pumping during the mid-1980s, (4) the 1996 hydraulic communication study when pumping was halted for about one

month, (5) the site-wide cessation of most groundwater pumping since 2001 (Table 6-2), and (6) the C-1 pumping test, which lasted about 5 months from August 2003 through January 2004. Hydrograph responses to several of these events are described above in Section 6.3.3.1.

#### **6.3.4.3.1 1996 Hydraulic Communication Study**

During the 1996 hydraulic communication study (GRC, 1997), all but one of SSFL pumping wells were turned off on June 11, and restarted on a staggered schedule during July 11-23, allowing some differentiation of the drawdown responses. Table 6-8 provides a summary of the study's pumping rates and monitoring well responses to the study. The study results provide support for the following interpretations:

- The transmissivity of the Burro Flats member between the North Fault and Shale 2 is relatively low; as a result, well yields and the extent of drawdown are fairly limited at roughly 10 gpm and 100 feet, respectively.
- The transmissivity and interconnectivity of the Sage member between Shale 2 and the Shear Zone are high, such that well yields and the extent of drawdown are relatively large (at up to 200 gpm and nearly 5,000 feet, respectively). Pumping influences do not cross the Shear Zone or Shale 2, except where Shale 2 is cut by the North Fault.
- The transmissivity of the Canyon and Bowl members east of the Shear Zone is low to moderate, with well yields of 20 gpm and drawdown extending nearly 1,000 feet, possibly enhanced along some fault traces.
- The influence of WS-9A on RD-5A demonstrates that the Sage member south of the Coca Fault is also fairly transmissive, possibly preferentially along certain fractures.

#### **6.3.4.3.2 Response to 2001 Site-Wide Cessation of Groundwater Pumping**

Figures 6-29a and 6-29b present a correlogram analysis of groundwater-level recoveries since the 2001 site-wide cessation of most groundwater pumping. Haley & Aldrich (2000) used a similar approach to evaluate hydraulic interconnectivity across the site using pre-2000 water levels. For the current analysis, the water-level records of 45 individual wells are each compared to the WS-6 water-level record for August 2001 through July 2009; the locations of most of these wells are shown in Figure 6-12. The groundwater-level elevations of WS-6 trended smoothly upward throughout this period, primarily in response to the cessation of WS-5 and WS-6 pumping by mid-2001. By plotting the WS-6 water levels along the horizontal axis of each correlogram, each plot coincidentally represents increasing time from left to right as a function of the continuously

upward water-level trend. The water-level data points of wells that correlate with WS-6 are plotted in blue, whereas those that do not are plotted in red.

As shown by these correlograms and summarized in Table 6-8, the water-level records of 21 individual wells plot nearly one-to-one against the WS-6 water-level record. This remarkably high degree of exact correlation, over distances ranging from 1,100 to 3,600 feet, demonstrates a very high degree of hydraulic interconnectivity throughout much of the Sage member, the North Fault Zone, and a portion of the Burro Flats member immediately north of the North Fault. The water levels of these wells not only recovered simultaneously at essentially identical rates, they shared an essentially flat-lying piezometric surface that rose gradually throughout this period. Twelve of these wells lie along the North Fault Zone, which strongly supports the interpretation that the fault zone has relatively high vertical hydraulic conductivity and is hydraulically connected with the Sage member at depth. Furthermore, relatively high hydraulic connectivity appears to extend north into a portion of the Burro Flats member, as demonstrated by the correlated response of RD-70.

The water-level records of another 8 wells correlate reasonably with WS-6, but less exactly, and demonstrate the approximate limits of the Sage member aquifer unit from which WS-5 and WS-6 produce (Table 6-8).

The water-level records of the remaining 16 wells considered for this analysis do not correlate with the WS-6 water-level recovery. These include wells completed in the Burro Flats member between Shale 2 and the North Fault, wells east of the Shear Zone, wells considerably north of the North Fault, and wells along and south of the Coca Fault other than RD-41B and RD-41C.

#### **6.3.4.3.3 C-1 Pumping Test**

A 152-day pumping test was performed east of the Shear Zone from August 2003 through January 2004 (MWH, 2004a). During this test, 600-foot deep corehole C-1 was pumped at an average rate of 40 gpm. C-1 is drilled into the Canyon member immediately south of the IEL Fault (Figure 6-13) and is interpreted to pass through the fault plane at depth. Measurable drawdown among the monitored wells occurred at a maximum distance of more than 1,300 feet. The IEL fault was not interpreted to act as either a barrier or conduit to flow during the test. The

test influence did not extend west across the Shear Zone, however. Similar to the 2001-2009 water-level recovery described above, drawdown resulting from the C-1 pumping test was described as “sub-planar,” i.e., water levels were lowered fairly uniformly across a large area, indicating a significant degree of hydraulic interconnectivity throughout the fractured sandstone.

#### **6.3.4.3.4 Western SSFL Tests**

Large-scale hydraulic testing in western SSFL generally is hindered by the relatively low hydraulic conductivity of Sandstone 2. In 2006, well RD-54B was pumped at a rate of 0.12 gpm for 165 days, achieving measurable drawdown in 6 of 16 monitored wells at a maximum distance of 400 feet. These results confirmed the fracture network within Sandstone 2 is significantly less conductive than elsewhere within SSFL (MWH, 2006a).

A tracer test was conducted in March 1993 by injecting a salt solution into WS-SP while pumping RD-9 at a rate of about 4 gpm about 53 feet away (Figure 6-12). A breakthrough concentration of the tracer arrived at RD-9 in approximately 5 hours, indicating a relatively high groundwater velocity of 250 feet per day as a result of fracture flow. However, the characteristically low pumping rate of RD-9 and other wells in western SSFL suggests that the extent of such high permeability fractures must be limited (GRC, 1993).

#### **6.3.4.4 Influence of Faults**

Table 6-10 summarizes groundwater monitoring and test data in the vicinity of SSFL faults and the various lines of evidence indicating whether these faults may perform as potential partial barriers and/or conduits to groundwater flow.

As described previously in Section 5 (Table 5-1), the attributes of the North Fault are considered in three segments: western (west of RD-56), middle (from RD-56 to Shale 2), and eastern (from Shale 2 to the Shear Zone). The western segment lacks mappable traces, but rather consists of a wide zone of closely spaced deformation bands. Although not explicitly monitored, this segment may serve as a partial barrier to flow given the low-permeability mineralization commonly associated with such features. The middle segment of the North Fault Zone demonstrates a high degree of hydraulic continuity with the Sage member, as demonstrated and discussed above (Section 4.3.4.3.2; Figure 6-29). The response of RD-37, located north of the fault, to pumping

and recovery by water-supply wells south of the fault indicates that the eastern segment is not an effective barrier to groundwater flow.

Several lines of evidence strongly indicate that the Shear Zone serves as an effective partial barrier to groundwater flow, as described and illustrated previously (Sections 6.3.1.1 and 6.3.4.3; Figure 6-17). These include: more than 200 feet of water-level off-set across the Shear Zone; the lack of hydraulic response from testing conducted on either side of the Shear Zone; and distinct boundaries in contaminant concentrations coinciding with the trace of the Shear Zone.

The occurrence of low yielding wells and elevated water levels along portions of the Coca Fault provide possible indications that it may serve as a low-permeability zone. However, groundwater levels in RD-41C, which is located on or immediately south of the fault, responded partially to the recovery of groundwater levels in the Sage member north of the fault (Figure 6-9b). Further west along the Coca Fault, a comparison of groundwater levels on either side of the fault in the vicinity of ES-17, -26, and -27 does not suggest a low-permeability barrier effect along the fault. The non-detection of contaminants in RD-61 along the Coca Fault near the eastern boundary of SSFL does not provide evidence that the fault serves as a conduit for groundwater flow.

As discussed in Section 5, as much as a mile of lateral off-set is interpreted to have occurred along the Burro Flats fault. Furthermore, low-permeability gouge as much as 1-foot thick has been observed to occur in places along the fault. However, the distribution of monitoring wells and hydraulic testing are insufficient for demonstrating the impact of this fault on groundwater levels and flow.

In northeastern SSFL, both the 1997 RD-73 and 2004-05 C-1 pumping tests demonstrated that the IEL Fault, and apparently the Woolsey Canyon Fault, does not act as significant barriers to groundwater flow. Figure 6-30 provides a set of groundwater level hydrographs for 13 wells along, between, south, and north of these two faults over the past two decades. These hydrographs exhibit similar patterns, most significantly in response to the C-1 pumping test. The non-detection of contaminants in RD-66 and the RD-43 cluster along the Woolsey and IEL

faults, respectively, to the immediate east of SSFL does not provided evidence that these faults serve as conduits for groundwater flow.

Hydraulic continuity along the southern trace of the Happy Valley Fault was demonstrated by the 1986-2000 response of groundwater levels in RD-10 to groundwater pumping by RD-1 (Figure 6-31), located approximately 600 feet to the west (Figure 6-13). During an initial test in July 1986, water levels in RD-10 responded after approximately 300 minutes as a result of pumping RD-1 at about 37 gpm. This and the continued pumping of RD-1 caused a reversal of the natural, more easterly gradient between the two wells. An interconnection between these wells was further demonstrated by a 1994-95 tracer test (GRC, 1996). This test involved the injection of 40,000 gallons of 9,000  $\mu\text{mhos/cm}$  salt solution into the 400-foot deep RD-10 during a 15-hour period on October 13, 1994, which rapidly diluted into a slug of groundwater with an electrical conductivity of about 3,000  $\mu\text{mhos/cm}$ . Meanwhile, groundwater extraction from the 506-foot deep RD-1 continued at rates of about 12 to 15 gpm, resulting in an average hydraulic gradient between the wells of 0.046 ft/ft over the next several months. On March 10, 1995, approximately five months after the tracer was introduced, the electrical conductivity of the water pumped from RD-1 rose and fell over a 19-hour period, peaking at greater than 2,000  $\mu\text{mhos/cm}$ , more than double typical background levels. This indicated a groundwater velocity of 4 feet/day as a result of the gradient induced by pumping RD-1. The potential for transport east of RD-10 toward the SSFL boundary has not been similarly evaluated, nor do any other wells exist to the east of RD-10 along the Happy Valley Fault.

Figure 6-31 compares the long-term water-level hydrographs of two wells located along the Bowl Structure, remedial extraction well RD-2 and monitoring well RD-44 approximately 800 feet to the east-southeast (Figure 6-13). After pumping from RD-2 ceased in 2000, its water levels recovered approximately 80 feet over the next 5 years, while water levels in RD-44 rose approximately 20 feet. The relatively muted response of RD-44 may indicate some degree of hydraulic connectivity along the Bowl Structure. Contaminants have not been detected in groundwater sampled from RD-44.

As listed in the remainder of Table 6-10, the available information for other SSFL faults remains inconclusive regarding their potential as groundwater flow pathways. For the most part, these are relatively minor faults internal to SSFL that do not lead off-site.

### 6.3.4.5 Estimated Groundwater Velocities

Based upon the hydraulic properties of the sandstone matrix and fractures discussed in Section 6.2, relatively high groundwater flow velocities are expected in fractures compared to significantly lower velocities in the surrounding porous medium. Flow through the dual porosity medium as a whole (fractures and matrix) is referred to as bulk flow.

An approximate range of bulk and fracture groundwater flow velocities at SSFL may be expressed as follows:

	Gradient (ft/ft)	Hydraulic Conductivity (cm/s)	Matrix Porosity	Fracture Porosity	Bulk Velocity	Fracture Velocity
			(%)		(ft/day)	
Groundwater flow across SSFL northwest boundary	0.4	$5 \times 10^{-6}$	14	0.01	0.04	60
Groundwater flow across southern SSFL boundary	0.1	$5 \times 10^{-5}$	14	0.01	1	140
Groundwater flow across fine-grained unit:						
High	10	$1 \times 10^{-7}$	7	0.01	0.04	30
Low	0.1	$1 \times 10^{-7}$	7	0.01	0.0004	0.3

As discussed in the following section, total groundwater flow is estimated at less than 150 gpm site-wide.

## 6.4 GROUNDWATER BUDGET

Recharge to and discharge from the groundwater system drives flow at the site. The details of each are discussed below.

### 6.4.1 Recharge

Groundwater recharge is water that enters the subsurface and reaches the saturated zone. Sources of recharge include precipitation, applied water (e.g., irrigation, leaks), and various forms of wastewater discharge. Recharge is the net amount from such sources that is not lost to evapotranspiration or off-site runoff.

Stable oxygen isotope data confirm that precipitation is the primary source of groundwater recharge and that water imported from the Calleguas Water District contributes negligibly to recharge. Isotope data also indicate that a portion of recharge derives from infiltration of precipitation runoff collected and partially evaporated in ponds (SCM Element 12 in Cherry, McWhorter and Parker, 2009).

Factors that influence the spatial and temporal variability of recharge across SSFL include:

- Seasonal and climatic precipitation patterns and variability
- Influences of topographic elevation and aspect on precipitation
- Geomorphic controls on runoff and ponding
- Soil, geologic, and ambient-moisture controls on infiltration capacity
- Type and extent of vegetative cover
- The location, nature, and variability of applied-water and wastewater practices

The nature and character of site runoff and ponding, and their association with the occurrence of shallow depths to groundwater, are described in previous SSFL reports (MWH, 2003b and c).

#### **6.4.1.1 On-Site Water Use and Disposal**

Table 6-2 and Figure 6-18 present the record of annual SSFL water production and use, which exceeded 220 million gallons per year (equivalent to 420 gpm) as recently as 1998. Some portion of this water re-enters the subsurface as recharge, although the portion previously derived from groundwater pumping does not constitute a net source of recharge.

Water and wastewater from various on-site uses has been and continues to be discharged on-site to the ground surface and subsurface. Surface discharges have been associated with various site operations and include the release of treated wastewater and remediated groundwater. In recent years, surface discharge has been limited to the Bell Creek drainage (MWH, 2003c). These discharges and storm runoff collect in five perennially filled basins (the R-1, R-2a, R-2b, and Coca ponds, and the Silvernale reservoir) and one intermittently filled basin (the Perimeter Pond). During periods of remedial groundwater extraction, treated groundwater from wells WS-5 and C-1 is discharged and collects in the R-1 pond, and treated groundwater from WS-6 and WS-9 collects in the Silvernale reservoir along with storm runoff. Formerly, the Silvernale

reservoir also collected operational discharge from the Alpha and Bravo test stands. Overflow from the Silvernale reservoir collects in the R-2 ponds, along with storm runoff and the discharge of treated groundwater when extracted from well WS-9A. The Coca pond appears to receive discharge from leaking water supply lines. The Perimeter pond is located at a relatively low elevation and collects seasonal runoff. These ponds likely contribute to groundwater recharge, but may also receive groundwater discharge during periods of elevated groundwater levels (MWH, 2003b). Discharge to the subsurface occurs from leaking buried pipeline and septic-system leach fields.

In prior years, process water from various site activities collected in eleven surface water impoundments identified as the APTF-1, APTF-2, ABSP, SPA-1, SPA-2, Delta, PLF, STL-IV-1, STL-IV-2, ECL-1, and ECL ponds. These likely leaked to the subsurface and have since been filled (GRC, 1987).

#### **6.4.1.2 Site-Wide Estimated Recharge**

As described below, site-wide recharge has been evaluated by two separate approaches: 1) chloride mass balance and 2) Darcy calculation in the vadose zone.

##### **6.4.1.2.1 Chloride Mass Balance**

Stable isotope results for dissolved chloride indicate that the chloride present in the Chatsworth Formation groundwater is natural chloride originating from modern sea water and conveyed to the site as precipitation and dry fallout (SCM Element 12 in Cherry, McWhorter and Parker, 2009).

The chloride mass balance approach is used to estimate long-term mean recharge to groundwater on a site-wide basis (SCM Element 10 in Cherry, McWhorter and Parker, 2009). This method estimates the portion of precipitation that becomes groundwater recharge by evaluating naturally occurring chloride deposition onto the ground surface from precipitation and dry fallout, and subsequent transport into the subsurface by the infiltration of precipitation. The calculation of recharge by this method is as follows:

$$R = P(C/C_R)$$

where  $R$  is groundwater recharge,  $P$  is precipitation,  $C$  is chloride concentration in precipitation and dry fallout, and  $C_R$  is chloride concentration in groundwater recharge.  $C_R$  is greater than  $C$  as a result of concentration of chloride mass in the vadose zone that occurs largely as a result of evapotranspiration. This equation is based on an assumed steady-state relationship between 1) chloride mass entering the vadose zone as a result of precipitation infiltration and 2) chloride mass exiting the vadose zone as a result of recharge to the saturated zone. In addition, it is assumed that the chloride in groundwater is derived from recharge and that the groundwater concentration may be taken as that of the recharge. This second assumption is based on the expectation that water of marine origin that was present in the rocks at the time of deposition has been since flushed away by percolating precipitation during the millions of years since the rocks were uplifted above sea level. Data recently collected from Corehole C-15 supports this line of reasoning. Both assumptions are consistent with estimation of a long-term mean value for recharge. Long-term mean values for both  $P$  and  $C$  were developed from site-specific data. The mean precipitation from 1960 through 2008 was 18.6 inches per year, and the mean chloride concentration in precipitation estimated from recent data is 2.5 mg/L. Also, a mean value for  $C_R$  of 54 mg/L was based on 228 groundwater chloride concentrations observed across the site over time. Development of this value involved 1) inspection and screening of the available concentration data for outliers and effects not related to recharge and 2) comparison to results derived from an independent dataset.

Long-term mean recharge is estimated to be 4.6% of precipitation, or 0.9 inches per year, which represents approximately 70 million gallons per year over the entire site. Uncertainty analysis has resulted in a range of estimates from 2 percent to 7 percent (0.4 to 1.3 inches per year). This range of values is expected to be conservatively high since the effects of runoff and resulting surface water transport of chloride off-site are unaccounted for. Such an accounting would reduce the precipitation concentration,  $C$ , and result in a proportional decrease in recharge,  $R$ .

#### **6.4.1.2.2 Darcy Calculation in the Vadose Zone**

The SSFL Groundwater Advisory Panel has estimated an upper bound of SSFL recharge rate based on estimated flow through unsaturated sandstone. This calculation is based on Darcy's law and the Brooks-Corey relation between unsaturated hydraulic conductivity and soil water

content. It estimates long-term average flow from the ground surface to the saturated zone using site-derived values of the sandstone matrix hydraulic conductivity, residual saturation, and mean water saturation. The resulting estimate of 0.35 inches/year is consistent with the lower range of values estimated by the chloride mass balance method.

## **6.4.2 Discharge**

Discharges from the groundwater system include extraction from wells; flows to springs, seeps and phreatophytes; and flows across hydrogeologic boundaries established for the site. Each of these categories is discussed below.

### **6.4.2.1 Extraction**

#### **6.4.2.1.1 Facility Water Supply**

As described by MWH (2000b) and Groundwater Resources Consultants (2000b), groundwater extraction began at the site in 1948 for the purpose of water supply. Seventeen supply wells were installed between 1948 and 1963 (Figure 6-19). These wells were hundreds to more than 2,000 feet deep and were completed as open boreholes from relatively shallow depths (Table 6-3). By the early 1960s, all but five of the wells located in the north-central portion of the site (WS-5, WS-6, WS-9A, WS-12 and WS-13) were abandoned or not used because of insufficient yield (Table 6-2). Groundwater extraction appears to have peaked in the late 1950s to early 1960s at over 150 million gallons per year, or an average continuous rate of approximately 300 gpm (Figure 6-18). As much as 500 feet of groundwater level drawdown had been induced in the most heavily pumped north-central area of the site by the late 1950s, creating a significant cone of depression. Importation of water from the Calleguas Water District began in 1963, such that little groundwater extraction occurred through the early 1970s. Possibly 60 percent of facility water use was satisfied by groundwater extraction from the late 1970s through 1986; however, little to no data are available for the period from 1964 through 1983.

#### **6.4.2.1.2 Interim Remedial Measures**

Groundwater extraction associated with remediation began in 1984. A combination of water-supply wells and newly installed extraction wells were used (Figure 6-19). The shallow new

wells were less than 40 feet deep and screened over much of their length, and the new deep wells were approximately 100 to 500 feet deep and completed as open boreholes from relatively shallow depths (Table 6-3). Review of pumping activities and locations (Table 6-2 and Figure 6-19) indicates that the spatial distribution of pumping changed somewhat during this more recent period of groundwater extraction as a result of addition of the new wells. However, the focus of the extraction remained deep and was largely allocated among the same wells as in the past (Figure 6-18).

Extraction rates increased through the 1980s and stabilized in the 1990s between 125 and 150 million gallons per year, or an average continuous rate of approximately 250 gpm. Remedial pumping has greatly decreased since 1999 for a variety of reasons that include 1) accommodation of subsurface characterization activities begun in 2000, 2) post-closure permit modification for some areas that occurred in 2001, and 3) damage to extraction well pipelines that occurred in late 2005 as a result of the Topanga Fire (MWH, 2008b; CH2M HILL, 2008a).

#### **6.4.2.1.3 Off-Site Groundwater Production**

A recent off-site well inventory (Appendix 2-E) identified 127 off-site wells, of which 73 are considered active, 30 are of unknown status, and the remainder are abandoned or destroyed. Off-site groundwater uses include residential and small agricultural (i.e., cattle watering and small plots of crops).

#### **6.4.2.2 Other Discharges and Outflows**

Estimates of groundwater discharge to seeps and phreatophytes sum to approximately half of the estimated average annual precipitation recharge for the mountain groundwater flow system encompassing SSFL (SCM Element 13 in Cherry, McWhorter and Parker, 2009).

Outflows along the study area's hydrogeologic boundaries consist of subsurface flow into adjacent areas; discharge to the ground surface through springs, seeps, and stream baseflow; and discharge to the atmosphere by phreatophytes. Groundwater flow into adjacent areas and discharge through phreatophytes has been estimated by groundwater modeling (Section 6.5). Discharges to seeps have been catalogued and the flows estimated during field mapping.

### 6.4.3 Balance of Inflows and Outflows

Based on the information and estimates presented above, a groundwater budget is assessed for the greater site area. Four groundwater budget periods are presented in Table 6-11. All of the groundwater budget components except outflow are estimated from site data as indicated in the table's notes. The outflow term was estimated by rearranging the standard groundwater budget equation. The standard groundwater budget equation is:  $\text{inputs} - \text{outputs} = \text{change in storage}$ . For the groundwater budget considered in this work, the output component is the sum of pumping, evapotranspiration, and outflow. Rearranging to solve for outflow yields:  $\text{outflows} = \text{inputs} - \text{change in storage} - \text{pumping} - \text{evapotranspiration}$ . This term is an estimate of bulk groundwater flow for each of the four periods considered and can be converted into an estimate of Darcy velocity through division by the perimeter length and depth of the area considered in the groundwater budget analysis. These estimates for the greater site area are averages across the study area and over the depth of the active flow system. Variations very likely occur 1) across the area as a result of variability in hydrostratigraphy and geologic structure, 2) with depth as a result of decreasing bulk hydraulic conductivity with depth and 3) over time as the best-estimate values used as parameters in the water budget may vary.

## 6.5 GROUNDWATER FLOW MODEL

A groundwater flow model for the site and adjacent areas has been constructed and its calibration optimized. Modeled groundwater flow is represented as an equivalent porous medium (EPM). The EPM approach represents the fractured bedrock system by applying hydrologic properties representative of bulk groundwater flow (e.g., bulk hydraulic conductivity).

The groundwater flow model integrates the hydrogeologic data discussed in this report in order to:

- Evaluate the significance of various aspects of SSFL hydrogeologic conceptual model.
- Aid in quantifying the overall water budget.
- Understand the nature, occurrence, and source areas of groundwater discharging from SSFL.

- Develop insight regarding historical variations in the pattern of groundwater flow as a function of groundwater withdrawals for water supply and interim remedial measures.
- Quantify the pattern, magnitude, and variability of Darcy fluxes from contaminant source areas.
- Evaluate the effectiveness of the groundwater monitoring network.

This section summarizes the modeling approach and results presented in Appendix 6-A as well as earlier model documentation (AquaResource/MWH, 2007).

### **6.5.1 Model Configuration**

The previously documented mountain-scale groundwater flow model (AquaResource/MWH, 2007) has been updated to reflect additional field data (Section 4.12), incorporate input from DTSC staff regarding the location of potential faults, and refine the finite element mesh to better represent the updated geology and support additional model functionality. Groundwater flow is simulated using FEFLOW (DHI-WASY, 2009), a three-dimensional, commercially-available modeling software package.

The mountain-scale model domain is approximately 20 square miles and coincides with the area and hydrogeologic boundaries shown in Figure 6-1. The base of the model domain is set at sea level based on a regional interpretation of the subsurface geology and water quality at depth. The spatial variability of hydrogeologic units and faults are represented by specifying hydraulic property zones within the finite element mesh that conform to mapped faults and hydrogeologic structures across the site. Specified boundary conditions are used to represent water entering and leaving the groundwater system. The modeled boundary conditions include recharge and groundwater discharge from pumping wells, seeps, phreatophytes, and perimeter outflow from the model domain. Additionally, the model simulates variably saturated conditions. Initial calibration was performed by manual adjustment of parameter values. Both steady-state and transient flow calibration were performed to estimate the hydraulic conductivity of the hydrogeologic units and faults, and estimate values of recharge and specific storage. Estimated hydraulic conductivities are assumed to decrease with depth due to gradual fracture closure.

## 6.5.2 Model Calibration

Calibration of the updated model has been optimized using PEST (Doherty, 2009). The simulation of steady-state pumping conditions was optimized relative to average 1995-1998 conditions, a period when SSFL groundwater extractions were fairly consistent. The optimization procedure involved the systematic adjustment of parameter values until the modeled state of the groundwater system—generally defined by hydraulic heads, head differences, and flows—best approximated those observed and interpreted for the site. Estimated parameters include bedding-parallel hydraulic conductivity, the anisotropy of hydraulic conductivity (i.e., bedding parallel versus bedding perpendicular), the effective hydraulic conductivity of faults, the decrease in hydraulic conductivity with depth, and recharge. In all, 599 parameter values were estimated. The optimized calibration best matches the model output based on five criteria related to observed aspects of SSFL groundwater system:

- Groundwater elevations at specific map locations and depths (i.e., heads).
- Groundwater elevation differences within well clusters and paired wells across stratigraphic or structural features (i.e., head differences).
- Flows to seeps and phreatophytes.
- Pumping well extraction rates.
- Percolation of discharged treated groundwater along site drainages.

The observations used for optimization include averaged head measurements and pumping rates for 1995-1998. Flows at seeps and water use by phreatophytes were estimated from more recent field data. Observations are weighted such that higher quality data (i.e., small variations in observed values; discrete measurement intervals; low measurement error; consistent period of measurement) receive greater weight. These weights also reflect the overall quality of each type of observation and the number of available observations. The weight ranking of data groups, in order of decreasing importance, is as follows: heads; head differences; pumping rates; and seep and phreatophyte discharge.

The resulting calibrated values of hydraulic conductivity are presented in Appendix 6-A, and are generally consistent with expected values for each lithologic type and the degree of geologic variability observed on-site. Estimates of spatially variable recharge range from 0 to 3.86 inches

per year, depending upon location at the site. The total for SSFL (Over 2850 acres) equates to 214 gpm. These values are also generally consistent with information presented above in Section 6.4.

A second model calibration has been performed to evaluate potential changes in recharge over time. Conditions in 1949 were simulated by 1) omitting pumping stresses and the associated discharge to drainages and 2) using hydraulic conductivity values estimated from the previous calibration (steady-state 1995-1998 conditions). Recharge values were estimated by matching the model output to pre-pumping water elevations in 12 water-supply wells. These water levels reflected the aggregate effects of hydrologic conditions at the site during the earlier time period. Consistent with the fact that average precipitation was lower during the 1949 timeframe relative to 1995-1998 (Section 6.3.1.3), the total site recharge estimated from this calibration was lower (90 gpm, or 3 percent of the long-term average precipitation) than that estimated for the more recent period.

The groundwater flow analysis presented in this report is based on updated model simulations that have been optimized, using the parameter estimation software PEST, to achieve the best-fit between observed and model-simulated water levels, head differences, groundwater seepage, and pumping rates. Optimization was performed on steady-state pumping (1995-1998) and non-pumping (1949) simulations. A historical simulation for 1949-2008 was completed based on the optimized steady-state models using externally estimated variable recharge.

### **6.5.3 Method of Evaluating Modeled Groundwater Flow**

Particle tracking is used to evaluate the three-dimensional groundwater flow system beneath SSFL. Particle tracking is a numerical modeling tool that can be used to evaluate the velocity and direction of groundwater flow under steady-state and transient conditions. The simulated three-dimensional head distribution and modeled hydraulic conductivity field are used to calculate the three-dimensional velocity distribution. Imaginary particles can then be placed at release locations within the model domain and their path traced either forward or backward. FEFLOW uses a fourth-order Runge-Kutta method to interpolate the three-dimensional velocity

field for particle tracking. In typical applications, porosity can be specified to evaluate advective travel times along the flow path (Darcy flux divided by porosity).

Particle tracking is used to illustrate SSFL groundwater flow directions and relative groundwater velocity using the Darcy flux. The dual porosity nature of the fractured rock at SSFL does not allow for specification of a single porosity value to represent groundwater flow velocities in the EPM model. The particle tracking presented in this report uses a default porosity of 1.0, which allows comparison of the Darcy flux (i.e., relative velocity) along flowpaths in different areas of the model. The particle tracks illustrated in this report are intended solely for the depiction of flow directions in a given model simulation. As such, the length of depicted particle tracks does not reflect contaminant transport distance or travel time.

For SSFL fractured-rock groundwater system, a discrete fracture network (DFN) model is used to represent appropriate transport mechanisms and analyze contaminant transport distance and travel times, as opposed to an EPM model. This work is documented in draft Appendix 8-A. The three-dimensional Darcy flux simulated by the FEFLOW model provides key input to the DFN model and serves to link the two analyses.

Forward particle tracking has been used to understand SSFL groundwater discharge areas, gain insight into variations in historical groundwater flow directions, and quantify the magnitude and variability of Darcy fluxes from source areas. Backward particle tracking has been used to evaluate the effectiveness of the groundwater monitoring network and identify areas contributing groundwater flow to seeps. Subsequent sections of this report use the results of particle tracking to help characterize groundwater flow and gain insight into contaminant distributions.

#### **6.5.4 Estimates of SSFL Groundwater Discharge**

Forward particle tracking has been used to evaluate groundwater discharge at SSFL and throughout the entire mountain-scale model domain. Sections 7 and 8 of Appendix 6-A provide a detailed description of this approach. In general, particles are released from the water table over a 50-meter grid and tracked through the simulated flow fields under both the steady-state pumping and non-pumping conditions. The particles are tracked to the point where they exit the

model domain and GIS is used to conduct spatial queries linking particle release and discharge locations. The results are color-coded for visual presentation.

Simulated discharge locations beneath SSFL under the steady-state pumping and steady-state non-pumping conditions are shown in Figures 6-32 and 6-33, respectively. Under the steady-state pumping condition, simulated groundwater discharge is influenced appreciably by extraction wells across broad areas of central SSFL (Figure 6-32). Additionally, this simulation indicates that groundwater in northwestern SSFL discharges to seeps and phreatophytes off-site to the north; groundwater in southwestern SSFL discharges to Bell Canyon seeps and phreatophytes; and most eastern and southern SSFL groundwater flows out the model perimeter along San Fernando Valley and Box Canyon. The steady-state non-pumping condition shown in Figure 6-33 indicates that the vast majority of SSFL groundwater discharges to seeps and phreatophytes off-site to the north and to Bell Canyon, and flows to the model perimeter boundaries along San Fernando Valley and Box Canyon. Some discharge is also simulated to seeps along Box Canyon in northeastern SSFL.

It is important to reiterate that these results reflect simulated flow conditions at infinite time (i.e., steady state), and that the three-dimensional groundwater flow model has been constructed, and its calibration optimized, to best represent the integration of geologic and hydrogeologic data collected at SSFL and its vicinity. When and where ever applicable, the understanding gained through groundwater modeling is considered in the context of the field data (e.g., contaminant distribution, seep sampling results, observed discharges). The flow model provides a means to understand both historic and future conditions of this complex system, particularly where the absence of data prevents the consideration of such conditions.

### **6.5.5 Additional Flow Analysis from Modeling**

Model results are presented in Sections 7 and 8 to analyze the following aspects of groundwater flow at SSFL:

**Forward Particle Tracking of Groundwater Flow from RI Areas:** Model results are used to illustrate and serve as a basis for discussing potential variations in flow directions and Darcy flux

under general pumping and non-pumping conditions. This analysis is based on forward particle tracking from multiple depths below RI sites. Particle tracking is applied to steady-state 'snapshots' of historical flow conditions to illustrate variations in flow direction within RI sites throughout SSFL's 60 year history. Results are presented in Section 7 and Appendix 6-A.

**Backward Particle Tracking to Areas Contributing Groundwater Flow to Monitoring**

**Wells:** This application of the model is used to illustrate and discuss the origins of groundwater flow to monitoring wells in various areas. These results help identify 1) wells that potentially monitor groundwater beneath RI sites under simulated steady-state pumping and non-pumping conditions. Results are presented in Section 7 and Appendix 6-A.

**Backward Particle Tracking in Areas Contributing Groundwater Flow to Seeps:**

This application illustrates and discusses areas contributing flow to seeps and flowing wells mapped in the model domain. The results are used to: 1) understand whether the seeps and flowing wells receive groundwater from on-site recharge areas; 2) identify seeps and flowing wells that potentially monitor groundwater beneath RI sites; and 3) interpret the origin of natural water chemistry sampled from seeps. Results are presented in Appendix 6-A and in Cherry, McWhorter, and Parker (2009).

**Specific Alternative Conceptualizations:** In this application, the model is used to optimize alternative conceptualizations, such as 1) continuous damage zones adjacent to faults and 2) higher rates of recharge. Results are presented in Appendix 6-A.

## 6.6 DATA GAPS

Section 6.3.4.4 identifies the following data gaps: The distribution of monitoring wells and hydraulic testing are insufficient for demonstrating the effect of the Burro Flats Fault and the Happy Valley Fault (east of RD-10) on groundwater levels and flow.

## **7.0 NATURE AND EXTENT OF CHEMICALS AND RADIONUCLIDES IN BEDROCK VADOSE ZONE AND GROUNDWATER**

This section describes the nature and extent of chemicals and radionuclides in the bedrock vadose zone and groundwater at SSFL. During the RCRA corrective action program, facility operations and areas potentially using chemicals have been identified as SWMUs and AOCs (SAIC 1994). These include operations or areas that have used, stored or handled various hazardous materials or substances and petroleum products. These areas have been grouped into RI sites (formerly called RFI sites in RCRA terminology) for evaluation. The locations of the RI sites are shown on Figure 2-2 and lie within each of the four administrative areas (i.e., Areas I, II, III and IV). The southern undeveloped area of SSFL has also been characterized in a separate RI group report (Group 10) although there were no known operational activities conducted there (CH2MHill, 2009a). Descriptions of confirmed sources of chemical releases are described in detail in the RI group and site reports and hence will not be presented in this report. The information contained in the surficial media group and site reports are incorporated into this groundwater RI report by reference.

### **7.1 CHEMICAL NATURE AND EXTENT INFORMATION CONTAINED IN SURFICIAL MEDIA RI REPORTS**

Material and information presented in surficial media site and group reports have been extensively used during the preparation of this report as these reports identify known or potential sources of chemical impacts to groundwater. As such, an overview of the surficial media characterization program is presented below.

Surficial media site and group reports include comprehensive reviews of historical documents generated during facility operations or in subsequent environmental investigations. This review is undertaken to identify chemicals known or suspected to have been used at each RI site along with the operational area at the site where these activities occurred. An overview of chemical use at SSFL is provided in Table 7-1.

The nature and extent of chemical impacts to groundwater have been evaluated for this groundwater RI report on a site-by-site basis for:

- Chemicals identified in surficial media RI site reports as a soil impact (soil matrix and soil vapor) exceeding soil screening levels;
- Chemicals identified in surficial media RI site reports as a groundwater impact exceeding groundwater screening levels;
- Chemicals recommended for further evaluation in the Feasibility Study (formerly referred to as the CMS) in the surficial media RI site reports; and
- Chemicals exceeding the groundwater screening levels described in Section 7.3.2 in the groundwater screening performed for this report.

Each chemical meeting any of the above conditions at an RI site were evaluated for that RI site. Monitoring wells were assigned to each RI site for this evaluation based on the assignments presented in the surficial media reports and on artificial group and RI site boundaries. Well assignments are presented in Table 7-2 and graphically depicted in Plate 7-1. The analysis of chemical impacts identified at RI sites is presented in detail in Appendix 7-A. Findings from this analysis and evaluation are used in the discussion of nature and extent of chemical impacts to the bedrock vadose zone and groundwater. A tabular summary of the findings is provided in Table 7-3.

## **7.2 NATURE AND EXTENT OF CHEMICAL CONTAMINANTS IN BEDROCK VADOSE ZONE**

The nature of contaminant releases to, and their transport through, the bedrock vadose zone is discussed below. A description of the available characterization results follows. It is important to recognize that the thickness of the bedrock vadose zone has varied over time at SSFL due to both natural conditions and anthropogenic activities and is not a static condition. The vadose zone thickness has been and will continue to be affected by annual fluctuations in recharge associated with varying precipitation events (longevity and intensity). Historical activities that have affected the thickness of the bedrock vadose zone include operational releases of water to support the mission of SSFL coupled with the extraction of groundwater for the same and subsequently for groundwater interim measures and characterization (i.e., pumping tests). Both have varied over time. Operational discharges have ceased and groundwater extraction since

2000 has been minimal as the shutdown of various extraction wells was required to support the characterization program. Thus, discussions as to the vadose zone thickness and the number of samples collected and analyzed from the vadose zone in the following sections of this report need to be considered in this context.

### **7.2.1 Nature of Releases and Contaminant Transport in the Bedrock Vadose Zone**

Table 7-1 presented a summary of chemical use and release mechanisms for the chemicals known to have been used or generated at SSFL. Contaminant phases released to, or beneath, the ground include solids (e.g., perchlorate salts), liquids (e.g., TCE and other solvents and fuels), gases (secondary releases from volatile liquids) and solutes (e.g., chemicals dissolved in operational discharge waters, surface water or recharge). Conceptual descriptions of the transport of these contaminant phases follow.

Throughout the history of operations at SSFL, VOC transport within the bedrock vadose zone at SSFL likely occurred in one or more of three different forms: gaseous-phase diffusion due to small releases at or just beneath the ground surface; dissolved-phase carried by recharge waters, surface waters, or seepage beneath ponds containing dissolved VOCs in operational discharges; or as an immiscible-phase from large and/or persistent releases of primarily TCE. TCE dense non-aqueous phase liquid (DNAPL) releases would have initially flowed through the alluvium or colluvium (where present) then into the fracture network where it spontaneously imbibed into the unsaturated bedrock matrix. TCE DNAPL penetration into the unsaturated rock matrix was restricted due to the relatively high vadose zone water content (i.e., ~70 percent on average). Equilibrium partitioning of the VOCs in the vadose zone bedrock has occurred, resulting in the exchange of mass between the vadose zone porewater, air, and sorption onto natural organic matter. Decades have passed since most releases of VOCs occurred. Currently, the vast majority of VOC mass is present in the rock matrix blocks of the vadose zone, with very little being present in the fracture network. VOC concentrations in the fracture network are in close equilibrium with concentrations present in the rock matrix near the fracture faces. Depending upon the transport mechanism and matrix block size, VOCs may be present throughout the unsaturated rock matrix or have penetrated into them a distance of a meter or more.

For contaminants that are not volatile (i.e., no gaseous phase diffusion) or enter the vadose zone as a separate phase (i.e., no DNAPL or light non-aqueous phase liquid [LNAPL] flow), transport of the contaminants will occur through recharge waters flowing primarily through the bedrock matrix block, as further explained in the complementary Site Conceptual Model document (Cherry, McWhorter and Parker, 2009).

### **7.2.2 Extent of Chemical Impacts**

Available data that characterize contaminants in the bedrock vadose zone include rock core sampling results for VOCs, extractable fuel hydrocarbons and perchlorate. Rock core sampling locations are shown in Figure 7-1 and sampling summaries are provided in Tables 7-4 and 7-5. Individual sample results are provided in searchable electronic format as an attachment in Appendix 7-A (i.e., database (Microsoft Access) or spreadsheet (Microsoft Excel)). Samples were collected at most of these locations from both the vadose zone and below the water table. All locations where bedrock samples have been collected for contaminant characterization are discussed below even though vadose zone samples were not collected from some locations as the data will be used in subsequent sections of this report.

Rock core samples have been collected from coreholes and well installations that have been installed for two primary purposes that include:

- Source zone characterization: These coreholes have been drilled at various locations throughout SSFL where chemicals entered the subsurface and include: 11 shallow groundwater coreholes that were subsequently converted to piezometers, and 12 deep bedrock coreholes as follows: RD-35B (IEL RI site), RD-46B (CTL-III RI site), C-1 (IEL RI site), C-2 (Canyon RI site), C-3 (LET/CTL-I RI site), C-4 (Bowl RI site), C-5 (Alfa RI site), C-6 (Delta RI Site), C-7 (ELV RI site), C-8 (FSDF RI site) and C-9 (B-1 RI site). Samples have been collected at all of these locations for VOC characterization and some for hydrocarbon characterization (C-1 through C-7). Rock core samples have also been collected at RD-77 for perchlorate characterization. Vadose zone rock core samples were collected from all 23 of these locations.
- Four additional coreholes were drilled to create a transect through a groundwater source area in the northeast portion of SSFL at the IEL RI site. Two previous coreholes (RD-35B and C-1) were supplemented with rock core collection from four additional locations (RD-31, RD-35C, C-10 and C-11). However, vadose zone samples were collected from only C-11 and analyzed for both VOCs and perchlorate.

- Plume characterization: Three coreholes were drilled to create a transect across the groundwater plume in the northeast portion of SSFL (C-12, C-13 and C-14). Vadose zone samples were collected from each of these locations and analyzed for VOCs.
- Rock core samples were also collected from four other locations that were drilled to characterize areas suspected to have possibly transported perchlorate. Vadose zone samples were collected and analyzed for perchlorate at RD-75, RD-76, RD-78 and RD-80.
- Two coreholes, C-16 and C-17, were drilled at the leading edge of the groundwater contaminant plume in the northeast portion of SSFL. Vadose zone samples were collected from C-16 to evaluate the potential occurrence of VOCs in a perched zone that is transient where sample results from a monitoring well (RD-39A) have shown sporadic low level detections of TCE.

Characterization of VOCs in the vadose zone bedrock has primarily targeted five chlorinated ethenes that include: TCE, cis- and trans-isomers of 1,2-dichloroethene (DCE), 1,1-DCE; and chlorofluorocarbon (CFC)-113. A subset of samples (about 5 percent) was also analyzed for a full suite of compounds included in EPA analytical method 8260. The list of 8260 compounds and their corresponding rock porewater detection limits is provided in Table 7-6. Two additional VOCs, chloroform and 1,1,1-TCA, were added to the rock core analytical suite when corehole C-6 was deepened from its original depth and for subsequent coreholes that were drilled starting with C8. Carbon tetrachloride was added to this set of eight VOCs for coreholes C-12 through C-15.

Samples were also collected and analyzed for extractable fuel hydrocarbons to the initial completion depths at coreholes C-1 through C-7. Coreholes C-1 and C-6 were both subsequently deepened but samples were not analyzed for extractable fuel hydrocarbons as the sampling results from the initial coring showed this constituent to have been present in only a few samples as will be later discussed. Extractable fuel hydrocarbon (EFH) was measured however as a target analyte in the EPA method 8260 list (i.e., in 5 percent of the samples).

The bedrock vadose zone has been characterized for perchlorate through the collection and analysis of rock core or drill cuttings from 6 locations (RD-75 through RD-78, RD-80 and corehole C-11). Locations where the bedrock vadose zone has been characterized are shown in Figure 7-2 and a sampling summary is provided in Table 7-5.

### 7.2.2.1 Summary of Chlorinated Ethene Sample Results

Much has been previously written about the nature and extent of chlorinated ethenes in rock porewater as described in the following reports:

*Evolution of TCE Source Zones and Plumes in the Chatsworth Formation Groundwater, Santa Susana Field Laboratory*, Parker and Cherry, 2000 (Appendix E in Montgomery Watson, 2000)

*Final Report, Source Zone Characterization at the Santa Susana Field Laboratory: Rock Core VOC Results for Core Holes C-1 through -C7* (Hurley et al., 2007a).

*Rock Core VOC Results for Corehole C-8: Source Zone Characterization at the Santa Susana Field Laboratory Addendum Report No. 1* (Hurley et al., 2007b).

*Rock Core VOC Results for Corehole -C9 (RD-84): Source Zone Characterization at the Santa Susana Field Laboratory Addendum Report No. 3* (Hurley et al., 2007c).

*Phase 2 Northeast Area Groundwater Characterization Technical Memorandum* (Parker et al., 2008)

The latter four of these five reports provide figures depicting the distribution of VOCs detected in the source zone and plume front corehole locations. These figures are provided in Appendix 7-B. Individual sample results are depicted in these figures for both chlorinated ethenes and the minor constituents detected at each location.

The rock core sampling results from each sampling location were separated into intervals where samples were collected from the vadose zone and below the water table (at the time the coreholes were drilled). The results are provided in Table 7-7. Sampling results discussed below are all presented in equivalent rock porewater concentrations in units of micrograms per liter and should be considered as approximate values due to the assignment of standard parameters that are used to calculate the equivalent porewater values. The methodology used to calculate these values is discussed in the reports identified above in the previous paragraph.

Locations where the maximum porewater concentration of a chlorinated ethene occurred in the vadose zone are shown below. As shown, the maximum porewater concentrations of parent chlorinated ethenes (i.e., PCE and TCE) measured in the vertical profile occur in the vadose zone at RD-46B, C-1, C-3, C-8, C-9 and C-11. Note, however, that the range in maximum concentrations between locations where detected varied over a factor of more than 200,000

(i.e., TCE maximum of 243,612 micrograms per liter ( $\mu\text{g/L}$ ) at C1, to four locations with no detects: RD-35B, C-12, C-14, and PZ006). This variability reflects the position of the corehole relative to the input location or in the plume. Alternately, the maximum concentrations of all chlorinated ethenes were found in the groundwater at C4, C6 and C7. TCE and 1,1-DCE were the chlorinated ethenes found most frequently at higher concentrations in the vadose zone than in the groundwater.

Location	Chlorinated Ethene				
	PCE	TCE	cDCE	tDCE	1,1-DCE
RD-35B					
RD-46B					
C-1					
C-2					
C-3					
C-4					
C-5					
C-6					
C-7					
C-8					
C-9/RD-84					
C-11					
C-12					
C-13					
C-14					
C-16					
PZ004					
PZ006					
PZ007					
PZ008					
PZ012					
PZ013					

Location	Chlorinated Ethene				
	PCE	TCE	cDCE	tDCE	1,1-DCE
PZ014					
PZ015					
PZ016					
PZ017					
PZ018					
Shading indicates maximum concentration of ethene occurred in vadose zone samples.					

Cumulative mass plots of equivalent TCE in rock porewater were also presented in Hurley et al. (2007a, b and c) and Parker et al. (2008a). Available cumulative mass plots for each location where both vadose zone and groundwater samples were collected are presented in Figure 7-3. The distribution of TCE in the vadose zone relative to that below the water table is also summarized in Table 7-7. As can be seen in the figure and table, the relative mass contribution of TCE in the unsaturated zone to the total mass profile within the coreholes is highly variable and ranges from a low of 1 percent in corehole C-6 at the Delta RI site in Area II to 95 percent at C-8 at the FSDF RI site in Area IV. Various factors affect this distribution and include: the total completion depth of the corehole, the thickness of the vadose zone, the distance from the input location, the total mass released into the ground, and the penetration of immiscible phase TCE below the water table.

### 7.2.2.2 Summary of Other VOCs Characterized at University Laboratories

#### 1,1,1-TCA

1,1,1-TCA was detected in three samples from corehole C-9, but at concentrations that could not be quantified because they were too low. Detections occurred at depths of 22 and 29 feet. It was not detected in any other rock core vadose zone samples from the source characterization coreholes.

Chloroform

Chloroform was found in five coreholes. Most of the concentrations detected were close to the method detection limit (MDL) and similar to what was observed in many of the blanks. This indicates that these detections may be the result of cross-contamination during storage and/or prior contamination of methanol used to decontaminate sampling equipment. Detections in the vadose zone included:

Location	Number of Vadose Zone Samples	Number of Detects	Average Concentration (µg/L)	Minimum Concentration (µg/L)	Maximum Concentration (µg/L)
C-9	91	76	4.3	1.1	12
C-11	205	74	4.0	1.1	7.4
C-13	138	7	9.0	3.7	13
C-14	135	5	15	1.4	32
C-16/C-17	42	2	3.3	2.4	4.2

CFC-113

CFC-113 was detected in vadose zone samples from nine source zone coreholes. A summary of the CFC-113 vadose zone detections is as follows:

Location	Number of Vadose Zone Samples	Number of Detects	Average Concentration (µg/L)	Minimum Concentration (µg/L)	Maximum Concentration (µg/L)
C-1	56	42	287	2.6	3,940
C-2	74	24	2.4	0.7	13
C-3	309	8	1.2	0.1	2.2
C-4	80	9	4.4	0.1	22
C-5	149	3	2.5	0.2	5.5
C-8	68	8	600	21	2,630
C-9	91	1	2.6	NA	NA
C-11	205	5	2.4	1.1	4.0
C-13	138	1	0.7	NA	NA
PZ004	13	3	1.3	2.9	6.1

Location	Number of Vadose Zone Samples	Number of Detects	Average Concentration (µg/L)	Minimum Concentration (µg/L)	Maximum Concentration (µg/L)
PZ006	2	2	12	5.3	18
PZ007	11	8	62	6.7	154
PZ008	26	8	55	5.1	353
PZ012	5	4	84	1.7	203
PZ013	9	8	120	31	277
PZ014	17	8	104	0.5	321
PZ015	8	8	8390	6.0	24,900
PZ016	22	6	3.0	1.3	6.4

These data indicate that CFC-113 is a minor contaminant in 5 of the 9 coreholes, and 8 of the 9 piezometers, with appreciable concentrations being encountered in C-1, C-8, and PZ015. Most of the higher concentrations detected in C-1 are within 20 feet of the water table. Alternately, all of the detections at C-8 are within 20 feet of the ground surface and appreciably above the Chatsworth Formation groundwater (i.e., more than 100 feet above).

### 7.2.2.3 Summary of EPA 8260 Target Analytes

The only other VOCs that were encountered in the vadose zone samples from the source zone characterization coreholes were chlorobenzene, 1,4-dioxane, toluene, 1,1-dichloroethane (DCA), and isopropylbenzene. Chlorobenzene was detected in five samples from C-1 between depths of 16 and 32 feet at concentrations that ranged between 240 and 293 µg/L. It was also detected in a single sample at both C-2 and C-4.

1,4-dioxane was encountered in the bedrock vadose zone in samples from C-1 through C-5, and piezometers PZ008, PZ014, and PZ016. Detections in the vadose zone included:

Location	Number of Vadose Zone Samples	Number of Detects	Average Concentration (µg/L)	Minimum Concentration (µg/L)	Maximum Concentration (µg/L)
C-1	9	3	241	228	252
C-2	3	1	211	NA	NA

Location	Number of Vadose Zone Samples	Number of Detects	Average Concentration (µg/L)	Minimum Concentration (µg/L)	Maximum Concentration (µg/L)
C-3	19	11	269	150	369
C-4	4	1	221	NA	NA
C-5	6	2	362	194	528
PZ008	2	1	1650	NA	NA
PZ014	1	1	132	NA	NA
PZ016	1	1	594	NA	NA

There were no other detections of 1,4-dioxane.

1,1-Dichloroethane was detected in one vadose zone sample at PZ007 (774 µg/L at 8 feet). Toluene was detected in one vadose zone rock sample from C-2 (375 µg/L at 81 feet) and C-7 (542 µg/L at 36 feet), and two samples at PZ008 (5337 µg/L at 49 feet and 22,233 µg/L at 66 feet). Toluene was also detected in the vadose zone at C-3 as follows:

Number of Vadose Zone Samples	Zone	Number of Detects	Average Concentration (µg/L)	Minimum Concentration (µg/L)	Maximum Concentration (µg/L)
20		8	596	265	1010

There were no other detections of toluene in vadose zone samples at the other coreholes.

Isopropylbenzene was encountered in one sample from corehole C-9 at a depth of 33 feet.

#### 7.2.2.4 Summary of Extractable Fuel Hydrocarbon Results

EFH was detected in vadose zone samples at only three source characterization coreholes, C-2, C-3 and C-9 (RD-84), and two piezometers PZ004 and PZ017. It was encountered in a total of six samples at two depth intervals (33-35 and 67-70 feet) at corehole C-2, with a maximum estimated porewater concentration of 8,600 µg/L (average of 5 samples: 4,028). At corehole

C-3, EFH was encountered in 2 vadose zone samples at depths of 28 and 44 feet at estimated concentrations of 647 and 10,100  $\mu\text{g/L}$ , respectively. At corehole C-9, EFH was detected in one of seven vadose zone samples at a depth of 33 feet and an estimated concentration of 1,120  $\mu\text{g/L}$ . At piezometer PZ004, EFH was detected in one vadose zone sample (of 13 samples) at a depth of 15 feet and a concentration of 21,900  $\mu\text{g/L}$ . At piezometer PZ017, EFH was detected at a depth of 12 feet at a concentration of 2,340  $\mu\text{g/L}$ .

### **7.2.2.5 Summary of Perchlorate Results**

Perchlorate was detected in bedrock vadose zone samples at source characterization location RD-77 (H&A, 2004). Perchlorate was detected in 20 of 71 vadose zone samples with the maximum concentration encountered in the bedrock vadose zone (150  $\mu\text{g/L}$  at a depth of 75 feet). The perchlorate rock porewater profile for RD-77 is provided in Appendix 7-B.

At locations drilled to characterize potential areas where perchlorate may have been transported via surface water or groundwater, it was not detected in vadose zone samples at RD-78, RD-80 or C-11. At RD-75, perchlorate was detected in 1 of 84 vadose zone samples at an estimated concentration of 1.5  $\mu\text{g/L}$ . At RD-76, perchlorate was detected in 2 of 31 vadose zone samples at concentrations of 3.6 and 4.4  $\mu\text{g/L}$ .

### **7.2.3 Summary of Vadose Zone Characterization**

A summary of the vadose zone rock core sample results is presented in Table 7-8. In summary, TCE is the primary contaminant of concern both in terms of the magnitude of measured concentrations and the frequency of detections found in the analysis of rock core vadose zone samples. TCE was detected at concentrations above the limit of quantitation in 958 of 1,580 rock core samples from the vadose zone (61 percent). The mass of equivalent TCE mass in the vadose zone relative to that below the water table also varies considerably ranging from a low of 1 percent to a high of 95 percent. Various factors affect this distribution and include: the total completion depth of the corehole, the thickness of the vadose zone, the distance from the input location, the total mass released into the ground, and the penetration of immiscible phase TCE below the water table. PCE was also frequently detected (52 percent of the samples) but at much lower concentrations. Two of the three DCE isomers (cDCE, and 1,1-DCE) were also

frequently detected in vadose zone rock core samples (20 percent and 22 percent, respectively), but again at much lower concentrations than TCE.

Minor detections of 1,4-dioxane, an acid scavenger for 1,1,1-TCA were also found in the vadose zone. 1,4-dioxane was encountered in 36 percent of the vadose zone samples at C-3 and was a minor contaminant at the other locations. However, 1,1,1-TCA was only detected in three vadose zone samples (from C-9). CFC-113 was found in 75 percent and 12 percent of the vadose zone samples from C-1 (also location of maximum concentration) and C-8, respectively, and was a minor contaminant at the other locations. Perchlorate was found in 31 percent of the vadose zone samples in RD-77, but was detected in only 3 other of the 243 vadose zone samples analyzed (at or below its screening level of 6 µg/L). The other analytes (chlorobenzene, toluene, isopropylbenzene, and EFH) that were detected in vadose zone rock core samples were found infrequently and are of minor importance relative to the chlorinated ethenes. Finally, it should be noted that about 45 other 8260 analytes were not detected in any vadose zone bedrock samples.

### **7.3 NATURE AND EXTENT OF CHEMICAL IMPACTS TO SSFL GROUNDWATER**

Data that are available to assess the nature of chemical impacts to SSFL groundwater include information on sources above the water table from the surficial media site reports and below the water table from the rock core sampling results (i.e., DNAPL flow). The rock core sampling results also provide data that can be used to assess the extent of impacts to groundwater. The majority of available data to assess the extent of groundwater impacts comes from the collection and analysis of water level measurements and groundwater samples from SSFL's monitoring network and samples from seeps. Individual sample results are provided in searchable electronic format as an attachment in Appendix 7-A (i.e., database (Microsoft Access) or spreadsheet (Microsoft Excel)).

#### **7.3.1 Nature of Chemical Impacts to Groundwater**

Sources of chemical impacts in surficial media to groundwater have been identified in the surficial media RI site reports as discussed in Section 7.1. Locations where sample results

indicate that chemicals in surficial media are likely sources to groundwater will be identified later in this section where the extent of chemical impacts is described for each individual chemical.

Additionally, there are areas where impacts may have occurred based on historical site activities or operational history, but where the potentially impacted unsaturated lithologies were removed due to excavation, closure or interim measure activities and hence were not sampled. Excavated areas include:

- Building 4021 leach field excavation (1978)
- Area I Burn Pit cleanup (1981)
- Closure of nine surface impoundments that are under post-closure care (1989)
- Advanced Propulsion Test Facility (2 impoundments)
- Alfa-Bravo Skim Pond (1 impoundment)
- Storable Propellant Area (2 impoundments)
- Engineering Chemistry Lab (1 impoundment)
- Delta Skim Pond (1 impoundment)
- Systems Test Laboratory IV (2 impoundments)
- Accelerated site cleanups (1993)
- All Ash Pile; LETF fluoride; arsenic at EEL; and the LOX clarifier removal (metals, total petroleum hydrocarbons [TPH] and VOCs).

Interim measure actions at:

- Happy Valley - Interim Measure #1 for excavation or detonation and removal of unexploded ordnance (1999) and Interim Measure #2 for excavation and off-site disposal/on-site treatment for perchlorate (2003)
- Building 359 - for in situ treatment or excavation and off-site disposal/on-site treatment for perchlorate (2003-2006)
- Building 203 - for removal of mercury from surface soils (2004)
- Former Sodium Disposal Facility - excavation and off-site disposal for radionuclides (1992/93), and excavation and off-site disposal for mercury, polychlorinated biphenyl (PCBs) and polychlorinated dibenzodioxins (PCDD)/dioxins and furans (DFs) (2000)
- Result of ISE (imminent and substantial endangerment order)

- LOX debris area in 2008
- Northern Drainage clay pigeon

These features are shown in Figure 7-4 and will also be displayed in the figures that depict results used to evaluate the extent of impacts for individual chemicals later in this section.

Chlorinated solvents present a separate and distinct potential source of impacts to the groundwater system due to their physical characteristics of being able to penetrate through the groundwater as a DNAPL. The significance of the nature of this type of release has been evaluated in detail and is presented in the complementary Site Conceptual Model document (2009).

The nature of the transport of chemicals to the groundwater system is similar to that described in Section 7.2.1 except that imbibition of DNAPL and gaseous phase diffusion do not occur in the saturated zone.

### **7.3.2 Groundwater Data Screening**

Groundwater samples collected from the groundwater monitoring network through the second quarter of 2008 were used in characterizing the nature and extent of chemical impacts to groundwater. The groundwater monitoring network includes off-site locations and a complete list of locations is presented in Table 7-2. The SSFL groundwater database was accessed on October 10, 2008 and the data set was “frozen” as of this date to provide sufficient time to analyze and evaluate the analytical results. Groundwater sampling results for individual chemicals are compared to screening levels (RWQBC, 2008) based on the following descending order of priority:

- Primary Maximum Contaminant Levels (MCLs) promulgated by the Safe Drinking Water Act (SDWA) and 22 CCR, sections 64431 through 64449 and 64672 (listed as Primary MCL and Cal MCL in report tables);
- Regulatory action levels (RALs) for lead and copper;
- Notification levels (NLs);
- Archived advisory levels (AALs);

- Secondary Maximum Contaminant Levels (SMCLs) which address aesthetics, such as taste and odor (listed as Secondary MCL in report tables);
- Site-specific values developed by DTSC (i.e., groundwater comparison concentrations for metals) (listed as SSFL Comparison in report tables), and
- Site-specific values developed for SSFL using risk assessment procedures assuming direct ingestion of groundwater (listed as SWGW RBSL (site-wide groundwater risk-based screening level) in report tables).

Appendix 7-C contains a technical memorandum describing the methodology used to develop the risk-based screening values for chemicals that are not metallic elements and where there are no agency-published values. Screening values for all chemicals or elements where such values were either available or developed specifically for this report are presented in Table 7-9. This comparison was partially performed as an assessment independent of the surficial media characterization work in that some chemicals either do not persist in surficial media (e.g., formaldehyde) or are transformed from a parent product in the groundwater system (e.g., 1,4-dioxane from 1,1,1-TCA).

Results of this screening evaluation for the historical groundwater data (i.e., data through June 2008) are presented in Table 7-10 and summarized in a diagram in Figure 7-5. There are a total of 529 analytes in the entire historical SSFL groundwater data set, not including radionuclides, which are evaluated separately in Section 7.4. Note that analytes were counted by names as listed in the groundwater database, thus both non-specific “totals” analytes and their individual isomers are counted separately (e.g., 1,2-DCEs and its cis- and trans- isomers). Analytes with dissolved and totals results were also counted separately. Two hundred three of these 529 analytes had regulatory agency-published screening values or site-specific values developed by the DTSC, of which 145 have been detected in at least one groundwater sample collected from the monitoring network. One hundred eleven of the analytes with agency-established screening values were detected in at least one groundwater sample at concentrations exceeding the screening values. Sixty-four were detected in at least one groundwater sample at concentrations exceeding agency-established screening values in samples collected from the third quarter monitoring event of 2007 through the second quarter monitoring event of 2008 (i.e., between July 1, 2007 and June 30, 2008). This timeframe is defined as the “recent” data set and is intended to represent current conditions defining the nature and extent of

chemical impacts. Results of the data screening for the “recent” period are summarized in Table 7-11.

Certain analytes that are not groundwater contaminants were removed from this list of analytes, leaving 47 analytes that present a concern to groundwater at SSFL. Analytes not appropriate for groundwater evaluation include total metals, non-specific analytes (e.g., 1,2-DCE versus the cis- and trans-isomers), and general water quality parameters. For metals, only the dissolved (i.e., filtered) results were evaluated.

There were 326 analytes with no agency-established screening values. One hundred thirty-five (135) of these 326 analytes had detections and were evaluated by screening the results against RBSLs that were developed for SSFL as outlined in Appendix 7-C. Groundwater RBSLs were developed for 62 of the 135 analytes with detections and no agency-established screening values. The 100 analytes for which groundwater RBSLs were not developed are either: not typically considered to be a human health concern, have no toxicity values, or are non-specific analyte for which a specific individual analyte was available. Some of these individual analytes were evaluated by including them into a toxicity equivalency quotient (TEQ) (e.g., dioxin congeners combined into a 2,3,7,8-TCDD TEQ). Nineteen (19) of the 62 analytes for which groundwater RBSLs were developed were detected in at least one sample above the screening levels in the historical data set. None of these 19 analytes were detected at concentrations exceeding their screening level in the July 2007 through June 2008 data set.

### 7.3.3 Groundwater Evaluation

The groundwater screening results were used to identify chemicals of concern for which to perform a focused site-wide evaluation on chemical extent in this report. The following eighteen chemicals were identified and site-wide maps of their spatial distribution were developed for each as an aid in defining their extent:

- Chlorinated solvents (12):
- Chlorinated ethenes (6): PCE, TCE, cDCE, tDCE, vinyl chloride, and 1,1-DCE;
- Chlorinated ethanes and by-products (4): 1,1,2,2-tetrachlorethane (PCA), 1,2-DCA, 1,1-DCA, 1,4-dioxane;

- Chlorinated methane (1): carbon tetrachloride;
- Chlorinated propane (1): 1,2,3-trichloropropane;
- Non-halogenated organics (2): formaldehyde and TPH ;
- Semi-volatile organic compounds (1): n-nitrosodimethylamine; and
- Inorganics (3): perchlorate, nitrate and fluoride.

This list is comprised of chemicals detected at concentrations exceeding screening values at five or more locations in recent data and chemicals detected at concentrations exceeding screening values at five or more locations historically, but not in recent data due to limited sample coverage in recent data. Chemicals with concentrations historically exceeding screening values at five or more locations but having adequate sampling coverage in recent data to indicate the chemical is no longer present at concentrations above the screening level (e.g., 1,1,1-TCA, chloroform, and benzene) were not included. Chemicals that are common laboratory contaminants (e.g., methylene chloride and bis(2-ethylhexyl)phthalate) and those that are naturally occurring and for which there is no known site-related anthropogenic source (e.g., sulfate) were also not included, even if they had concentrations exceeding screening values at five or more locations. Although site-wide data displays have not been developed for all of the other chemicals that exceed groundwater screening levels, their extent is also considered and evaluated in this section (see Sections 7.3.5.19 and 7.3.5.20).

Note that there are off-site wells included in SSFL groundwater monitoring network that do not appear on the site-wide maps as they lie at distances far enough from site boundary that they fall off the edge of the view of the map. These locations are listed as “off-site” in Table 7-2 and are not assigned to any reporting group.

#### **7.3.4 Content of Maps Depicting Chemical Extent Data**

The groundwater results are presented on plan view maps for each of these 18 chemicals along with locations where impacts have been identified in surficial media (Plates 7-2 through 7-19).

Groundwater monitoring locations within SSFL and in the immediate perimeter around SSFL have been displayed on each plate. These include wells/piezometers that have historically been identified as “near-surface” monitoring locations (i.e., those that are screened within granular

lithologies and/or weathered bedrock), wells that have historically been identified as “Chatsworth Formation” monitoring locations (i.e., those that are screened predominantly in the unweathered portions of the Chatsworth Formation bedrock), and locations identified as springs or seeps. Monitoring locations where groundwater is perched above (i.e., separated by an unsaturated zone) the regional water tables are identified using a different symbol. Note that perched groundwater can be a transient condition. All groundwater monitoring locations and historical extraction wells are displayed on the plate independent of their completion interval as a function of depth. All locations are included on this plate based on the assessment of the groundwater flow system, which shows that any perched groundwater present at SSFL flows into the regional Chatsworth Formation groundwater.

Groundwater sampling results in the plan view maps show both “recent” and “historical” sampling information. “Recent” data is defined as results from samples collected from the third quarter 2007 through the second quarter 2008 (between July 1, 2007 and June 30, 2008). “Historical” data is defined as all historical data collected at SSFL through second quarter 2008 (through June 30, 2008). Groundwater monitoring locations are color-coded to indicate (from lowest to highest priority) non-detects, detections below the screening level, and detections exceeding the screening level for maximum concentrations in recent and historical data. Locations where the detection limit exceeded the screening level for all results at that location are also noted. Colors posted at each monitoring location are based on the maximum concentration in the recent dataset if sampled during that timeframe and on the historical maximum concentration if no analytical results in the recent dataset were available. For wells with multiple vertically-discrete sampling locations, the color representing the maximum concentration detected in the vertical profile is depicted. Results posted at each groundwater monitoring location beneath the location ID are the concentration value and date for the most recent analytical result.

Additionally, tabulated results are also provided on the plan view maps for monitoring locations where sampling results have exceeded screening values in historical and recent data. The tabulated results show the maximum concentration detected in both “historical” and “recent” sampling results. This allows for an assessment to be made as to the concentration trend over

time. Note that the maximum results reported here do not match the most recent results posted beneath the location IDs unless the maximum result occurred in the most recent sample collected at a location. Likewise, colors posted at each monitoring location may not correspond with the posted most recent results depending on whether the most recent result type matches the maximum result type (exceeding screening level (SL), detected below SL, or not detected).

Well data sheets have been prepared for nearly all locations with ES-, RS-, SH-, WS-, RD- and HAR- prefixes and are presented on well data sheets provided in Appendix 7-D. The well data sheets depict the well construction and stratigraphic completion information for each of these locations. These data sheets also show hydrographs and chemical concentrations over time for halogenated ethenes, ethanes and methanes. The information presented on these well data sheets should be used in conjunction with the data and information displayed on these plan view maps to obtain a full understanding of the variability in chemical concentrations over time and with varying hydraulic head at any location of interest.

Statistical probability distribution plots are included on the upper right corner of the plates depicting the maximum concentration detected in each groundwater monitoring location in the historical dataset. All groundwater monitoring locations in SSFL monitoring network, on-site and off-site, are included. Only locations where the chemical has been detected are presented on these plots. Locations where the chemical has not been detected in any sample have been excluded from these plots.

Surficial media data presented on the plates include soil matrix and soil vapor results and FS areas. The highest concentration soil matrix or vapor result measured in the vertical profile at each sampling location is displayed. "FS Areas" are areas that have been identified for further evaluation in the Feasibility Study. Shapes identified as FS areas for surficial OU Groups 1A, 4, 5, 6, 7 and 8 (shaded yellow) encompass areas comprising elevated concentrations of the specific chemical displayed on the plate. Shapes for surficial OU Groups 2 and 3 (shaded yellow) include the area within the RI site boundary, as more specific areas of elevated concentrations were not identified. FS Areas for Group 9 have not been included, as the report was submitted just prior to this report and there was insufficient time to incorporate its findings.

This approach of combining recent and historical groundwater data locations in a plan view map along with temporal variability in graphs for many locations allow for one to interpret the extent of the chemical impacts in both space and through time.

### **7.3.5 Extent of Chemicals in Groundwater**

Analysis of surficial media, rock core and groundwater data show that TCE is detected frequently in all media and at concentrations well above its screening level. Historical records also indicate it was used extensively throughout SSFL to support its mission of testing rocket engines, particularly in the late 1950's and early 1960's as reported in CH2MHill (1993). As such, its extent in the groundwater will be the first presented and will be used as a basis for comparison for the extent of subsequent chemicals.

#### **7.3.5.1 Extent of TCE in Groundwater**

##### Sources to Groundwater

In summary, TCE was encountered in surficial media at concentrations above RBSLs at 29 RI sites and was recommended for further evaluation in the feasibility study for surficial media at 23 RI sites and at one additional RI site under VOCs as a group. Areas recommended for further evaluation in the feasibility study are shown in yellow in Plate 7-2 along with soil matrix, soil vapor and groundwater sampling results. TCE has reportedly been released to the ground at SSFL in large volumes at the six former test stands (CH2MHill, 1993). These test stands occur at the Canyon, Bowl, Alfa, Bravo, Delta and Coca RI sites. A detailed assessment of groundwater impacts at the locations that have been characterized by rock core sampling results is presented in the complementary Site Conceptual Model document (Cherry, McWhorter, and Parker, 2009).

The RBSLs were evaluated for protection of groundwater by modeling the transport of TCE from vadose zone soils to groundwater using the modeling code SESOIL as presented in Appendix 7-F. The ECL RI site was chosen for modeling the transport of chemicals from the vadose zone because of the shallow depth to groundwater (~10 feet bgs). Hence, modeling results from this location are expected to be protective of other RI sites where groundwater is

encountered at greater depth. The transport of other chemicals was similarly modeled and results are presented in Section 8 along with a description of the modeling effort.

Additional locations where sources are suspected but were not confirmed by surficial media sampling results include the following RI sites: Building 204 in Area II, Bldg 65 metals clarifier, SNAP, Bldg 56 landfill, and the Bldg 009 leach field (excavated in 1978), all in Area IV. Surficial media sampling results may not indicate the presence of historical releases as certain areas may not have been sampled due to the lack of soil or because sufficient time has lapsed whereby the mass remaining in the soil profile has been transferred either deeper into the subsurface or volatilized to the atmosphere.

### Groundwater Sampling Summary

TCE has been sampled in groundwater at 485 locations at SSFL of which it has been detected on at least one occasion at 337 locations and exceeded the screening level of 5 µg/L at 239 locations with a maximum concentration of 110,000 µg/L at RD-35A at the IEL RI site. In the July 07/June 08 dataset, TCE was sampled in groundwater at 182 locations, detected at 107 locations, and exceeded the screening level at 71 locations, with a maximum concentration of 16,000 µg/L at WS-9 at the Bravo RI site.

### Lateral Extent of TCE in Groundwater

Data used to evaluate the lateral extent of TCE in groundwater include sampling results from the monitoring well network and from seeps. Plate 7-2 depicts the locations from which samples have been collected and analyzed for TCE along with concentration data. The data indicate that boundaries encompassing concentrations of TCE in excess of the screening level of 5 µg/L can be drawn over eight distinct areas of the site. Table 7-12 presents information on each of the eight areas of impacted groundwater and these areas are graphically summarized in Figure 7-6. In summary, about 626 acres of land are estimated to contain groundwater at concentrations above the screening level for TCE. Other noteworthy observations about the distribution of TCE in groundwater include:

- Concentrations in well WS-9 have increased appreciably since groundwater extraction from this well stopped in July 2002 (from about 70 µg/L during pumping to about 16,000 µg/L in 2008).
- Concentrations in wells located at the SPA RI site decreased from values above the screening level to below the screening level over the past few years.
- Similarly, concentrations at RD-33A on the western periphery of impacted groundwater at the FSDF RI site have also decreased below the screening level.

### Vertical Extent of TCE in Groundwater

Available sampling results used to evaluate the vertical extent of TCE impacts to groundwater include the following:

- Groundwater sampling results through time at 21 vertical monitoring well clusters,
- One-time rock core sampling results from 21 continuously-cored locations, and
- Groundwater sampling results from vertically-discrete intervals in multi-level monitoring systems subsequently installed in 4 of the 21 continuously-cored locations.

Review of the data presented in Plate 7-2 at monitoring well clusters indicates that the vertical extent of TCE has been defined at 18 of the 21 well clusters. TCE is present at concentrations above the 5 µg/L screening level in groundwater samples collected from the deepest well from the RD-35 (RD-35B), RD-49 (RD-49C) and RD-55 (RD-55B) well clusters. These well clusters are located at or near the IEL, Alfa and STL-IV RI sites, respectively.

Rock core sampling results from the vertical coreholes support the sampling results from well clusters. Sampling results from the RD-35C corehole provide information on the vertical extent of TCE at the RD-35 cluster at the IEL RI site. These sampling results show that the range of TCE concentrations detected in rock porewater in the bottom 50 feet of the corehole range between 0.7 and 111 µg/L, with an average of 9.4 µg/L (total of 42 samples, with 9 results non-detect).

Rock core sampling results from corehole C-15 information on the vertical extent of TCE at the Delta RI site. These sampling results show that TCE was detected in 4 rock core samples from the bottom 50 feet of the corehole (between depths of 1350 and 1400 feet bgs) at porewater concentrations ranging from 4 to 73 µg/L. The mean concentration was 3 µg/L when assigning a

value of ½ of the method detection limit to samples where TCE was not detected (total of 46 samples, with 42 results non-detect).

### Groundwater Transport Evaluation

An evaluation of groundwater flow directions (advective transport of contaminants) from known or suspected TCE sources was completed using forward 3-dimensional particle tracking based on the results of the 3-dimensional groundwater flow model. It should be recognized that as new site information is evaluated boundaries of identified TCE source areas are updated. Plots presented here are based on source representations as defined over the last few years and may not fully reflect the most recent refinements.

For each source, multiple particles were released at 10 m depth increments starting at the elevation of the simulated water table and extending to a depth of 200 m. A total of 6,645 particles were released from the water table and tracked through the simulated steady-state flow field under both the pumping (i.e., 1995-1998) and non-pumping conditions and results are depicted in Figures 7-7 and 7-8, respectively. Results were exported to a geographic information system (GIS) and the points representing the particle tracks were truncated at a travel distance of 1000 m. These truncated particle tracks were used to generate corresponding groundwater pathlines. Both the individual particle and line files were spatially queried to identify flow paths intersecting one or more sources. The 1000 m flow path length was selected to illustrate general flow directions during a period when no change in the groundwater flow field occurs, steady-state flow. This distance was also used to suggest the likely maximum transport distance of TCE. Transport modeling using a 2D fracture porous block representation of hydrogeologic conditions at the site commonly found that plume boundaries (defined as a reduction in source concentrations of five orders of magnitude (a factor of 100,000)) generally extended only about 1000 m from the source areas. The map view of the 1000 m flow path length is a two dimensional representation of a 3-dimensional pathline, thus the flow path length displayed in plan view will be shorter than the modeled path length.

It is important to state that these flow path representations were generated under steady state conditions representing a period of average flow during a period of active pumping and a second

period prior to when pumping was initiated (i.e., circa 1950) . As such, they do not represent the absolute TCE transport distance from an identified or suspected source, but, this analyses provides insight as to the general direction of groundwater flow and likely contaminant migration paths. Furthermore no velocity or time of travel is represented for the flow path as: 1) the time for groundwater to flow along this distance is based on a dual-porosity system which is not represented in the EPM model, and 2) other processes, such as matrix diffusion, sorption, or biological or abiotic decay that would further limit transport, are not represented.

### **7.3.5.2 Extent of PCE in Groundwater**

#### Sources to Groundwater

In summary, PCE was encountered in surficial media at concentrations above RBSLs at 27 RI sites and was recommended for further evaluation during the feasibility study for surficial media at 11 RI sites and at one additional RI site under VOCs as a group. Surficial media areas recommended for further evaluation in the feasibility study are shown in yellow in Plate 7-3 along with the PCE soil matrix, soil vapor and groundwater sampling results. PCE was found to be a chemical of concern in surficial media at three RI sites (LOX, Ash Pile/Bldg 515 STP, and ELV) but has not been found in groundwater samples at concentrations above PCE's screening level.

#### Groundwater Sampling Summary

PCE has been sampled in groundwater at 485 locations at SSFL of which it has been detected on at least one occasion at 94 locations and exceeded the screening level of 5 µg/L at 33 locations with a historical maximum concentration of 2,100 µg/L at SH-04 at the ECL RI site. In the July 07/June 08 dataset, PCE was sampled in groundwater at 182 locations of which it was detected at 16 locations and exceeded the screening level at five locations with a maximum concentration of 15 µg/L at HAR-16 at the APTF RI site.

#### Lateral Extent of PCE in Groundwater

Data used to evaluate the lateral extent of PCE in groundwater include sampling results from the monitoring well network and from seeps. Plate 7-3 depicts the locations from which samples

have been collected and analyzed for PCE along with concentration data. The data indicate that boundaries encompassing concentrations of PCE in excess of the screening level of 5 µg/L can be drawn over seven separate areas of the site. Table 7-13 presents information on each of the seven areas of impacted groundwater and these areas are graphically summarized in Figure 7-9. In summary, the area of PCE in groundwater at concentrations exceeding the screening level encompasses about 21 acres of land and is coincident with about 3 percent of the TCE-impacted area. These results are consistent with the rock core PCE sampling results, which show PCE to be present at concentrations much below those of TCE. Six of the seven PCE areas are coincident with the areas of TCE-impacted groundwater. The maximum concentration of PCE detected in groundwater in the July 07/June 08 dataset is three times above the screening value of 5 µg/L.

#### Vertical Extent of PCE in Groundwater

Available sampling results used to evaluate the vertical extent of PCE impacts to groundwater include the following:

- Groundwater sampling results through time at 21 vertical monitoring well clusters,
- One-time rock core sampling results from 21 continuously-cored locations, and
- Groundwater sampling results from vertically-discrete intervals in multi-level monitoring systems subsequently installed in 4 of the 21 continuously-cored locations.

Review of the data presented in Plate 7-3 at monitoring well clusters indicates that the vertical extent of PCE has been defined at 19 of the 21 well clusters. PCE is present at concentrations above its screening level in groundwater samples collected from the deepest well from the RD-49 (RD-49C) and RD-55 (RD-55B) well clusters. These well clusters are located at or near the Alfa and STL-IV RI sites, respectively. Rock core sampling results from the vertical coreholes support the sampling results from well clusters.

### **7.3.5.3 Extent of cDCE in Groundwater**

#### Sources to Groundwater

In summary, cDCE was encountered in surficial media at concentrations above RBSLs at 19 RI sites and was recommended for further evaluation during the feasibility study for surficial media at eight RI sites and also at one RI site under 1,2-dichloroethenes and one RI site under VOCs as a group. Areas recommended for further evaluation in the feasibility study are shown in yellow in Plate 7-4 along with the cDCE soil matrix, soil vapor and groundwater sampling results. However, the primary source of cDCE in groundwater is from the transformation of TCE to cDCE through biological reduction in the groundwater system. Detailed descriptions of the chlorinated ethene degradation assessment are provided in the complementary site conceptual model document (Cherry, McWhorter, and Parker, 2009).

#### Groundwater Sampling Summary

cDCE has been sampled in groundwater at 477 locations at SSFL of which it has been detected on at least one occasion at 255 locations and exceeded the screening level of 6 µg/L at 171 locations with a historical maximum concentration of 11,000 µg/L at HAR-7 at the Delta RI site. In the July 07/June 08 dataset, cDCE was sampled in groundwater at 182 locations of which it was detected at 99 locations and exceeded the screening level at 63 locations with a maximum concentration of 2,300 µg/L at HAR-7 at the Delta RI site.

#### Lateral Extent of cDCE in Groundwater

Data used to evaluate the lateral extent of cDCE in groundwater include sampling results from the monitoring well network and from seeps. Plate 7-4 depicts the locations from which samples have been collected and analyzed for cDCE along with concentration data. The data indicate that boundaries encompassing concentrations of cDCE in excess of the screening level of 6 µg/L can be drawn over 11 separate areas of the site. Table 7- 14 presents information on each of the 11 areas of impacted groundwater and these areas are graphically summarized in Figure 7-10. In summary, the area of cDCE in groundwater at concentrations exceeding the screening level encompasses about 352 acres of land and covers about 56 percent of the TCE-impacted area.

The 11 areas of cDCE impact generally all coincide with TCE-impacted areas except for the western portion of the Group 3 central TCE-impacted area and the eastern portion of the B056 Landfill/SNAP TCE-impacted area. Rock core cDCE sampling results are similar to the groundwater sampling results in that cDCE is found in rock porewater samples at a lower frequency than TCE and at lower maximum concentrations. These data are consistent with the transformation of TCE to cDCE via biologic pathways as has been previously reported and is further described in the complementary site conceptual model document (Cherry, McWhorter, and Parker, 2009). The occurrence of cDCE in groundwater is consistent with its occurrence in surficial media RI sites as shown in Plate 7-4.

#### Vertical Extent of cDCE in Groundwater

Available sampling results used to evaluate the vertical extent of cDCE impacts to groundwater include the following:

- Groundwater sampling results through time at 21 vertical monitoring well clusters,
- One-time rock core sampling results from 21 continuously-cored locations, and
- Groundwater sampling results from vertically-discrete intervals in multi-level monitoring systems subsequently installed in 4 of the 21 continuously-cored locations.

Review of the data presented in Plate 7-4 at monitoring well clusters indicates that the vertical extent of cDCE has been defined at all 21 well clusters. Rock core sampling results from the vertical coreholes support the sampling results from well clusters in that the occurrence and concentration of cDCE toward the bottom of the coreholes are fewer and lower than TCE.

#### **7.3.5.4 Extent of tDCE in Groundwater**

##### Sources to Groundwater

In summary, tDCE was encountered in surficial media at concentrations above RBSLs at seven RI sites and was recommended for further evaluation during the feasibility study for surficial media at two RI sites and also at one RI site under 1,2-dichloroethenes and one RI site under VOCs as a group. Areas recommended for further evaluation in the feasibility study are shown in yellow in Plate 7-5 along with the tDCE soil matrix, soil vapor and groundwater sampling

results. However, the primary source of tDCE in groundwater is from the transformation of TCE to tDCE through biological reduction in the groundwater system.

### Groundwater Sampling Summary

tDCE has been sampled in groundwater at 485 locations at SSFL of which it has been detected on at least one occasion at 182 locations and exceeded the screening level of 10 µg/L at 100 locations with a historical maximum concentration of 6,400 µg/L at ES-03 at the CTL-III RI site. In the July 07/June 08 dataset, tDCE was sampled in groundwater at 182 locations of which it was detected at 59 locations and exceeded the screening level at 18 locations with a maximum concentration of 130 µg/L at HAR-7 at the Delta RI site.

### Lateral Extent of tDCE in Groundwater

Data used to evaluate the lateral extent of tDCE in groundwater include sampling results from the monitoring well network and from seeps. Plate 7-5 depicts the locations from which samples have been collected and analyzed for tDCE along with concentration data. The data indicate that boundaries encompassing concentrations of tDCE in excess of the screening level of 10 µg/L can be drawn over nine separate areas of the site. Table 7-15 presents information on each of the nine areas of impacted groundwater and these areas are graphically summarized in Figure 7-11. In summary, the area of tDCE in groundwater at concentrations exceeding the screening level encompasses about 75 acres of land and covers about 12 percent of the TCE-impacted area. The nine areas of cDCE impact generally all coincide with TCE-impacted areas except for the western portion of the Group 3 central TCE-impacted area. Rock core tDCE sampling results are similar to the groundwater sampling results in that tDCE is found in rock porewater samples at a much lower frequency (typically 1-5%) than TCE and at concentrations in the low hundreds of µg/L. These data are consistent with the minor transformation of TCE to tDCE via biologic pathways as has been previously reported and is further described in the complementary site conceptual model document (Cherry, McWhorter, and Parker, 2009). Where tDCE has been found in surficial media, it is also found in groundwater as shown in Plate 7-5.

### Vertical Extent of tDCE in Groundwater

Available sampling results used to evaluate the vertical extent of tDCE impacts to groundwater include the following:

- Groundwater sampling results through time at 21 vertical monitoring well clusters,
- One-time rock core sampling results from 21 continuously-cored locations,
- Groundwater sampling results from vertically-discrete intervals in multi-level monitoring systems subsequently installed in 4 of the 21 continuously-cored locations.

Review of the data presented in Plate 7-5 at monitoring well clusters indicates that the vertical extent of tDCE has been defined at all 21 well clusters. Rock core sampling results from the vertical coreholes support the sampling results from well clusters in that the occurrence of tDCE toward the bottom of the coreholes is very infrequent, and when detected concentrations are very low (see Appendix 7-B).

#### **7.3.5.5 Extent of Vinyl Chloride in Groundwater**

##### Sources to Groundwater

In summary, vinyl chloride was encountered in surficial media at concentrations above RBSLs at 12 RI sites and was recommended for further evaluation during the feasibility study for surficial media at six RI sites and at one additional RI site under VOCs as a group. Areas recommended for further evaluation in the feasibility study are shown in yellow in Plate 7-6 along with the vinyl chloride soil matrix, soil vapor and groundwater sampling results. However, the primary source of vinyl chloride in groundwater is from the transformation of cDCE to vinyl chloride through biological reduction in the groundwater system. The transformation of cDCE to vinyl chloride is closely associated with strongly reducing conditions in the groundwater system.

##### Groundwater Sampling Summary

Vinyl chloride has been sampled in groundwater at 485 locations at SSFL of which it has been detected on at least one occasion at 114 locations and exceeded the screening level of 0.5 µg/L at 102 locations with a historical maximum concentration of 3,900 µg/L at SH-04 at the ECL RI site. In the July 07/June 08 dataset, vinyl chloride was sampled in groundwater at 182 locations

of which it was detected at 39 locations and exceeded the screening level at 31 locations with a maximum concentration of 64  $\mu\text{g/L}$  at HAR-18 at the STL-IV RI site.

#### Lateral Extent of Vinyl Chloride in Groundwater

Data used to evaluate the lateral extent of vinyl chloride in groundwater include sampling results from the monitoring well network and from seeps. Plate 7-6 depicts the locations from which samples have been collected and analyzed for vinyl chloride along with concentration data. The data indicate that boundaries encompassing concentrations of vinyl chloride in excess of the screening level of 0.5  $\mu\text{g/L}$  can be drawn over nine separate areas of the site. Table 7-16 presents information on each of the nine areas of impacted groundwater and these areas are graphically summarized in Figure 7-12. In summary, the area of vinyl chloride in groundwater at concentrations exceeding the screening level encompasses about 187 acres of land and covers about 30 percent of the TCE-impacted area. Vinyl chloride is found in groundwater samples above its screening level from wells in areas that are fully within the areas of cDCE-impacted groundwater. The fact that vinyl chloride is found above its screening level in more areas and over a larger area than tDCE can be attributed to two factors: its lower screening value and the preferential production of transformation products via the biological pathway. There have been no detections of vinyl chloride in rock core samples partly due to the fact that only about 5 percent of the samples have been analyzed and the method detection limit of the methods used to quantify its presence are elevated (see Table 7-6 for the detection limits). Where vinyl chloride has been found in surficial media, it is also found in groundwater as shown in Plate 7-6.

#### Vertical Extent of Vinyl Chloride in Groundwater

Available sampling results used to evaluate the vertical extent of cDCE impacts to groundwater include the following:

- Groundwater sampling results through time at 21 vertical monitoring well clusters,
- One-time rock core sampling results from 21 continuously-cored locations, and
- Groundwater sampling results from vertically-discrete intervals in multi-level monitoring systems subsequently installed in 4 of the 21 continuously-cored locations.

Review of the data presented in Plate 7-6 at monitoring well clusters indicates that the vertical extent of vinyl chloride has been defined at 19 of the 21 well clusters. Vinyl chloride is present at concentrations above its screening level in groundwater samples collected from the deepest well from the RD-49 (RD-49C) and RD-58 (RD-58C) well clusters. These well clusters are located at or near the Alfa and STL-IV RI sites, respectively.

### **7.3.5.6 Extent of 1,1-DCE in Groundwater**

#### Sources to Groundwater

In summary, 1,1-DCE was encountered in surficial media at concentrations above RBSLs at 19 RI sites and was recommended for further evaluation during the feasibility study for surficial media at eight sites and at one additional site under VOCs as a group. Areas recommended for further evaluation in the feasibility study are shown in yellow in Plate 7-7. Soil sampling results of 1,1,1-TCA are shown on this plate, along with the 1,1-DCE groundwater sampling results. 1,1,1-TCA surficial media sampling results were selected to depict potential sources of 1,1-DCE in the groundwater since 1,1-DCE is a known abiotic transformation product of 1,1,1-TCA (Vogel & McCarty, 1987).

#### Groundwater Sampling Summary

1,1-DCE has been sampled in groundwater at 485 locations at SSFL of which it has been detected on at least one occasion at 136 locations and exceeded the screening level of 6 µg/L at 76 locations with a historical maximum concentration of 12,000 µg/L at RD-35A at the IEL RI site. In the July 07/June 08 dataset, 1,1-DCE was sampled in groundwater at 182 locations of which it was detected at 50 locations and exceeded the screening level at 14 locations with a maximum concentration of 1,200 µg/L at RS-54 at the FSDF RI site.

#### Lateral Extent of 1,1-DCE in Groundwater

Data used to evaluate the lateral extent of 1,1-DCE in groundwater include sampling results from the monitoring well network and from seeps. Plate 7-7 depicts the locations from which samples have been collected and analyzed for 1,1-DCE along with concentration data. The data indicate that boundaries encompassing concentrations of 1,1-DCE in excess of the screening level of

6 µg/L can be drawn over seven separate areas of the site. Table 7-17 presents information on each of the 7 areas of impacted groundwater and these areas are graphically summarized in Figure 7-13. In summary, the area of 1,1-DCE in groundwater at concentrations exceeding the screening level encompasses about 64 acres of land and covers about 10 percent of the TCE-impacted area. However, 1,1-DCE is an abiotic transformation product of 1,1,1-TCA in groundwater and is a likely transformation product of TCE at SSFL. Groundwater sampling results typically measure lower concentrations of 1,1-DCE and less frequently than rock core sampling results of 1,1-DCE. Six of the seven 1,1-DCE areas are coincident with the areas of TCE-impacted groundwater. 1,1-DCE is found in one area where TCE is not present above screening levels, within the Group 7 RI reporting area. Additionally, 1,1-DCE impacted groundwater extends westward to the SPA RI site in the central part of SSFL, where TCE is not present at concentrations above its screening level. It is possible that the source of the 1,1-DCE at these locations results from historic small releases of 1,1,1-TCA.

#### Vertical Extent of 1,1-DCE in Groundwater

Available sampling results used to evaluate the vertical extent of 1,1-DCE impacts to groundwater include the following:

- Groundwater sampling results through time at 21 vertical monitoring well clusters,
- One-time rock core sampling results from 21 continuously-cored locations, and
- Groundwater sampling results from vertically-discrete intervals in multi-level monitoring systems subsequently installed in 4 of the 21 continuously-cored locations.

Review of the data presented in Plate 7-7 at monitoring well clusters indicates that the vertical extent of 1,1-DCE has been defined at all 21 well clusters. Rock core sampling results from the vertical coreholes show that 1,1-DCE is found in rock porewater at low concentrations in certain coreholes throughout the total depth (e.g., C2 and C3, see profiles in Appendix 7-B) but is found only infrequently in other coreholes (e.g., C5, C7, C10).

### **7.3.5.7 Extent of 1,1,2,2-Tetrachloroethane**

#### Sources to Groundwater

1,1,2,2-PCA was encountered in surficial media at concentrations above RBSLs at one RI site and was not recommended for further evaluation during the feasibility study for surficial media except for at one site under VOCs as a group. Therefore, surficial media sampling results do not show this solvent to be a current major source to groundwater. Historical groundwater sampling results showed that this chemical was present above its screening level. Additionally, 1,1,2,2-PCA has been observed to transform to 1,2-DCA (through 1,1,2-TCA) under anaerobic conditions and to TCE abiotically (Field and Sierra-Alvarez, 2004). As such, it was evaluated to assess its current distribution relative to its screening level of 1 µg/L as shown in Plate 7-8.

#### Groundwater Sampling Summary

1,1,2,2-PCA has been sampled in groundwater at 484 locations at SSFL of which it has been detected on at least one occasion at 9 locations and exceeded the screening level of 1 µg/L at 7 locations with a historical maximum concentration of 840 µg/L at RD-35A at the IEL RI site. In the July 07/June 08 dataset, 1,1,2,2-PCA was sampled in groundwater at 182 locations and it was not detected. Since 1,1,2,2-PCA is not present at concentrations exceeding its screening level in recent sample results, its lateral and vertical distribution do not require discussion.

### **7.3.5.8 Extent of 1,2-DCA**

#### Sources to Groundwater

1,2-DCA was encountered in surficial media at concentrations above RBSLs at four RI sites and was recommended for further evaluation during the feasibility study for surficial media at one site under VOCs as a group. Areas recommended for further evaluation in the feasibility study for surficial media are shown in yellow in Plate 7-9. Soil vapor and matrix sampling results of 1,2-DCA are shown on this plate, along with the groundwater sampling results. As mentioned previously, 1,2-DCA has been observed as a transformation product of 1,1,2,2-PCA under anaerobic conditions (through transformation from 1,1,2-TCA).

## Groundwater Sampling Summary

1,2-DCA has been sampled in groundwater at 484 locations at SSFL of which it has been detected on at least one occasion at 56 locations and exceeded the screening level of 0.5 µg/L at 51 locations with a historical maximum concentration of 250,000 µg/L at SH-04 at the ECL RI site. In the July 07/June 08 dataset, 1,2-DCA was sampled in groundwater at 182 locations of which it was detected at 9 locations and exceeded the screening level at 8 locations with a maximum concentration of 21 µg/L at RS-54 at the FSDF RI site.

## Lateral Extent of 1,2-DCA in Groundwater

Data used to evaluate the lateral extent of 1,2-DCA in groundwater include sampling results from the monitoring well network and from seeps. Plate 7-9 depicts the locations from which samples have been collected and analyzed for 1,2-DCA along with concentration data. The data indicate that boundaries encompassing concentrations of 1,2-DCA in excess of the screening level of 0.5 µg/L can be drawn over three separate areas of the site. Table 7-18 presents information on each of the three areas of impacted groundwater and these areas are graphically summarized in Figure 7-14. In summary, the area of 1,2-DCA in groundwater at concentrations exceeding the screening level encompasses about eight acres of land.

## Vertical Extent of 1,2-DCA in Groundwater

Available sampling results used to evaluate the vertical extent of 1,2-DCA impacts to groundwater include the following:

- Groundwater sampling results through time at 21 vertical monitoring well clusters,
- One-time rock core sampling results from 10 continuously-cored locations, and
- Groundwater sampling results from vertically-discrete intervals in multi-level monitoring systems subsequently installed in 4 of the 21 continuously-cored locations.

Review of the data presented in Plate 7-9 at monitoring well clusters indicates that the vertical extent of 1,2-DCA has been defined at all 21 well clusters. Rock core sampling results from the vertical coreholes support the sampling results from well clusters in that there were no detections

of 1,2-DCA in the 5 percent of the rock core samples analyzed at a commercial laboratory, although the detection limits were about 530 µg/L equivalent porewater.

### **7.3.5.9 Extent of 1,1-DCA**

#### Sources to Groundwater

1,1-DCA was encountered in surficial media at concentrations above RBSLs at eight RI sites and was recommended for further evaluation during the feasibility study for surficial media at two sites and at one additional site under VOCs as a group. Areas recommended for further evaluation in the feasibility study for surficial media are shown in yellow in Plate 7-10. Soil vapor and matrix sampling results of 1,1-DCA are shown on this plate, along with the groundwater sampling results. As mentioned previously, 1,1-DCA has been observed as a transformation product of 1,1,1-TCA under anaerobic conditions.

#### Groundwater Sampling Summary

1,1-DCA has been sampled in groundwater at 485 locations at SSFL of which it has been detected on at least one occasion at 100 locations and exceeded the screening level of 5 µg/L at 48 locations with a historical maximum concentration of 2,800 µg/L at RS-54 at the FSDF RI site. In the July 07/June 08 dataset, 1,1-DCA was sampled in groundwater at 182 locations of which it was detected at 21 locations and exceeded the screening level at 10 locations with a maximum concentration of 1,400 µg/L at RS-54 at the FSDF RI site.

#### Lateral Extent of 1,1-DCA in Groundwater

Data used to evaluate the lateral extent of 1,1-DCA in groundwater include sampling results from the monitoring well network and from seeps. Plate 7-10 depicts the locations from which samples have been collected and analyzed for 1,1-DCA along with concentration data. The data indicate that boundaries encompassing concentrations of 1,1-DCA in excess of the screening level of 5 µg/L can be drawn over six separate areas of the site. Table 7-19 presents information on each of the six areas of impacted groundwater and these areas are graphically summarized in Figure 7-15. In summary, the area of 1,1-DCA in groundwater at concentrations exceeding the screening level encompasses about 19 acres of land and its occurrence is coincident with the

locations where 1,1-DCE is present (Figure 7-13). Where 1,1-DCA has been found in surficial media, it is also found in groundwater as shown in Plate 7-10. This comparison was made to assess the possible correlation of these two constituents as both are believed to be associated with historic releases of 1,1,1-TCA.

#### Vertical Extent of 1,1-DCA in Groundwater

- Available sampling results used to evaluate the vertical extent of cDCE impacts to groundwater include the following:
- Groundwater sampling results through time at 21 vertical monitoring well clusters,
- One-time rock core sampling results from 10 continuously-cored locations, and
- Groundwater sampling results from vertically-discrete intervals in multi-level monitoring systems subsequently installed in 4 of the 21 continuously-cored locations.

Review of the data presented in Plate 7-10 at monitoring well clusters indicates that the vertical extent of 1,1-DCA has been defined at all 21 well clusters. Rock core sampling results from the vertical coreholes support the sampling results from well clusters in that there were no detections of 1,1-DCA in the 5 percent of the rock core samples analyzed at a commercial laboratory, although the detection limits were about 990 µg/L equivalent porewater.

#### **7.3.5.10 Extent of 1,4-Dioxane in Groundwater**

##### Sources to Groundwater

In summary, 1,4-dioxane was not encountered in surficial media at any RI sites at concentrations of concern. Soil sampling results of 1,1,1-TCA are shown in Plate 7-11 along with the 1,4-dioxane groundwater sampling results. 1,1,1-TCA surficial media sampling results were selected to depict potential sources of 1,4-dioxane in groundwater since 1,4-dioxane was commonly added as an acid scavenger to 1,1,1-TCA (Jackson and Dwarakanath, 1999).

##### Groundwater Sampling Summary

1,4-dioxane has been sampled in groundwater at 241 locations at SSFL of which it has been detected on at least one occasion at 76 locations and exceeded the screening level of 3 µg/L at 32 locations with a historical maximum concentration of 797 µg/L at RD-73 at the IEL RI site.

In the July 07/June 08 dataset, 1,4-dioxane was sampled in groundwater at 33 locations of which it was detected at 21 locations and exceeded the screening level at 7 locations with a maximum concentration of 67 µg/L at HAR-14 at the SPA RI site.

#### Lateral Extent of 1,4-dioxane in Groundwater

Data used to evaluate the lateral extent of 1,4-dioxane in groundwater include sampling results from the monitoring well network and from seeps. Plate 7-11 depicts the locations from which samples have been collected and analyzed for 1,4-dioxane along with concentration data. The data indicate that boundaries encompassing concentrations of 1,4-dioxane in excess of the screening level of 3 µg/L can be drawn over nine separate areas of the site. Table 7-20 presents information on each of the nine areas of impacted groundwater and these areas are graphically summarized in Figure 7-16. In summary, the area of 1,4-dioxane in groundwater at concentrations exceeding the screening level encompasses about 59 acres of land. The occurrence of 1,4-dioxane at concentrations above screening levels at 7 of the 9 areas is coincident with 1,1-DCE impacted groundwater (Figure 7-13). This comparison was made to assess the possible correlation of these two constituents as both are believed to be associated with historic releases of 1,1,1-TCA. 1,4-dioxane is found in two areas where 1,1-DCE is not present above screening levels, the CTL-III RI site in Group reporting area 1B, and the Building 204 RI site in Group reporting area 3. Alternately, 1,1-DCE is present in groundwater at concentrations exceeding screening levels where 1,4-dioxane is absent, one in Group reporting area 7 and the other at the Delta RI site in Group reporting area 4. The occurrence of 1,4-dioxane also closely parallels that of 1,1-DCA (see Figure 7-15).

#### Vertical Extent of 1,4-Dioxane in Groundwater

Available sampling results used to evaluate the vertical extent of 1,4-dioxane impacts to groundwater include the following:

- Groundwater sampling results through time at 21 vertical monitoring well clusters, and
- One-time rock core sampling results from 10 continuously-cored locations.

Review of the data presented in Plate 7-11 at monitoring well clusters in or near areas with 1,4-dioxane impacted groundwater indicates that sample results define the vertical extent of 1,4-dioxane at the RD-49, -55 and -58 well clusters. 1,4-dioxane is present at concentrations above its screening level in groundwater samples collected from the deepest well at RD-35 (RD-35C) well cluster. Sample results from other well clusters where 1,4-dioxane is found in groundwater have detection limits exceeding the screening level. These clusters include RD-33, -34, -38, -39, -41, -46, -54, -56, -59, and -68. However, it is expected that 1,4-dioxane concentrations at depth would be low. Rock core sampling results from the vertical coreholes support this expectation as 1,4-dioxane is infrequently found at depth and, when found, is encountered at low concentrations (see profiles in Appendix 7-B).

### **7.3.5.11 Extent of Carbon Tetrachloride**

#### Sources to Groundwater

Carbon tetrachloride was encountered in surficial media at concentrations above RBSLs at four RI sites and was recommended for further evaluation during the feasibility study for surficial media at two RI sites and at one additional RI site under VOCs as a group. Areas recommended for further evaluation in the feasibility study for surficial media are shown in yellow in Plate 7-12. Soil vapor and matrix sampling results of carbon tetrachloride are shown on this plate, along with the groundwater sampling results.

#### Groundwater Sampling Summary

Carbon tetrachloride has been sampled in groundwater at 484 locations at SSFL of which it has been detected on at least one occasion at 36 locations and exceeded the screening level of 0.5 µg/L at 34 locations with a historical maximum concentration of 29,000 µg/L at SH-04 at the ECL RI site. In the July 07/June 08 dataset, carbon tetrachloride was sampled in groundwater at 182 locations of which it has been detected at 7 locations and exceeded the screening level at 5 locations with a maximum concentration of 64 µg/L at SH-03 at the ECL RI site.

### Lateral Extent of Carbon Tetrachloride in Groundwater

Data used to evaluate the lateral extent of carbon tetrachloride in groundwater include sampling results from the monitoring well network and from seeps. Plate 7-12 depicts the locations from which samples have been collected and analyzed for carbon tetrachloride along with concentration data. The data indicate that boundaries encompassing concentrations of carbon tetrachloride in excess of the screening level of 0.5 µg/L can be drawn over nine separate areas of the site. Table 7-21 presents information on each of the nine areas of impacted groundwater and these areas are graphically summarized in Figure 7-17. In summary, the area of carbon tetrachloride in groundwater at concentrations exceeding the screening level encompasses about 15 acres of land. The occurrence of carbon tetrachloride at concentrations above screening levels is coincident with other areas of impacted groundwater.

### Vertical Extent of Carbon Tetrachloride in Groundwater

Available sampling results used to evaluate the vertical extent of carbon tetrachloride impacts to groundwater include sampling results through time at 20 of 21 vertical monitoring well clusters. Carbon tetrachloride is present at concentrations above its screening level in groundwater samples collected from the deeper well from the RD-35 (RD-35B; not sampled at RD-35C) well cluster located at the IEL RI site. Otherwise, the vertical extent of carbon tetrachloride in groundwater has been defined at the remaining well clusters.

#### **7.3.5.12 Extent of 1,2,3-Trichloropropane**

##### Sources to Groundwater

1,2,3- trichloropropane (TCP) was not encountered in surficial media at concentrations above RBSLs at any of the RI sites and was not recommended for further evaluation during the feasibility study for surficial media except at one site under VOCs as a group. Therefore, surficial media sampling results do not show this solvent to be a source to groundwater. However, historical groundwater sampling results showed that this chemical was present above its screening level as shown in Plate 7-13.

### Groundwater Sampling Summary

1,2,3-TCP has been sampled in groundwater at 199 locations at SSFL of which it has been detected on at least one occasion at 15 locations and exceeded the screening level of 0.005 µg/L at seven locations with a historical maximum concentration of 0.04 µg/L at RD-60 at the Building 204 RI site. In the July 07/June 08 dataset, 1,2,3-TCP was sampled in groundwater at seven locations of which it was detected at two locations and exceeded the screening level at one location with a maximum concentration of 0.014 µg/L at HAR-16 at the APTF RI site.

### Lateral Extent of 1,2,3-TCP in Groundwater

Data used to evaluate the lateral extent of 1,2,3-TCP in groundwater include sampling results from the monitoring well network and from seeps. Plate 7-13 depicts the locations from which samples have been collected and analyzed for 1,2,3-TCP along with concentration data. The data indicate that boundaries encompassing concentrations of 1,2,3-TCP in excess of the screening level of 0.005 µg/L can be drawn over five separate areas of the site. Table 7-22 presents information on each of the five areas of impacted groundwater and these areas are graphically summarized in Figure 7-18. In summary, the area of 1,2,3-TCP in groundwater at concentrations exceeding the screening level encompasses about five acres of land. The occurrence of 1,2,3-TCP at concentrations above screening levels is coincident with other areas of impacted groundwater.

### Vertical Extent of 1,2,3-TCP in Groundwater

Available sampling results used to evaluate the vertical extent of 1,2,3-TCP impacts to groundwater include sampling results through time at 15 of 21 vertical monitoring well clusters. Review of the data presented in Plate 7-13 at monitoring well clusters closest to the areas of 1,2,3-TCP-impacted groundwater indicate that 1,2,3-TCP is defined vertically (i.e., RD-36, and RD-45 well clusters). Sample results from 5 other well clusters at the site have not shown 1,2,3-TCP to be present above its screening level. Sample results from 8 other well clusters have reporting limits that exceed the screening value of 0.005 µg/L, while samples have not been collected at the 6 remaining clusters. However, considering the low concentrations at which

1,2,3-TCP has been detected and its apparent minimal use (based on sampling results), vertical transport is expected to be minimal.

### **7.3.5.13 Extent of Formaldehyde in Groundwater**

#### Sources to Groundwater

Formaldehyde was encountered in surficial media at concentrations above RBSLs at one RI site and was recommended for further evaluation during the feasibility study for surficial media at one site and at one additional site under VOCs as a group. The fact that formaldehyde was not found to be broadly distributed in surficial media is likely a function of it being a break-down product of monomethylhydrazine, which was used as a rocket fuel at SSFL, and its short half-life in soil (reference). Surficial media areas recommended for further evaluation in the feasibility study are shown in yellow in Plate 7-14 along with the formaldehyde soil matrix and groundwater sampling results.

#### Groundwater Sampling Summary

Formaldehyde has been sampled in groundwater at 119 locations at SSFL of which it has been detected on at least one occasion at 47 locations and exceeded the screening level of 100 µg/L at 15 locations with a historical maximum concentration of 2,000 µg/L at WS-5 near the Canyon and LETF/CTL-1 RI sites. In the July 07/June 08 dataset, formaldehyde was sampled in groundwater at 49 locations of which it was detected at 29 locations and exceeded the screening level at 7 locations with a maximum concentration of 160 µg/L at 3 different wells: RD-49B (Alfa RI site), RD-58B (STL-IV RI site), and RD-41B (Delta RI site).

#### Lateral Extent of Formaldehyde in Groundwater

Data used to evaluate the lateral extent of formaldehyde in groundwater include sampling results from the monitoring well network and from seeps. Plate 7-14 depicts the locations from which samples have been collected and analyzed for formaldehyde along with concentration data. The data indicate that boundaries encompassing concentrations of formaldehyde in excess of the screening level of 100 µg/L can be drawn over 4 separate areas of the site. Table 7-23 presents information on each of the four areas of impacted groundwater and these areas are graphically

summarized in Figure 7-19. In summary, the area of formaldehyde in groundwater at concentrations exceeding the screening level encompasses about 24 acres of land. Occurrences of formaldehyde at concentrations above screening levels at three of the four areas occur in only one or two wells (Figure 7-19).

#### Vertical Extent of Formaldehyde in Groundwater

Available sampling results used to evaluate the vertical extent of formaldehyde impacts to groundwater include sampling results through time at 12 vertical monitoring well clusters. Review of the data presented in Plate 7-14 at monitoring well clusters in or near areas of formaldehyde impacted groundwater indicates that sample results define the vertical extent of formaldehyde at the RD-58 well cluster. Sample results from the RD-41 well cluster are inconclusive as RD-41B is impacted by formaldehyde, while samples have not been analyzed from RD-41C. Formaldehyde is present at concentrations above the 100 µg/L screening level in groundwater samples collected from the deepest well from the RD-49 (RD-49C) well cluster. This well cluster is located at or near the Alfa RI site.

#### **7.3.5.14 Extent of TPH**

Both immiscible phase and dissolved concentrations of petroleum hydrocarbons have been found in groundwater at SSFL. The immiscible phase petroleum hydrocarbons have been encountered at RD-49A at the Coca RI site and corehole C-2 at the Canyon RI site. Immiscible phase petroleum hydrocarbons are nearly all less dense than water and as such they are frequently found as a separate phase above the water table. They are also referred to as LNAPL. LNAPL was discovered in RD-49A during the removal of Snap samplers (see Section 4.8) and in corehole C-2 during the collection of a video log in late 2009.

LNAPL samples were collected from both locations and characterized. An LNAPL sample was collected from RD-49A in August 2009 and submitted for total petroleum hydrocarbon analysis by EPA Method 8015. The measured thickness of LNAPL at RD-49A prior to sample collection was 0.03 feet. Results of the analysis were reported in Haley & Aldrich, 2009c and indicate that the sample was comprised of 1.7 percent TPH as C<sub>8</sub> through C<sub>11</sub>, 38 percent TPH as C<sub>12</sub> through C<sub>14</sub>, 51 percent TPH as C<sub>15</sub> through C<sub>20</sub>, and 9.3 percent TPH as C<sub>21</sub> through C<sub>30</sub>, where C

represents the number of carbon atoms in the hydrocarbon chain. TPH in the C<sub>8</sub>-C<sub>15</sub> range was analyzed for in rock core samples collected from corehole C-5 but was not detected in any samples. Corehole C-5 is located about 220 feet northeast of RD-49A, but is both down dip of, and at a higher elevation than, RD-49A.

An LNAPL sample was collected from C-2 in October 2009 and analyzed for C<sub>3</sub>-C<sub>44</sub> hydrocarbon fingerprint analysis, simulated distillation, and volatile solvent identification. The analytical laboratory report is included in Appendix 7-E. The LNAPL appeared is a light, straw-colored translucent liquid and contained hydrocarbons in the range C<sub>10</sub> to C<sub>16</sub>, with a distribution characteristic of kerosene and kerosene-based jet fuels. The simulated distillation showed the LNAPL to have a boiling range from 290<sup>0</sup>F to 600<sup>0</sup>F. These results were compared to information contained in 1967 product specifications on the color and formulation for RP-1 (rocket propellant 1, military specification MIL-P-25576C)). The LNAPL sample from C-2 showed differences from the RP-1 specification in both color and the upper boiling point range, which are reported as including a red dye and upper boiling point range of 525<sup>0</sup>F for the RP-1. Analysis of the LNAPL sample for volatile solvent composition showed 1,2-DCE to be present along with traces of TCE, which were estimated to comprise less than 0.1 percent of the sample. Petroleum hydrocarbons in the C<sub>8</sub>-C<sub>15</sub> range were analyzed for in rock core samples collected from corehole C-2 and were encountered at depths of about 35 feet (2 samples) and 70 feet (3 samples) at estimated equivalent porewater concentrations ranging from about 1 to 9 milligrams per liter.

The findings on the composition of LNAPL at RD-49A and C-2 were incorporated into the assessment of the distribution of dissolved concentrations of TPH in groundwater at SSFL. This was done by evaluating TPH analytical laboratory results from groundwater samples that are within the carbon range between C<sub>4</sub> and C<sub>30</sub>.

#### Other Sources to Groundwater

TPH in the carbon range of C<sub>4</sub> to C<sub>30</sub> was encountered in surficial media at concentrations above RBSLs at 42 RI sites and was recommended for further evaluation during the feasibility study for surficial media at one site for TPH as gasoline and at one site for petroleum hydrocarbons.

Additionally, as discussed above, petroleum hydrocarbon LNAPL was recently discovered to be present at two locations. Surficial media areas recommended for further evaluation in the feasibility study are shown in yellow in Plate 7-15 along with the locations of LNAPL occurrence and TPH C<sub>4</sub>-C<sub>30</sub> soil matrix and groundwater sampling results. Note that any TPH results reported within the range of C<sub>4</sub> to C<sub>30</sub>, which covers gasoline, jet fuel, kerosene, diesel, and light oil range hydrocarbons, or with reported results having a majority of carbon atoms falling in this range were included for both soil and groundwater.

### Groundwater Sampling Summary

TPH in the carbon range of C<sub>4</sub> to C<sub>30</sub> has been sampled in groundwater at 111 locations at SSFL of which it has been detected on at least one occasion at 34 locations and exceeded the screening level of 50 µg/L for TPH C<sub>4</sub>-C<sub>12</sub> or 100 µg/L for TPH C<sub>12</sub>-C<sub>30</sub> at 23 locations with a historical maximum concentration of 15,000 µg/L at RD-73 at the IEL RI site. The agency-published screening level for TPH C<sub>4</sub>-C<sub>12</sub> is 5 µg/L (taste/odor threshold). However, typical analytical laboratory method reporting limits (MRLs) are 50 µg/L, so this value was used for screening TPH C<sub>4</sub>-C<sub>12</sub> groundwater results in order to assess the data under appropriate limits. In the July 07/June 08 dataset, TPH C<sub>4</sub>-C<sub>30</sub> was sampled in groundwater at 30 locations of which it was detected at 9 locations and exceeded the screening level at each of these locations with a maximum concentration of 2,700 µg/L also at RD-73 (same location as historical).

### Lateral Extent of TPH C<sub>4</sub>-C<sub>30</sub> in Groundwater

Data used to evaluate the lateral extent of TPH C<sub>4</sub>-C<sub>30</sub> in groundwater include sampling results from the monitoring well network. Plate 7-15 depicts the locations from which samples have been collected and analyzed for TPH C<sub>4</sub>-C<sub>30</sub> along with concentration data. The data indicate that boundaries encompassing concentrations of TPH C<sub>4</sub>-C<sub>30</sub> in excess of the screening levels of 100 µg/L and 50 µg/L can be drawn over ten separate areas of the site. Table 7-24 presents information on each of the ten areas of impacted groundwater and these areas are graphically summarized in Figure 7-20. In summary, the area of TPH C<sub>4</sub>-C<sub>30</sub> in groundwater at concentrations exceeding the screening levels encompasses about 109 acres of land.

Occurrences of TPH C<sub>4</sub>-C<sub>30</sub> at concentrations above screening levels at seven of the ten areas occur in only one or two locations (Figure 7-20).

#### Vertical Extent of TPH C<sub>4</sub>-C<sub>30</sub> in Groundwater

Available sampling results used to evaluate the vertical extent of TPH C<sub>4</sub>-C<sub>30</sub> impacts to groundwater include sampling results through time at six vertical monitoring well clusters. Review of the data presented in Plate 7-15 at these well clusters indicates that TPH C<sub>4</sub>-C<sub>30</sub> is defined vertically in the RD-45 well cluster in the northeast portion of SSFL and in the RD-36 and RD-38 well clusters, both off-site in the northeast. Reporting limits exceed the screening value in the other three well clusters (RD-41, RD-55 and RD-58), all located in the mid-west portion of SSFL. Considering the low concentrations at which TPH has been detected, vertical transport is expected to be minimal.

#### **7.3.5.15 Extent of NDMA in Groundwater**

##### Sources to Groundwater

N-nitrosodimethylamine (NDMA) was encountered in surficial media at concentrations above RBSLs at one RI site and was recommended for further evaluation during the feasibility study for surficial media at one site. The fact that NDMA was not found to be broadly distributed in surficial media is likely a function of it being a break-down product of unsymmetrical dimethyl hydrazine (UDMH), which was used as a limited rocket fuel at SSFL, and its short half-life in soil (reference). Surficial media areas recommended for further evaluation in the feasibility study are shown in yellow in Plate 7-16 along with the NDMA soil matrix and groundwater sampling results.

##### Groundwater Sampling Summary

NDMA has been sampled in groundwater at 242 locations at SSFL of which it has been detected on at least one occasion at 46 locations and exceeded the screening level of 0.01 µg/L at 29 locations with a historical maximum concentration of 110 µg/L at SH-04 at the ECL RI site. In the July 07/June 08 dataset, NDMA was sampled in groundwater at 39 locations of which it was

detected at 14 locations and exceeded the screening level at 10 locations, with a maximum concentration of 6.8  $\mu\text{g/L}$  at HAR-16 at the APTF RI site.

#### Lateral Extent of NDMA in Groundwater

Data used to evaluate the lateral extent of NDMA in groundwater include sampling results from the monitoring well network and from seeps. Plate 7-16 depicts the locations from which samples have been collected and analyzed for NDMA along with concentration data. The data indicate that boundaries encompassing concentrations of NDMA in excess of the screening level of 0.01  $\mu\text{g/L}$  can be drawn over nine separate locations at the site. Table 7-25 presents information on each of the nine areas of impacted groundwater and these areas are graphically summarized in Figure 7-21. In summary, the area of NDMA in groundwater at concentrations exceeding the screening level encompasses about 71 acres of land. Occurrences of NDMA at concentrations above screening levels at six of the nine areas occur in either one or two wells (Figure 7-21). Further sampling at these locations may show some of these to be false positives, due to the lack of a source and a consistent distribution pattern in groundwater. Where NDMA was recommended for further evaluation in the surficial media FS (ELV RI site), it was not found in groundwater. Alternately, where it was found in groundwater, it has not been found in surficial media samples. Its occurrence in groundwater however, is consistent with the use of UDMH as a rocket fuel at test areas (i.e., APTF, Alfa, SPA, Delta, STL-IV).

#### Vertical Extent of NDMA in Groundwater

Available sampling results used to evaluate the vertical extent of NDMA impacts to groundwater include groundwater sampling results through time at 21 vertical monitoring well clusters. Review of the data presented in Plate 7-16 at monitoring well clusters closest to the areas of NDMA-impacted groundwater indicate that NDMA is defined vertically (i.e., RD-41, -55, -58, -36, -38, -45, and -49 well clusters). Also, sample results from the following well clusters also provide vertical definition: RD-5, RD-43, -48 -51, and -52. Sample results from other well clusters have reporting limits that exceed the screening value of 0.01  $\mu\text{g/L}$ .

### **7.3.5.16 Extent of Perchlorate in Groundwater**

#### Sources to Groundwater

Perchlorate was encountered in surficial media at concentrations above RBSLs at 12 RI sites and was recommended for further evaluation during the feasibility study for surficial media at eight sites. Surficial media areas recommended for further evaluation in the feasibility study are shown in yellow in Plate 7-17 along with the perchlorate soil matrix and groundwater sampling results.

#### Groundwater Sampling Summary

Perchlorate has been sampled in groundwater at 332 locations at SSFL of which it has been detected on at least one occasion at 48 locations and exceeded the screening level of 6 µg/L at 27 locations with a historical maximum concentration of 1,600 µg/L at HAR-16 at the APTF RI site. In the July 07/June 08 dataset, perchlorate was sampled in groundwater at 80 locations of which it was detected at 6 locations and exceeded the screening level at each location where it was detected with a maximum concentration of 308 µg/L at RD-77 at the Building 359 RI site.

#### Lateral Extent of Perchlorate in Groundwater

Data used to evaluate the lateral extent of perchlorate in groundwater include sampling results from the monitoring well network and from seeps. Plate 7-17 depicts the locations from which samples have been collected and analyzed for perchlorate along with concentration data. The data indicate that boundaries encompassing concentrations of perchlorate in excess of the screening level of 6 µg/L can be drawn over three separate areas of the site. Table 7-26 presents information on each of the three areas of impacted groundwater and these areas are graphically summarized in Figure 7-22. In summary, the area of perchlorate in groundwater at concentrations exceeding the screening level encompasses about 47 acres of land. Occurrences of perchlorate at concentrations above screening levels at one of the three areas occur in only one well (Figure 7-22).

#### Vertical Extent of Perchlorate in Groundwater

Available sampling results used to evaluate the vertical extent of perchlorate impacts to groundwater include the following:

- Groundwater sampling results through time at 21 vertical monitoring well clusters, and
- One-time rock core sampling results from 6 locations.

Review of the data presented in Plate 7-17 at monitoring well clusters indicates that perchlorate is defined vertically in all 21 well clusters. Perchlorate rock core sampling results are consistent with the groundwater sampling results in that perchlorate was not detected at depth in any of the 5 locations drilled outside of the source area at the Building 359 RI site.

#### **7.3.5.17 Extent of Nitrate**

##### Sources to Groundwater

Nitrate was not encountered in surficial media at concentrations above RBSLs at any of the RI sites and hence was not recommended for further evaluation during the feasibility study for surficial media. Therefore, surficial media sampling results do not show sources to groundwater. However, leach fields are a source of nitrate, as shown in Plate 7-18, along with the nitrate soil matrix and groundwater sampling results.

##### Groundwater Sampling Summary

Nitrate has been sampled in groundwater at 296 locations at SSFL of which it has been detected on at least one occasion at 195 locations and exceeded the screening level of 45,000  $\mu\text{g/L}$  at 22 locations with a historical maximum concentration of 193,000  $\mu\text{g/L}$  at HAR-15 at the SPA RI site. For the purpose of this evaluation, results for nitrate-N were converted to nitrate- $\text{NO}_3$  in order to assess all nitrate data collected at SSFL and get a more comprehensive understanding of the distribution of nitrate in groundwater relative to a threshold. In the July 07/June 08 dataset, nitrate was sampled in groundwater at 79 locations of which it was detected at 24 locations and exceeded the screening level at 2 locations where it was detected at a maximum concentration of 64,000  $\mu\text{g/L}$  at PZ-005 at the DOE Leach Field 3 RI site.

##### Lateral Extent of Nitrate in Groundwater

Data used to evaluate the lateral extent of nitrate in groundwater include sampling results from the monitoring well network and from seeps. Plate 7-18 depicts the locations from which samples have been collected and analyzed for nitrate along with concentration data. The data indicate that boundaries encompassing concentrations of nitrate in excess of the screening level of 45,000  $\mu\text{g/L}$  can be drawn over eight separate areas of the site. Table 7-27 presents information on each of the eight areas of impacted groundwater and these areas are graphically summarized in Figure 7-23. In summary, the area of nitrate in groundwater at concentrations exceeding the screening level encompasses about 24 acres of land. Occurrences of nitrate at concentrations above screening levels at five of the eight areas occur in only one or two wells (Figure 7-23). Nitrate impacts to groundwater occur in two areas where no other chemicals have been encountered at concentrations exceeding screening levels: RD-40 at the Coca RI site and the area near the DOE Leach Field 3 RI site.

#### Vertical Extent of Nitrate in Groundwater

Available sampling results used to evaluate the vertical extent of nitrate impacts to groundwater include sampling results through time at 21 vertical monitoring well clusters. Review of the data presented in Plate 7-18 at monitoring well clusters indicates that nitrate is defined vertically in all 21 well clusters.

#### **7.3.5.18 Extent of Fluoride**

##### Sources to Groundwater

Fluoride was encountered in surficial media at concentrations above RBSLs at two RI sites but none were recommended for further evaluation during the feasibility study for surficial media. Plate 7-19 displays the fluoride soil matrix and groundwater sampling results.

##### Groundwater Sampling Summary

Fluoride has been sampled in groundwater at 284 locations at SSFL of which it has been detected on at least one occasion at 278 locations and exceeded the screening level of 800  $\mu\text{g/L}$  at 48 locations with a historical maximum concentration of 6,400  $\mu\text{g/L}$  at a seep located off-site of SSFL (FDP-810). In the July 07/June 08 dataset, fluoride was sampled in groundwater at 34

locations and was detected at all and exceeded the screening level at 2 locations where it was detected with a maximum concentration of 6,000 µg/L at artesian flowing well OS-2.

#### Lateral Extent of Fluoride in Groundwater

Data used to evaluate the lateral extent of fluoride in groundwater include sampling results from the monitoring well network and from seeps. Plate 7-19 depicts the locations from which samples have been collected and analyzed for fluoride along with concentration data. The data indicate that boundaries encompassing concentrations of fluoride in excess of the screening level of 800 µg/L can be drawn over four separate areas of the site. Table 7-28 presents information on each of the four areas of impacted groundwater and these areas are graphically summarized in Figure 7-24. In summary, the area of fluoride in groundwater at concentrations exceeding the screening level encompasses about seven acres of land. Occurrences of fluoride at concentrations above screening levels at three of the four areas occur in only one or two wells (Figure 7-24).

#### Vertical Extent of Fluoride in Groundwater

Available sampling results used to evaluate the vertical extent of fluoride impacts to groundwater include sampling results through time at 21 vertical monitoring well clusters. Review of the data presented in Plate 7-19 at monitoring well clusters indicates that fluoride is defined vertically in all but two of the well clusters, both of which are located off-site (RD-59 and -68 clusters). However, no appreciable fluoride sources have been identified near these clusters and the occurrence of fluoride at concentrations above the screening level at these locations is believed to be the result of natural geochemical changes in the hydrogeologic system.

#### **7.3.5.19 Metals in Groundwater**

Metals in groundwater beneath SSFL were evaluated in detail because of their natural occurrence in the groundwater, some of which are discussed in the complementary site conceptual model document (Cherry, McWhorter, and Parker, 2009). Comparison concentrations for metals were established by the DTSC and presented in the Site-wide Risk Assessment Methodology, Revision 2 (MWH, 2005a). Discussions of metals in groundwater in this section of the report

apply to dissolved concentrations (i.e., filtered to remove suspended solids) and not total concentrations (i.e., unfiltered) because dissolved phase concentrations comprise the major mobile component of metals in groundwater. Additionally, sampling methods and analytical procedures for dissolved metals in groundwater at SSFL have improved significantly over the past 20 years. Much data have been analyzed and evaluated in the surficial media site and group reports about metals in groundwater, the primary purpose of which was to conservatively identify metals that should be included as chemicals of potential concern for inclusion in the human health and ecological risk assessments.

For this groundwater RI report, both the sampling results of metals in surficial media and groundwater were re-evaluated to assess the extent of metals in groundwater. As additional background, metals have not been used in appreciable quantities at SSFL except for some specialized work associated with nuclear reactor development in Area IV of SSFL. In this area, both sodium and potassium were used in support of the research activities conducted on behalf of DOE. Otherwise, releases of metals to the environment across SSFL were limited and occurred in local areas.

Transport modeling of metals from vadose zone soils to shallow alluvial groundwater was performed to further support, and provide context for, evaluating the extent of metals in groundwater at SSFL. The transport modeling is discussed in detail in appendix 7-F. The ECL RI site in the Group 5 reporting area was selected for this modeling effort because of its relatively shallow depth to groundwater (i.e., about 10 feet) and the fact that groundwater is present in alluvium. This latter feature is important for this modeling exercise because the results of the vadose zone transport model (SESOIL) can be coupled with a groundwater transport model (AT 123D) to evaluate metals transport in alluvial groundwater. The AT 123D groundwater transport code is not applicable to the fractured bedrock because it is not a discrete fracture model that incorporates diffusion. The model was used to simulate the transport of 23 different metals from the vadose zone to groundwater and subsequently within the groundwater. Results from the modeling effort showed the following key points:

- Breakthrough times varied between 1 and 60 years, reflecting the broad range in distribution coefficients that each metal exhibits,

- Groundwater retardation factors ranged from a low of 14.5 (boron) to more than 4,000 (nickel),
- Because of their strong retardation, metals were transported only very short distances beyond the footprint where they were released, and
- Concentrations in groundwater beneath the release location persist over long periods of time.

To provide additional context regarding the nature and extent of metals in groundwater at SSFL, the potential transport of boron in groundwater was further evaluated. Boron was selected for this evaluation because it has the lowest distribution coefficient and would therefore reflect the upper range of potential metals transport in groundwater.

The transport of boron from the vadose zone to groundwater and in alluvium groundwater was evaluated in three ways. First, a hypothetical “contaminated” source condition in soil was simulated by loading the first 3 sub-layers (30 centimeters (cm) or ~1 foot) of soil in the model with concentrations of boron 100 times above those measured at the ECL. This “contaminated” source condition was modeled in addition to that of the base case source condition, which applied calculated median concentrations of boron in soils at ECL throughout the soil profile. The base case concentrations of 2.75 milligrams per kilogram (mg/kg) (0-100 cm) and 1.7 mg/kg (100-201 cm) in soils at ECL are less than the background boron concentration of 9.7 mg/kg. Second, a sensitivity analysis was conducted that increased the longitudinal dispersivity by factors of 2, 5 and 10 above the base case value of 1 meter. Third, hypothetical points of compliance were established a distance of 50, 60 and 70 meters from the center of the source (0, 0), noting that the source area extends 45 meters beyond the center in each principal direction. Model results for the four longitudinal dispersivities over a 100-year period are depicted in Figure 7-25. Results are presented relative to boron’s groundwater comparison concentration (GWCC) of 0.34 mg/L (used as  $C_0$  for the purpose of displaying the results). Model results presented in Figure 7-25 show the following key points:

- The model over-predicts boron concentrations in groundwater under the natural source condition by a factor of 3 to 4 above the GWCC of 0.34 mg/L (i.e., is conservative, referred to below as modeled background).
- The 100-fold increase in soil concentrations in the first 3 sub-layers increases the predicted boron groundwater concentrations beneath the source by a factor of 20.

- Breakthrough at 5 meters (m) beyond the downgradient source area boundary under both source conditions occurs at all four longitudinal dispersivity values.
- Breakthrough in the “contaminated” source condition extends to 25 m beyond the source area boundary at the highest longitudinal dispersivity, but not at concentrations above the modeled background.
- For the “contaminated” source condition, concentrations above modeled background occur at the higher longitudinal dispersivities at a distance of 5 m beyond the source area boundary and reach values about 10 times above the modeled background. These elevated values also persist (i.e., they are not sporadic).

Similar simulations for a “contaminated” source condition were also completed for iron (Kd of 25), mercury (Kd of 70), barium (Kd of 213) and zinc (Kd of 590). Breakthrough at a distance of 5 meters beyond the downgradient extent of the source area was not predicted to occur within 100 years.

These modeling results showed that groundwater monitoring locations with detected concentrations of metals exceeding the comparison values needed to be positioned at or adjacent to source areas identified as a result of surficial media sampling or based on documented operational use. It is emphasized that the model results were not used in this evaluation in absolute terms, but to gain a better understanding as to their expected behavior of various metals in the context of evaluating potential the nature and extent of metals in SSFL groundwater.

Table 7-29 identifies monitoring locations where metals have exceeded the GWCCs for more than two consecutive sampling events at any time in their sampling history. Concentration through time graphs for these metals are provided in Appendix 7-G, Supplement I, while Supplement II in Appendix 7-G provides distribution plots of electrical conductivity (mean of 900  $\mu\text{mhos/cm}$ ) and pH (mean of 7.3) in groundwater across SSFL as additional background information. The elevated metals results from certain groundwater monitoring locations were further evaluated by reviewing the surficial media sampling results. The results of this evaluation are also provided in Appendix 7-G, Supplement III. Additional evaluations were performed to determine if elevated concentrations of metals in soil had impacted local groundwater. The results of that evaluation are also provided in Appendix 7-G, Supplement III.

The database was queried to identify locations in soil where metals concentrations exceeded background values by a factor of 100 or more. Five locations were identified where this criteria was met and where a monitoring well(s) was positioned close to the impacted soil. Metals evaluated for this condition included copper at the Happy Valley and LOX RI sites, mercury and cadmium at the LETF/CTL-I RI site, and mercury at the SRE RI site. This evaluation showed that groundwater was not impacted at concentrations above their respective GWCCs at any of these five locations.

A summary of the overall impacts of metals to groundwater from these evaluations show the following:

- Groundwater near the former Delta impoundment at the Delta RI site has likely been impacted by arsenic, copper and vanadium, and
- Groundwater at the former FSDF pond at the FSDF RI site has been impacted by boron, cadmium, cobalt, copper, molybdenum and nickel.

Locations where metals have impacted groundwater are shown in Figure 7-26.

#### **7.3.5.20 Other Chemicals in Groundwater**

Other chemicals in groundwater beneath SSFL at concentrations exceeding screening levels typically occur in very local areas (i.e., one or two wells dispersed throughout the site).

Beyond the chemicals evaluated and discussed in previous sections, there were ten remaining chemicals encountered in groundwater at concentrations exceeding screening levels over the July 2007/2008 timeframe. None of these chemicals are found at concentrations exceeding screening levels at more than two locations site-wide. The 10 chemicals exceeding screening levels in the July 2007/2008 dataset include the following:

- Chlorinated ethanes: 1,1,2-trichloroethane (one location), 1,1,1-trichloroethane (one location);
- Chlorinated methanes: Chloroform (two locations), methylene chloride (1 location);
- Non-halogenated VOCs: benzene (two locations);
- Semi-volatile organic compounds: bis(2-ethylhexyl)phthalate (two locations);

- Pesticides: aldrin (two locations), heptachlor (two locations), heptachlor epoxide (one location); and
- Inorganics: Sulfate (two locations, related to natural geochemistry).

Locations where these chemicals exceed their screening levels are shown in Figure 7-26 and a summary is provided in Table 7-30.

The groundwater database was queried for all historical results with concentrations greater than their screening levels. This evaluation shows an additional 31 chemicals as being present in SSFL groundwater in at least one sample. Results are shown in Table 7-31 and reveal that none of these chemicals exceed their screening value at more than three locations, except for chloromethane, toluene, and chloride. Results of these chemicals were further evaluated at the locations where screening values were exceeded to determine if concentrations in the most recent sample results remained above screening levels. This analysis revealed that there are 11 chemicals that were detected above screening values in the most recent sample results:

- Halogenated methanes: dichlorodifluoromethane (one location);
- Non-halogenated VOCs: toluene (one location);
- Halogenated benzenes: 1,2,3-trichlorobenzene (one location);
- SVOCs: 1,3-dinitrobenzene (one location), 2,6-dinitrotoluene (one location), 4,6-dinitro-o-cresol (one location), benzidine (one location);
- Polycyclic aromatic hydrocarbons (PAHs): benzo(a)pyrene TEQ (one location) and benzo(a)anthracene (one location);
- Inorganics: chloride (seven locations)
- Dioxins/Furans: 2,3,7,8-TCDD TEQ (seven locations)

Six chemicals were not detected in the most recent sample results but had reporting limits above the screening level:

- Halogenated propene/propanes: trans-1,3-dichloropropene (one location); and
- SVOCs: 2,6-dinitrotoluene (one location), 3,3'-dinitrobenzidine (one location), kepone (one location), n-nitrosodi-n-propylamine (two locations), and pentachlorophenol (two locations)

These chemicals and the locations where they have been detected are shown in Table 7-32 and Figure 7-26.

### **7.3.5.21 Completeness Reviews**

#### Evaluation of Results from Samples Collected After June 2008

As a completeness review, SSFL groundwater database was queried to determine if any additional chemicals were present in the groundwater post the “recent” dataset. Results from July 2008 through March 2009 are summarized in Table 7-33. New chemicals identified as a result of this query include:

- Methyl-tertiary-butyl-ether (MTBE), which was added to the list of target analytes in mid-2008,
- Dissolved gases including: acetylene, propane and propylene (acetylene not detected), these were included as analytes for characterizing TCE transformation pathways, and
- 2,4-diamino-6-nitrotoluene and 2,6-diamino-4-nitrotoluene (both non-detect), which were included for characterizing explosive by-products.
- Results of groundwater samples collected in May 2009 from piezometers in Administrative Areas I, II and III (see Appendix 4-M) are generally consistent with the descriptions of chemical impacts presented in this document. A review of the results indicates that a slight modification to the lateral extent of the area of TCE-impacted groundwater is warranted at the Alfa RI site. A slight modification for NDMA is warranted near the SPA RI site. MTBE was also detected in a piezometer at the Building 2204 RI site just south of an area of TPH-impacted groundwater. These modifications can be made for the Final Groundwater RI Report.

#### Extent of MTBE

Based on the most recent dataset results from July 2008 through March 2009, MTBE was identified as a new chemical posing a concern to SSFL groundwater as it was detected at concentrations above its screening level at 12 locations and thus its extent is discussed in this section. Note that the data used to evaluate the extent of MTBE is from a different timeframe than was used for other chemicals in groundwater, since MTBE was added to the list of target analytes for groundwater monitoring in mid-2008 and there were no prior detections of MTBE.

### Sources to Groundwater

MTBE was not encountered in surficial media at concentrations above RBSLs and was not recommended for further evaluation during the feasibility study for surficial media at any RI sites. TPH C<sub>4</sub>-C<sub>30</sub> soil matrix results are shown as a source for MTBE on Plate 7-20.

### Groundwater Sampling Summary

MTBE has been sampled in groundwater at 60 locations at SSFL of which it has been detected on at least one occasion at 14 locations and exceeded the screening level of 5 µg/L at 12 locations with a historical maximum concentration of 27.6 µg/L at RD-35B at the IEL RI site. In the July 08/March 09 dataset, MTBE was sampled in groundwater at 22 locations of which it was detected at 14 locations and exceeded the screening level at 12 of these locations with a maximum concentration of 27.6 µg/L also at RD-35B (all detections and exceedances were between July 08 and March 09).

### Lateral Extent of MTBE in Groundwater

Data used to evaluate the lateral extent of MTBE in groundwater include sampling results from the monitoring well network and from seeps. Plate 7-20 depicts the locations from which samples have been collected and analyzed for MTBE along with concentration data. The data indicate that boundaries encompassing concentrations of MTBE in excess of the screening level of 5 µg/L can be drawn over six separate areas of the site. Table 7-34 presents information on each of the six areas of impacted groundwater and these areas are graphically summarized in Figure 7-27. In summary, the area of MTBE in groundwater at concentrations exceeding the screening level encompasses about 53 acres of land. Occurrences of MTBE at concentrations above screening levels all six areas occur in only one or two wells if well clusters are considered as one well location (Figure 7-27).

### Vertical Extent of MTBE in Groundwater

Available sampling results used to evaluate the vertical extent of MTBE impacts to groundwater include sampling results through time at ten vertical monitoring well clusters. Review of the

data presented in Plate 7-20 at the ten well clusters indicates that MTBE is defined vertically in six well clusters: 3 off-site well clusters in the northeast and 3 well clusters in the north central portion of SSFL. MTBE is present at concentrations above the 5 µg/L screening level in groundwater samples collected from the deepest well from the RD-35, RD-41, RD-49, and RD-55 well clusters. However, considering the low concentrations at which MTBE has been detected, vertical transport is expected to be minimal.

### 7.3.5.22 Assessment of Groundwater Monitoring Network

The 3-dimensional groundwater flow model was used to help evaluate the effectiveness of the monitoring network by tracking particles from monitoring wells backward in the flow field to their starting point in the flow system. Details of the particle tracking approaches and results are presented in Appendix 6-A. Results of the backward particle analysis from monitoring wells under the steady-state pumping and steady-state non-pumping conditions are depicted in Figures 7-28 and 7-29, respectively. Flow paths were assigned colors based on their length. For this analysis, a vertical string of particles was released at 5 m depth intervals from wells across their entire screen or open-interval and tracked backward through the simulated flow field until they reach the water table (the recharge location for that flow path). No flow velocity or travel time is computed or implied, but the complete flow path is traced.

Using GIS, queries of the path lines were made to determine particle paths that flowed through a 3-dimensional projection of each RI site. The vertical dimension of the projection extended from the ground to a depth of 200 m for RI sites where TCE DNAPL was suspected to have historically been present. Historical DNAPL presence was made based on operational use or needs as reported in the surficial media RI reports and/or soil, rock core and groundwater sampling results as presented in previous sections of this report. Flow through the following RI sites was evaluated under the assumption that DNAPL was historically present:

IEL	APTF	LETF/CTL-I	Canyon
Bowl	CTL-III	LOX	ELV
Alfa	Bravo	Coca	Delta
Compound A	ECL	STL-IV	FSDF

At the remaining RI sites, the vertical dimension of the projection extended to a depth of 50 m to reflect transport of chemicals dissolved in recharge waters. The particles were then linked backed to the well of origin to determine the wells receiving flow from sources. This process conservatively highlights specific wells that have the potential to monitor chemical transport at each RI site. This method is conservative in that it does not account for any widening of the contaminant distribution as it expands through the flow field (i.e., dispersion).

Results of the simulated flow system from monitoring wells through RI sites shows that under steady-state pumping conditions two areas are not monitored (Building 4064 Leach field and Building 4065 Metals Clarifier), and under non-pumping conditions three are not monitored (Building 4065 Metals Clarifier, SE Drum Yard and CTL-V). Of these locations, potential surficial media impacts are such that bedrock groundwater at CTL-V should be characterized. Review of both the simulated flow field from sources (Figures 7-7 and 7-8) coupled with the simulated flow field to the monitoring wells shown in Figures 7-28 and 7-29 and surficial media sampling results indicates that additional characterization of groundwater beneath the Area I Burn Pit is also warranted.

#### **7.4 NATURE AND EXTENT OF RADIONUCLIDES IN BEDROCK AND GROUNDWATER**

Available information used in evaluating the nature and extent of radionuclide impacts to the bedrock vadose zone and groundwater at SSFL includes the following:

- Atomic International communications regarding well installations at SRE (Rockwell, 1973; AI, 1974, 1977a, 1977b; Rockwell, 1993a)
- Historical Site Assessment of Area IV (Sapere and Boeing, 2005),
- Draft Gap Analysis Report for Area IV EIS (Camp Dresser McKee (CDM), 2008),
- Radionuclides Related to Historical Operations at SSFL Area IV (SAIC, 2009),
- Reports on soils/bedrock excavations for radiochemistry impacts,
- Radiochemistry groundwater and seep sampling results (database through the 1st quarter 2009),
- Report on Data Gap Investigation for Radiological Constituents in Groundwater (Haley& Aldrich, see Appendix 4-P), and

- Data Summary – Construction and Testing of Core Borings SB\_Trit-01 and SB\_Trit-02 (Haley & Aldrich, see Appendix 4-P).

Further work regarding the characterization of potential radiological impacts to the environment is in the planning stages by EPA Region IX (Inter-Agency Agreement, 2009). This work reportedly includes the following three elements:

- Conducting a background study to determine site-specific background values for radiological contaminants,
- Initiating a historical site assessment evaluating past radiological activities in Area IV at SSFL, and
- Developing and implementing a work plan to complete a radiation survey, including: conducting a surface gamma scan, collecting and analyzing surface and subsurface soil samples and groundwater sampling. EPA estimates that approximately 10,000 soil samples will be collected. The EPA's SSFL radiological background study and Area IV radiological survey should be useful in evaluating cleanup options at SSFL and to support the preparation of SSFL's Area IV Environmental Impact Statement.

#### **7.4.1 Potential Sources of Radionuclide Impacts**

As described in Appendix 2-B of this report, nuclear operations at SSFL were conducted in Area IV. Nuclear facilities in Area IV were designed and operated to contain any accidental releases of nuclear materials within negative-pressure, high efficiency particulate air-ventilated structures whenever possible. Over 3,000 soil samples have been collected and analyzed for radionuclides to evaluate and assess releases to the environment. Furthermore, releases of nuclear material that may have escaped from structures and reached surficial media were characterized and cleaned up through excavation and off-site disposal as part of the radiological decommissioning and decontamination (D&D) process. Based on current information, areas remediated through excavation would represent potential radiological impacts to the bedrock vadose zone and groundwater. However, many former radiological facilities in Area IV have been released for unrestricted use and are not potential sources of radiological impact to SSFL groundwater.

In addition to the clean-up of historical releases reported as part of the radiological D&D process, other historical documents were reviewed to identify any areas where excavations were conducted for radiological clean-up and determine the nature or basis for the clean-up. Findings from this effort are depicted in Figure 7-30 and summarized in Table 7-35. Thirty-five different

excavations were identified. (Note: 32 excavation areas are shown in Figure 7-30 because multiple excavations were conducted at a few of the locations noted (e.g. Building 4020 and Building 4064 sideyard). These excavated areas are considered potential radiological sources to the bedrock vadose zone and groundwater.

#### **7.4.2 Bedrock Vadose Zone Radionuclide Characterization**

Rock core samples have been collected and analyzed for tritium from eight locations. Six locations were converted to groundwater monitoring wells while the remaining two coreholes were subsequently filled with grout. Locations from which samples were collected are within the vicinity of Building 4010 where characterization work was done to fill data gaps as described earlier in Section 4 of this report. Thirty-three rock core samples from the vadose zone were collected and analyzed for tritium as shown in Table 7-36. This table also shows that the rock core samples were collected from depths at or below the groundwater table. As stated earlier in this report, groundwater levels can fluctuate by significant amounts depending upon variations in rainfall duration and intensity, which recharges the groundwater system. Hence, the thickness of the bedrock vadose zone can vary accordingly.

Rock core sample results reported tritium in all 33 samples collected from the vadose zone. Statistical results of the samples showed the following: a minimum value; 74 picoCuries per liter (pCi/L); a median value; 19,500 pCi/L; an average value; 56,100 pCi/L and a maximum value; 247,000 pCi/L.

#### **7.4.3 Extent of Radionuclide Impacts to Groundwater**

The extent of the radionuclide impacts to groundwater was evaluated by querying the SSFL groundwater database for radiochemistry, which contains results from more than 1,400 samples dating back to 1989. Groundwater samples have been collected from 160 monitoring locations across SSFL and 12 seeps around the perimeter of SSFL and analyzed for general ionizing radiation (i.e., gross alpha and beta activity) and 49 radionuclides. Locations at SSFL that have been sampled for radiochemistry are shown in Figure 7-31. Sampled locations are not indicative of radiological impacts to groundwater, but provide a sense as to the magnitude and spatial

distribution of the sampling program. Individual sample results are provided in searchable electronic format as an attachment in Appendix 7-A (i.e., database (Microsoft Access) or spreadsheet (Microsoft Excel)).

Figures depicting both locations where excavations were conducted for radiological clean-up (i.e., potential sources that were described above) and wells that have been sampled for various isotopes of specific radioactive elements are presented in Appendix 7-H. Figures of the following ionizing radiation or radioisotopes are included in this appendix: Gross alpha, Gross beta,  $^{241}\text{Americium}$  (Am),  $^{137}\text{Cesium}$  (Cs),  $^{60}\text{Cobalt}$  (Co),  $^{152}\text{Europium}$  (Eu),  $^{154}\text{Eu}$ , and  $^{155}\text{Eu}$ ,  $^{238}\text{Plutonium}$  (Pu),  $^{239}\text{Pu}$ , and  $^{239/240}\text{Pu}$  (included on figure with uranium isotopes),  $^{228}\text{Thorium}$  (Th),  $^{230}\text{Th}$ ,  $^{232}\text{Th}$ , and  $^{234}\text{Th}$ ,  $^{90}\text{Strontium}$  (Sr),  $^{(233/234)}\text{Uranium}$  (U),  $^{234}\text{U}$ ,  $^{235}\text{U}$ ,  $^{236}\text{U}$ , and  $^{238}\text{U}$ , and  $^3\text{Hydrogen}$  (tritium).

A statistical summary of results from a database query of radiochemistry database is provided in Table 7-37. Excluding tritium, both filtered and unfiltered samples have been analyzed for radionuclides with most of the samples having been filtered prior to analysis. Tritium has been analyzed using only unfiltered samples (i.e., total) as its activity is minimally affected by sorption to aquifer solids. The radiochemistry results depicted on this table also identify the potential origin of each of the radionuclides characterized in SSFL groundwater. Radionuclides have been created under primordial or cosmogenic conditions (e.g.,  $^{238}\text{U}$ ), atmospheric testing of nuclear weapons (i.e., fallout from non-SSFL related activities), and/or from operations conducted for DOE in Area IV. Radionuclides analyzed in SSFL groundwater samples were compared to the list of radionuclides potentially generated and persistent/relevant at SSFL (SAIC, 2009, see Table 2 in Appendix 2-B). Seven radionuclides have not been analyzed for in either surficial media or groundwater samples: Beryllium-10, Cadmium-113m, Curium-224, Neptunium-237,  $^{240}\text{Pu}$  and  $^{241}\text{Pu}$ , and Promethium-147. Should their presence in surficial media be confirmed when additional sampling and analysis is conducted in the future, then groundwater samples from nearby wells should be collected and analyzed for any of these radionuclides detected.

Review of the results presented in Table 7-37 show the following regarding potentially-related radiation and radionuclide occurrence at SSFL:

- Groundwater samples for gross alpha activity, gross beta activity, radium, uranium and tritium exceed groundwater screening levels. The groundwater screening levels used for this evaluation are the national drinking water standards which are listed in Table 7-37 where applicable.
- Five site-related radionuclides have been detected in at least one SSFL groundwater sample:  $^{241}\text{Am}$ ,  $^{134}\text{Cs}$ ,  $^{137}\text{Cs}$ ,  $^{60}\text{Co}$ , and  $^{90}\text{Sr}$ .

Historical results of groundwater samples collected from wells installed in the 1970s at the SRE RI site also show local exceedances of gross beta activity. Results of each are further discussed below.

#### **7.4.4 Gross Alpha Activity in Groundwater**

The history of gross alpha groundwater sampling results was evaluated by comparing reported results to the gross alpha screening level of 15 pCi/L. Sample results from 133 locations were evaluated. Sampling locations are shown on the gross alpha in groundwater figure in Appendix 7-H. According to EPA drinking water regulations, the gross alpha screening level applied to this evaluation (primary drinking water MCL) excludes uranium activity (Federal Register, 2000). When available, isotopic uranium results for the wells sampled for gross alpha activity were subtracted from the gross alpha results.

This comparison showed that gross alpha results from at least one sampling event exceeded the screening value as follows: filtered samples-18 wells; unfiltered samples-17 wells; and filtered and unfiltered samples-9 wells. Therefore, a total of 44 unique wells had at least one sample result where the gross alpha activity exceeded the screening level. Thirty-nine of the 44 wells exceeded the screening value because there were no corresponding uranium isotope results that could be subtracted from the gross alpha activity. The remaining 5 wells had gross alpha activity exceedances even after isotopic uranium results were subtracted. Adjusted gross alpha data for these 5 wells are summarized in Table 7-38.

A review of gross alpha activity and uranium results from the 5 wells with at least a single sample result exceeding the screening value of 15 pCi/L showed the following:

- Unfiltered sample results from 2 wells, RS-05 and RD-97 had gross alpha activity above the screening level, while filtered sample results collected and analyzed on the same date had results below the screening value.
- A single filtered sample from RD-28 and two filtered samples from both RS-28 and RS-54 had adjusted gross alpha results above the screening value. Unadjusted gross alpha results from other sampling events for these wells also exceeded the screening value, because there were no corresponding uranium results to allow for any adjustments. When uranium results were available for these three wells, adjusted gross alpha results were below the screening level.

These results potentially reflect historical sampling methods at these locations and not degradation of the groundwater by gross alpha activity. This interpretation is based on the infrequent and sporadic nature of the elevated results, application of a screening methodology that was developed after many of the samples were collected, and an understanding of the behavior of the impacts in the groundwater system.

Impacts to groundwater from past radionuclide releases generating gross alpha activity would exhibit persistent results above the screening level at the locations monitored. The analysis of the nature of stable metal isotope (i.e., non-radioactive) detections presented earlier in Section 7 can be used as an analog for radionuclides as both species are strongly sorbed to aquifer solids (except for tritium, discussed further below).

The nature of gross alpha exceedances at locations without uranium data was further evaluated by graphing all gross alpha sampling results from each location over time. Graphs are presented in Appendix 7-I, Supplement I. For the group of wells where isotopic uranium data were not collected and the unadjusted gross alpha activity persistently exceeded the 15 pCi/L screening level, samples should be collected and analyzed for gross alpha activity and isotopic uranium to obtain representative results (e.g., HAR-18, RS-08, etc.).

#### **7.4.5 Gross Beta Activity in Groundwater**

The history of gross beta activity groundwater sampling results was evaluated by comparing reported results to the gross beta screening level of 50 pCi/L. Results were reviewed from historical groundwater investigation reports conducted at the SRE RI site in the 1970s and from groundwater monitoring network samples collected starting in the late 1980s.

Gross beta results from samples collected in a Wash Cell Valve Pit at the SRE RI site and wells referred to as Well #2, #3 and #5 were reported by AI and Rockwell in written communications from 1973, 1977 and 1993. Gross beta sampling results exceeded screening levels at Wells #2 and #5. The reports indicate that water was present in Well #5 for only a month or two in 1977 and was likely associated with a leak from a water-filled storage pit within the SRE building. The interpreted positions of these wells and reported gross beta activity results are graphically presented in Appendix 7-I, Supplement II. In 2004, wells RD-85 and RD-86 were installed in close proximity to Wells #2 and #3, respectively. Samples were collected from both of these wells in 2004 and 2005 and analyzed for gross beta; results were below the screening level. Piezometers PZ-150, PZ-160 and PZ-161 were installed in 2008 in proximity to Well #5 at DTSC's direction, but groundwater has not accumulated to the depth intercepted by their screened intervals during quarterly gauging and sampling events. Gauging and monitoring at the three piezometers will continue into 2011.

Gross beta sample results from 133 locations in the groundwater monitoring well network were also evaluated. Locations sampled are shown on the gross beta in groundwater figure in Appendix 7-H. According to EPA drinking water regulations (2000), the gross beta screening level applied for this evaluation (primary drinking water MCL) excludes  $^{40}\text{K}$ , which is naturally occurring. Where available,  $^{40}\text{K}$  results for the wells sampled for gross beta activity were subtracted from the gross beta results.

This analysis showed that gross beta results exceeded the screening level in four wells during a sampling event in 1989. The 1989 sampling program occurred during the implementation of the radiochemistry groundwater sampling program at SSFL. Because these samples were not analyzed for  $^{40}\text{K}$ , this naturally occurring radionuclide was not subtracted from the gross beta result. Wells with gross beta exceedances in this timeframe included: HAR-11, OS-12, RS-22 and WS-8. It also appears that the original samples from the 1989 sampling program were not filtered, but that filtered samples (referred to previously as decanted samples) were analyzed in later sampling events. Filtered sample data do not show gross beta activity above the 50 pCi/L screening level at these four well locations. This would suggest that the exceedances were due to high levels of suspended solids containing naturally-occurring  $^{40}\text{K}$  and beta-emitting decay

products of uranium and thorium. Graphs of the results are presented in Appendix 7-I, Supplement III.

There are also filtered samples from four other wells where the gross beta activity screening level was exceeded one time: HAR-15, RD-19, RD-25 and RD-54A. Re-analysis of the primary samples from HAR-15 and RD-19 reported results below the screening level. Analysis of split samples from RD-25 also reported results below the screening level. All other results for these locations were below the screening level. Graphs of the results are presented in Appendix 7-I, Supplement III. Based on the evaluation of the full dataset, there are no exceedances of gross beta activity in SSFL groundwater at the 133 locations sampled.

#### **7.4.6 Isotopic Radium in Groundwater**

The  $^{226}\text{Ra}$  (potentially site-related) and  $^{228}\text{Ra}$  (naturally occurring) sampling results from the historical database were summed and compared to the screening level of 5 pCi/L (primary drinking water MCL). Eighty-seven monitoring locations have been sampled and analyzed for dissolved  $^{226}\text{Ra}$  and 56 locations have been sampled and analyzed for dissolved  $^{228}\text{Ra}$ . The comparison of the combined radium isotopes to the 5 pCi/L screening level showed that eight wells had at least one exceedance above the screening level: HAR-15, HAR-16, RD-18, RD-27, RD-33A, RD-54B, RD-63 and RD-97. Graphs of the sum of these two radium isotopes over time for the eight wells are provided in Appendix 7-I, Supplement IV. Exceedances of  $^{226+228}\text{Ra}$  at RD-27, RD-33A and RD-63 occurred only once, with all other results below the screening level, while there were 2 exceedances at RD-54B (5.12 and 5.17 pCi/L). The RD-97 sample result exceeding the screening level was for an unfiltered sample. A filtered sample collected during the same sampling event showed  $^{226+228}\text{Ra}$  to be below the screening level. The sample results for RD-18 and HAR-16 are more than 16 years old and the wells should be re-sampled for radium isotopes, particularly HAR-16 as one of the reported results appears to be an extremely high outlier (~460 pCi/L) potentially the result of sampling or laboratory error.

#### 7.4.7 Isotopic Uranium in Groundwater

The history of isotopic uranium sampling results was evaluated by comparing reported results to the screening level of 20 pCi/L for total uranium (California MCL). Locations sampled and analyzed for uranium varied by isotope from one location for dissolved  $^{236}\text{U}$  to 80 locations for  $^{235}\text{U}$ . Locations sampled for the various isotopes are shown on the uranium and plutonium in groundwater figure in Appendix 7-H. At least one sample result from eight wells contained total uranium activities exceeding the screening level. Sample results from these eight locations were evaluated by characterizing the uranium isotopic composition in each well. Graphs of the  $(^{233/234}\text{U})$  to  $^{238}\text{U}$ , and  $^{235}\text{U}$  to  $^{238}\text{U}$  ratios over time are provided in Appendix 7-I, Supplement V. The calculated uranium isotope ratios were evaluated to determine if the total uranium exceedances are the result of site-related activities or due to naturally occurring uranium.  $(^{233/234}\text{U})/^{238}\text{U}$  and  $^{235}\text{U}/^{238}\text{U}$  isotope ratios in the range of 1.03 and 1.05, respectively, are indicative of naturally occurring conditions. When uranium isotope ratios significantly exceed the natural occurring uranium isotope ratios, anthropogenic releases of uranium can be suspected. Calculated uranium isotope ratios, including quantifying the uncertainty associated with the analytical method, are provided in Table 7-39. As shown on the table and in the graphs of Supplement V of Appendix 7-I, where total uranium has been detected above the 20 pCi/L screening level, nearly all of the uranium isotope ratios fall in the range of naturally occurring uranium.

#### 7.4.8 Tritium in Groundwater (Site-related)

Samples have been collected from 132 locations and analyzed for site-related tritium releases. The number of monitoring locations does not include the collection of samples that have been analyzed for low-level tritium during the characterization of groundwater flow paths at and from SSFL as described earlier in Section 4 and in the complementary Site Conceptual Model document (Cherry, McWhorter, and Parker, 2009). These low-level tritium occurrences result from atmospheric testing (i.e., non-SSFL) of nuclear weapons in the 1950s and early 1960s (Clark and Fritz, 1997).

The occurrence and distribution of tritium in groundwater was investigated in detail at Building 4010 as a result of the data gap sampling work performed between 2004 and 2007 (see Appendix 4-P). Prior to this work, there were no exceedances of tritium's screening level of 20,000 pCi/L in any sample from SSFL monitoring locations. Using both rock core and groundwater sampling results, the data gap sampling work identified an area of tritium in groundwater at concentrations above its screening level.

#### **7.4.8.1 Saturated Rock Core Sampling Summary**

Rock core samples have been collected and analyzed for tritium from the same eight locations used to characterize the bedrock vadose zone (Section 7.1.2). Ninety-five rock core samples from the saturated zone were also collected and analyzed for tritium as shown in Table 7-36. Rock core sample results from the saturated zone showed that tritium was found in all samples analyzed. Statistical results of the samples showed the following: minimum value; 16 pCi/L; a median value; 41,800 pCi/L; an average value; 75,200 pCi/L; and a maximum value; 931,000 pCi/L.

#### **7.4.8.2 Lateral Extent of Tritium in Groundwater**

Data used to evaluate the lateral extent of tritium in groundwater include sampling results from the groundwater monitoring well network and seeps. Samples from four monitoring wells, RD-88, RD-90, RD-93 and RD-95, contain tritium at concentrations above its screening level. The area of tritium-impacted groundwater is shown in Figure 7-32 and is estimated to encompass about 4.4 acres of land.

#### **7.4.8.3 Vertical Extent of Tritium in Groundwater**

Sampling results used to evaluate the vertical extent of tritium impacts at Building 4010 include the rock core sampling results from coreholes SB\_Trit-01 and SB\_Trit-02. SB\_Trit-01 and SB\_Trit-02 were drilled to depths of 128.5 and 220.0 feet, respectively. The average concentration of tritium in rock core in the bottom 50 feet (i.e., 79.75 feet to 127.25 feet) of SB\_Trit-01 was 70,900 pCi/L (10 samples). The average concentration of tritium in a similar interval in SB\_Trit-02 (i.e., 78.25 feet to 128.25 feet) was 57,600 pCi/L (11 samples). The average concentration of tritium in the bottom 50 feet (i.e., 172.25 to 219.25 feet) of SB\_Trit-02

was 8,400 pCi/L (12 samples) and none of the samples reported a tritium activity above 20,000 pCi/L. The rock core sampling results from the bottom 50 feet of SB\_Trit-02 indicate that the base of tritium impacts at this location have been defined relative to the tritium screening level. Tritium sampling results from vertical monitoring well clusters positioned in and around SSFL do not show impacts at depth.

Additional details and displays of tritium in groundwater are provided in Appendix 4-P.

#### 7.4.9 Other Radionuclides in Groundwater

Five other site-related radionuclides have been detected in at least one SSFL groundwater sample and include the following: <sup>241</sup>Am, <sup>134</sup>Cs, <sup>137</sup>Cs, <sup>60</sup>Co, and <sup>90</sup>Sr. The detections of <sup>241</sup>Am, <sup>134</sup>Cs, <sup>137</sup>Cs, and <sup>60</sup>Co have been infrequent and measured in only a few wells. However, <sup>90</sup>Sr has been detected in all sampling events from one well (RD-98), but at concentrations below the 8 pCi/L screening level. Isotope <sup>241</sup>Am was detected in well RD-33B during a single sampling event. A summary of the sampling results for these five radionuclides is provided below.

Radionuclide	Well	Number of Detections	Number of Sampling Events	Percent Detected (percent)	Comment
<sup>241</sup> Am	RD-33B	1	1	100	Detected in Primary (Dissolved) Sample; Unfiltered Primary and Field Duplicate Samples – ND.
<sup>134</sup> Cs	RS-54	1	19	5	Detected in Primary Sample.
<sup>137</sup> Cs	RD-17	1	16	6	Detected in Primary Sample (J Value); Unfiltered Sample (Same Date) – ND.
	RD-23	2	30	7	1 <sup>st</sup> Detect in Field Duplicate Sample; Primary Sample – ND; Unfiltered Sample (Same Date) – ND. 2 <sup>nd</sup> Detect in Primary Sample Only (Different Date).
	RD-33B	2	27	7	1 <sup>st</sup> Detect in Primary Sample; Lab Repeat – ND. 2 <sup>nd</sup> Detect in Primary Sample Only (Different Date).
	RD-34A	2	26	8	1 <sup>st</sup> Detect in Primary Sample; Lab Repeat – ND. 2 <sup>nd</sup> Detect in Primary Sample; Lab Repeat – ND (Different Date).

Radionuclide	Well	Number of Detections	Number of Sampling Events	Percent Detected (percent)	Comment
<sup>60</sup> Co	RD-33B	1	22	5	Detect in Primary Sample; Lab Repeat – ND.
	RD-34A	1	19	5	Detect in Primary Sample; Lab Repeat – ND.
	RD-34B	1	23	4	Detect in Primary Sample.
<sup>90</sup> Sr	RD-98	3	3	100	Detects in Three Primary (Dissolved) Samples; One Detect in an Unfiltered Sample on 11/14/2008.

#### 7.4.10 Summary of Radionuclides in Bedrock and Groundwater

The clean-up of radiological facilities in SSFL Area IV has also involved the identification, delineation, and removal by excavation of radiological impacts to surficial media. Documents and materials were reviewed to identify the locations of excavation that have been conducted during this clean-up. These former locations of radiological impacts to surficial media are considered potential sources of radioactivity and radionuclides to vadose zone bedrock and groundwater.

A data gaps analysis of potential groundwater impacts was performed in 2004. Data gaps were filled by collecting and analyzing rock core samples for tritium, and installing and sampling 14 additional groundwater monitoring wells. The data gaps work resulted in the identification and characterization of an area of groundwater impacted with tritium at concentrations above the 20,000 pCi/L screening level that includes four wells (RD-88, RD-90, RD-93 and RD-95). The area of impact covers about 4.4 acres and extends about 300 feet or so from the suspected release location. Characterization of the vadose and saturated zone bedrock for the occurrence and distribution of tritium was also conducted through the analysis of rock core. Tritium was detected in 33 vadose zone samples collected from locations within the impacted area at an average concentration of 56,000 pCi/L. Tritium was also detected in 95 saturated zone bedrock samples at an average concentration of 75,300 pCi/L. The presence of tritium in the porewater from rock core samples is primarily due to its attenuation and retardation by diffusion.

The extent of radionuclide impacts to groundwater was further evaluated by querying the SSFL groundwater database for radiochemistry, which contains sample results dating back to 1989. Groundwater samples have been collected and analyzed for general ionizing radiation (i.e., gross alpha and beta activity) and 49 radionuclides from 160 monitoring locations across and around SSFL with the sampling emphasis appropriately focused on wells within and around Area IV. A comparison of the list of radionuclides that have been analyzed for in SSFL groundwater samples to the list of radionuclides potentially generated and persistent/relevant at SSFL shows that groundwater samples have not been analyzed for seven radionuclides that may have been generated from Area IV operations. Should their presence in surficial media be confirmed when additional sampling and analysis is conducted in the future, then groundwater samples from nearby wells should be collected and analyzed for any of the seven radionuclides detected in surficial media. Review and evaluation of the sampling results included in the database showed the following:

- Exceedances of gross alpha and beta activity, radium, and total uranium above screening levels and the detections of  $^{241}\text{Am}$ ,  $^{134}\text{Cs}$ ,  $^{137}\text{Cs}$ ,  $^{60}\text{Co}$ , are infrequent and sporadic and are not representative of impacts to SSFL groundwater.
- A few wells should be re-sampled for both gross alpha activity and uranium to determine the validity of older data where uranium results were not available to evaluate the effect of naturally-occurring uranium on the gross alpha activity results.
- The detections of  $^{90}\text{Sr}$  have been persistent at one well (RD-98), indicating that it is present in groundwater. However, the  $^{90}\text{Sr}$  levels in RD-98 have been below the 8 pCi/L screening level.

## 7.5 SUMMARY

Work performed on the surficial media operable unit at SSFL has resulted in the identification of the chemicals used and released into the environment (Table 7-1). Known or potential releases have been characterized using appropriate methods for the chemicals encountered with approval and oversight by the DTSC. Remedial investigation reports have been issued for RI sites within the 11 Group reporting areas. Since the Group 9 report (NASA, 2009b) was issued nearly concurrent with this draft groundwater RI report, its results have not been incorporated as there was insufficient time to do so. Results from the surficial media reports were used in identifying and evaluating sources of releases to the bedrock vadose zone and groundwater.

### 7.5.1 Bedrock Vadose Zone

The bedrock vadose zone has been characterized at both sources and above plumes through the collection of rock core at 17 locations and the analysis of up to 1,580 samples. A summary of the vadose zone rock core sample results is presented in Table 7-8. In summary, TCE is the primary contaminant of concern both in terms of the magnitude of measured concentrations and the frequency of detections found in the analysis of rock core vadose zone samples. TCE was detected 61 percent of the vadose zone samples analyzed. The equivalent TCE mass in the vadose zone relative to that below the water table also varies considerably ranging from a low of 1 percent (C6, Delta RI site) to a high of 95 percent (FSDF RI site). Various factors affect this distribution and include: the total completion depth of the corehole, the thickness of the vadose zone, the distance from the input location, the total mass released into the ground, and the penetration of immiscible phase TCE below the water table. PCE was detected in 52 percent of the samples, but at much lower concentrations. Two of the three DCE isomers (cDCE, and 1,1-DCE) were also frequently detected (20 percent and 22 percent, respectively), but again at much lower concentrations than TCE.

Minor detections of 1,4-dioxane, an acid scavenger for 1,1,1-TCA were also found in the vadose zone. 1,4-dioxane was encountered in 58 percent of the vadose zone samples at C3 and was a minor contaminant at the other locations. However, 1,1,1-TCA was only detected in three vadose zone samples (from C9). CFC-113 was found in 75 percent and 12 percent of the vadose zone samples from C1 (also location of maximum concentration) and C8, respectively, and was a minor contaminant at the other locations. Perchlorate was found in 31 percent of the vadose zone samples in RD-77. At the other 5 wells or coreholes where rock core samples were analyzed for perchlorate, it was detected in only 3 of 243 vadose zone samples analyzed, with the detected concentrations being at or below its screening level of 6 µg/L. The other analytes (chlorobenzene, toluene, isopropylbenzene, and EFH) that were detected in vadose zone rock core samples were found infrequently and are of minor importance relative to the chlorinated ethenes. Finally, it should be noted that about 45 other EPA method 8260 analytes were not detected in any vadose zone bedrock samples. Characterization of the bedrock vadose zone for

tritium impacts showed that it was found in all 33 samples tested, demonstrating its diffusion into the bedrock.

### 7.5.2 Groundwater

Two broad areas of impacted groundwater, defined as that containing concentrations of chemicals exceeding screening values, have been identified in SSFL groundwater: an area encompassing about 247 acres along the eastern portion of SSFL, and a second area encompassing about 470 acres in the central and western part of SSFL. Four other areas have been identified totaling about 15 acres and ranging in size from 0.8 to 8.9 acres. The total area of impacted groundwater is about 732 acres. Summary of the lateral extent of impact is shown in Table 7-40. Locations are shown in Figure 7-33. Chemicals contained within these areas include the following list of 52:

- Chlorinated solvents (18):
  - Chlorinated ethenes (6): PCE, TCE, cDCE, tDCE, vinyl chloride, and 1,1-DCE;
  - Chlorinated ethanes and by-products (5): 1,1,2-TCA, 1,1,1-TCA, 1,2-DCA, 1,1-DCA, and 1,4-dioxane;
  - Chlorinated methanes (4): carbon tetrachloride, chloroform, methylene chloride, and dichlorodifluoromethane;
  - Chlorinated Benzene (1): 1,2,3-trichlorobenzene
  - Chlorinated propane/propenes (2): 1,2,3-trichloropropane and trans-1,3-dichloropropene;
- Non-halogenated organics (5): formaldehyde, TPH C<sub>4</sub>-C<sub>30</sub>, benzene, MTBE, and toluene;
- Semi-volatile organic compounds (12): n-nitrosodimethylamine, bis-2-ethylhexyl-phthalate, 1,3-dinitrobenzene, 2,6-dinitrotoluene, 3,3'-dichlorobenzidine, 4,6-dinitro-*o*-cresol, benzidine, kepone, n-nitrosodi-n-propylamine, and pentachlorophenol;
  - Polyaromatic hydrocarbons (2): benzo(a)pyrene TEQ and benzo(a)anthracene;
- Pesticides (3): Aldrin, Heptachlor, and Heptachlor epoxide;
- Dioxins/furans (1): 2,3,7,8-Tetrachlorodibenzo-p-dioxin TEQ
- Metals (8): arsenic, boron, cadmium, cobalt, copper, molybdenum, nickel, and vanadium; and
- Inorganics (5): perchlorate, nitrate, fluoride, sulfate, and chloride.

Immiscible-phase kerosene-range hydrocarbons were also found on the water table at two monitoring locations, one at the Alfa RI site and the other at the Canyon RI site.

The vertical extent of most of these chemicals has been defined based on results of collection and analysis of samples from monitoring well clusters and from bedrock core. Table 7-42 provides a summary assessment of the vertical extent for the 18 chemicals that were detected at more than five locations across SSFL. This table shows that the vertical extent of impacts has not been defined to concentrations below screening levels at the following well clusters: TCE and PCE at RD-49 and -55; TCE, 1,4-dioxane, and carbon tetrachloride at RD-35; vinyl chloride at RD-49 (co-located with TCE and PCE) and RD-58; formaldehyde at RD-49; MTBE at RD-35 (co-located with TCE and 1,4-dioxane), RD-41, RD-49 (co-located with PCE, TCE, vinyl chloride, and formaldehyde), and RD-55 (co-located with PCE and TCE). However, concentrations at the deepest well within these clusters are typically only a factor of 1 or 2 above the screening levels. For some chemicals, the depth of impacts could not be confirmed by sampling results due to reporting limits exceeding screening values or because no samples had been collected (as shown in Table 7-42). Fluoride at the RD-59 and RD-68 well clusters is attributed to natural conditions and not site-related impacts.

Characterization of radiological impacts shows an area of tritium in groundwater at concentrations exceeding 20,000 pCi/L that covers about 4.4 acres. Detections of tritium in porewater from rock core samples demonstrate its attenuation and retardation by diffusion even though sorption plays no role. Additional sampling of the existing well network should be conducted to evaluate the potential occurrence of seven potentially site-related radionuclides for which the groundwater has not been characterized should future surficial media sample collection and analysis show them to be present in environmental media.

## **7.6 SITE CHARACTERIZATION DATA GAPS**

Analysis of surficial media characterization results for the CTL-V, Area I Burn Pit and Coca RI sites indicates these sources have not been characterized for potential impacts to bedrock groundwater, primarily from VOCs. These sites should be evaluated through the collection of field data to characterize the nature of any impacts. Groundwater flow path analyses for CTL-V

and Area I Burn Pit RI sites indicate that the position of existing monitoring wells may not intercept groundwater flowing through a portion of these sites. Any identified impacts to groundwater beneath CTL-V or Area I Burn Pit sites should be characterized through collection of additional data. Groundwater flow path analyses from the Coca RI site indicates that existing wells are positioned such that groundwater flowing from this area is monitored.

The former pond at the SRE RI site is recommended for further characterization based on historical use of the pond, its proximity to the northern property boundary, and groundwater flow path and Darcy flux analyses. Should impacts to bedrock groundwater be identified, their extent should be characterized.

Collection and analysis of samples from select wells within the groundwater monitoring network for a specified set of target analytes should also be conducted to confirm their vertical and/or lateral extent of impacts to bedrock groundwater. Locations and target analytes will be specified in the sampling and analysis plan to be submitted in mid-April 2010.

## 8.0 TRANSPORT AND FATE

This section discusses potential migration pathways for the chemicals present in the bedrock vadose zone and groundwater. Chemical releases occurred as liquid product (both lighter and denser than water), gas (i.e. vapor), solutes in water (or other liquids) and as solids (from which solutes were generated) as described in Section 7.0. Chemicals encountered based on the surficial media and groundwater characterization work are addressed in this section. Physical properties of these chemicals that affect their transport in air, soil, bedrock, and groundwater, and the inter-phase partitioning that occurs among these media, are discussed. The processes that influence transport and fate of these COCs are then discussed. Predictions of transport and fate for specific chemicals throughout the site are evaluated and compared with corresponding analytical results and the results of numerical simulations of chemical transport.

The processes to be addressed involve one or more fluid phases in a heterogeneous, fractured porous solid. In some cases, chemicals migrate not only as a separate phase but also in the gaseous phase and as a dissolved constituent in the aqueous phase. Contaminant transport is complicated further by inter-phase partitioning among all the phases, including the solid phase. All of these processes are dependent on local values of the controlling parameters such as porosity, permeability, density, fluid content, organic carbon content, rock mineralogy, and capillary properties. Finally, the contaminant distribution is affected by spatially and temporally variable infiltration, recharge and contaminant inputs.

Due to this complexity, values for the parameters above, including detailed spatial and temporal variations, cannot feasibly be obtained. However, application of established principles coupled with knowledge of empirical values can provide important qualitative and conceptual insights into the distribution and transport of contaminants in such a system. The discussion that follows was developed in this context.

## 8.1 TRANSPORT ROUTES

The potential routes of chemical transport include the following:

### **From chemicals within alluvial or colluvial soil:**

- Gaseous phase diffusion to the atmosphere, vadose zone bedrock, and groundwater;
- Dissolution of site chemicals in surface soils into recharge waters and transport to vadose zone bedrock and groundwater; and
- Flow of non-aqueous liquids and dissolution to the aqueous phase, volatilization and sorption to solid surfaces.

### **From chemicals within vadose zone bedrock:**

- Gaseous phase diffusion to the atmosphere and groundwater;
- Imbibition of non-aqueous phase liquids to the rock matrix and partitioning to the vapor, aqueous and solid phases; and
- Aqueous phase transport to groundwater by recharge waters.

### **From chemicals dissolved in groundwater:**

- Advection and diffusion; and
- Volatilization from groundwater into vadose zone bedrock and soil gas.

### **From DNAPLs that may be present below the water table:**

- Dissolution into groundwater by advection; and
- Advection and diffusion after dissolution.

A diagram depicting a number of these transport pathways is shown on Figure 8-1.

## 8.2 PROCESSES AFFECTING CHEMICAL TRANSPORT

A number of processes affect the transport and fate of chemicals present at the surface and in the subsurface. If a chemical is released to the ground as a solid or non-aqueous phase substance, the solubility of the chemical in water (designated *S*) determines the mass of the chemical that can dissolve in vadose zone pore water and groundwater. The solubility is also important if

aqueous chemical concentrations approach saturation, as the solubility limit represents the maximum mass of a chemical that can be dissolved in a unit volume of water.

Vapor pressure and the Henry's Law constant for volatile chemicals are important parameters influencing transport and fate. Vapor pressure expresses the pressure of the vapor phase of a chemical (usually in millimeters [mm] of mercury [Hg]) in equilibrium with the pure liquid phase (i.e., non-aqueous phase liquid). At a minimum, vapor pressure values provide a qualitative indication of the tendency of a pure chemical to volatilize. The Henry's Law constant for a chemical may also be important in determining transport and fate in the vadose zone because it determines the partitioning into the dissolved (i.e., pore water) and vapor (i.e., soil gas) phases. The Henry's Law constant is calculated according to an equation of the form:

$$\text{Henry's Law Constant} = \frac{\text{vapor pressure} * \text{molecular weight}}{\text{solubility}}$$

and the values are adjusted according to the desired units. The Henry's Law constant is also important in the saturated zone as it indicates a chemical's propensity to transfer from the aqueous phase to the gas phase with possible subsequent diffusive transport to the vadose zone.

Chemicals dissolved in pore water in the vadose zone can be transmitted to groundwater by recharge waters. Vertical permeability and porosity of the vadose zone material affects this transport mechanism. If DNAPL is present, fracture characteristics such as aperture width and capillarity, along with fluid characteristics such as viscosity, influence whether DNAPL can enter and migrate through fractures. Values of hydraulic apertures for these were discussed in Section 6 of this report. The persistence of DNAPL is described further below in Section 8.5.

In fractured vadose zone rocks, gaseous diffusion often represents the primary mechanism for transport of a volatile chemical. Air diffusivity describes the tendency of a chemical to diffuse in air, while air permeability describes the capacity for diffusion to occur in soil or the unsaturated bedrock matrix. The air diffusion coefficient ( $D_{\text{air}}$ ) is calculated according to:

$$D_{\text{air}} (\text{cm}^2/\text{s}) = 0.001 T^{1.75} M_r^{1/2} / P (V_A^{1/3} + V_B^{1/3})^2$$

where:

T = Temperature in degrees Kelvin

$M_r$  is a function of molecular weight:  $M_r = (M_a + M_b) / M_a / M_b$ , and

where:

$M_A$  is the molecular weight of air, approximately 28.97 g/mol

$M_B$  is the molecular weight of the compound of interest, and

$V_A$  is the molar volume of air (approximately 20.1 cm<sup>3</sup>/mol)

$V_B$  is the molar volume of the compound of interest

Once a chemical has been transported to the water table, transport occurs through advection, hydrodynamic dispersion and diffusion. Advective processes, or the bulk motion of flowing groundwater, were previously described in Section 6.0. Hydrodynamic dispersion, or the tendency of a solute to spread out more than predicted by advective flow, consists of two components: mechanical mixing and molecular diffusion.

Mechanical mixing occurs during groundwater flow in response to microscopic features such as the tortuosity of flow paths and variations in pore size and pore wall roughness along a flow path. Mechanical mixing is difficult to measure in the field, and reliable values are not available in the literature. Rough estimates for mechanical mixing are often estimated on a site-specific basis based on chemical distributions in an aquifer.

Molecular diffusion in an aqueous medium describes the tendency of a chemical to diffuse in water, and is expressed by a water diffusion coefficient ( $D_{\text{water}}$ ). The water diffusion coefficient is calculated according to:

$$D_{\text{water}} = 13.26 \times 10^{-5} / \eta^{1.14} (V_B')^{0.589}$$

where:

$\eta$  is the viscosity of water

$V_B'$  is the LaBas estimate of molar volume

Molecules of a chemical diffuse in response to concentration gradients. Diffusion often occurs so slowly that it is not considered a significant factor influencing the transport and fate of

chemicals in groundwater. However, Foster (1975) described how diffusion often occurs at a sufficiently rapid rate in fractured rocks to be a significant influence, if not the predominant influence, on chemical transport in groundwater. It should be noted that diffusion acts simultaneously as a mechanism for both transport and retardation, as described further below. Diffusion processes in SSFL groundwater are described further in Sections 8.4 and 8.5.

The transport of constituents in groundwater is retarded by various processes, including adsorption, degradation, and diffusion. Adsorption to the aquifer matrix is largely determined by the bulk density ( $\rho_b$ ) and organic carbon content of the aquifer ( $f_{oc}$ ). Adsorption is also influenced by properties of the chemical. Many organic pollutants are hydrophobic, which indicates that they have a low affinity for solution in water (a polar liquid), and prefer solution in non-polar liquids. These pollutants are readily taken up in organic matter in soil and rock solids. The tendency to be adsorbed is related to the distribution coefficient of the chemical in a non-polar liquid (usually taken to be octanol). The ratio of the equilibrated concentrations of an organic substance in a two-phase system consisting of octanol and water is represented by the symbol  $K_{ow}$ . The organic carbon-water partition coefficient, designated  $K_{oc}$ , is related to  $K_{ow}$ , according to a chemical-specific equation of the form:

$$\text{Log}_{10}K_{oc} = x * \text{Log}_{10}K_{ow} + \text{constant}$$

where:

x is experimentally determined. These properties are included in the distribution or partition coefficient ( $K_d$ ), given by:

$$K_d (\text{ml/g}) = \frac{\text{mass of solute on the solid phase per unit mass of solid mass}}{\text{concentration of solute in solution}}$$

$$K_d = f_{oc} * K_{oc}$$

The parameters described above act to retard solute transport in groundwater according to:

$$v_{gw}/v_s = 1 + \rho_b/n_e * K_d$$

where:

$v_{gw}$  = velocity of groundwater (cm/s)

$v_s$  = velocity of solute (cm/s)

$\rho_b$  = bulk density (g/ml)

$n_e$  = effective porosity (unitless)

The right side of the equation is described by the “*retardation factor*”, designated “*R*”.

A chemical may also undergo biotic degradation (i.e., biodegradation) or abiotic transformation. Both processes result in attenuation of the degrading chemical and increased mass (and corresponding concentration) of the chemical that is produced (i.e., daughter product). Biological degradation may occur under aerobic conditions (i.e., in the vadose or saturated zone) or anaerobic conditions (in the saturated zone). The rate at which degradation proceeds is described by a degradation constant or, a half-life, for the chemical. While the half-life of a radionuclide is purely dependent on its identity, the half-lives of organic chemicals also depends on the environmental conditions. Degradation of TCE and its daughter products cDCE and vinyl chloride have been extensively studied at SSFL and these studies are summarized and discussed in Section 8.6.

Half-lives of chemicals are used to estimate their persistence in the environment. Chemical-specific half-lives are calculated according to the general decay equation:

$$A = A_0 e^{-(0.693 t / T_{1/2})}$$

where:

$t$  = time since decay began (days)

$A$  = the quantity of substance remaining at time  $t$  (mg)

$A_0$  = initial quantity of substance present at time  $t_0$  (mg)

$T_{1/2}$  = half-life for decay (*days*)

### **8.3 PHYSICAL PROPERTIES OF SITE CHEMICALS AFFECTING THEIR MOBILITY AND PERSISTENCE**

Values for the transport and fate of chemicals at SSFL were discussed in Sections 5.0 and 6.0. Values for properties of groundwater flow that influence transport and fate, such as hydraulic gradient, bulk hydraulic conductivity and fracture porosity were discussed in Section 6.0 and Appendix 6-A. Properties of the individual chemicals that are present in SSFL groundwater are discussed in this section.

Properties that affect the mobility of the chemicals encountered are presented in Table 8-1. For presentation and discussion purposes, the chemicals presented in this table are grouped according to the following categories:

- Halogenated Volatile Organic Compounds
- Non-Halogenated Volatile Organic Compounds
- Emerging Contaminants (Perchlorate, 1,4-Dioxane, NDMA)
- Gasoline Range Total Petroleum Hydrocarbons
- Diesel, Kerosene, and Lubricant Oil Range Petroleum Hydrocarbons, SVOCs
- PCBs and PCDD/Fs
- Metals

The physical properties that are discussed for these chemicals include solubility, Henry's Law constant, octanol-water partitioning coefficient, organic carbon-water partitioning coefficient, distribution coefficient, biodegradation constant, and vapor pressure are shown on Table 8-1.

#### **8.3.1 Halogenated and Non-Halogenated Volatile Organic Compounds**

The properties of the majority of halogenated VOCs detected at SSFL are provided in Table 8-1. The halogenated and non-halogenated VOCs are grouped as follows:

- Halogenated ethenes (e.g., PCE, TCE, 1,1-DCE)
- Halogenated ethanes (e.g., 1,1,1-TCA, 1,1-DCA)
- Halogenated methanes (e.g., chloroform, trichlorofluoromethane)

- Halogenated benzenes, propenes, and propanes (e.g., chlorobenzene, 1,2,3-trichloropropane)
- Non-halogenated compounds (e.g., benzene) and formaldehyde

Halogenated VOCs generally have moderate to high solubilities (10 to 13,000 mg/L) in water. They have a high tendency to volatilize to air (Henry's Law constants from 0.01 to 106) and moderate to high vapor pressures (1.0 to 122,000 millimeters of mercury [mm Hg]). Halogenated VOCs have variable tendency to dissolve preferentially in organic liquids compared to water (i.e., low to high log  $K_{ow}$  values), and have moderate tendency to sorb to organic matter in soil ( $K_{oc}$  values ranging from 6 to 1,700 liters per kilogram [L/kg]). These physical properties indicate that chlorinated VOCs can readily dissolve in water and quickly be transported through soil and into groundwater. As noted in Section 7.0, TCE (halogenated ethene) is present in groundwater over an estimated 20% of the site and vertically to depths beyond 900 feet below the ground surface (at the Delta RI site). TCE has been detected at the highest frequency and at the highest concentrations in groundwater.

A number of halogenated and non-halogenated VOCs have a tendency to degrade in the environment, under a variety of conditions. However, there is little data on the degradation of VOCs in fractured porous sandstones, hence the development and/or discussion regarding half-lives is currently premature. Field and laboratory studies have been conducted to evaluate TCE and daughter product transformation at SSFL as summarized later in this section. In laboratory studies of cDCE transformation, surface-normalized transformation rates of cDCE were estimated to be  $1.3 \times 10^{-5}$  liters per square meter per day ( $L m^{-2} d^{-1}$ ) in live microcosms (Darlington, 2008).

Non-halogenated VOCs, when compared to halogenated VOCs, are 20 to 30 times more soluble in water, less volatile, and less likely to sorb to organic matter (Table 8-1). The chemical properties of non-halogenated VOCs indicate that they tend to be more mobile in soil and groundwater than halogenated VOCs. However, as presented in Section 7.3, non-halogenated VOCs have been detected in fewer groundwater samples, and at lower concentrations, than halogenated VOCs. This results from the fact that non-halogenated solvents were used in much

lower quantities at SSFL than the halogenated solvents and the fact that they rapidly undergo biological decay in aerobic conditions.

### **8.3.2 Chemicals of Recent Interest (Perchlorate, 1,4-Dioxane, NDMA, 1,2,3-TCP and MTBE)**

The chemical properties of perchlorate, 1,4-dioxane, NDMA, 1,2,3-TCP and MTBE are summarized in Table 8-1. All five compounds have high solubilities (431,000 mg/L to 2,090,000 mg/L) in water. They have either low volatility to air or are non-volatile (indicated by low Henry's Law constants ( $7.46 \times 10^{-5}$  to  $7.25 \times 10^{-1}$ ) and moderately high vapor pressures (2.7 to 39.9 mm Hg). They all have a low tendency to adsorb to organic matter in soil, indicated by a low tendency to dissolve preferentially in organic liquids compared to water ( $K_{oc}$  values ranging from 2.6 to 13 liter per kilogram (L/kg)). These physical properties indicate that perchlorate, 1,4-dioxane, NDMA, 1,2,3-TCP and NDMA readily dissolve in water and migrate through soil and groundwater (in granular aquifers) at rates similar to the average linear groundwater velocity.

### **8.3.3 Gasoline Range Total Petroleum Hydrocarbons**

Gasoline typically consists of over 200 individual compounds. Because physical-chemical property data are not available for many of the individual compounds present in gasoline, subsets or fractions of the full suite of compounds are often used to evaluate the transport and fate of the entire mixture. Hydrocarbon mixtures separate and partition according to the physical-chemical properties of each compound; therefore, it is important not to consider gasoline as behaving as a pure liquid.

Individual compounds present in gasoline may be alkanes (straight-chain hydrocarbons) or aromatics (ring-structured hydrocarbons). Alkanes include straight-chain alkanes (e.g., hexane), straight-chain alkenes (e.g., hexene), branched-chain alkanes (e.g., isobutane), branched-chain alkenes (e.g., 3-methyl-1-butene), cycloalkanes (e.g., cyclohexane), and cyclohexenes (e.g., cyclohexene). Aromatics include compounds such as benzene, toluene, ethylbenzene and xylene (BTEX).

The properties of each hydrocarbon fraction vary strongly according to carbon number (or *equivalent* carbon number). Gasoline is considered to include alkanes and aromatics consisting of up to 10 carbon atoms. Compounds containing a higher number of carbon atoms are regarded as diesel and lubricant oil range hydrocarbons. These are discussed in a subsequent section.

The chemical properties of gasoline compounds are summarized in Table 8-1. Gasoline compounds have moderate to high solubilities (up to  $6.6 \times 10^{-1}$  milligrams per liter (mg/L)) in water. They have a moderate to high tendency to volatilize to air (indicated by a low Henry's Law constant of  $1.26 \times 10^2$ ) and a moderate to high vapor pressure ( $1.78 \times 10^{-2}$  mm Hg). The higher solubility and higher tendency to volatilize are associated with the lower carbon number compounds. Gasoline compounds have variable (low to high log  $K_{ow}$  values) tendency to dissolve preferentially in organic liquids compared to water, and variable tendency to sorb on to organic matter in soil ( $K_{oc}$  value of  $2.43 \times 10^4$  L/kg). These physical properties indicate that gasoline compounds can readily dissolve in water and thus migrate through soil and into groundwater.

Many gasoline compounds, including BTEX, readily degrade to non-toxic compounds under aerobic conditions. Alkane compounds are degraded to smaller carbon-chain alkanes. Aromatic compounds degrade aerobically to carbon dioxide and water. Other compounds, such as benzoate, may be generated as intermediate products. The tendency to degrade generally decreases with increasing carbon number.

#### **8.3.4 Diesel, Kerosene, and Lubricant Oil Range Petroleum Hydrocarbons, and Semi-Volatile Organic Compounds**

Diesel, kerosene, lubricant oil range petroleum hydrocarbons are similar to gasoline compounds, consisting of many different compounds, but are characterized by higher carbon numbers. The higher carbon numbers result in lower solubilities, lower tendency to volatilize, and a significantly greater tendency to sorb on to organic matter in soil. The chemical properties of diesel, kerosene, lubricant oil range petroleum hydrocarbons, and SVOCs are summarized in Table 8-1.

The lower carbon number compounds in this group (e.g., naphthalene) biodegrade readily. Higher carbon number compounds (e.g., anthracene) show little tendency to degrade, either biotically or abiotically. Preferential degradation of a mixture of hydrocarbon compounds, such as diesel, may result in a heavy-end, recalcitrant residual in the soil and/or groundwater.

### **8.3.5 PCBs and PCDD/Fs**

The chemical properties of PCBs and PCDD/Fs are summarized in Table 8-1. All three compound groups have low aqueous solubility (greater than 0.07 mg/L) and have little potential to dissolve in groundwater (log  $K_{ow}$  of greater than 6.0). They are considered semi-volatile compounds (extremely low Henry's Law constants and vapor pressures) and these compounds are highly adsorptive ( $K_d$  values greater than 1,730 L/kg). Compared to halogenated VOCs, these compounds are more than three orders of magnitude less soluble, are more strongly sorbed to organic carbon in soil and rock, and are much less volatile.

PCBs and PCDD/Fs are persistent in the environment and are resistant to biodegradation in soil and groundwater. Both typically persist in soil and water for decades. The rate of degradation decreases with increasing number of chlorine atoms.

Because of their low volatility, vapor is not considered a migration pathway for PCBs and PCDD/Fs. Because of their high tendency to sorb to solids, they are unlikely to migrate vertically through the vadose zone. Furthermore, their low solubility and low tendency to dissolve in water indicates that transport by groundwater flow is unlikely.

### **8.3.6 Metals**

A summary of chemical properties of metals, including the 23 metals detected in more than one groundwater sample (aluminum, antimony, arsenic, barium, beryllium, boron, cadmium, chromium, copper, iron, lead, manganese, nickel, selenium, silica, strontium, and zinc), is provided in Table 8-1. Metals are not volatile, with the exception of elemental mercury. Metals are relatively insoluble in water, unless dissolved in highly acidic groundwater (pH of less than about 4 pH units [Hem, 1992]). Metals are usually highly adsorptive and can readily precipitate from solution and attenuate in soil. It should be noted that degradation is not applicable for

metals because they are transformed, but not degraded, in the environment. These properties cause metals to occur and persist primarily in shallow soil.

### **8.3.7 Summary**

The subsequent discussion of transport and fate focuses on TCE, and in some cases other chemicals that are typically mobile in granular aquifers but are retarded in the Chatsworth Formation bedrock due to diffusion (e.g., perchlorate, NDMA, 1,4-dioxane and MTBE). The transport of TCE in the vadose zone was selected to be representative of all VOCs due to its widespread distribution in soil, bedrock vadose zone, and groundwater across SSFL. Transport simulations of TCE are displayed and supplemented by simulations of other chemicals in groundwater to assess their transport characteristics relative to TCE. In addition, rock porewater sampling results from a number of the coreholes indicate that TCE penetrated through the groundwater as a DNAPL. Therefore, TCE can also be used to illustrate DNAPL flow and fate through the vadose and saturated zones. Other chemicals selected for transport analysis have properties representative of low sorption to the solid phase, high solubilities, and little degradation.

## **8.4 TRANSPORT AND FATE PROCESSES IN THE VADOSE ZONE**

Chemical transport in vadose zone soils has been evaluated using SESOIL as described in Appendix 7-G. The primary purpose of applying SESOIL to vadose zone soils was to characterize the behavior of metals transport from soil to groundwater and to evaluate the level of protection of groundwater associated with risk-based screening levels for select VOCs.

SESOIL is a one-dimensional vertical transport screening-level model for the vadose zone and is designed to simulate transport and fate of chemical compounds based on diffusion, adsorption, volatilization, biodegradation, and hydrolysis processes. SESOIL is based on mass balance and partitioning of the chemical between the dissolved, sorbed, vapor, and pure phases. SESOIL was coupled with AT 123D, which is a three-dimensional groundwater fate and transport model used to simulate transport of chemical compounds. Concentrations of chemical compounds transported, dispersed, degraded, and sorbed in the saturated zone can be estimated. AT 123D's

transport mechanisms include advection, dispersion, sorption, decay/biodegradation, and heat losses. Modeling results can be used to estimate the distance a chemical plume will migrate and evaluate risks at discrete locations and time periods. It is recognized that the application of the AT 123D groundwater transport model is not appropriate for modeling chemical transport in the fractured Chatsworth Formation where groundwater flows primarily in discrete fractures. The latter condition is addressed separately later in this section. The SESOIL model results indicate that the RBSLs for the 11 VOCs evaluated are protective of groundwater. The SESOIL modeling results for metals also provided context for evaluating results of metals concentrations in groundwater as described in Section 7.3.5.19.

Two analyses are presented in the following subsections to further characterize the transport and fate of TCE (as an indicator chemical) in the vadose zone. Section 8.4.1 analyzes the transport of TCE to the atmosphere from groundwater that has been impacted (i.e., no known soil source). Second, an analysis will be presented in Section 8.5.2.9 to characterize the effect that a vadose zone source has on groundwater.

Attenuation of TCE and other volatile VOCs in the vadose zone occurs as a result of (1) volatilization to the atmosphere, (2) aerobic biodegradation, (3) sorption to organic carbon contained in the bedrock matrix and (4) mass transfer to the groundwater. Partitioning of TCE among the sorbed, gaseous, and aqueous phases in pore water can be calculated based on the measured concentrations in soil gas and use of the appropriate partition coefficients ( $K_d$  and Henry's Law constant, listed in Table 8-1. The calculated concentrations from a range of TCE values measured in soil gas as reported in surficial media RI reports (i.e., 1000, 400, 100 and 10  $\mu\text{g}/\text{L}_v$ ) are provided in Table 8-2. Although degradation of TCE in the vadose zone soils is apparent from the occurrence of daughter products, it has not been evaluated quantitatively, hence it will not be considered in the subsequent sections.

#### **8.4.1 Volatilization to the Atmosphere Through the Vadose Zone Above Areas of Impacted Groundwater**

A modified version of the Johnson-Ettinger vapor migration model has been used to characterize the vapor migration pathway from groundwater through the vadose zone in the surficial media RI

reports. The standard version of the model has been modified to predict indoor air concentrations using VOC concentrations in Chatsworth Formation groundwater as a source term based on an analysis performed by McWhorter (2004). The model estimates the transport of VOCs through bedrock and any overlying soil to the ground surface and then to indoor or outdoor air. The indoor air concentrations are then used as exposure point concentrations in the residential exposure scenario. The model was modified to estimate the flux of VOCs to the atmosphere from groundwater according to the following equation:

$$F = C_o R / \exp (RT/D) - 1$$

where:

F = Steady mass flux of VOC to ground surface ( $\mu\text{g}/\text{cm}^2\text{-s}$ )

Co = Mass concentration of VOC in pore water ( $\mu\text{g}/\text{L}$ )

R = Steady recharge rate (cm/s)

T = thickness of vadose zone (cm)

D = Bulk diffusion coefficient ( $\text{cm}^2/\text{s}$ )

The bulk diffusion coefficient is calculated from the equation:

$$D = \phi_{m,w} S_w^{10/3} t_o D_w + K_{HD} [\phi_{f,w} + \phi_{m,w} S_g^{10/3} t_o] D_g$$

The terms and values used in the above equation are defined in Table 8-3. The situation is depicted as Scenario 1 on Figure 8-2. TCE partitions from the dissolved phase in groundwater into the gaseous phase in the vadose zone and is transported first through the unweathered bedrock, then through the weathered bedrock and into the soil prior to discharging at the ground surface. This analysis assumes that the ground surface is not covered by any natural or man-made lower permeability surface.

This modified version of the vapor transport model has been subject to field validation. Validation methodologies are described in the *Vapor Migration Modeling Validation Study Work Plan* (MWH, 2005c). Reports describing the results of this study have been submitted to DTSC (MWH, 2007b and 2008c). The vapor validation study report concludes that the proposed model conservatively over-predicts migration from Chatsworth Formation groundwater based upon flux

chamber measurement results. Further descriptions of the modified Johnson-Ettinger vapor migration models are provided in Revision 2 of the SRAM (MWH, 2005a). Application of the model and the results of characterizing the vapor transport pathway above areas of impacted groundwater for the purposes of human health and ecological risk assessments are presented in Appendix 9-A.

## **8.5 CHEMICALS WITHIN THE GROUNDWATER SYSTEM**

The transport of contaminants in fractured porous media like the Chatsworth Formation is fundamentally different from transport in granular aquifers. This fundamental difference is attributed to the transfer of VOC mass from the groundwater flowing through the fracture network into the nearly stagnant groundwater that is resident in the porous rock matrix by molecular diffusion. This transfer of mass into the rock matrix effectively slows the rate at which TCE is transported in groundwater flowing through the fracture network (by orders of magnitude relative to the average linear groundwater velocity).

As presented in Section 7.3 and noted earlier in this section, TCE is the dominant chemical of concern at SSFL because of the reportedly large volumes used, its frequent detection and elevated concentration (particularly relative to its MCL) and significant lateral extent. This section first evaluates the persistence of TCE as a dense, non-aqueous phase liquid, and then evaluates the transport of TCE in groundwater using a two-dimensional fracture network model and ends by comparing site TCE data to the simulation results.

### **8.5.1 DNAPL Persistence**

When TCE is released as DNAPL and penetrates below the water table in a fractured porous media, it begins to dissolve in the flowing groundwater. This condition marks the onset of TCE DNAPL dissolution and diffusive mass transfer to the matrix and begins forming a plume of dissolved contaminants. In most fractured rock, fractures provide the paths of least resistance to fluid flow and therefore, generally dominate the bulk fluid movement. This causes the volume of DNAPL in the fractures to continually decline and the VOC mass in the matrix to continually increase. The mass in the matrix is dissolved in the pore water and sorbed to rock matrix solids. The dissolution of DNAPL by mass transfer and diffusion to the matrix is a major factor causing

DNAPL to become immobile. As DNAPL dissolves into the rock matrix through diffusion and loses its mass, disconnected segments of DNAPL develop.

The complete dissolution of DNAPL to dissolved and sorbed phases through matrix diffusion in fractured bedrock results when the mass storage capacity of the rock matrix exceeds the mass storage capacity of the fractures. This DNAPL dissolution process is also referred to as “DNAPL disappearance” (Parker et al., 1994). Calculations presented in the *TCE Technical Memorandum* (Montgomery Watson, 2000a) were made using Chatsworth Formation data to estimate the ratio of the rock matrix storage capacity to the fracture network storage capacity. These results showed that the Chatsworth Formation sandstone can store between 5 and 100 times the mass of DNAPL within the matrix than within the fracture network, hence DNAPL disappearance due to matrix diffusion would be expected.

#### 8.5.1.1 Complete DNAPL Dissolution Due to Diffusion Only

The effect that matrix diffusion has on DNAPL dissolution can be quantified using a solution to Fick’s second law. The time for complete DNAPL dissolution from Chatsworth Formation fractures can be calculated by solving Fick’s second law and results in the following equation for a single parallel-plate fracture:

$$t_D = \frac{\pi \rho^2 (2b)^2}{16 S_w^2 \phi_m^2 D_e R_m}$$

where:

$t_D$  = DNAPL disappearance time

$\rho$  = density of TCE

$2b$  = fracture aperture

$S_w$  = aqueous solubility of TCE

$\phi_m$  = matrix porosity

$D_e$  = diffusion coefficient

$R_m$  = retardation in the matrix due to sorption, calculated by

$$R_m = 1 + (\rho_b/\phi_m)(K_{oc} \times f_{oc})$$

where:

$\rho_b$  = dry bulk density

$\phi_m$  = matrix porosity

$K_{oc}$  = octanol-water partition coefficient for TCE

$f_{oc}$  = fraction of organic carbon

DNAPL disappearance times by diffusion only were calculated using representative values for physical properties and hydraulic apertures presented throughout this report and in the complementary Site Conceptual Model document (2009). Results from these calculations are presented in Table 8-4. The calculations show that matrix diffusion alone causes DNAPL to completely dissolve from fractures in timeframes ranging from 0.3 to 290 years for apertures ranging from 10 to 300 microns, with the time for disappearance for the calculated mean aperture of 100 microns being about 32 years. These times for diffusion-only are worse-case, given that dissolution in groundwater flowing in fractures can significantly reduce disappearance times as examined below.

#### **8.5.1.2 Complete DNAPL Dissolution Due to Diffusion into the Matrix and Advection in the Fracture**

The effect of DNAPL dissolution in groundwater flowing in a fracture in addition to diffusion into the matrix was also evaluated, including relative permeability effects due to DNAPL presence in the fracture. For the purposes of the DNAPL disappearance calculations, a hydraulic gradient ( $i$ ) of 0.01 and DNAPL source length in the fracture is 10 m. Further, the initial DNAPL saturation is assumed to be 1.0 meaning the fracture is initially NAPL filled (so that calculations can be directly related to the diffusion-only disappearance time estimates). However, it is important to note that the groundwater velocity and dissolution estimates are based on the hydraulic fracture aperture. The actual physical fracture aperture (referred to as the volume aperture) within which the NAPL resides may be larger, such that the actual initial NAPL saturation would be lower. Details of the calculations are presented in the complementary Site Conceptual Model document (2009). Results are presented in Table 8-4 where a comparison of disappearance times can be made for the scenarios of (1) diffusion-only,

(2) diffusion and dissolution in groundwater flowing in the fracture neglecting relative permeability effects, and (3) same as (2) but including relative permeability effects. These calculations show that groundwater flow through fractures significantly decreases the time for DNAPL to completely dissolve relative to the diffusion only case. Calculations of hydraulic apertures from measurements made at SSFL show that more than 95% of the measurements show apertures below 300 microns. With advection in fractures, calculated DNAPL disappearance times range from about 0.3 to 5 years for fracture apertures ranging from 10 to 300 microns when relative permeability effects are neglected, and range from 0.3 to 40 years when relative permeability effects are included. However, as noted above, the estimates including relative permeability effects are biased high based on the form of the relative permeability function and by assuming the fracture is initially NAPL-filled. These results can also be compared to the estimates of diffusion only, which range from 0.3 to 290 years. Results from these analyses were used to support the duration of the source term of 20 years for most of the numerical transport modeling in discrete fracture networks that is presented later in this section.

TCE concentration results from the analysis of rock core from source zone coreholes provide field confirmation that little to no DNAPL remains in the Chatsworth Formation fracture network as described in this report and the complementary Site Conceptual Model document (2009). All but 3 of the more than 4,600 rock core samples collected and analyzed from source areas had concentrations below TCE's aqueous solubility limit, with nearly all samples being a factor of 10 below the aqueous solubility. The field data confirm that TCE that entered at input locations to the Chatsworth Formation during the period of major releases to the ground in mid-1950's to early 1960's has disappeared from nearly all fractures. The complete dissolution of TCE DNAPL is due to the combined effects of groundwater flow, matrix diffusion, volatilization and sorption. If any TCE DNAPL remains, it does so only in the largest fractures and exists as small immobile disconnected layers or globules.

### **8.5.2 TCE Transport and Retardation in Groundwater**

Molecular diffusion, like Darcy's law, is a gradient flux law that was first described by Fick in 1852. Stephen Foster (1975) was the first to apply the concept of molecular diffusion to

groundwater flow and solute transport in a fractured porous media. In this case, the concept was applied to the diffusion of atmospheric tritium into the fractured Chalk Formation in England. Freeze and Cherry (1979) extended the concept of retardation of a solute plume front due to matrix diffusion. Additional work done by the members of SSFL groundwater advisory panel extended the concept of matrix diffusion to the disappearance of immiscible phase liquids in fractured geologic media (Parker et al., 1994, 1997). Material from this work was used to evaluate complete DNAPL dissolution timeframes. The application of matrix diffusion to TCE in the Chatsworth Formation was initially published in the *TCE Technical Memorandum* (Montgomery Watson, 2000a). Comparison of the concentrations of TCE between the source zone and plume transects that were drilled in the northeast portion of SSFL demonstrate the strong attenuation effects of matrix diffusion.

#### **8.5.2.1 Field Assessment of TCE Transport**

The transport of chemicals in bedrock groundwater was characterized with field data through the installation of source zone and plume transects in an area of impacted groundwater in the northeast part of SSFL. Mean porewater concentrations of TCE in 3 source zone transect coreholes (C-1, RD-35 and C10; mean of 2,544 µg/L; detected in 1,295 of 1,655 samples [78 percent]) are more than a factor of 100 higher than mean TCE concentrations in 2 plume transect coreholes (C-13 and C-14; mean of 23 µg/L; detected in 102 of 810 samples [13 percent]) over a horizontal distance of 2,140 feet. These data provide compelling and conclusive evidence of the strong attenuation effect of matrix diffusion on contaminant transport in the Chatsworth Formation at SSFL.

#### **8.5.2.2 Modeling Assessment**

Two-dimensional (2-dimensional) steady-state flow and transient transport fracture network simulations were performed to evaluate the effect of matrix diffusion on TCE transport in Chatsworth Formation groundwater with specific conditions relative to individual source areas. Fracture network transport modeling was first performed as described below in Section 8.5.2.4 as a general case to evaluate variations in source conditions and contaminant type. Additional simulations were also performed as described in Section 8.5.3 where output from the 3-dimensional groundwater flow model is coupled with 2-dimensional fracture network models.

### **8.5.2.3 Background on Transport Simulations**

Simulations were conducted to evaluate the rate and distance of solute transport in DFN in a sandstone rock (with a porous matrix between the fractures) using a 2-dimensional numerical model (FRACTRAN, Sudicky and McLaren, 1992, 2003). The 2-dimensional DFN code FRACTRAN used for this assessment accommodates orthogonal fracture networks with randomly generated fractures having variable apertures, lengths and fracture density / spacing. Rock matrix properties can also vary spatially. Steady-state groundwater flow is assumed and the code simulates the transient evaluation of contaminant plumes from assigned source zones where source concentrations can vary over time. Groundwater flow and contaminant transport (including matrix diffusion and advection in the porous matrix) are rigorously treated in both fractures and porous matrix blocks. Chemical reactions in the form of first-order decay and linear equilibrium sorption are also accommodated.

### **8.5.2.4 Two Dimensional Model Domain and Fracture Network**

The “base case” model domain for these simulations consists of a 2-dimensional vertical cross-section with a length of 500 meters (m) and height of 100 m as shown on Figure 8-3. The hydraulic conductivity utilized for the sandstone matrix was  $1 \times 10^{-6}$  cm/s and matrix porosity was 12 percent. The bases for these values are the large number of physical property measurements collected from Chatsworth Formation sandstones as presented in the complementary Site Conceptual Model document (2009).

The fracture network consists of randomly generated horizontal and vertical fractures (single realization of random fracture network) with horizontal and vertical fracture lengths ranging from 10 m to 20 m and 5 m to 10 m, respectively. Histograms of horizontal and vertical fracture lengths are shown in Figure 8-4. The density of fractures assigned to generate the random fracture network was 0.050 and 0.075 fractures/m<sup>2</sup> in the vertical and horizontal directions, respectively. This fracture density produced a total of 2500 vertical and 3750 horizontal fractures within the domain. The average spacing of horizontal and vertical fractures, based on fracture counts along four lines in each direction (i.e., at distances of 100, 200, 300, and 400 m along the x-axis, and 20, 40, 60, and 80 m along the vertical axis), was determined to be about 1.5 and 3.8 m, respectively.

Fracture apertures vary on a fracture-by-fracture basis, and are randomly generated according to a lognormal distribution with a mean aperture of 100 microns. Figure 8-5 provides histograms of the hydraulic apertures of both horizontal and vertical fractures. The generated fracture apertures range from about 20 to over 1000 microns.

#### 8.5.2.5 Groundwater Flow Conditions in the 2-Dimensional Model Domain

The hydraulic head was specified along all four sides of the model domain to provide an average horizontal hydraulic gradient of 0.5 percent and a vertical (downward) gradient of 0.2 percent. Steady-state hydraulic head contours are shown on Figure 8-6. Based on the numerical flow solution, values for bulk hydraulic conductivity can be estimated, in both the horizontal and vertical directions, using the following variation of Darcy's Law:

$$K_{bh} = \frac{Q_h}{i_h A_h} \quad K_{bv} = \frac{Q_v}{i_v A_v}$$

where  $K_{bh}$  and  $K_{bv}$  are the bulk hydraulic conductivities in the horizontal and vertical directions, respectively,  $Q_h$  and  $Q_v$  are the total flow rates in the horizontal and vertical directions (calculated as the average of the inflow and outflow along the left and right, or top and bottom boundaries, respectively),  $i_h$  and  $i_v$  are the average horizontal (0.5 percent) and vertical (0.2 percent) gradients and  $A_h$  and  $A_v$  are the areas for flow in the horizontal (100m by 1m) and vertical (500m by 1m) directions, respectively. For this realization, the bulk hydraulic conductivities were determined to be about  $8.0 \times 10^{-5}$  and  $2.3 \times 10^{-5}$  cm/sec in the horizontal and vertical directions, respectively, resulting in an anisotropy factor (ratio of  $K_{bh}$  to  $K_{bv}$ ) of 3.5. The presence of fractures has increased the bulk hydraulic conductivity by 80 times in the horizontal direction and 23 times in the vertical direction, compared to the hydraulic conductivity of the sandstone matrix ( $K_m = 10^{-6}$  cm/s). These bulk hydraulic conductivity values were selected to be representative of values resulting from the optimized flow model results.

The average linear groundwater velocity across the domain (bulk medium) where the fractures control groundwater flow ( $\bar{v}_f$ ) can be estimated using:

$$v_f = \frac{K_b i}{\phi_f}$$

where  $\phi_f$  is the bulk fracture porosity. This calculation assumes that all flow occurs in fractures and does not take into account the lack of flow in dead-end fractures or flow in the matrix, and therefore, provides a rough estimate of average flow velocities through the fracture network. This calculation is considered conservative as the accounting for the two conditions described above would result in a slower groundwater flow rate across the domain. More details on the concept of average linear groundwater velocity can be found in Appendix E of the *TCE Technical Memorandum* (Montgomery Watson, 2000a). Using the overall bulk fracture porosity ( $\phi_f = 1.3 \times 10^{-4}$ ), calculated by the model based on the generated fracture network, the average linear groundwater velocities are estimated to be 925 (~3050 feet per year) and 105 meters per year (m/yr) in the horizontal and vertical directions, respectively. The horizontal values are similar to those calculated from the field data. Actual groundwater velocities in individual fractures vary considerably from the estimated average linear groundwater velocities, depending on local fracture apertures and gradients, with some larger aperture fracture pathways showing much higher velocities. For this case, groundwater velocities in horizontal fractures vary from -2850 m/yr to 11,500 m/yr and in vertical fractures from -12,300 m/yr (downward) to 9160 m/yr (upward). Therefore, flow in some fractures occurs opposite to the average hydraulic gradients. However, these individual fracture velocities are not useful for calculating groundwater travel times through the fracture network because the actual tortuous path taken by the groundwater would also need to be known, which is not currently feasible to determine.

#### 8.5.2.6 TCE Properties and Source Conditions

A TCE free-solution diffusion coefficient ( $D_o$ ) of  $1.0 \times 10^{-9}$  square meters per second ( $m^2/sec$ ), calculated for 25°C, was used in these simulations. A tortuosity factor ( $\tau$ ) of 0.10, based on laboratory diffusion tests on SSFL sandstone samples (Golder, 1997), was applied to the free-solution diffusion coefficients to estimate effective diffusion coefficients ( $D_e$ ) for TCE. A matrix retardation factor ( $R_m$ ) of 2.0 was used for TCE based on the  $f_{oc}$  measurements.

The position and conditions of the TCE source used in the simulations are shown in Figure 8-7. The TCE source was placed along the left model boundary, extending over a 25 m vertical interval, and was assumed to be constant over a 20-year time period, after which time the source was set to zero. The source duration used in the TCE simulations is based on calculated DNAPL disappearance time as described earlier. The position of the source is based on the historical existence of DNAPL as described in the complementary Site Conceptual Model document (2009). Available data indicate that DNAPL migrated downward in the fractures before becoming immobile, where it would have persisted for a few decades until the DNAPL mass was gradually depleted and completely dissolved in groundwater flowing in fractures and diffused into the sandstone matrix. The fracture dispersivity was assumed to be 0.10 m for all simulations, which is small enough to not have any significant impact on plume front transport rates.

#### **8.5.2.7 TCE Transport Simulation Results**

Figure 8-8 shows concentration contours for TCE at 20, 50 and 100 years after the point of initial release for the base case numerical simulations. Figure 8-9 shows the same except for timeframes of 50, 100 and 150 years after the point of initial release. Fractures are not superimposed on the contour plots for easier viewing of the concentration contours. Concentrations are expressed relative to the source concentration ( $C/C_0$ ) over a five order-of-magnitude range. For TCE, this would represent a concentration of about 11  $\mu\text{g/L}$ , since TCE solubility is about 1,100,000  $\mu\text{g/L}$ . This is above the MCL for TCE, however the model provides exact 'point' concentrations within the fractures, whereas in the field such concentrations would be diluted during sampling over larger vertical intervals, such that concentrations would likely be close to or below the MCL. As indicated in the contour plots, the  $C/C_0=10^{-5}$  contour levels, the TCE plume has migrated about 340 m (~1100 feet) downgradient from the source 50 years after the initial release. The 50-year contours are intended to be representative of current conditions at SSFL in that the initial releases of TCE to the subsurface were believed to have occurred in the mid-1950s.

In comparison to the rapid rates of groundwater flow in fractures, as discussed above, the rate of advance of the TCE plume fronts are orders-of-magnitude slower than the average linear

groundwater velocity due to matrix diffusion. The apparent retardation factor ( $R_A$ ) at 50 years after the initial release as indicated by these simulations is about 140. Additionally, The simulated TCE migration rate of the plume front ( $C/C_0=10^{-5}$ ) declined over time, from an average of about 8.8 m/yr between 0 to 20 years to 1.9 m/yr between 50 and 100 years. This decline in the plume front migration rate over time occurs due to the greater surface area for matrix diffusion to occur as the plume expands, with some further retardation effect from the finite source conditions after long time periods. In addition to causing significant plume front retardation, matrix diffusion also causes concentrations within the plume to decline following the end of the constant source period, which is evident by examining the contours near the source at 50 and 100 years in Figure 8-8.

#### **8.5.2.8 Effects of Vadose Zone Impacts on TCE Transport in Groundwater**

As noted in Section 8.1, characterization of one of the transport pathways is needed to evaluate the effect that chemicals present in the unsaturated zone have on the transport rate in groundwater. TCE was again selected as the indicator chemical for this evaluation. The 2-dimensional fracture network transport simulations discussed above were used to evaluate the effect that TCE mass has on the transport of TCE in the groundwater. The analysis of the vadose zone impacts is shown as scenario 2 on Figure 8-2.

A vadose source representative of the one measured at the IEL RI site was targeted for simulation. The soil gas sampling data discussed in previous sections of this report were used to develop a source term, along with the vadose zone rock core data from corehole C-1. A concentration of 10,000  $\mu\text{g/L}$  in vadose zone porewater was selected as an initial concentration for this analysis. This concentration in porewater equates to a soil gas concentration of 4,220  $\mu\text{g/L}_v$ , which is higher than any TCE soil gas concentration measured in the local area. The initial length of the source that was selected for the simulation was 100 m. This source length is about three times longer than the actual measured distance of the 1,000  $\mu\text{g/L}_v$  isoconcentration contour within the IEL RI site. Two source durations were simulated, one allowing the source to persist for 50 years and a second allowing the source to persist for 100 years. The simulations used the current time frame (i.e., 50 years after the initial release) as the starting point for this analysis. The simulation results showing TCE concentration contours

without any vadose zone source for periods of 50, 100, and 150 years after the initial release are provided on Figure 8-10. These simulations are the same as the base case TCE results shown on Figure 8-8 except that the results are shown for 150 years after the initial release.

The TCE simulation results for the vadose zone case where the source persists for 50 years are shown on Figure 8-10 and the results for a 100-year source condition are shown on Figure 8-11. The source conditions are also shown on these two figures. A comparison of the plumes at 100 and 150 years between no vadose zone source (base case), the 50-year vadose zone source and the 100-year vadose zone source shows the plumes to be nearly identical. The only notable difference is the invasion of TCE into the matrix blocks in the first 10 m of rock in the vertical dimension and the first 200 m in the horizontal dimension. Concentrations in these matrix blocks increase by about a factor of 10. It should be noted however that these differences are only an artifact of initiating the vadose zone impacts after 50 years. In the field, such impacts would be experienced from the initial release. Hence, the true impacts on the plume are likely less than observed in the simulations. Furthermore, observable effects on either the lateral or vertical extent of the plume in either of the vadose zone cases are indistinguishable compared to the base case.

#### **8.5.2.8.1 Vadose Zone Source Only**

Two additional transport simulations were run to evaluate the effects of a TCE vadose zone source only on groundwater plume development. The simulations were run consistent with those described in previous sections. The variable that was changed involved that of the source term. The source along the left vertical edge of the simulations that represented a DNAPL source term (duration of 20 years) was removed and the source representing a constant vadose zone source as described above was applied along the top of the model domain at the upgradient edge as described above. Simulation results are displayed in Figure 8-12 for periods of 20, 50, 100 and 150 years for source durations of 50 years and 100 years. These two periods were chosen to allow an evaluation of the potential benefit that may result from vadose zone source mass removal. Inspection of the differences between the two source term cases show that internal concentrations in the 100 year source term case are greater than those in the 50 year case. Overall plume extent is not appreciably different between the two cases.

### **8.5.2.9 TCE Degradation in Groundwater**

Additional transport simulations presented in the complementary Site Conceptual Model document (2009) show that even slow rates of contaminant degradation can further retard plume front migration and appreciably contribute to the overall attenuation of the contaminant plume. The simulations indicate that even slow rates of degradation (i.e., with half-lives ranging between 5 and 20 years) can cause plume fronts to retreat and collapse within 150 to 200 years. The fate of chlorinated ethenes is further discussed in Section 8.6.

### **8.5.2.10 Other COCs Within the Groundwater System**

Significant interest exists in certain other chemicals that are associated with rocket engine testing, namely perchlorate, 1,4-dioxane, NDMA, and MTBE primarily because their transport in granular aquifer groundwater systems is not retarded relative to the groundwater flow velocity. Hence, these chemicals can produce extensive plumes in granular aquifers. Because of these features and the interest in these chemicals by regulatory agencies, they were selected for groundwater transport analysis. The simulations provide a basis for comparing the relative rates of transport of these constituents due to their differing physical properties (diffusion coefficients, sorption characteristics), source conditions and range in concentrations of interest.

#### **8.5.2.10.1 Chemical Properties and Source Conditions**

In addition to the TCE simulations previously discussed, simulations were also conducted for three different solutes and source conditions: (1) perchlorate, (2) NDMA and (3) 1,4-dioxane. Table 8-5 summarizes the relevant transport properties for these compounds that were used in the simulations. The main differences between the solutes, for the purposes of these simulations, are in the assigned values for the free-solution diffusion coefficient and retardation factors. Given the similarities in transport properties for NDMA and 1,4-dioxane, a single transport simulation was performed to demonstrate transport conditions and concentration variability relative to TCE and perchlorate. Free-solution diffusion coefficients for TCE, NDMA and 1,4-dioxane are all about  $1.0 \times 10^{-5}$  cm<sup>2</sup>/sec (or slightly higher), while the value for perchlorate is a factor of 1.8 higher. Estimated matrix retardation factors (associated with sorption) for regular 'sandstone' are about 1.8 for TCE and 1.0 to 1.1 for 1,4-dioxane and NDMA, respectively (Table 8-5), while perchlorate is assumed to be conservative ( $R_m = 1.0$ ). As mentioned earlier, the TCE retardation

factor used was 2.0 ( $R_m$ ). The other three compounds are assumed to be non-sorbing ( $R_m = 1.0$ ) for simulation purposes. To convert the free-solution diffusion coefficients ( $D_o$ ) to effective diffusion coefficients ( $D_e$ ) the following correlation is used:

$$D_e = D_o \tau \text{ where } \tau \text{ is the tortuosity factor.}$$

Values for the tortuosity factor were assigned to be 0.10 for unweathered sandstone, based on laboratory diffusion tests on SSFL sandstone samples (Golder, 1997).

In contrast to TCE, perchlorate is believed to have been released as a powder at the ground surface, and would have entered the subsurface as a dissolved solute in recharge water. Hence, the source zone was positioned along the top boundary as shown on Figure 8-13. A constant source period of ten years was used given the high solubility of perchlorate (Table 8-5). A perchlorate release would probably not have been uniformly distributed, and likely would have dissolved faster from much of the release area. Therefore, assuming a long (50 m) and uniform concentration source over a ten-year period is considered conservative.

For NDMA and 1,4-dioxane, the source was assumed to be present over a similar vertical interval as that for TCE. The source position was placed from the top of the model domain to a distance of 25 m below the water table as shown on Figure 8-13. A ten-year source duration was used given the high solubility of these compounds (Table 8-5). The ten year source duration for 1,4-dioxane was selected to reflect the preferential dissolution of 1,4-dioxane from a chlorinated solvent due to its greatly enhanced solubility relative to the host solvent (e.g., 1,1,1-TCA) in which it was dissolved. Initial concentrations, however, would be orders of magnitude lower than the pure-phase solubility based on multi-component NAPL dissolution, where the effective solubility is a function of both pure-phase solubility and its mole fraction in the mixture (e.g., see Feenstra and Guiger, 1996). NDMA was likely released in the dissolved phase as a breakdown product of unsymmetrical dimethyl hydrazine. Therefore, assuming a ten-year constant source period is also considered conservative.

### 8.5.2.11 Perchlorate Simulation Results

Figure 8-14 shows the concentration contours for perchlorate at 20, 50 and 100 years after the point of initial release for the “base case” numerical simulations. Again, the concentrations are expressed relative to the source concentration ( $C/C_o$ ). Fractures are not superimposed on the contour plots for easier viewing of the concentration contours. Table 8-6 provides a comparison of the distances and relative rates of plume front migration between perchlorate and TCE. The plume front for these comparisons is assumed at  $C/C_o=10^{-4}$ , representing a four order-of-magnitude (OM) decline from the source concentrations. For perchlorate, using the drinking water action level of 6  $\mu\text{g/L}$ , the source concentration could be as high as 60,000  $\mu\text{g/L}$ . As indicated in the contour plots, the  $C/C_o=10^{-5}$  contour levels, which are approaching the lower limit of model stability, are not much further downgradient than the  $10^{-4}$  level for in these simulations. The perchlorate plume extends about 320 m (~1100 feet) downgradient from the source 50 years after the initial release at a  $C/C_o=10^{-4}$ . This equates to an apparent retardation factor of 144.

Comparisons of the contours shown on Figure 8-14 with the TCE contours shown on Figure 8-8 suggest that perchlorate transport distances are only slightly longer than for TCE. This is due both to the difference in the position of the source (i.e., vertical for TCE and horizontal for perchlorate) and to differences in matrix parameters ( $D_e$ ,  $R_m$ ). Variations in advance rates are also expected due to differences in migration pathways that are related to the different source locations for perchlorate and TCE (see Figures 8-13 and 8-7, respectively). However, most of the difference is likely attributable to the difference in source positions, with the downgradient limit of the perchlorate source 50 m beyond the TCE source, given the similarity in plume front advance rates. In both cases, the plumes remain within the model domain over the 100-year simulation period and show similar plume front migration rates for these two solutes. This is likely attributable to the higher  $D_e$  for perchlorate compared to TCE, which would enhance the relative rate of matrix diffusion of perchlorate. However, this is off-set by the lack of sorption for perchlorate compared to TCE, which enhances the relative rate of TCE mass transfer by diffusion into the matrix.

### 8.5.2.12 NDMA/1,4-Dioxane Simulation Results

The simulation results depicting NDMA/1,4-dioxane transport results are shown on Figure 8-15 for 20, 50 and 100 years after initial release. Comparison of the NDMA/1,4-dioxane results to the TCE transport simulation results show that NDMA/1,4-dioxane would be about 60 m (~200 feet) further downgradient than TCE at a  $C/C_0=10^{-4}$  50 years after the initial release. It should be noted that the simulation results for NDMA/1,4-dioxane are depicted to  $C/C_0=10^{-4}$ , which is one order-of-magnitude higher than the simulation results for TCE and perchlorate. This higher relative concentration was selected because of the mechanism of release of these two chemicals into the subsurface as described earlier in this section. Initial source concentrations for NDMA of 100  $\mu\text{g/L}$  were selected as a starting point to allow for resolution of NDMA transport simulations to the drinking water action level of 0.01  $\mu\text{g/L}$ . Similarly, the initial source concentration for 1,4-dioxane of 30  $\text{mg/L}$  was selected as a starting point to allow for resolution of the 1,4-dioxane transport simulations to the drinking water action level of 3  $\mu\text{g/L}$ . The maximum concentrations of NDMA and 1,4-dioxane measured in groundwater in the northeast are 110  $\mu\text{g/L}$  and 797  $\mu\text{g/L}$ , respectively. Using the results from the transport simulations, the apparent retardation factor 50 years after the initial release for TCE at a  $C/C_0=10^{-4}$  is 165, while the apparent retardation factor for NDMA/1,4-dioxane at the same relative concentration is 136. The calculated apparent retardation factor for NDMA/1,4-dioxane is quite remarkable when compared to the lack of any significant retardation of these constituents in granular aquifers. These results show the strong effect of molecular diffusion on retarding the transport of various solutes under conditions encountered at SSFL.

### 8.5.2.13 Field Data of the Diffusion of Perchlorate, 1,4-dioxane and NDMA

Rock core results source zone coreholes provide field confirmation that 1,4-dioxane diffuses into the porous bedrock matrix. Rock core results from RD-77 provide field confirmation that perchlorate also diffuses into the porous bedrock matrix of the Chatsworth Formation. Rock core samples have not been analyzed for the presence of NDMA.

Additionally, analytical data collected during the C-1 pumping test also provide field confirmation on the molecular diffusion of perchlorate, 1,4-dioxane and NDMA. Groundwater samples were collected from the groundwater extracted from C-1 weekly and submitted for

perchlorate and 1,4-dioxane analysis, along with other constituents as specified in the Temporary Authorization Permit (DTSC, 2003). Results of these analyses have been previously reported (MWH, 2004a). Additionally, samples were also collected from the groundwater extracted from C-1 at start-up and before shut-down of pumping and submitted for NDMA analysis. 1,4-dioxane was consistently detected in the groundwater samples collected weekly from the groundwater extracted from C-1. Perchlorate was also consistently detected in groundwater samples from the groundwater extracted from C-1 after the first three weeks of pumping. NDMA was detected in the C-1 groundwater samples at the beginning and at the conclusion of the test. As discussed in MWH 2004a, the pumping performed at C-1 removed most of the groundwater from the fracture network within the first few days of extraction. The groundwater extracted after these first few days of pumping was being provided primarily from storage in the rock matrix. Hence, chemicals detected in the extracted groundwater after the first few days of pumping had to have been present in the rock matrix porewater. These data provide additional field confirmation that perchlorate, 1,4-dioxane and NDMA diffuse into the porous bedrock matrix of the Chatsworth Formation.

### **8.5.3 Linking EPM Flow Hydraulic Characteristics with DFN Hydraulics and Contaminant Transport**

This section provides an overview of the methodology applied to link results from the 3-dimensional EPM groundwater flow simulations and particle tracking results from SSFL source areas to 2-dimensional DFN-derived contaminant transport evaluation. While EPM models can be applied to sites situated on fractured porous media for estimating bulk groundwater flow (e.g., Darcy Flux), such models cannot be used for contaminant transport, particularly in scenarios involving a porous rock matrix where contaminant transport is strongly influenced by diffusion into the rock matrix. Chapter 6 (Field-Scale Flow and Transport Models) in NRC, 1996 provides a more detailed discussion of simulation approaches in fractured rock, ranging from continuum models, dual porosity models and discrete fracture network models and their advantages and limitations both for groundwater flow and solute transport.

The mechanisms by which solutes are transferred from water flowing in fractures to relatively more stagnant waters in adjacent matrix blocks, mostly via diffusion processes, are well known

and understood. The effects of such mass transfer on the rate of solute transport in a single uniform fracture sandwiched between infinite matrix blocks can be calculated from analytical models. One of the important insights provided by this calculation is that the progression of the solute front in the fracture is slowed by the diffusion of solute from the fracture to the matrix. The degree to which the solute front is retarded compared to the rate of groundwater flow in the fracture is shown to depend on the magnitude of water flux in the fracture (which is a function of the hydraulic fracture aperture and hydraulic gradient), the effective diffusion coefficient, solute adsorption on solid surfaces (fracture surface and/or within the matrix blocks), biotic and abiotic reactions and radioactive decay (when applicable), and matrix porosity.

At SSFL, solute transport occurs within a complex, three dimensional, network of interconnected fractures and matrix blocks. The above simple model suggests that the progression of the solute front will be slowed, even in this much more complex system, where the magnitude of water flux within the network is expected to be highly variable owing to spatial variability of fracture length, orientation, aperture and spacing. The model FRACTRAN provides a means of quantifying solute transport as affected by the most important of the complicating factors that occur in the real system at SSFL. While FRACTRAN calculates transport in only a two-dimensional plane and within an orthogonal fracture network, the calculation is made with realistic spatial variability of fracture spacing, aperture, and length. The FRACTRAN network is tied to the real SSFL network by using the observed statistics for spacing, aperture and length to generate the FRACTRAN network. As well, groundwater fluxes and hydraulic gradients obtained using the site-wide 3-dimensional EPM groundwater flow model along particle traces from SSFL source areas are used to constrain and condition the FRACTRAN simulations.

However, it is not expected that the fracture network used in the numerical calculations in FRACTRAN matches any specific part of the actual fracture network at SSFL, other than in these statistics. For this reason and because FRACTRAN computes only 2-dimensional transport, it is not expected that calculated concentrations should be numerical matches to observed concentrations. It is expected that FRACTRAN calculates concentration distributions that are stylistically similar to observed distributions. FRACTRAN does not simulate actual plumes; rather it is a tool that reliably informs and bounds our judgment concerning how far and

how rapidly solute fronts are likely to move under a wide variety of circumstances, using input parameters tailored to conditions at SSFL to the extent feasible.

### **8.5.3.1 Linking Approach**

The approach taken to link the EPM-derived groundwater flow simulation results and particle tracking with DFN-transport simulations is shown schematically in Figures 8-16a & b. EPM Darcy flux ( $q$ ) along pathlines from particles released from sources, along with hydraulic gradients ( $i$ ) and positions of major structural features such as faults or shale units were used as input parameters for designing DFN representations of conditions along the flowpath (Figure 8-16a).

The primary goal of these simulations is to provide estimates of the expected travel distance of the plume front under the Darcy fluxes from source areas obtained from the 3-dimensional flow model using DFN transport simulations, and then use these distances as a basis for truncating the pathlines in the flow model (Figure 8-16b). The DFN simulations account for plume attenuation caused by dispersion in the fracture network and diffusion into and sorption in the rock matrix. Degradation is not included in these simulations, but its effect was discussed previously in Section 8.5.2.9 and show that even slow rates of degradation can be an important factor in further attenuating the plume.

For Darcy flux, the conditions along the first 1000 m of the particle tracks were used, along with incorporation of distances to the first (or multiple) low  $K$  zones encountered (e.g., faults). The incorporation of such low  $K$  zone(s) in the 2-dimensional DFN simulations was a means to control the  $q$  by varying the degree of hydraulic connectivity across these units (i.e., by using lower fracture density, lengths and apertures). This then allows incorporation of field-derived ranges in fracture network parameters (e.g., fracture lengths, apertures and spacing in sandstone units) and hydraulic gradients to the extent possible while still maintaining  $q$  in the target range. This is supported by the field observations and flow model particle tracking results that show generally large hydraulic head declines across some units.

Using the  $q$  and  $i$  along with positions of major structural features that generally have a strong influence on hydraulic gradient along the flowpaths from the 3-dimensional EPM model,

2-dimensional DFN representations were constructed. The DFN simulations incorporate field ranges in parameters for both the rock matrix (e.g., porosity, tortuosity, sorption) and fracture network characteristics (e.g., fracture spacing, lengths and apertures) to the extent possible. Matrix parameters represent average sandstone-derived values, while variations in fracture network characteristics are included through the use of randomly generated fracture networks that incorporate variability in parameters such as fracture density, lengths and apertures. However, actual fracture networks are extremely complex and simulations are simplified through assumptions of 2-dimensional orthogonal fracture networks with individual fractures having uniform apertures and steady state flow conditions, as described above.

Since the simulations are intended to represent conditions along a streamline, the DFN model boundaries were established with constant head boundaries at the inflow and outflow ends of the domain, providing a similar hydraulic gradient as along the EPM streamlines, and no flow across the lateral boundaries. It was also assumed that the fracture network is oriented along a vertical section so that the orthogonal fractures represent bedding plane fractures and joints. Generally the domain used is 1000 m in the direction of flow and 200 m in the lateral direction. The lateral dimension was selected to be large enough to accommodate variation in fracture network statistics and flow conditions such that simulation results do not change significantly between different realizations of fracture networks with the same statistics, and also to allow transverse spreading of contamination from the source positioned along the middle portion of the upgradient boundary.

Fracture network conditions were then adjusted to provide the desired bulk  $q$  for each of the selected source areas. Generally, this required several flow simulations, adjusting fracture network characteristics (generally fracture lengths, fracture density and/or mean apertures in the sandstone zones, and/or the degree of fracture connectivity across the low  $K$  units) to provide the desired  $q$ .

#### **8.5.3.2 Source Areas Selected for EPM Flow to DFN Transport Assessment**

Simulations linking location-specific results from the EPM-flow model to DFN-transport were performed for three RI sites: (1) IEL (northeast area), (2) ELV, and (3) Delta. These areas were

selected to be representative of the full range of Darcy fluxes from sites of known or suspected TCE sources. Mean Darcy fluxes under the non-pumping condition for the RI sites evaluated are shown in Figure 8-17 and the three selected sites are noted. IEL was selected to represent the moderate  $q$  scenario, ELV a high  $q$  scenario, and Delta a low  $q$  scenario.

However, the target  $q$  values used for the EPM-flow to DFN-transport simulations generally differ from the average values, in some cases representing a higher end value from a specific subset of particles from each source zone as discussed below. Additional considerations in the selection of the sites for this assessment were (a) presence of a known TCE source area, (b) availability of nearby source zone core data, and (c) location of the area to potential receptors.

### 8.5.3.3 Overview of Results

In all DFN simulations, average sandstone matrix parameters were applied: matrix porosity ( $\Phi_m$ ) of 13%, tortuosity ( $\tau$ ) of 0.10, matrix hydraulic conductivity ( $K_m$ ) of  $3e-9$  m/s and TCE matrix retardation factor ( $R_m$ ) of 1.8. No contaminant degradation is included in these simulations. The lower  $K$  zones (e.g., faults) have an assumed thickness of 10 m. An average hydraulic gradient, consistent with conditions along the flow model particle traces over the first 1000 m for each source zone, is established using constant head boundaries at the upgradient and downgradient ends of the domain. For all simulations, a source zone is placed along the middle portion of the upgradient boundary with an assumed lateral extent of 40 m. The source is assumed constant for a period of 20 years, representing the assumed period of TCE releases followed by DNAPL disappearance due to diffusion into the rock matrix and dissolution into groundwater flowing in fractures.

The Darcy flux for the fractured rock mass is obtained from the numerical flow simulation using the total flow through the system ( $Q$ ) and area for flow ( $A$ ) (i.e., 200 m wide domain with unit thickness):

$$q = \frac{Q}{A}$$

The overall bulk hydraulic conductivity ( $K_b$ ) of the fractured rock mass can be calculated as previously described.

When assessing the plume front position, a relative concentration ( $C/C_o$ ) of  $10^{-5}$  is used, close to the ratio of the TCE MCL (0.005 mg/L) to its aqueous solubility (1100 mg/L) or  $5 \times 10^{-6}$ . It must be noted that the simulations provide ‘point’ concentrations, whereas in the field concentrations would generally represent ‘depth-averaged’ values from wells which would be lower, so that the plume front position is conservative (further) than would be the case if concentrations were depth averaged values. Such an analysis was not conducted here, which would require using flux-averaged concentrations weighted to groundwater flow rates and concentrations in fractures within assumed monitoring intervals. The following is an overview of the simulations and results for each of the three selected source areas.

#### IEL Area (Northeast)

IEL is in an area of moderate  $q$  (Figure 8-17) with an overall mean of  $1.1 \times 10^{-4}$  m/d for all released particles under non-pumping conditions (see particle traces and  $q$  histogram in Figure 8-18). The DFN transport simulations for the IEL area use conditions along a higher  $q$  pathline (see representative head and gradient profiles along the flowpath in Figure 8-18) under non-pumping conditions, with  $q$  of  $3.4 \times 10^{-4}$  m/d, which is about three times greater than the mean  $q$ . The DFN scenario incorporates two lower  $K$  zones positioned at similar distances to faults and the Happy Valley Member along the higher  $q$  flowpath (Figure 8-18(c)).

Figure 8-19 shows the DFN generated to represent IEL conditions, with sandstone zones separated by the two lower  $K$  zones at 380 m and 550 m from the source boundary. Fractures have a mean aperture of 70 microns in the sandstone units with a lognormal distribution such that some fractures have apertures in the few hundred micron range (see example aperture profile and histogram in Figure 8-20). Fracture lengths range from 10 to 150 m in the horizontal plane (bedding plane fractures) and 3 to 30 m in the vertical plane (joints) with a uniform probability distribution applied for fracture lengths. Horizontal fractures in the sandstone units terminate at the low  $K$  zones. To provide the hydraulic connection across these low  $K$  zones, separate sets of fractures were generated within the low  $K$  units, with lower fracture density, lower mean

apertures (30 microns) and shorter lengths (5 to 25 m) compared to the sandstone units. The fractures generated in the low K zones were allowed to extend beyond the low K units, such that many of the fractures connect across the low K zone to fractures in the sandstone units.

Figure 8-19 shows simulated hydraulic head contours for this scenario, with an overall assigned gradient of 5% consistent with the field results along the selected pathline (Figure 8-19(c)). As shown in the hydraulic head contour plot and example head and gradient profiles along  $z=100$  m, significant head declines occur across the lower K zones which is consistent with the EPM flow model results (Figure 8-18(c)). In the DFN transport simulations, the local hydraulic gradients vary significantly depending on local fracture network conditions. For the DFN generated to represent IEL conditions, the overall  $K_b$  is  $8.7 \times 10^{-8}$  meters per second (m/s) and  $q$  is  $4.3 \times 10^{-9}$  m/s ( $3.8 \times 10^{-4}$  m/d), which is slightly higher than the EPM flow model-derived  $q$  of  $3.4 \times 10^{-4}$  meters per day (m/d) along the pathline. Two additional realizations of randomly generated fracture networks using the same fracture network statistics provided  $q$  values of  $3.5 \times 10^{-4}$  and  $5.0 \times 10^{-4}$  m/d, respectively.

After 50 years, the plume front (at  $C/C_0=10^{-5}$ ) extends to about 800 m downgradient for the base case scenario as shown in Figure 8-21. For the two other realizations of fracture networks, the transport distance is slightly shorter for the scenario with lower  $q$  and slightly longer for the scenario with higher  $q$ , and remains within the 1000 m long domain after 50 years. As indicated above, the DFN transport simulations for IEL use a  $q$  that is at the higher-end of the range at IEL, which causes greater plume transport distances so these should be regarded as conservative estimates. Also, as discussed later, several assumptions inherent in the DFN simulations may be expected to cause conservative (longer) plume transport distances.

#### ELV Area – Higher $q$

ELV is in an area of high  $q$  (Figure 8-17) with an overall mean Darcy flux of  $1.5 \times 10^{-3}$  m/d for all released particles under non-pumping conditions (see particle traces and  $q$  histogram in Figure 8-22). The DFN simulations for the ELV area use conditions from a representative subset of particles released near corehole C-7, with an average  $q$  of  $1.8 \times 10^{-3}$  m/day which is 20% higher than the average  $q$  for all particles, and a factor of five higher than the target  $q$  value used for the

IEL simulations. Representative hydraulic head and gradient results along one of these pathlines are shown in Figure 8-22. The low K zone is positioned at 150 m from the source boundary, consistent with the average distance to the North Fault which is the first lower K zone encountered by these particles.

Figure 8-23 provides the DFN generated to represent ELV conditions, with sandstone zones separated by a single low K zone at 150 m from the source boundary. As with the IEL area, fractures have a mean aperture of 70 microns in the sandstone units with a lognormal distribution and similar fracture lengths. However, the higher ELV  $q$  is accommodated by use of a denser network of fractures in sandstone zones, more hydraulic connectivity across the single fault and also higher average hydraulic gradient.

Figure 8-23 shows simulated hydraulic head contours for this scenario, with an overall gradient of 10% consistent with the field results along representative pathlines (Figure 8-23). The head contours and example head and gradient profile show a significant head drop across the low K zone. Results from the EPM flow model show much less head loss across the North Fault as its hydraulic conductivity in the model is similar to that of the surrounding sandstone rock. For this fracture network representing ELV conditions, the overall  $K_b$  is  $2.1 \times 10^{-7}$  m/s and  $q$  is  $2.1 \times 10^{-8}$  m/s ( $1.8 \times 10^{-3}$  m/d), which is similar to the target value. One additional realization of a randomly generated fracture network was performed using the same fracture network statistics but this time with the domain extended to 1500 m, and the  $q$  for this simulation was  $2.0 \times 10^{-3}$  m/d.

After 50 years, the plume front (at  $C/C_0=10^{-5}$ ) for the base case ELV scenario extends beyond the end of the 1000 m long domain as shown in Figure 8-24. For the other realization with the domain extended, the plume front also extends beyond the end of the 1500 m domain after 50 years, but only at relative concentrations lower than  $C/C_0=10^{-4}$ . At 50 years, for this scenario the plume front at  $C/C_0=10^{-4}$  reaches to about 1300 m. As discussed later, several assumptions inherent in the DFN simulations are expected to return conservative (i.e., longer) simulated plume transport distances.

### Delta Area – Lower q

Delta is in an area of lower q relative to other source areas (Figure 8-17) with an overall mean of  $2.6 \times 10^{-5}$  m/d for all released particles under non-pumping conditions (see particle traces and q histogram in Figure 8-25).

The DFN simulations for the Delta area use conditions from a representative subset of particles released south of the Delta structure, with an average q of  $2.0 \times 10^{-4}$  m/day, which is much greater than the overall mean in this area by nearly a factor of 8 but still about a factor of two lower than the target q value used for the IEL simulations. Representative hydraulic head and gradient results along one of these pathlines are shown in Figure 8-25. A single low K zone is positioned at 570 m from the source boundary, consistent with the average distance to the Burro Flats Fault, which is the first low K zone encountered by these particles.

Figure 8-26 provides the DFN generated to represent Delta conditions, with sandstone zones separated by a single low K zone at 570 m from the source boundary. In this case, the fracture apertures have a mean of 60 microns in the sandstone units with a lognormal distribution, and shorter horizontal fracture lengths in the range of 10 to 80 m, both smaller than in the previous simulations for the IEL and ELV areas, and also a sparser fracture network to provide the desired smaller q.

Figure 8-26 shows simulated hydraulic head contours for this scenario, with an overall average gradient of 6% consistent with the field results along representative pathlines. The head contours and example head and gradient profile for the DFN simulation show a significant head drop across the low K zone consistent with the EPM model.

For this fracture network representing Delta conditions, the overall  $K_b$  is  $5.0 \times 10^{-8}$  m/s and q is  $3.0 \times 10^{-9}$  m/s ( $2.6 \times 10^{-4}$  m/d), which is about 30% greater than the target value. Two additional realizations of randomly generated fracture network were performed using the same fracture network statistics providing q values of  $2.3 \times 10^{-4}$  and  $3.0 \times 10^{-4}$  m/d. After 50 years, the plume front (at  $C/C_0=10^{-5}$ ) for the base case Delta scenario extends to about 650 m downgradient as

shown in Figure 8-27. Plume transport distances are similar or slightly shorter for the two other realizations of fracture networks.

#### 8.5.3.4 Assumptions Causing Conservative Estimates of Transport Distances in DFN Simulations

Based on several assumptions inherent in the 2-dimensional DFN simulations, it is likely that the results are conservative producing greater simulated plume transport distances than may be expected under field conditions. An overview of some of these assumptions and effects on simulated plume transport distances is provided below:

1. **Current DFN simulations are constrained to two-dimensional orthogonal fracture networks.** This has the effect of (a) neglecting dispersion in the fracture network in the third dimension, which can cause strong attenuation due to mixing and dilution with water flowing in fractures not connected to the source, (b) neglecting attenuation due to diffusion into the rock matrix with this additional spreading, and (c) causes source zones to be infinitely wide in the third dimension whereas actual source zones would have finite extents.
2. **Source applied over relatively large area along boundary and assumed constant for 20 years.** Besides infinite source width inherent in 2-dimensional simulations, the source term is applied over a fairly large extent (40 m) along the upgradient boundary and is assumed to be constant for a 20 year duration, which represents the time-period assumed for complete DNAPL dissolution. In reality, the source zone from DNAPL releases is much more complex, likely discontinuous and of shorter duration in some zones than assumed, which would result in greater attenuation. This condition is discussed in additional detail in the complementary Site Conceptual Model document (2009).
3. **DFN Transport simulations assume most contaminant transport in sandstone units.** Besides the relatively thin low K zones, the DFN simulations assume all sandstone. However if some of the transport occurs within lithologies such as siltstone, shale, or interbedded zones, greater rates of mass loss to the matrix due to sorption would be expected compared to transport in sandstone only, which would cause even stronger plume attenuation and shorter transport distances given their higher organic carbon content. For example, core logs for corehole C-7 in the ELV area and VOC results show much mass occurs in the vicinity of finer-grained lithologies.
4. **Incorporation of lower fracture density due to computational limits.** For representative contaminant transport in DFN simulations, the density of the computational grid has to be high to capture processes of matrix diffusion off fractures. In general, it may be expected that the actual field fracture spacing is smaller than that applied in the simulations. The effect of maintaining the same  $q$  with tighter fracture spacing would provide higher surface area for diffusion of mass from fractures to the

rock matrix and therefore cause greater plume front attenuation, unless fracture spacing becomes too close whereby diffusion profiles from adjacent fractures overlap.

5. **Simulations neglect degradation in the rock matrix and fractures.** Incorporation of even slow degradation in the rock matrix, in addition to diffusion and sorption, has been shown in other simulations presented in the complementary Site Conceptual Model document (2009) to cause much greater attenuation of transport distances. Degradation in the matrix allows higher concentration gradients for diffusion to be maintained and therefore causes more mass transfer from fractures to the matrix, in addition to the direct contaminant mass removal via degradation.

## 8.6 CHEMICAL FATE

As presented in previous sections of this report, chlorinated ethenes represent the vast majority of impacts to groundwater beneath SSFL. As such, much of work performed to date and the current understanding of the chemical fate is focused on chlorinated ethenes as will be discussed in this section. The fate of other chlorinated solvents that have been used at SSFL will be considered in the context of what is known about the groundwater geochemical conditions, groundwater sampling results, and fate pathways that have been reported in the scientific literature (McCarty, 1999 and Field and Sierra-Alvarez, 2004).

It is important to consider a number of site conditions in the context of the characterization of the groundwater geochemical conditions and sampling results and they are as follows:

- The measurements of nitrate in groundwater monitoring wells and their use in characterizing the groundwater redox conditions have been affected by anthropogenic releases of nitrate to the subsurface associated with SSFL operations. Nitrate sources include releases from leach fields that were used early in SSFL's operating history for the collection and management of sanitary wastes and from the use of red fuming nitric acid as a rocket fuel. Characterization of nitrate releases to SSFL groundwater was presented in previous section of this report.
- Historical groundwater withdrawals to support operations and for groundwater interim measures likely altered the natural geochemical conditions in local areas beneath SSFL.
- Samples obtained from groundwater monitoring locations are dominated by flow from the most-transmissive fracture zones intercepted by the monitoring instrument. Flow characterization from fractures intercepted by wells indicates that the bulk of the flow from the formation is dominated by one to two fracture zones at each location (Williams et al. 2002; Williams and Knutson, 2009). Furthermore, the transmissivity of the Chatsworth Formation is highest at the shallowest depths due to a reduction in fracture

transmissivity with depth associated with lithostatic loading of the rock mass. As such, these conditions induce a bias in the groundwater sample results that are used to characterize the groundwater geochemistry and chemical occurrence and concentration. Samples from vertical well clusters (and rock core) reduce this bias are expected to be more representative of the conditions with depth.

- Anthropogenic releases of other chemicals and their subsequent transformation may also affect local geochemical conditions and enhance the potential and rate of transformation of other chemicals (e.g., acetate production from the abiotic transformation of 1,1,1-TCA (Vogel & McCarty, 1987) that can serve as an electron donor to enhance reductive dechlorination of chlorinated ethenes).
- The geochemical and microbiological conditions occur within a dual-porosity system where the groundwater flows predominately in the fractures with its storage predominately in the rock matrix.

A summary of the redox conditions at the site is provided in Table 8-7 and is described in further detail in the complementary Site Conceptual Model document (2009) and by Pierce (2005). It is within this context that the following discussion of chemical fate is considered.

Both field and laboratory studies have been conducted to evaluate the fate of chlorinated VOCs in SSFL groundwater. Chlorinated ethenes have been the primary focus of the field and laboratory studies because of their occurrence in SSFL groundwater and the potential for their complete transformation to non-hazardous by-products under the appropriate geochemical environment (Freedman & Gossett, 1989). Four field studies have been conducted at SSFL to assess the fate of chlorinated VOCs in groundwater. The first study was conducted by Beak International at the ECL RI site in 1997 (Beak Environmental, 1997). A second field study of TCE transformation in the bedrock matrix was conducted by Jennifer Hurley. A third study covered a much broader area of SSFL and was initiated by Amanda Pierce in 2003. A fourth, focused field study was initiated in 2008 by Laura Zimmerman. These latter 3 studies were conducted under the direction of Dr. Beth Parker at the University of Guelph. Two laboratory studies have been conducted using saturated SSFL rock core to aid in the understanding of the transport and fate of TCE and its daughter products at the site. Both studies were performed by Dr. Ramona Darlington in the laboratory and under the direction of Dr. Freedman at Clemson University. Each of these six studies is described in further detail in the following sections.

### **8.6.1 1997 Field Study**

In 1997, Beak Environmental conducted a field study whose goal was to assess the nature and extent of intrinsic biodegradation of a number of chlorinated compounds including chlorinated methanes, ethenes and ethanes. The approach included collecting geochemical data from seven existing wells and a French Drain along the flowpath at the ECL RI site. Results of the study showed the reduction-oxidation conditions to be mildly aerobic throughout. Field data supporting reductive dechlorination included low concentrations of dissolved oxygen (DO), the continual presence of partial dechlorination products such as 1,2-DCE and 1,1-DCA, and the presence of complete dechlorination products (ethene and methane) from samples collected during a February 1997 monitoring event. Evidence for aerobic conditions included high concentrations of DO in upgradient groundwater and elevated oxidation-reduction potential (ORP) during the February 1997 monitoring event. These results indicated aerobic conditions exist in some portions of the site during the wet portion of the year. The presence of methane, ethane, ethene, propane and ammonia indicated there is a potential for aerobic cometabolic processes to occur under these conditions but mass losses due to cometabolic processes could not be estimated with these data alone.

Study authors concluded that reductive dechlorination was a major process that was occurring at the site and that aerobic biodegradation processes were also likely playing a role in reducing the mass of VOCs in site groundwater. The study indicated that these processes may be occurring in sequential manner, both spatially and temporally. This was partially attributed to a shallow depth to groundwater and large seasonal changes in groundwater levels associated with variations in precipitation.

### **8.6.2 2000/2001 Field Study**

TCE transformation in the rock matrix under natural conditions was evaluated by Jennifer Hurley using analytical results from the collection and analysis of more than 3,250 rock core samples from nine coreholes that were positioned at or near locations across SSFL where chlorinated solvents, primarily TCE, entered the subsurface (Hurley et al., 2007a, b and c). Laboratory analysis of the rock samples primarily targeted five chlorinated ethenes that included:

PCE, TCE, cDCE, tDCE, 1,1-DCE, and CFC-113. A sub-set of samples (about 5 percent) was also analyzed for a full suite of compounds included in EPA analytical method 8260. Sample results found frequent and appreciable detections of cDCE. cDCE is frequently cited in the literature as the most common transformation product resulting from the microbial reductive dechlorination of TCE, (e.g., Weidemeier et al., 1999; Chappelle, 2001). Results showed that the molar concentrations of cDCE exceeded that of TCE in many of the samples in which both analytes were detected. These results indicate that TCE transformation to cDCE is active and widespread in the Chatsworth Formation, but spatially variable.

Rock core sample results for tDCE showed infrequent detections and concentrations that never exceeded TCE. Results also showed that concentrations of cDCE nearly always greatly exceeded tDCE. The literature on the microbial reductive dechlorination of TCE reports that tDCE is a common transformation product, but that it is typically produced at much lower concentrations than cDCE, commonly at a ratio of five or less (Weidemeier et al., 1999). In the context of cDCE and tDCE, the rock core results are consistent with the literature on the transformation of TCE to DCE by microbial reductive dechlorination.

The rock core VOC analyses performed on five percent of the samples using EPA Method 8260 did not show an accumulation of vinyl chloride (VC), although the detection limit of VC using this method was approximately 450 µg/L in porewater. Further evaluations were conducted by reviewing the results of routine sampling and analysis of monitoring wells at SSFL for VC occurrences. Sampling results from 85 wells in the fall of 2001 showed that the highest concentration of VC was 13 µg/L. These results indicated that either transformation of the cDCE and tDCE isomers along the typical microbial reductive dechlorination pathway is not occurring, or that VC is rapidly being transformed to non-hazardous end products.

1,1-DCE was also found to be present in rock core samples from all nine coreholes at measurable concentrations. Concentrations of 1,1-DCE oftentimes exceeded TCE in many of the samples in which both compounds were detected. Additionally, concentrations of 1,1-DCE exceeded cDCE in the majority of the samples in which the two were detected. The abundance of 1,1-DCE was unexpected because its occurrence at TCE contamination sites is rare. The occurrence of abundant 1,1-DCE in groundwater is most oftentimes attributed to the transformation of

1,1,1-trichloroethane (1,1,1-TCA). However, the use of 1,1,1-TCA as a solvent at the locations investigated using rock core analyses showed its potential use at only 2 of 9 locations, with sampling results collected from monitoring wells located near this corehole confirming the presence of 1,1,1-TCA in groundwater. Additional information on 1,1,1-TCA occurrence in rock core samples analyzed using EPA Method 8260 showed no detections, although the detection limit was 320 µg/L in porewater. Based on the above and a review of the available literature, Hurley proposed that 1,1-DCE in rock porewater is a TCE transformation product, potentially through abiotic pathways in association with pyrite and sulphidogenic bacteria.

### 8.6.3 2003/2004 Field Study

The third field study assessed the transformation of chlorinated ethenes and was initiated by Amanda Pierce in 2003 (Pierce, 2005). The goals of the study were to characterize the reduction-oxidation conditions throughout SSFL and to assess the transformation pathways TCE, and cDCE. Isotopic and hydrogeochemical methods were used to characterize the groundwater and provide insight into the origin of major ions and the reduction-oxidation conditions. Compound-specific carbon isotope analyses of TCE and cDCE were used to identify and quantify the degradation of these two chlorinated ethenes.

The study used groundwater samples that were collected in 2003 and 2004 from 122 bedrock monitoring wells and were analyzed using:

- Field measurements of pH, oxidation-reduction potential (ORP), dissolved oxygen (DO), and alkalinity, and
- Laboratory measurements of major ions, minor and trace inorganics, dissolved inorganic carbon, dissolved organic carbon, VOCs, dissolved gases (methane, propene, propane, ethene, ethane, and acetylene), the ratios of naturally occurring stable isotopes, ( $^{18}\text{O}/^{16}\text{O}$ ,  $^2\text{H}/^1\text{H}$ ,  $^{13}\text{C}/^{12}\text{C}$ ,  $^{34}\text{S}/^{32}\text{S}$ ) and compound-specific carbon isotope analysis of TCE and cDCE.

The study results showed that the reduction-oxidation conditions at the site are highly variable. Concentrations of DO, nitrate, manganese(II), iron(II), and methane, as well as dissolved hydrogen concentrations and  $\delta^{34}\text{S}$  values, indicate redox conditions ranging from nitrate

(NO<sub>3</sub><sup>2-</sup>)-reduction to methanogenesis. Redox conditions are predominately Fe(III)-reducing with local occurrences of NO<sub>3</sub><sup>2-</sup>, Mn(IV)-, sulfate (SO<sub>4</sub><sup>2-</sup>)-reduction and methanogenesis.

Study results also showed that 37 wells contained detectable concentrations of TCE, with 32 of the 37 having one or more of the following degradation products: cDCE, trans-1,2-DCE (tDCE), 1,1-DCE, VC, and/or ethene. Results also showed that 42 of the 122 wells had quantifiable concentrations of cDCE with a maximum concentration of 2,300 µg/L. tDCE was present in 29 wells with a maximum concentration of 107 µg/L. The common presence of cDCE and tDCE is consistent with the microbial reductive dechlorination of TCE. The δ<sup>13</sup>C values for TCE ranged from -30.5 to -11.9 ‰, also consistent with microbial reductive dechlorination of TCE and indicate that 1.4 to 95.2% of the TCE has been degraded. The δ<sup>13</sup>C values for cDCE range from -25.5 to -20.8 ‰ and indicate microbial reductive dechlorination of cDCE is small. Low concentrations of VC and ethene in groundwater support this conclusion. The presence of acetylene is indicative of abiotic degradation of TCE and cDCE.

#### 8.6.4 2008 Field Study

A fourth, focused field study was initiated in 2008 by Laura Zimmerman under the direction of Dr. Beth Parker at the University of Guelph. The goal of this study was to collect groundwater samples from 14 wells using specialized sampling devices to ascertain the occurrence and concentration of highly volatile end products of the complete transformation of chlorinated ethenes. Specialized sampling techniques were used to avoid volatilization of these products that normally occurs using standard sample collection methods and produce concentrations representative of *in situ* conditions. Data collected from this third field study continue to be reduced and evaluated as of the date of this report. Results obtained from this study were compared to sampling results from the same set of wells using conventional well purging methods as reported by Pierce (2005). Key preliminary findings, also reported in the complementary Site Conceptual Model document (2009), include:

- The characterization of samples for redox parameters show conditions favorable to biological reduction of chlorinated ethenes.
- Concentrations of TCE daughter products were found at much higher concentrations in some samples providing further evidence of complete reductive dechlorination.

- Acetylene, an indicator of abiotic transformation of TCE, was absent in the Snap samplers when compared to the samples collected from wells at the same locations. Its absence is attributed to acetylene's instability, which is suspected to quickly volatilize or decay in the well bore after its production occurs in the rock matrix.

### 8.6.5 2003-2005 Laboratory Study

The first laboratory study of chlorinated ethene degradation involved establishing microcosms to address the degree to which biotic and abiotic transformation is occurring for TCE, cDCE, and vinyl chloride, and the potential role of biological oxidative processes for removing cDCE and vinyl chloride (Freedman and Darlington, 2006).

Rock core samples containing different types of mineralogy were collected from corehole C-6 within the Delta RI site. Subsections from depths of approximately 531, 568, 732, and 872 feet were crushed and used to prepare microcosms with groundwater taken from a nearby well (WS-9A). For each depth and compound, treatments consisted of live anaerobic conditions; autoclaved anaerobic controls; oxidized controls (by adding peroxide), and distilled water-only controls. A  $^{14}\text{C}$ -labeled compound was added to each bottle, yielding initial TCE, cDCE and vinyl chloride concentrations of approximately 260, 760, and 110  $\mu\text{g/L}$ , respectively.

The results of this microcosm study confirmed the field observations of TCE attenuation at the site and demonstrated the potential for reductive and oxidative transformations in fractured sandstone. Transformation of TCE was predominantly biological. cDCE was the predominant isomer formed, providing evidence that the process is biotic. Reduction of TCE to cDCE in the microcosm studies is consistent with field data that correlates TCE attenuation with cDCE accumulation. Reductive dechlorination was a significant fate process only in the live microcosms; very little occurred in the autoclaved controls. The process was abrupt rather than gradual in the bottles in which TCE reduction occurred. This suggests a lag phase preceding the onset of growth by microbes that chlororespire TCE. The electron donor for reductive dechlorination was not ascertained during this study, but may be from organic carbon or reduced iron and sulfide minerals in the sandstone. Molecular studies of the microcosms indicated the presence of a microbe associated with anaerobic oxidation of iron (II) coupled to nitrate reduction. Polymerase chain reaction (PCR) amplification of microbes that are known to

chlororespire TCE to cDCE (i.e., *Dehalobacter*, *Desulfuromonas*, *Dehalospirillum*, and *Desulfitobacterium*) were negative, suggesting that a novel type of microbe is responsible for this activity in SSFL sediment.

Accumulation of soluble, non-strippable residue (NSR) in autoclaved controls and  $^{14}\text{CO}_2$  in as-is treatments suggested that a combination of biotic and abiotic mechanisms is involved in transformation of [ $^{14}\text{C}$ ]cDCE. Work done by concentrating NSR by lyophilization indicates that glycolate and formate are two of the three likely compounds formed from [ $^{14}\text{C}$ ]cDCE. Both would be readily oxidized to  $\text{CO}_2$  in the presence of microbes. In microcosms that did not undergo rapid reduction of TCE to cDCE, statistically significant zero-order rates of TCE transformation ranged from 0.27 to 0.41 micrograms per meter per year ( $\mu\text{g}/\text{m}/\text{yr}$ ) above water controls.

#### 8.6.6 2005-2007 Laboratory Study

A second laboratory study was performed by Darlington (2008). The objectives of the second laboratory study were to:

- Identify the microorganism(s) responsible for reductive dechlorination of TCE to cDCE,
- Confirm the main chemical constituents present in NSR,
- Determine if pyrite in the sandstone is responsible for catalyzing the abiotic transformation of cDCE to soluble products and  $\text{CO}_2$ ,
- Quantify the rate of cDCE transformation, and
- Evaluate the effect of autoclaving as a method of sterilization for measuring abiotic transformation of cDCE in fractured sandstone.

The work included repeatedly enriching microcosms for the TCE dechlorinator to identify the microbe and to identify and quantify the chemicals that comprise the NSR. This latter activity was intended to more fully develop the TCE and cDCE transformation pathways. *Pseudomonas stutzeri* was identified as the organism in the community responsible for the reduction of TCE to cDCE. PCR-denaturing gradient gel electrophoresis (DGGE) analysis of DNA extracted from enrichments of the microorganisms provided a sequence that matched 100 percent to *Pseudomonas stutzeri*. Only one other facultative aerobe is known that can dechlorinate TCE to

cDCE under anaerobic conditions, strain MS-1. *Desulfovibrio putealis*, a sulfate reducer, was also found to be present in the community. These results suggest that a combination of abiotic and biotic transformation processes is responsible for attenuation of TCE and cDCE in the fractured sandstone aquifer. Tracking the distribution of  $^{14}\text{C}$  during the microcosm study was essential for observing these phenomena.

Microcosms (2 liter (L) glass bottles equipped with mini-nert valves) were prepared with groundwater and approximately mg/L cDCE (including some  $^{14}\text{C}$ -labeled) plus pyrite, pyrite-rich sandstone, and typical sandstone that was crushed and autoclaved. During 120 days of incubation, the highest level of cDCE transformation occurred with typical sandstone (11-14%  $^{14}\text{CO}_2$ , 1-3 percent  $^{14}\text{C}$ -soluble products), followed by pyrite-rich sandstone (2-4 percent  $^{14}\text{CO}_2$ , 1%  $^{14}\text{C}$ -soluble products). Transformation in the treatment with pyrite was only slightly higher than groundwater-only controls, indicating that pyrite was not the principal mineral involved.

A second experiment was performed using only the typical sandstone, with three treatments (live, autoclaved, and sterilized with propylene oxide). Surface-normalized transformation rates for cDCE were higher for the live treatment ( $1.31\text{E-}05 \text{ L m}^{-2} \text{ d}^{-1}$ ) versus the autoclaved treatment ( $1.08\text{E-}05 \text{ L m}^{-2} \text{ d}^{-1}$ ). Although the extent of transformation in the autoclaved sandstone was higher initially, the ultimate extent of transformation was similar in both treatments (approximately 7 percent of the [ $^{14}\text{C}$ ]cDCE added converted to  $^{14}\text{CO}_2$  +  $^{14}\text{C}$ -soluble products). The presence of glycolate, formate and acetate as components of the soluble products was confirmed. Small amounts of vinyl chloride, ethene, ethane and acetylene were detected in the live treatment, while only acetylene was detected in the autoclaved treatment. Use of propylene oxide to sterilize the sandstone resulted in substantial inhibition of cDCE transformation. X-ray photoelectron spectroscopy (XPS) analysis of the sandstone indicated the presence of magnetite and goethite. The presence of ferrous and ferric oxides and hydroxides suggest that these minerals may be central to cDCE transformation under field conditions. The results of this study provide further insight into the co-occurrence of abiotic and biotic transformation process for chlorinated ethenes in fractured sandstone.

### 8.6.7 Integrated Assessment of Chlorinated Ethene Fate

The understanding of chlorinated ethene fate at SSFL comes from the results of the studies mentioned above, other rock core and conventional groundwater sampling that has been conducted to assess their nature and extent. A tabulated summary of the results from these studies and other sampling activities is provided in Table 8-8. Further discussions of the transformation pathways for the chlorinated ethenes are provided below.

PCE has not been used extensively as a chlorinated solvent at SSFL as reflected in the review of historical records and surficial media and groundwater sampling results (from both wells and rock core). In most areas of SSFL, when PCE is present it is suspected as being a contaminant in the neat TCE that was used throughout SSFL to support operations. PCE has been shown in numerous laboratory and field studies to be reduced to TCE in nearly any anaerobic environment (Weidemeier et al., 1999). Where PCE was used as a neat solvent and entered the groundwater system (e.g., the B-1 RI site in the northeast area of SSFL), it is expected to be transformed to TCE by reductive dechlorination. Field data for this transformation at SSFL can be found in the rock core sampling results for corehole C-9 where the ratio of PCE to TCE in the groundwater is 1:20, while in the vadose zone it is 1.5:1. Locations where both PCE and TCE have been detected in groundwater at concentrations above screening levels are shown in Figure 8-28.

Additional insight into the biological reduction of PCE (and TCE, discussed further below) at SSFL can also be gained from review of the rock core sampling results from the 1 of the 3 plume transect coreholes (C-12) drilled north of the B-1 RI site. Results from corehole C-12 show the only chemical detected in the rock core is PCE and it was found in only 3 of 285 samples of rock core at low concentrations (maximum of ~50 µg/L equivalent porewater). Hydrogeochemical analysis of samples from two wells in this area (RD-66 and -71) conducted by Pierce in 2003, showed Fe(III)- to sulfate-reducing conditions. However, it is believed that the native microbial population has yet to become acclimated to the presence of PCE at this location thus accounting for the absence of TCE. A similar condition exists for TCE at the plume front corehole pair C16/C17 where TCE is found in 12 percent of the rock core samples (22 of 185) with 1,1-DCE being the only other chlorinated ethene encountered in 1.6% of the rock core samples (3 of 185).

Chapelle (2001) discusses the acclimation of microbes to xenobiotics (i.e., carbon compounds not typically found in nature) in groundwater systems. He discusses acclimation responses in both “contaminated” and “pristine” groundwater. The position of corehole C-12 relative to the source can be considered an area of “pristine” (i.e., un- or minimally-contaminated, or plume front) groundwater as demonstrated by the presence of only PCE in only ~1 percent of the samples. Chapelle discusses the results of a few studies done on microbial acclimation to xenobiotics. The results indicated that the response of microbial communities to the presence of xenobiotic compounds will not be uniform and that the response can be concentration-dependent. The studies attribute the concentration-dependence of a microbial response to the induction of specific enzyme systems.

The first set of Clemson University laboratory studies of chlorinated ethene degradation at SSFL provide insight regarding microbial acclimation in “contaminated” groundwater at SSFL. In this context, “contaminated” groundwater is considered to occur in former input locations and mid-plume. The Clemson studies utilized rock core from a source zone (C6 at the Delta RI site) and groundwater samples from well WS-9A, a well impacted by chlorinated ethenes. The Clemson studies showed relatively little time lag in the microbial response to the hydrogenolysis of TCE to cDCE (i.e., the cleaving of a carbon-chlorine single bond by hydrogen) using carbon-14 labeled product (Freedman and Darlington, 2006). These results are consistent with the acclimation response study in a contaminated aquifer reviewed and discussed by Chapelle. The results of that study showed that contaminants in sediments from the contaminated portion of the aquifer were much more mineralized than from the uncontaminated portion of the aquifer.

The fate of TCE in groundwater is affected by 3 different and distinct transformation pathways. Biological reduction of TCE to predominantly cDCE, and to much lesser degrees tDCE and 1,1-DCE, is the major transformation pathway. Locations where both TCE and cDCE have been detected in groundwater at concentrations above screening levels are shown in Figure 8-29, TCE and tDCE are shown in Figure 8-30 and TCE and 1,1-DCE are shown in Figure 8-31. TCE is also expected to abiotically transform to 1,1-DCE, organic acids including glycolate, formate and acetate, and carbon dioxide as minor transformation pathways. The abiotic reactions that transform TCE occur in the rock matrix and along fracture faces in association with pyrite and

sulphidogenic bacteria (producing 1,1-DCE) and with ferrous and ferric oxides and hydroxides (producing acetylene, glycolate, formate, acetate and carbon dioxide).

The biological reduction of TCE to primarily cDCE at SSFL has been documented in sampling results from monitoring locations and rock core, in carbon-specific isotope analyses of TCE, and in carbon-14 labeled laboratory studies. The biological and abiotic transformation of TCE to 1,1-DCE in the rock matrix has been documented in rock core sampling results, where 1,1-DCE is found as frequently as cDCE (18 percent and 17 percent of samples, respectively), but at lower average concentrations (316 and 1,864 µg/L, respectively). Samples collected from monitoring locations and analyzed for both 1,1-DCE and cDCE show that 1,1-DCE is found less frequently than cDCE (28 percent and 54 percent of locations sampled). Its less frequent occurrence in samples from wells can be attributed to lower concentrations in the rock matrix. It is important to remember that 1,1-DCE is also an abiotic transformation product of 1,1,1-TCA and its concentration is elevated in areas where there have been historical releases of 1,1,1-TCA. This is most recently observed in sampling results collected in Zimmerman's 2008 special study where 1,1-DCE was detected at concentrations at least an order of magnitude higher in areas of historical 1,1,1-TCA releases (i.e., B-1 and STL-IV RI sites) than in areas where only TCE was released. The abiotic transformation pathway of TCE to organic acids and carbon dioxide is shown as a result of the laboratory studies done by Darlington. Field data to support this pathway is problematic to obtain due to the rapid rate of biologically-mediated organic acid transformation to carbon dioxide.

The transformation of cDCE to vinyl chloride and beyond by reductive dechlorination is characterized as a minor transformation pathway. Locations where both cDCE and vinyl chloride have been detected in groundwater at concentrations above screening levels are shown in Figure 8-32. Results from both field and laboratory studies indicate the transformation of cDCE to vinyl chloride at fewer locations and at low concentrations. The Pierce cDCE carbon isotope analyses and Darlington laboratory studies show limited transformation of cDCE to daughter products, although some transformation was noted. The periodic detections of ethene and ethane in groundwater samples from select wells indicate some complete dechlorination is occurring. Ethene has been shown to be mineralized to carbon dioxide under sulfate-reducing

conditions (Bradley & Chapelle, 2002). Locations where concentrations of vinyl chloride are present above its screening level and any detections of ethene and ethane in groundwater are shown in Figure 8-33.

These data show that microbially-mediated complete dechlorination of chlorinated ethenes is occurring at SSFL. The reductive dechlorination observed is consistent with cometabolism by sulphate- or iron-reducing bacteria present within the Chatsworth Formation. Gantzer and Wackett (1991) present half-life constants for reductive dechlorination of chlorinated ethenes by bacterial transition-metal coenzymes and they are summarized in Table 8-9. Field and laboratory results also show the complete mineralization of TCE and cDCE due to abiotic reactions with ferric and ferrous oxides and oxyhydroxides in the rock matrix. A summary diagram of the transformation pathways of the chlorinated ethenes is shown in Figure 8-34 along with that of two other chlorinated solvents that have been used at SSFL, 1,1,1-TCA and carbon tetrachloride.

#### **8.6.8 Other Chlorinated Solvents**

1,1,1-TCA is known to abiotically transform to 1,1-DCE and acetic acid (Vogel & McCarty, 1987). For the recent period used in this report to characterize the current groundwater conditions (i.e., July 2007 through June 2008), only one well (RS-54) contains concentrations of 1,1,1-TCA above its 200 µg/L screening level. In the historical dataset, 12 monitoring locations contained concentrations of 1,1,1-TCA above its screening level. The fact that there remains only one well with 1,1,1-TCA above its screening level are supportive of its transformation to lower chlorinated daughter products. Figures depicting the current distribution of 1,1-DCE, the abiotic transformation product of 1,1,1-TCA and 1,1-DCA, the reductive dechlorination transformation product of 1,1,1-TCA were presented in Section 7. Locations where both 1,1-DCE and 1,1-DCA were present in samples from groundwater monitoring wells at concentrations exceeding their screening levels are shown in Figure 8-35. As depicted in this figure, 1,1-DCE is more broadly distributed than 1,1-DCA, most likely due to the abiotic transformation of TCE to 1,1-DCE as discussed above.

The reductive dechlorination product of 1,1-DCA is chloroethane and groundwater sampling results show that it is detected less frequently and at lower concentrations than 1,1-DCA based

on results from the “recent” groundwater sampling data set. 1,1-DCA was detected in samples from 21 wells, while chloroethane was found in samples from 9 wells. These results are consistent with the redox conditions of the groundwater system characterized and described in the complementary Site Conceptual Model document (2009). Research literature indicates that complete transformation of 1,1-DCA to chloroethane then to ethane requires methanogenic conditions (Vogel & McCarty, 1987, and de Best et al., 1999), which locally occur beneath SSFL. Similar to the transformation of chlorinated ethenes, the reductive dechlorination of 1,1-DCA to chloroethane likely results from cometabolism by iron- and sulfate-reducing bacteria.

Chloroethane has been documented to transform to ethanol by hydrolysis (Washington, 1995), which may also attribute to its infrequent occurrence at low concentrations. Finally, 1,4-dioxane is known to have been used as a stabilizer in 1,1,1-TCA. Its occurrence in groundwater at concentrations above its screening along with that of 1,1-DCE and 1,1-DCA is shown in Figures 8-36 and 8-37, respectively.

Carbon tetrachloride has been shown to transform to chloroform via hydrogenolysis under a range of reducing conditions (Egli et al., 1987, Egli et al., 1988, and Galli & McCarty, 1989). Carbon tetrachloride can also transform to carbon monoxide and carbon dioxide, carbon disulfide and formate via one- or two-electron reduction processes (Krone et al., 1991). At SSFL in the recent groundwater dataset, carbon tetrachloride is found in groundwater at concentrations above 1 µg/L at three RI sites (SPA (1 well), FSDF (1 well) and ECL (2 wells & French drain)).

Chloroform is found at concentrations similar to carbon tetrachloride in samples from wells at both the SPA and FSDF RI sites and at higher concentrations in two of three wells at the ECL RI site. Additionally, chloroform is found in an additional well at the FSDF RI site. Methylene chloride, the reductive dechlorination product of chloroform is not detected at the SPA RI site, is detected in the well with only chloroform at the FSDF RI site and in only 1 of 3 locations at the ECL RI site. Sulfate-reducing or methanogenic conditions are reportedly needed to reductively dechlorinate chloroform to methylene chloride.

Chloromethane, the final chlorinated methane in the reductive dechlorination pathway has not been found in wells at the ECL RI site, is found in a different well at the FSDF RI site and is found in the same well at the SPA RI site and an additional well. All concentrations detected are less than 1 µg/L. Methane was also detected in the same two wells at the SPA RI site in sampling conducted by Pierce in 2004. There are little to no field data available to evaluate the reduction processes of carbon tetrachloride and chloroform noted earlier as the resultant products are not discernable from their generation associated with unrelated biogeochemical processes.

### **8.6.9 Perchlorate**

A preliminary evaluation of the natural biodegradation of perchlorate in SSFL groundwater is presented in the complementary Site Conceptual Model document (2009). The literature review concludes that the potential for biodegradation of perchlorate in SSFL groundwater via autotrophic organisms is likely although the transformation rates will be slow and limited by the supply of electron donor. The broadest area and highest concentration of perchlorate impacted groundwater at SSFL occurs in the northeast area beneath the Building 359 and Happy Valley North RI sites (see Figure 7-22). However, this area has also been impacted by anthropogenic nitrate releases (see Figure 7-23). Pierce (2005) characterized the geochemical conditions of a well (RD-77) in this area and found nitrate at 3.5 mg/L, manganese at 0.01 mg/L, non-detectable concentrations of iron, and sulfate at 64 mg/L. The presence of elevated concentrations of nitrate in this area from historical operations will likely extend the persistence of perchlorate as the natural organisms adapt and first consume the available nitrate.

### **8.6.10 Tritium**

The half-life of tritium through radioactive decay (beta emission) is well established to be 12.3 years. The fate of other radionuclides will not be further discussed as current information shows that none are present in wells for which they were sampled at concentrations exceeding screening levels.

## 8.7 SUMMARY OF TRANSPORT AND FATE

Transport evaluations were conducted by coupling site data with analytical and numerical models to:

- Gain insight into the transport of metals in soil and to alluvium groundwater (presented in Section 7 to support the evaluation of their nature and extent),
- Estimate vapor fluxes to the ground surface from chlorinated solvents in bedrock groundwater,
- Consider the effects of vadose zone sources on VOC distributions and their longevity in groundwater,
- Estimate the persistence of immiscible-phase TCE (DNAPL) below the water table,
- Inform and provide bounds for judging how far and how rapidly the fronts of different solutes are likely to move under a wide variety of circumstances, using input parameters tailored to conditions at SSFL where feasible,
- Provide insight into the effects of degradation, and decay on plume expansion and longevity, and
- Help in identifying data gaps.

Use of, or insight gained from, transport evaluations indicate:

- The transport of metals from anthropogenic sources in alluvium groundwater is strongly retarded with the smallest retardation factor being 14 (boron) leading to very short transport distances (i.e., less than 10 m).
- Vapor fluxes to ground surface from bedrock groundwater have been used in surficial media RI risk assessments to evaluate potential impacts to receptors.
- Coupled TCE vadose zone- and DNAPL-sources do not show discernable differences in either the lateral or vertical extent of groundwater plumes relative to a DNAPL-only source. For a TCE vadose zone-only source, the overall extent of a groundwater plume is not appreciably different when the source is continuously present for either 50 or 100 years. This is attributed to the fact that mass transfer to the saturated rock matrix started decades ago after initial releases and continued for the last 50 years or so. Nearly all the mass resides in the saturated rock matrix where its further transport is diffusion controlled.
- TCE DNAPL completely dissolves in nearly all fractures within 10s of years after it entered the subsurface and is consistent with field sampling results.
- Extents of the various contaminants found in groundwater based on field data, including source and plume transects and longsect, are consistent with the ranges predicted by the DFN simulations

- Slow rates of contaminant degradation can cause additional plume front retardation and appreciably contribute to the overall attenuation of the contaminant plume. Field data indicate conditions for degradation or decay exist at SSFL. Degradation rates with half-lives ranging between 5 and 20 years can cause plume fronts to retreat and collapse within a few hundred years or sooner.
- Further field characterization is warranted to evaluate potential contaminant transport as presented in Section 8.8.

Fate evaluations were conducted by evaluating field and laboratory data from conventional groundwater samples, and from special studies, and were coupled with fate information contained in the scientific literature. The evaluations using site data show that microbially-mediated complete dechlorination of chlorinated ethenes is occurring at SSFL. The reductive dechlorination observed is consistent with cometabolism by sulphate- or iron-reducing bacteria present within the Chatsworth Formation. Field and laboratory results also show the complete mineralization of TCE and cDCE due to abiotic reactions with ferric and ferrous oxides and oxyhydroxides in the rock matrix. The redox conditions are also consistent with reductive dechlorination of other chlorinated solvents used at SSFL. Field results also show the abiotic transformation of 1,1,1-TCE. A literature review of perchlorate biodegradation concludes that the potential exists in SSFL groundwater via autotrophic organisms, although the transformation rates will be slow and limited by the supply of electron donor. Tritium's fate is evident from its spatial distribution and it has a relatively short radioactive half-life (12.4 years). Although tritium is the only radionuclide that has been found in groundwater at SSFL above screening levels, other radionuclides were historically found in soil at SSFL and remediated. As sampling results from the existing well network and seeps have not shown other radionuclides to be present in groundwater above screening levels, their fate is not addressed in this report.

## **8.8 TRANSPORT AND FATE DATA GAPS**

Additional characterization of the extent of VOC impacts at the ELV RI site is warranted. Characterization of contaminant transport by combining the results from the 3-dimensional groundwater flow model with 2-dimensional discrete-fracture network transport simulations indicate that the position of existing monitoring wells may not intercept groundwater flowing through this site. Characterization results presented in this report show that this area is

characterized by higher Darcy fluxes due to projected steep gradients along simulated 3-dimensional flow paths. This condition, coupled with ELV's proximity to the northern property border, warrant further characterization of potential impacts to the bedrock groundwater.

Insights into the groundwater flow system gained from the 3-dimensional groundwater flow model indicate that evaluation of two faults in the northwest portion of SSFL is warranted (i.e., FSDF structures). Flow model optimization represents these features as more conductive than the surrounding bedrock, which makes them unique in their hydraulic character relative to the field data and flow model's characterization of the remaining faults at SSFL.

Seeps around the perimeter of SSFL should be sampled and analyzed for VOCs to confirm the absence of impacts to off-site receptors.

This Page Intentionally Left Blank

## **9.0 GROUNDWATER IMPACT ASSESSMENT**

Human health and ecological risk assessments were prepared and reported in the surficial media RI reports. Appendix 9-A presents the results of those risk assessments as they relate to groundwater underlying the site. Risk assessments for groundwater in some areas of SSFL indicate incremental lifetime cancer risks and/or hazard index values that exceed values in regulatory guidance. In accordance with standard protocols, these risk assessments assumed complete or nearly complete groundwater exposure pathways. However, as described below, the potential exposure pathways for groundwater contaminants are expected to be predominantly incomplete. The purpose of this section is to describe the expected on-site and off-site impacts to human and ecological receptors from groundwater contamination within and originating at SSFL. The analyses presented in this section are based upon and incorporate the data and analyses presented in Sections 2 through 8 and their associated appendices, surficial OU reports, and in the complementary Site Conceptual Model document (Cherry, McWhorter and Parker, 2009).

### **9.1 CONSIDERATION OF ON-SITE GROUNDWATER CONTAMINANT IMPACTS**

The extensive site investigations and their support of the Site Conceptual Model provide strong evidence that the nature and extent, and the transport and fate of contaminants in groundwater at SSFL are well understood. Access to SSFL is restricted by the property owners and no water supply wells are planned for domestic or other use on-site. It is anticipated a groundwater use prohibition will be imposed on the site to restrict access to groundwater in perpetuity, thus controlling drinking water and other direct exposure pathways.

Three on-site seasonally variable seeps in the south western portion of the property periodically discharge site groundwater contaminated with VOCs to the land surface. This potential discharge is currently controlled by groundwater pumping as part of an interim measures program. Remedying this potential exposure pathway to human or ecological receptors will be addressed in the Remedial Action Plan.

Limited exposure potential is expected for VOC vapors emanating from groundwater as described in the surficial media risk assessments. This potential exposure pathway will be addressed in the Remedial Action Plan.

## **9.2 GROUNDWATER INVESTIGATION FINDINGS CONCERNING POTENTIAL OFF-SITE IMPACTS**

In this section, the results of SSFL site investigations and the SCM are used to assess the likelihood that site contaminated groundwater will impact off-site human and environmental receptors, now and in the future. Figure 7-33 shows areas where on-site and off-site groundwater contamination is known and projected to exist in the bedrock groundwater system based on monitoring well and seeps sampling results. This information and results generated from field data and the calibrated and optimized 3-dimensional mountain scale numerical groundwater flow model were used to evaluate the potential for the transport of contaminants towards off-site locations. The possibility that off-site exposure of human and ecological receptors to site impacted groundwater at the rural hillside locations adjacent to the site or at more distant locations such as Simi Valley, Chatsworth, and the San Fernando Valley has been assessed.

Site data show that a plume extends off-site in only one portion of SSFL (in the northeast area). Areas with groundwater contamination are characterized by numerous types of field data, and the integration and interpretation of these data. The characterization of site groundwater contamination includes extensive hydrochemical data sets. These data show plumes are nearly stationary and of limited extent. The near-stationary status of the plumes is supported by the following:

- Matrix diffusion has been confirmed by rock core results.
- Rock core results demonstrate the nature of the vertical extent of plumes and concentrations in former source areas. Multi-level groundwater monitoring also provides information about the vertical extent of contamination.
- Plumes are monitorable. The lateral extent of groundwater plumes has been characterized by existing field data including rock core, and monitoring well and seep data sets.

- Strong natural attenuation of plumes is indicated by field monitoring results, laboratory studies and modeling of contaminant transport and fate. Attenuation is attributed to matrix diffusion, dispersion, chemical, and microbial processes. Plume front retardation and attenuation have been confirmed by the plume and source transect and longsect investigations performed in the northeast portion of the site and by plume characterization efforts evaluating the tritium plume in the northwest part of the site.
- Atmospheric derived tracers (e.g., tritium and carbon-14) have been used to characterize groundwater flow and solute attenuation.

Since the termination of site operations and releases to the subsurface, source zone data sets show strong attenuation of initial concentrations due to dissolution, diffusion and degradation processes. Groundwater monitoring results and rock core data confirm that contaminant concentrations in former source areas decrease over time. Concentrations in source areas have attenuated and are not easily distinguished from other portions of site plumes because nearly all contaminant mass exists as dissolved and sorbed phases residing in the rock matrix.

Potential groundwater exposure pathways are limited:

- A small number of domestic wells are known to exist near the site for potable water use. These wells have been sampled and the data indicate no impacts from contaminants in groundwater originating from SSFL.
- Off-site seep sampling results indicate no discharge of site contaminants, thus no off-site exposure is occurring.
- Such information has also been previously communicated in the *Offsite Data Evaluation Report* (MWH, 2007g).

### 9.3 CONSIDERATION OF OFF-SITE CONTAMINANT IMPACTS

The analysis of groundwater flow from SSFL indicates that about half of the groundwater originating on SSFL flows to exit points on the hill slopes adjacent to SSFL (local groundwater discharge) and about half follows deeper flow paths extending beyond the Simi Hills into the adjacent valleys (regional discharge). Although contaminants such as TCE and perchlorate have been periodically detected in wells located in the surrounding valleys, these compounds are commonly used in a variety of industrial and commercial off-site operations. Their presence in valley wells can be attributed to local industrial sources and not SSFL. It is scientifically implausible for groundwater from SSFL to impact the water quality of wells in the valleys so

distant from SSFL. It is not scientifically plausible for contaminants to migrate to outlying communities at concentrations causing human and ecological impacts due to the observed concentrations in plumes, the transport distance required, the strength of attenuation and retardation in the bedrock, and the small contaminant mass discharge available for advective transport in contaminant plumes at SSFL.

An intensive investigation was conducted to locate and describe seeps on and near SSFL. These seeps exist on the hill slopes peripheral to where releases occurred at SSFL. These releases occurred at elevations much higher than the elevation of nearly all seeps identified. Figure 9-1 shows the location of the seeps found. The identification of seeps involved the use of aerial photography and on-the-ground field mapping. A small portion of the area was not investigated in the field due to the lack of access. A total of 154 seeps were identified of which 69 had insufficient water to allow sampling. Samples were collected from more than 60 seeps and analyzed for targeted SSFL contaminants (e.g., VOCs and perchlorate) and other flow system indicators. Sample results show that there have been no confirmed detections of site-related contaminants at the off-site seeps sampled. Although the sampling did not include all seeps, the group sampled included seeps that have diverse characteristics and are widely spatially distributed (representative of the entire site and vicinity). Future work will include additional seeps sampling. The absence of site-related contaminants at seeps is consistent with what is known about the migration, attenuation, and retardation of groundwater contaminant plumes originating at SSFL. Sampling of off-site wells in and beyond the seeps areas is part of ongoing monitoring at SSFL. The sampling results show no presence of site-related contaminants in wells sampled, which is consistent with the results from seeps sampling and the understanding of contaminant transport and fate.

Community water supply sources in the surrounding valleys are a combination of surface water from northern California (the State Water Project) and local groundwater. Water supply wells in both the Simi Valley and San Fernando Valley are more than 3 miles from SSFL, much farther than the predicted transport distances of SSFL contaminants.

In summary, available data indicate there are no known impacts to off-site human or ecological receptors from groundwater originating beneath SSFL. This report recommends that additional field data be collected to further evaluate this conclusion.

This Page Intentionally Left Blank

## **10.0 SUMMARY AND CONCLUSIONS**

A substantial body of data has been collected during the remedial investigation of groundwater at SSFL over more than two decades. The primary purpose of this RI report has been to review and interpret these data, as well as collect new data, with the objectives of fully describing the characterization of contaminants in groundwater and identifying data gaps related to that characterization. This report is supported and complemented by numerous prior published site documents and the Site Conceptual Model report prepared by the SSFL Groundwater Advisory Panel (2009).

### **10.1 WORK PERFORMED**

More than 20,000 groundwater samples have been collected from over 485 groundwater monitoring locations over nearly a quarter century and have produced nearly a half-million chemical records. Samples collected from the monitoring network cover an area of about 11 square miles and extend to depths beyond 1,000 feet. Over 1,400 groundwater samples have been collected and analyzed for radiological characterization. Approximately 7,800 rock core samples have been collected from more than 40 locations to depths of 1,400 feet and analyzed for sorbing and non-reactive chemicals and for non-reactive radionuclides over the last 12 years to supplement the groundwater sampling results. Additional investigations of the groundwater system have been performed to characterize various hydrogeologic parameters of the fractured bedrock and the groundwater flow system influencing contaminant transport and fate.

The characterization program at SSFL has generated one of the largest data sets in the world that describe a fractured rock site. Scales of investigations conducted in support of the groundwater RI program extend from regional flow modeling that encompasses an area of about 336 square miles, to the use of electron microscopy and X-ray photospectroscopy instruments to inspect minerals on the surface of rock particles. Examples of the multi-scaled data sets include:

- Rock matrix porosity and permeability measurements;
- Compound-specific stable isotope analyses;
- Microbiological and fracture network characterization;

- Isotopes to trace the origins and composition of the groundwater system; and
- Dry-fall and rock core chloride measurements.

A number of recent activities have been performed to support the groundwater remedial investigation project at SSFL as outlined in the Work Plan, Site-wide Groundwater Characterization (MWH, 2008a), that was approved by DTSC (2009). Consistent with the site-wide work plan, the following work has been performed:

- Installation, purging, monitoring and sampling of four multilevel monitoring systems;
- Installation of a corehole to a depth of 1,400 feet and analysis of hundreds of rock core samples for VOCs;
- Completion of three plume transect coreholes off the northeast perimeter of SSFL and the analysis of hundreds of rock core samples for VOCs and the installation of multilevel monitoring systems;
- Hydraulic conductivity profiling, borehole geophysical logging, high-resolution fluid temperature logging, and analysis of rock core samples for chloride;
- Field and laboratory TCE degradation studies, including collection of samples from wells for dissolved gases; and
- Seeps sampling and analysis.

Further work beyond that described in the site-wide work plan was also performed to either fill data gaps identified during review of the available data (consistent with the approach presented in the site-wide work plan) or to further reduce uncertainties related to the characterization of groundwater at SSFL. This additional work included:

- Field mapping of the geology in the southern undeveloped land area of SSFL and in off-site areas to the north and east, including the mapping of joints observed in surface outcrops across the site;
- Integration of fracture surface mapping and borehole geophysical fracture analysis results;
- Installation of 34 piezometers to evaluate the occurrence of groundwater within Areas II, III and IV of SSFL;
- Collection and analysis of samples from on- and off-site monitoring wells for additional geochemical characterization;
- Optimization and uncertainty evaluation of the 3-dimensional groundwater flow model using parameter estimation techniques;

- Collection of groundwater samples to complete the characterization of the transport pathway from surficial media to groundwater;
- Reporting of rock core sampling and analyses results from shallow piezometers; and
- Reporting of well and corehole installation and sampling results from groundwater characterization work to fill radiological data gaps.

This recent work, performed mostly since early 2008, supplements the large body of work previously performed. The quantity and quality of the data that have been collected at SSFL throughout its history are robust and may be unprecedented in regards to the characterization of a sedimentary rock aquifer contaminated with industrial chemicals. These data have formed the basis of the current understanding of the hydrogeologic system, the nature and extent and transport and fate of chemical and radiological constituents, and the impacts to the site vadose zone bedrock and groundwater.

## **10.2 PHYSICAL SETTING**

The SSFL occupies approximately 2,850 acres of hilly terrain that expresses approximately 1,100 feet of topographic relief near the crest of the Simi Hills. The highest surface elevation at SSFL occurs near the center of the site at an approximate elevation of 2,245 feet msl. The highest surface elevations at SSFL occur along two general ridges that trend northeast-southwest. The Simi Valley lies north-northwest of SSFL about 800 feet below, and the western edge of the San Fernando Valley lies to the east about 900 feet below.

Climate at SSFL and surrounding area is Mediterranean. Precipitation at SSFL is normally in the form of rain, although snow has occasionally fallen during winter months. Precipitation at SSFL has averaged approximately 18.5 in/yr between 1960 and 2008, varying over a broad range (minimum of 6.15 (2007) and maximum of 41.24 in/yr (1998)).

Most surface water that collects and drains at SSFL is intermittent and is conveyed off-site via one of four drainages: the Northwestern drainage, the Northern drainage, the Happy Valley drainage, and the Bell Creek drainage, the last of which drains about 60% of SSFL land surface. Operational discharges of water, which have now ceased, have historically occurred within the central portion of SSFL in the Bell Creek drainage.

### 10.3 GEOLOGY

SSFL is located in the Western Transverse Ranges physiographic province of southern California. The province's geology and physiography reflects at least 70 million years of earth history. The sedimentary rocks in the portion encompassing SSFL range from coarse-grained conglomerates and sandstones to fine-grained siltstones and shales. This geologic history is reflected in multiple fold, fault and fracture orientations in the vicinity of SSFL.

Underlying much of the province and exposed across most of SSFL is the Chatsworth Formation, a turbidic sandstone with interbedded shale, siltstone and conglomerate approximately 6,000 feet thick and more than 65 million years old. As a result of geologic folding, the Chatsworth Formation dips moderately to the northwest at SSFL, along the southern limb of the Simi Valley syncline.

By conducting detailed geologic mapping at the site and surrounding area to refine published geologic maps, the Chatsworth Formation at SSFL has been subdivided into upper and lower units. The lower unit is exposed in southeastern SSFL and dips to the northwest beneath the remainder of the site. The upper Chatsworth Formation is exposed across much of the remainder of the site. Numerous steeply dipping to near-vertical faults have off-set site stratigraphy. Fault gouge and fracturing ancillary to faults are observable at some locations.

The Chatsworth Formation contains a ubiquitous fracture network consisting of a systematic arrangement of bedding-parallel fractures and bedding-perpendicular fractures (joints). Variations in the mechanical properties of the rock as a function of composition, compaction and cementation result in local variations in fracture character and density. Joints typically cross the full thickness of one or several sandstone beds, often terminating at the contact with shale beds. Joints extending fully across thick shale units are less common.

Unconsolidated deposits at SSFL include alluvium, artificial fill and thin soils over bedrock. The alluvium generally consists of silty sand and occurs in topographic lows and along ephemeral drainages. These deposits are typically 1 to 15 feet thick but range to more than 30 feet thick.

Areas with five or more feet of alluvium cover more than 300 acres of SSFL, or about 11 percent of the site.

#### **10.4 HYDROGEOLOGY**

The SSFL's geologic framework and its hydraulic properties provide the template within which the 3-dimensional groundwater system is recharged, stored, moves and discharges.

For purposes of this investigation, the boundaries of the mountain groundwater system encompassing SSFL are considered to include the water table present under the site and surrounding area, groundwater discharge locations focused at hillside seeps and stands of phreatophytes located in surrounding canyons, and at lateral outflow boundaries present at depth where the Simi Hills meet the floor of Simi and San Fernando valleys. The potential for subsurface groundwater outflow (lateral outflow boundaries) exists along the entire mountain perimeter except due west of SSFL where the boundary is approximately parallel to inferred directions of groundwater flow (no boundary flux would occur). These lateral boundaries encompass an area of 20 square miles, of which SSFL occupies approximately 22 percent.

Historical and ongoing groundwater production from SSFL wells demonstrates that portions of the Chatsworth Formation comprise locally productive aquifer units. These units generally consist of the fractured sandstone members of the upper Chatsworth Formation, many of which are up to several hundred feet thick. Separating the major sandstone units are a series of relatively thin shale and siltstone members, some of which behave as aquitards. Properties relevant to the aquifer and aquitard characteristics include lithologic heterogeneity, thickness and lateral continuity, type and degree of cementation, geologic structures, matrix porosity, and the effective porosity and interconnection of fractures.

Faults influence the hydrogeologic structure in several ways including off-setting or truncating permeable zones and fractures, juxtaposing of different units and fold orientations, the creation of low-permeability boundaries formed along fault planes, and likely discontinuous zones of enhanced permeability from fracturing along the fault core and within adjacent damage zones. Major faults subdivide SSFL into roughly ten large blocks. These are further subdivided by

shale beds. In addition, the Chatsworth Formation contains a systematic network of bedding-parallel and bedding-perpendicular fractures that result in a hydraulic continuum of groundwater flow through all parts of the system.

The physics of groundwater occurrence, storage, and movement are controlled by hydrogeologic properties that include porosity, hydraulic conductivity, and storage coefficients. The bulk porosity of the Chatsworth Formation includes the affects of the effective porosity of the rock matrix (~14 percent) and the bulk fracture porosity, which is several orders of magnitude smaller (~0.01 percent). Each type of porosity has particular significance with regard to groundwater storage, movement, hydrochemistry, and solute transport and fate.

The small magnitude of bulk fracture porosity estimated for the Chatsworth Formation indicates that fractures contribute little to the total rock porosity. However, several lines of evidence indicate that fractures form a well interconnected network where active groundwater flow can occur.

The bulk hydraulic conductivity of fractured Chatsworth Formation sandstone is generally several orders of magnitude greater than the hydraulic conductivity of the unfractured sandstone matrix. Compared to “textbook” ranges of bulk hydraulic conductivity for indurated sandstones and estimates reported in the literature, the estimated bulk hydraulic conductivity for SSFL may be described as low to moderate. As a result of increased overburden pressures, the bulk hydraulic conductivity is estimated to decrease with depth and eventually approach the matrix hydraulic conductivity; however, this trend varies locally.

## **10.5 CHEMICAL NATURE AND EXTENT**

Work performed on the surficial media operable unit at SSFL has resulted in the identification of the chemicals used and released into the environment. With the approval and oversight of DTSC, known or potential releases of chemicals at SSFL have been characterized using appropriate methods. Remedial investigation reports have been issued for the 11 Group reporting areas. Results from these reports were reviewed and evaluated using additional groundwater sampling results to confirm or update similar information presented in the surficial media RI reports. The

results from these reports were used in identifying and evaluating sources of releases of COC's to the bedrock vadose zone and groundwater. Surficial media sampling results are depicted on plates that have been developed to evaluate groundwater characterization as appropriate.

### **10.5.1 Bedrock Vadose Zone**

TCE is the primary contaminant of concern both in terms of the magnitude of measured concentrations and the frequency of detections found in the analysis of rock core vadose zone samples. TCE was detected in 61 percent of the vadose zone samples analyzed. The equivalent TCE mass in the vadose zone relative to the mass below the water table at a release site also varies considerably ranging from a low of 1 percent (C6, Delta RI site) to a high of 95 percent (C8, FSDL RI site). Various factors affect the characterization of contaminant distributions: the total completion depth of the coreholes, thickness of the vadose zone, distance from the input location, total mass released into the ground, and the degree of penetration of immiscible phase TCE below the water table.

### **10.5.2 Groundwater**

Two broad areas of impacted groundwater, defined as that containing concentrations of chemicals exceeding screening values, have been identified in SSFL groundwater: an area encompassing about 247 acres along the eastern portion of SSFL, and a second area encompassing about 470 acres in the central and western part of SSFL. Four other areas have been identified totaling about 15 acres and ranging in size from 0.8 to 8.9 acres. One area extends off-site to the northeast of SSFL and groundwater periodically emerges at the ground surface in another area in the southwest portion of SSFL along the Burro Flats fault. The total area of impacted groundwater is about 732 acres. Fifty-two different chemicals are contained within these areas. Consistent with site operations, immiscible-phase kerosene-range hydrocarbons were also found on the water table at two monitoring locations, one at the Alfa RI site and the other at the Canyon RI site.

The vertical extent of chemicals has been defined based on results of collection and analysis of samples from monitoring well clusters and from bedrock core. A summary assessment of the

vertical extent for the 18 chemicals that were detected at more than five locations across SSFL shows that the total vertical extent of groundwater contamination has not been defined at certain locations when concentrations below screening levels are used to define the vertical contaminant extent. However, concentrations at the deepest well within these clusters are typically only a factor of 1 or 2 above the screening levels indicating that the plume extent is being approached.

## **10.6 RADIOLOGICAL NATURE AND EXTENT**

The clean-up of radiological facilities in SSFL Area IV has also involved the identification and excavation/removal of radiological impacts to surficial media. Documents and materials were reviewed to identify the locations of excavations that have been conducted for this clean-up. These locations are considered potential sources of radioactivity and radionuclides to vadose zone bedrock and groundwater. Thirty-five (35) different excavations were identified.

A data gaps analysis of potential groundwater impacts was performed in 2004 and 14 groundwater monitoring wells and 2 coreholes were installed in response. The data gaps work resulted in the identification and characterization of an area of groundwater impacted with tritium at concentrations above the 20,000 pCi/L screening level that includes 4 wells (RD-88, RD-90, RD-93 and RD-95). The area of impact covers about 4.4 acres and extends about 300 feet or so from the suspected release location. No other radionuclides have been found at concentrations above screening levels in samples collected from the well network. However, detections of <sup>90</sup>Strontium have persisted at the well where it was detected (RD-98), indicating that it is present in groundwater, although at concentrations below the 8 pCi/L screening level. Additional sampling of the existing well network should be conducted to evaluate the potential occurrence of seven potentially site-related radionuclides for which the groundwater has not been characterized, should future surficial media sample collection and analysis show them to be present in surficial media.

## **10.7 TRANSPORT AND FATE**

Transport evaluations based on-site data and analytical and numerical models indicate the following:

- The transport of metals from anthropogenic sources in alluvium groundwater is strongly retarded with the smallest retardation factor being 14 (boron) leading to very short transport distances (i.e. less than 10 m).
- Coupled TCE vadose zone- and DNAPL-sources do not show discernable differences in either the lateral or vertical extent of groundwater plumes relative to a DNAPL-only source. For a TCE vadose zone-only source, the overall extent of a groundwater plume is not appreciably different when the source is continuously present for either 50 or 100 years. This is attributed to the fact that mass transfer to the saturated rock matrix started decades ago after initial releases and continued for the last 50 years or so. Nearly all the mass resides in the saturated rock matrix where its further transport is diffusion-controlled.
- TCE DNAPL completely dissolves in nearly all fractures within 10s of years after it entered the subsurface and this is consistent with field sampling results.
- Extents of the various contaminants found in groundwater based on field data, including source and plume transects and longsects, are consistent with the ranges predicted by the DFN simulations
- Slow rates of contaminant degradation can cause additional plume front retardation and appreciably contribute to the overall attenuation of the contaminant plume. Field data indicate conditions for degradation or decay exist at SSFL. Degradation rates with half-lives ranging between 5 and 20 years can cause plume fronts to retreat and collapse within a few hundred years (or sooner).
- Further field characterization is warranted to evaluate potential contaminant transport as presented in Section 8.8.

Fate evaluations were conducted by evaluating field and laboratory data including conventional groundwater samples, and special studies, and were coupled with fate information contained in the scientific literature. The evaluations using site data show that microbially-mediated complete dechlorination of chlorinated ethenes is occurring at SSFL. The reductive dechlorination observed is consistent with cometabolism by sulphate-, iron-reducing, or methanogenic bacteria present within the Chatsworth Formation. Field and laboratory results also show the complete mineralization of TCE and cDCE due to abiotic reactions with ferric and ferrous oxides and oxyhydroxides found in the rock matrix. The redox conditions are also consistent with reductive dechlorination of other chlorinated solvents used at SSFL. Field results show the abiotic transformation of 1,1,1-TCA. A literature review of perchlorate biodegradation concludes that the potential for biodegradation exists in SSFL groundwater via autotrophic organisms, although the transformation rates will be slow and limited by the supply of electron donor. Tritium's fate is controlled by its relatively short radioactive half-life (12.4 years). Although tritium is the only

radionuclide that has been found in groundwater at SSFL above screening levels, other radionuclides were historically found in soil at SSFL and remediated. As sampling results from the existing well network and seeps have not shown other radionuclides to be present in groundwater above screening levels, their fate is not addressed in this report.

## **10.8 IMPACT ASSESSMENT**

Human health and ecological risk assessments were conducted for groundwater during preparation of surficial media RI site and group reports. For hypothetical on-site receptors, both cancer and non-cancer endpoints were characterized in the risk assessments for both indirect (i.e., exposure by inhalation of VOCs transported from groundwater) and direct exposure pathways (i.e., use and exposure to groundwater by consumption and other direct contact pathways). Groundwater below portions of SSFL is impacted with contaminants with calculated Incremental Lifetime Cancer Risk and Hazard Index values that exceed regulatory guidance. It is anticipated a groundwater use prohibition will be imposed on the site to restrict access to groundwater in perpetuity, thus controlling drinking water and other direct exposure pathways.

For off-site receptors, the preponderance of site data supports the conclusion that it is not scientifically plausible for contaminants to migrate to wells in outlying communities at concentrations that may cause human and ecological impacts.

## **10.9 CONCLUSIONS**

The groundwater remedial investigation at SSFL has been guided by eight decision questions developed through the data quality objective process as described in Section 2.8. The decision questions were formed based on review of the substantial body of site data available in 2000. Subsequent work plans were prepared to address those decision questions and supplemental field data were collected. This groundwater RI report presents site data and its interpretation as related to the characterization of groundwater contamination at SSFL.

### 10.9.1 Decision Questions

The decision questions are presented below, with a summary of how each has been addressed in this RI report.

1. *Is the subsurface mass of chemicals present consistent with the estimated mass of TCE that may have been released and consistent with the conceptual site model (i.e. highest concentrations adjacent to the input locations)?*

The estimate of subsurface mass of chemicals present at SSFL is consistent with estimates of the mass of chemicals released at the identified source areas within the bounds of uncertainty. Rock core data have defined detailed TCE and other VOC concentration profiles at nine DNAPL sources areas. Based on these profiles the total estimated in situ mass was computed by using reasonable assumptions of the source area volume (a cylindrical volume centered on each corehole). Rock core sampling results support the conclusion that the bulk of the infiltrated VOC mass remains at or near DNAPL input locations. The majority of TCE and other VOC mass are stored in low permeability porous sandstone underlying former input locations. There are no formal estimates of how much mass of other COC's entered the subsurface and therefore, comparisons cannot be made between inputs and present day *in situ* estimates of mass (based on groundwater sampling and core analyses). However, as with the TCE, the rock core taken at source areas show perchlorate and tritium have also diffused into the low K rock matrix. As with the TCE and other VOC compounds, this process has limited the distance of contaminant from input locations.

2. *Has the maximum depth-of-penetration of COCs been characterized?*

The characterization of the maximum depth of penetration of the COC's is considered sufficient to assess the contaminant transport, fate, and impacts of the COC's on potential receptors. The maximum depth of penetration of COC's at SSFL has been assessed in two different contexts by: 1) examining concentrations of COC's versus depth from vertical well sampling results, and 2) calculating the mean equivalent rock porewater concentration over the bottom 50 ft of various coreholes. These results were compared to groundwater screening values to characterize the vertical extent of COC impacts.

3. *Does the presence of COCs in the unsaturated portions of the Chatsworth Formation contribute to the further migration of the plume fronts?*

Formation of all of the contaminant plumes in the Chatsworth Formation was initiated decades ago due to contaminant migration through the unsaturated zone into the groundwater zone and the contributions today from the unsaturated zone are currently too small to be influential. The contaminant mass that governs plume front behavior today is the accumulated mass over decades now present in the groundwater zone. The positions of plume fronts today, after many years of groundwater transport, are no longer appreciably influenced by contaminant mass remaining in the unsaturated zone because the annual contribution of mass from this zone is very small relative to the mass already residing in the bedrock groundwater. Field observations and mathematical modeling indicate that the plume fronts today are stationary (or nearly so) due to the combined effects of matrix diffusion, sorption, transverse dispersion, and, in many cases, degradation or decay.

4. *Has the three-dimensional flow of groundwater been defined such that the direction of COC solute transport can be predicted?*

Understanding of the complex 3-dimensional groundwater flow system has been defined through the integration of spatial and temporal site field data into a calibrated and optimized flow model. The nature of the 3-dimensional groundwater flow system is supported by multiple lines of evidence including (i) more than a thousand spatial groundwater hydraulic head values; (ii) a hydrogeologic framework developed from intensive geologic mapping, core inspections, and borehole geophysics; (iii) a comprehensive seeps inventory, (iv) and geochemical analyses interpretations including the distribution and concentrations of atmospheric tritium and carbon-14. The 3-dimensional groundwater model was based on detailed analyses of the geological framework of the SSFL site and surrounding area. Site stratigraphy and structures were incorporated into the hydrogeologic framework. Once this model structure was examined, tested and calibrated, the framework was parameterized based on thousands of field-based hydrologic data sets. Numerical methods solved basic groundwater flow equations and the 3-dimensional flow system was simulated. Groundwater movement is driven principally by local and regional recharge and historical site operations. Results of this modeling effort provide insight as to the key physical and hydrological components influencing groundwater movement

under natural, highly stressed and periods of groundwater recovery at SSFL. These modeling efforts provide a 3-dimensional framework within which more sophisticated discrete fracture and porous block groundwater modeling tools were formulated to represent the transport and fate of site COC's.

5. *Has the migration of COC solute at the plume front become effectively stable relative to a concentration threshold?*

Based on groundwater concentrations obtained from site monitoring wells over many years monitored COC plumes within the Chatsworth Formation are stable and plume fronts are stable (i.e., stationary). Plume fronts are defined as the location, in the direction of groundwater flow away from the contaminant input locations (source area), where the concentrations at the periphery of the plume are at regulatory limits for drinking water (i.e. the MCL or other screening values). For example the MCL for TCE is 5 µg/L, perchlorate 6 µg/L, and tritium 20,000 pCi/L. In some instances a plume front may change only very slowly over time and for practical purposes is considered a stable plume. Stationary plumes occur at SSFL because the processes causing advective transport of a contaminant are counteracted by other physical and geochemical processes, such as diffusion into the rock matrix, transverse dispersion, sorption, and degradation.

6. *Does the current groundwater monitoring program adequately characterize the temporal and spatial variability of COC solute?*

The temporal and spatial variability of COCs in groundwater have been characterized through the groundwater monitoring program that includes data from wells and seeps, source area characterization, and numerical modeling. Analyses of the source locations, vertical extent of contaminants, and the local transient groundwater flow system at each source area, in concert with the location and construction data of monitoring wells, were used to assess whether the presence and migration of contaminants were likely to be observed by the existing monitoring network. Site-wide and for most source locations, plumes are adequately monitored by the current observation well network. However, opportunities to improve the network have been identified as data gaps in a few areas and are described in subsequent sections.

7. *Have the attenuation effects of dispersion and biodegradation been considered and quantified?*

The effects of COC dispersion and degradation have been investigated through the collection and interpretation of field data and laboratory studies. Field data confirm the presence of a ubiquitous interconnected fracture network that enables transverse dispersion of COCs. Detection of COCs in monitoring wells with discrete sampling devices, short screened sections, and completed as open boreholes provide evidence that contaminant dispersion is occurring. Dispersion results from an extensive and dense interconnected fracture network at SSFL. Hydrodynamic dispersion contributes to plume attenuation through spreading of the mass throughout a larger volume of rock matrix. Transverse dispersion produces plumes in fractured sedimentary rock (i.e., Chatsworth Formation) that are monitorable by conventional means and quantifiable by numerical methods.

Geochemical and microbiological investigations at SSFL provide evidence of degradation of chlorinated solvents through abiotic and biotic processes. The degradation of many of the other COCs is known to occur under conditions that exist at SSFL. Radionuclides have documented half-lives that quantify their decay rates. Although degradation in the field is difficult to quantify, its occurrence at SSFL increases the degree of plume attenuation.

8. *Is restoration of the Chatsworth Formation groundwater technically practicable?*

This Groundwater Remedial Investigation report presents the substantial body of conventional and high-resolution field data that have been collected and interpreted to characterize groundwater beneath SSFL. The characterization confirms that consideration of any remedial technology must address the fact that at SSFL the majority of the mass resides in the low permeability rock matrix. Such considerations have been made and are presented in the Feasibility Study Work Plan (MWH, 2009d) and Treatability Study Work Plans (MWH, 2009e). The technical practicability of restoration of the Chatsworth Formation groundwater will be evaluated in the site Feasibility Study.

### 10.9.2 Data Gaps

The following is a summary of data gaps which have been previously described in sections 6 through 8 of this report. Data gaps will be addressed in a sampling and analysis plan scheduled for submittal in 2010.

Analysis of surficial media characterization results for the CTL-V, Area I Burn Pit and Coca RI sites indicates these sources have not been characterized for potential impacts to bedrock groundwater, primarily from VOCs. Groundwater flow path analyses for CTL-V and Area I Burn Pit RI sites indicate that the position of existing monitoring wells may not intercept groundwater flowing through a portion of these sites. Any identified impacts to groundwater beneath CTL-V or Area I Burn Pit sites should be characterized through collection of additional data. Groundwater flow path analyses from the Coca RI site indicates that existing wells are positioned such that groundwater flowing from this area is monitored.

The former pond at the SRE RI site is recommended for further characterization based on historical use of the pond, its proximity to the northern property boundary, and groundwater flow path and Darcy flux analyses. Should impacts to bedrock groundwater be identified, their extent should be characterized.

Collection and analysis of samples from select wells within the groundwater monitoring network for a specified set of target analytes should also be conducted to confirm their vertical and/or lateral extent. Locations and target analytes will be specified in the sampling and analysis plan to be submitted in mid-April 2010.

Additional characterization of the extent of VOC impacts at the ELV RI site is warranted. Characterization of contaminant transport by combining the results from the 3-dimensional groundwater flow model with 2-dimensional discrete-fracture network transport simulations indicate that the position of existing monitoring wells may not intercept groundwater flowing through this site. Characterization results presented in this report show that this area is characterized by higher Darcy fluxes due to projected steep gradients along simulated 3-dimensional flow paths. This condition, coupled with ELV's proximity to the northern property border, warrants further characterization of potential impacts to the bedrock groundwater.

The distribution of monitoring wells and hydraulic testing are insufficient for demonstrating the effect of the Burro Flats Fault and the Happy Valley Fault (east of RD-10) on groundwater levels and flow. Furthermore, insights into the groundwater flow system gained from the 3-dimensional groundwater flow model indicate that evaluation of two faults in the northwest portion of SSFL is warranted (i.e. FSDF structures). Flow model optimization represents these features as more conductive than the surrounding bedrock, which makes them unique in their hydraulic character relative to the field data and the flow model's characterization of the remaining faults at SSFL.

Seeps around the perimeter of SSFL should be sampled and analyzed for VOCs to confirm the absence of impacts to off-site receptors.

### 10.9.3 Key Conclusions

Analysis of available site data supports the following conclusions:

- Groundwater flow paths from site sources to off-site exposure points are long (i.e. typically >1,000 meters), and contaminant transport distances are short relative to the average linear groundwater velocity.
- Chemical and radiological constituents that entered the groundwater at SSFL remain within the local groundwater and sandstone matrix, extending only a few hundred to a few thousand feet from former input locations.
- Contaminant transport has been influenced by sorption to aquifer solids, diffusion from the fracture network into the nearly immobile porewater in the rock matrix, biological and abiotic transformations, and/or radioactive decay.
- Transport of chemicals and radionuclides by groundwater flow in the fracture network and diffusion into the rock matrix creates plumes that are identifiable and detectable using monitoring wells and/or seeps.
- Nearly all groundwater contaminant mass resides in the low permeability rock matrix blocks between fractures local to where the contaminants entered the ground.
- Contaminant plumes are generally stable and plume fronts are generally stationary.
- TCE is the chemical detected at the highest concentration relative to a regulatory threshold, is detected most frequently, and comprises the vast majority of impacts to groundwater beneath SSFL.
- Contaminant impacts to groundwater have been identified on-site and off-site at concentrations that exceed drinking water standards, as defined in agency regulations. It

is anticipated a groundwater use prohibition will be imposed on the site to restrict access to groundwater in perpetuity, thus controlling drinking water and other direct exposure pathways.

- Application of standard risk assessment protocols confirms that hypothetical on-site receptors inhaling volatiles from shallow groundwater beneath former release locations at SSFL show both cancer- and non-cancer endpoints above the acceptable risk range as defined in agency regulations.
- The preponderance of site data supports the conclusion that it is not scientifically plausible for contaminants to migrate to wells in outlying communities at concentrations that may cause human and ecological impacts.
- Groundwater characterization is sufficient for the preparation of feasibility and treatability studies.

This groundwater remedial investigation report confirms the nature and extent of contamination in groundwater beneath SSFL have been characterized at nearly all locations, the transport and fate of contaminants in groundwater are well understood, the nature of groundwater plumes are defined and monitorable, and the Site Conceptual Model (Cherry, McWhorter, and Parker, 2009) is a valid tool for guiding site risk management decisions.

## **10.10 ACKNOWLEDGEMENTS**

Many individuals have contributed to the preparation of this report. Names, qualifications and roles of principal contributors are provided in Table 10-1. The guidance, direction and thought of Professors John Cherry (Emeritus), Dave McWhorter (Emeritus), Beth Parker and Bill Woessner are greatly appreciated. In addition to the remaining contributors identified in Table 10-1, the contributions of Cheryl Yee, Jackie Zipp, Elaine Smith, Mike Luebke, Drew Lassen, Krissi McIlvenna, Sarah Oh, Jasmine Leehang-Austin, Cathy Henderson, and Jason Dioguardi at MWH in the preparation and production of this report are also greatly appreciated.

## 11.0 REFERENCES

- AMEC Earth and Environmental, 2003a. Standardized Risk Assessment Methodology Work Plan, Surficial Operable Unit, Revision 1, Santa Susana Field Laboratory, Ventura County California. April.
- AMEC, 2003b. Addendum to the Biological Conditions Report, Santa Susana Field Laboratory, Ventura County, California. July. Included as Appendix G in SRAM Work Plan, Revision 7, Draft by AMEC (2003a).
- Antonelli, M A. and Aydin, 1994. Effect of Faulting on Fluid Flow in Porous Sandstones: Petrophysical Properties. American Association of Petroleum Geologists Bulletin, Vol. 78, No.3, pp-355-377.
- AquaResource, Inc/MWH. 2007. Three-Dimensional Groundwater Flow Model Report, Santa Susana Field Laboratory, Ventura County, CA. November.
- Atomics International (AI), 1974. Letter from W.F. Heine to R.L. Westby, U.S. Atomic Energy Commission, Water Samples from SRE Was Cell Valve Pit and Shallow Surveillance Wells. March 14. (HDMSe00024571)
- AI, 1977a. Letter from R.J. Tuttle to Calvin D. Jackson, Energy Research and Development Administration regarding Leakage of Radioactively Contaminated Water at SRE. August 23. (HDMSe00024494)
- AI, 1977b. Letter from R.J. Tuttle to Calvin D. Jackson, Energy Research and Development Administration, regarding Leakage of Radioactively Contaminated Water at SRE-Final Report. October 25. (HDMSe00024498)
- Atwater, T., 1998. Plate Tectonic History of Southern California with Emphasis on the Western Transverse Ranges and Santa Rosa Island. in Weigand, P. W., ed., Contributions to the Geology of the Northern Channel Islands, Southern California. American Association of Petroleum Geologists, Pacific Section, MP 45, pp. 1-8.
- Beak Environmental, 1997. Evaluation of Intrinsic Biodegradation of Chlorinated VOCs in Groundwater at the Environmental Chemistry Laboratory. October.
- The Boeing Company (Boeing), 1998. Building 64 Side Yard Core Sampling Plan. March 6. HDMSe00022461.
- Boeing, 1999a. Area 4064, Final Status Survey Report. April 13.
- Boeing, 1999b. Final Report, Decontamination & Decommissioning of Fuel Storage Facility, 4064. September 11. HDMSe00022472
- Boeing, 1999c. 17th Street Drainage Area, Final Status Survey. October 7. HDMSp00131444.
- Boeing, 2000a. Operations Report for 17th Street Decontamination. August 28.
- Boeing, 2000b. 17th Street Drainage Area, Final Status Survey. September 19. HDMSp00131444.

- Boeing, 2001a. Hot Laboratory Decontamination and Dismantlement Final Report. November 27. HDMSP00012823.
- Boeing, 2001b. Letter from Phil Rutherford, Boeing, to Stephen Hsu, DTSC, regarding: Request for Approval to Ship from SRE to a Landfill. September 25.
- Boeing, 2003. Grid S19/T19 Interim Soil Remediation. November 19, 2003. HDMSe00731642.
- Boeing, 2004. Site Environmental Report for Calendar Year 2003 DOE Operations at the Boeing Company, Rocketdyne Propulsion and Power. September. HDMSP00079
- Boeing, 2006a. Email from Philip D. Rutherford to Daniel M. Trippeda regarding RMHF Slope. April 24. HDMSP00038287.
- Boeing, 2006b. Internal Letter from Phil Rutherford and Dan Trippeda to Brian Sujata regarding Contract DE-AC03-99SF21530 – RMHF Slope Remediation. June 9. HDMSP00038299.
- Boeing, 2007. Personal communication between Wonnie Kim, MWH and P. Rutherford, Boeing, regarding: Building 4064 Excavations.
- Boeing, 2009. Phil Rutherford Comments on Draft Building 4133 RFI Report Site History Text. May 15, 2009. HDMSe00731422.
- Boeing, 2008. Letter to Mr. James Pappas, DTSC from David Dassler, Boeing requesting approval of modifications to corehole location C-13. October 19.
- Bradley, Paul M & Francis H. Chapelle, 2002. Microbial Mineralization of Ethene Under Sulfate-Reducing Conditions. Bioremediation Journal 6 (1): 1-8.
- Cabrera Services (Cabrera), 2006. Final Status and Survey Report: Characterization and Final Status Survey Radioactive Materials Handling Facility Perimeter, Santa Susana Field Laboratory, Ventura County. March. HDMSE00714226.
- Cabrera, 2007. Characterization and Final Status Survey Radioactive Materials Handling Facility Holdup Pond (Site 4614). March. HDMSE00714288.
- Caine, J.S., Evans, J.P., and Forster, C.B., 1996. Fault Zone Architecture and Permeability Structure. Geology, v. 24, n. 11, pp. 1025-1028.
- Camp Dresser McKee (CDM), 2008. Draft Gap Analysis Report Prepared for SSFL Area IV Environmental Impact Statement. June 1.
- CH2MHill, 1993. Records Search and Trichloroethylene Assessment for Santa Susana Field Laboratory, Ventura County, CA. Technical Report, Volumes 1 and 2. June.
- CH2MHill, 2008. Draft Group 5 Central Portion of Areas III and IV RCRA Facility Investigation Report, Santa Susana Field Laboratory, Ventura County, California, November.
- CH2MHill, 2009a. Draft Group 10 Remedial Investigation Report at the Santa Susana Field Laboratory, Ventura County, California. March.
- CH2MHill, 2009b. Draft Group 1B Remedial Investigation Report at the Santa Susana Field Laboratory, Ventura County, California. September.

- Chappelle, F. H., D. A. Vroblesky, J. C. Woodward and D. R. Lovely, 1999. Practice Considerations for Measuring Hydrogen Concentrations in Groundwater, *Environmental Science and Technology*, Vol. 31, No. 10.
- Chappelle, Frances H., 2001. *Ground-water Microbiology and Geochemistry*, Second Edition. John Wiley and Sons, 477 pp.
- Cherry, John A., David B. McWhorter and Beth L. Parker (SSFL Groundwater Advisory Panel), 2009. Site Conceptual Model for the Migration and Fate of Contaminants in Groundwater at the Santa Susana Field Laboratory, Simi, California (Draft). Volumes I through IV. In Association with the University of Guelph, Montgomery Watson Harza, Haley & Aldrich and AquaResource Inc. December.
- Clark, Ian and Peter Fritz, 1997. *Environmental Isotopes in Hydrogeology*, 2nd printing, 1999, CRC Press. 328 pp.
- Darlington, R., 2008. Laboratory Evaluation of Chlorinated Ethene Transformation Processes in Fractured Sandstone, Ph.D. Dissertation, Clemson University. May.
- deBest, J.H., A. Hage, H.J. Doddema, D.B. Jansen and W. Harder, 1999. Complete Transformation of 1,1,1-trichloroethane to Chloroethane by a Methanogenic Mixed Population. *Appl. Microbiol. Biotechnol.* 51: 277-283
- Department of Toxic Substances Control (DTSC), 1995a. Hazardous Waste Facility Post-Closure Permits, Permit Numbers PC-94/95-3-02 and PC 94/92 3 03, Permits for Areas I and III and Area II, respectively, effective 11 May 1995.
- DTSC, 1999. Letter from Jim Pappas, DTSC, to Dave Dassler, Boeing regarding Operable Unit Formalization, Standardized Risk Assessment Methodology Work Plan, Santa Susana Field Laboratory, Ventura County, California. November 2.
- DTSC, 2003. Temporary Authorization for The Boeing Company, Treatment of Corehole C-1 Effluent at WS-5 Treatment System, Santa Susana Field Laboratory, Area I, EPA ID CAD093365435. June 30.
- DTSC, 2005. Letter from Gerard Abrams to David Dassler, The Boeing Company. Approval of Northeast Area Chatsworth Formation Work Plan, Phase II, Santa Susana Field Laboratory, Ventura County, CA. November
- DTSC, 2007a. Consent Order for Corrective Action, Docket No. P3-07/08-003, In the Matter of Santa Susana Field Laboratory, Simi Hills, Ventura County, California. August.
- DTSC, 2007b. Letter from James M. Pappas to David Dassler, Boeing. Conditional Approval of the Work Plan for the Phase 2 Groundwater Site Conceptual Model, Santa Susana Field Laboratory, Ventura County, California, Dated April 2007. September 14.
- DTSC, 2007c. Letter from James M. Pappas to David Dassler, Boeing. Conditional Approval of the Work Plan for the Phase 3 Groundwater Site Conceptual Model, Santa Susana Field Laboratory, Ventura County, California, Dated June 2007. September 14.
- DTSC, 2008a. Group 4 RFI Report. Comment letter from T.M. Seckington/DTSC to G. Abrams/DTSC. October 15.

- DTSC, 2008b. Group 8 RFI Report. Comment letter from T.M. Seckington/DTSC to G. Abrams/DTSC. December 10.
- DTSC, 2009. Letter from Tom Seckington to Allen Elliott, NASA, Tom Gallacher, Boeing and Thomas Johnson, DOE, Conditional Approval of Work Plan, Site-Wide Groundwater Characterization Work Plan. June 2.
- DHI-WASY, 2009. FEFLOW® 5.4. Finite Element Subsurface Flow and Transport Simulation System
- Dibblee, T. W., 1992. Geologic Quadrangle Maps: Los Angeles and Ventura Counties, California. Dibblee Foundation Geologic Maps. (a) Moorpark Quadrangle; (b) Simi Quadrangle; (c) Santa Susana Quadrangle; (d) Oat Mountain Quadrangle; (e) Camarillo and Newbury Park Quadrangles; (f) Thousand Oaks Quadrangle; (g) Calabasas Quadrangle; (h) Canoga Park Quadrangle; (i) Point Mugu and Triunfo Pass Quadrangles; (j) Point Dume Quadrangle; (k) Malibu Beach Quadrangle; (l) Topanga Quadrangle
- Doherty, 2009. Manual and Addendum for PEST v.11.8, Model Independent Parameter Estimation, WATERMARK Numerical Computing, Brisbane, Australia.
- Edwards, H. E., Becker, A. D. Howell, J. A., 1993. Compartmentalization of an Aeolian Sandstone by Structural Heterogeneities: Permo-Triassic Hopeman Sandstone, Moray Firth, Scotland. From North, C.P. and Prosser, D. J. (eds), 1993 Characterization of Fluvial and Aeolian Reservoirs, Geologic Society of America Special Publication No 73, pp 339-365.
- Egli C, Scholtz R, Cook AM & Leisinter T, 1987. Anaerobic Dechlorination of Tetrachloromethane and 1,2-dichloroethane to degradable Products by Pure Cultures of Desulfobacterium sp. and Methanbacterium sp FEMS Microbiol, Lett. 43: 257-261.
- Egli C, Tschan T, Scholtz R, Cook AM & Leisinger T, 1988. Transformation of Tetrachloromethane to Dichloromethane and Carbon-dioxide by Acetobacterium Woodii. Appl. Environ. Microbiol. 54: 2819-2824.
- Energy Technology Engineering Center (ETEC), 1988. Radiological Survey of the ESG Salvage Yard (Old), Rocketdyne Barrel Storage Yard and New Salvage Yard (T583). August 22. HDMS00022327.
- ETEC, 1998. Building 64 Side Yard Core Sampling Plan. February 16. HDMS00022461.
- Environmental Protection Agency (EPA), 1988. Guidance for Conducting Remedial Investigations/Feasibility Studies Under CERCLA, Interim Final. EPA/540/G-89/004. October.
- EPA, 1994. Guidance for the Data Quality Objectives Process, EPA QA/G-4. September.
- Federal Register, 2000. Environmental Protection Agency, 40 CFR Parts 9, 141, and 142, National Primary Drinking Water Regulations; Radionuclides; Final Rule. Volume 65, Number 236, pp 76708-76753. December 7.
- Feenstra and Guiger, 1996. Chapter 7 in: Dense Chlorinated Solvents and other DNAPLs in Groundwater, James F. Pankow and John A. Cherry, Waterloo Press. 522 pp.

- Field, J.A. and Sierra-Alvarez, R., 2004. Biodegradation of Chlorinated Solvents and Related Chlorinated Aliphatic Compounds, *Environmental Science & Biotechnology* (2004) 3: 185-254.
- Forster, C.B., Goddard, J.V., and Evans, J.P., 1994, Permeability Structure of a Thrust Fault, in Hickman, S.H., Sibson, R., and Bruhn, R.L., eds., 1994, *Proceedings of Workshop LXIII The Mechanical Involvement of Fluids in Faulting*, 6-10 June, 1993, USGS open-file report 94-228, pp. 216-223.
- Foster, Stephen S.D., 1975. The Chalk Groundwater Tritium Anomaly – A Possible Explanation, *Journal of Hydrology*, 25: 159-165.
- Freedman, David L. and Darlington, Ramona, 2006. Laboratory Evaluation of In-Situ Chlorinated Ethene Removal in the Chatsworth Formation. June 14.
- Freedman, David L. and Gossett, James M, 1989. Biological Reductive Dechlorination of Tetrachloroethylene and Trichloroethylene to Ethylene under Methanogenic Conditions. *Applied and Environmental Microbiology*, p. 2144-2151, September.
- Gantzer, Charles J. and Lawrence P. Wackett, 1991. Reductive Dechlorination Catalyzed by Bacterial Transition-Metal Coenzymes, *Environmental Science and Technology*, Vol. 25, No. 4.
- Galli, R & McCarty PL, 1989. Biotransformation of 1,1,1-Trichloroethane, Trichloromethane and Tetrachloromethane by *Clostridium* sp. *Appl. Microbiol.* 55: 837-844.
- Golder Associates, Ltd, 1997. Matrix Diffusion Testing on Rock Core Samples, Rocketdyne Santa Susana Field Laboratory. May 15.
- Groundwater Resource Consultants, Inc. (GRC), 1987. Hydrogeologic Assessment Report, Volume I Santa Susana Field Laboratory, Rocketdyne Division, Rockwell International Corp. November 30.
- GRC, 1993. Results of Pilot Tracer Testing at Wells RD-9 & WS-SP, Rockwell International. Rocketdyne Division. Ventura County, California. August 16.
- GRC, 1995a. Sampling and Analysis Plan, Hazardous Waste Facility Post-Closure Permit PC-94/95-3-02, Area IV. June 5.
- GRC, 1995b. Sampling and Analysis Plan, Hazardous Waste Facility Post-Closure Permit PC-94/95-3-03, Areas I and III. June 5.
- GRC, 1996. Results of Pilot Tracer Testing at Wells RD-1 and RD-10, Rockwell International Corporation, Rocketdyne Division, Santa Susana Field Laboratory, Ventura County, California. March 28.
- GRC, 1997. Hydraulic Communication Study, Rockwell International Corporation, Rocketdyne Division, Santa Susana Field Laboratory, Ventura County, California. June 3.
- GRC, 1999. Results of Dewatering Operations at Construction Pit B/056, Area IV. July 23.
- GRC, 2000. Summary of Pre-1960 Historic Groundwater Levels and Well Pumping Test Data. February 7.

- Haley & Aldrich, Inc. 2000. Appendix B to Technical Memorandum, Conceptual Site Model, Movement of TCE in the Chatsworth Formation, Santa Susana Field Laboratory, Ventura County, CA (Montgomery Watson). April.
- Haley & Aldrich, 2004. Data Summary, Construction and Testing of Monitor Wells RD-75, RD-76, RD-77, RD-78 and RD-80, November and December 2003. Santa Susana Field Laboratory, Ventura County, California. June.
- Haley & Aldrich, 2007. Report on Annual Groundwater Monitoring, 2006. Santa Susana Field Laboratory, Ventura County, California. February.
- Haley & Aldrich, 2008. Report on Annual Groundwater Monitoring, 2007. Santa Susana Field Laboratory, Ventura County, California. February.
- Haley & Aldrich. 2009a. Report on Annual Groundwater Monitoring, 2008. Santa Susana Field Laboratory, Ventura County, California. February.
- Haley & Aldrich. 2009b. Report on Quarterly Groundwater Monitoring, First Quarter 2009, January through March 2009. Santa Susana Field Laboratory, Ventura County, California. May.
- Haley & Aldrich. 2009c. Report on Quarterly Groundwater Monitoring, Third Quarter 2009, July through September 2009. Santa Susana Field Laboratory, Ventura County, California. May.
- Hem, John D., 1992. Study and Interpretation of the Chemical Characteristics of Natural Water, 3rd Edition, U.S. Geological Survey Water-Supply Paper 2254
- Hurley, J.C., B.L. Parker and J.A. Cherry, 2007a. Source Zone Characterization at the Santa Susana Field Laboratory: Rock Core VOC Results for Coreholes C1-C7. Final. Department of Earth Sciences, University of Waterloo. June.
- Hurley, J.C., S.W. Chapman and B.L. Parker, 2007b. Rock Core VOC Results for Corehole C8, Source Zone Characterization at the Santa Susana Field Laboratory Addendum Report No. 1. Department of Earth Sciences, University of Waterloo. June.
- Hurley, J.C. and B.L. Parker, 2007c. Rock Core VOC Results for Corehole C9 (RD-84), Source Zone Characterization at the Santa Susana Field Laboratory Addendum Report No. 3. Department of Earth Sciences, University of Waterloo. June.
- ICF Kaiser Engineers (ICF), 1993a. Current Conditions Report and Draft RCRA Facility Investigation Work Plan, Areas I and III, Santa Susana Field Laboratory, Ventura County, California. October.
- ICF, 1993b. Current Conditions Report and Draft RCRA Facility Investigation Work Plan, Area II and Area I LOX Plant, Santa Susana Field Laboratory, Ventura County, California. October.
- ICF, 1993c. Current Conditions Report and Draft RCRA Facility Investigation Work Plan, Area IV, Santa Susana Field Laboratory, Ventura County, California. October. HDMS00011714, HDMS00011932, and HDMS00012436.

- Ingersoll, R.V., and Rumelhart, P.E., 1999. Three-stage evolution of the Los Angeles Basin, Southern California. *Geology*, v. 27, n. 7, pp. 593-596.
- Inter-Agency Agreement, 2009. Amendment 4, Radiological Characterization of Area IV at Santa Susana Field Laboratory, DE-AI30-08CC60036, United States Department of Energy and United States Environmental Protection Agency. April.
- Jackson, R. and V. Dwarakanath, 1999. Chlorinated Degreasing Solvents: Physical-Chemical Properties Affecting Aquifer Contamination and Remediation. *Applied and Environmental Microbiology*, 57 (4), 2039-2046.
- Killingsworth, 1958. Geologic and Hydrologic Survey of the Underground Water Conditions at PFL Facility, Santa Susana Mountains, California. June.
- Krone, UE, Thauer RK, Hogenkamp HPC & Steinbach K, 1991. Reductive Formation of Carbon-monoxide from CCl<sub>4</sub> and Freon-11, Freon-12 and Freon-13 Catalyzed by Corrinoids. *Biochem.* 30: 2713-2719.
- Ladeira, F.L., and Price, N.J., 1981. Relationship Between Fracture Spacing and Bed Thickness. *Journal of Structural Geology*, v. 3, pp. 179-183.
- Link, M. H., Squires, R. L, Colburn, I. P., 1981. Simi Hills Cretaceous Turbidites, Southern California, Field Trip Guidebook, Pacific Section of the Society of Economic Paleontologists and Mineralogists.
- Loomer, D., Al, T., and Parker, B.L., 2009, Mineralogical Characterization of Drill Core Samples from the Santa Susana Field Laboratory, Ventura County, California. Prepared for The Boeing Company, NASA, and USDOE. July.
- McCarty, Perry L, 1999. Biotic and Abiotic Transformations of Chlorinated Solvents in Ground Water, in Proceedings of the Symposium on Natural Attenuation of Chlorinated Organics in Ground Water, EPA/54/R-97/504. May.
- Montgomery, John H. Groundwater Chemicals Desk Reference, 1997.
- Montgomery Watson, 2000a. Conceptual Site Model, Movement of TCE in the Chatsworth Formation, Santa Susana Field Laboratory, April.
- Montgomery Watson. 2000b. Work Plan for Additional Field Investigations, Chatsworth Formation Operable Unit, Santa Susana Field Laboratory, Ventura County, California, October.
- Montgomery Watson Harza, Inc. (MWH) 2001. Work Plan for Additional Field Investigations, Revision 2.2, Former Sodium Disposal Facility, December.
- MWH, 2002a. Geologic Characterization of the Eastern Portion of the Santa Susana Field Laboratory, February, 2002.
- MWH, 2002b. Spring and Seep Sampling Work Plan. Santa Susana Field Laboratory, Ventura County, CA. March.
- MWH, 2002c. Technical Memorandum, Collection of Various Bedrock Properties Using Borehole Geophysical Logging Methods in the Eastern Portion of the Santa Susana Field Laboratory. June.

- MWH, 2002d. Technical Memorandum, Collection of Various Bedrock Properties Using Borehole Geophysical Logging Methods at the Former Sodium Disposal Facility. November.
- MWH, 2003a. RCRA Facility Investigation Work Plan Amendment, Area I and Area II Landfills Investigation Work Plan, SWMU 4.2 and SWMU 5.1, Santa Susana Field Laboratory, Ventura County California. Revised Final. October.
- MWH, 2003b. Near-Surface Groundwater Characterization Report, Santa Susana Field Laboratory, Ventura County, CA. November.
- MWH, 2003c. Analysis of Groundwater Recharge, Santa Susana Field Laboratory, Ventura County, California. December.
- MWH, 2003d. Perchlorate Characterization Work Plan (Revision 1). Santa Susana Field Laboratory, Ventura County, California. December, 2003.
- MWH, 2004a. Report of Results, Phase I of Northeast Investigation Area Groundwater Characterization, Santa Susana Field Laboratory, Ventura County, CA. Volumes I-III. July, 2004.
- MWH, 2004b. RCRA Facility Investigation Program Report. Santa Susana Field Laboratory, Ventura County, CA. July.
- MWH, 2005a. Revision 2, Standardized Risk Assessment Methodology (SRAM) Work Plan. Santa Susana Field Laboratory, Ventura County, California. September.
- MWH, 2005b. Northeast Area Chatsworth Formation Work Plan: Phase 2. Santa Susana Field Laboratory, Ventura County, CA. October.
- MWH, 2005c. Vapor Migration Modeling Validation Study Work Plan, Santa Susana Field Laboratory, Ventura County, CA. November.
- MWH, 2006a. Draft Report of Results Former Sodium Disposal Facility Groundwater Characterization, Santa Susana Field Laboratory, Ventura County, California, Appendix B RD-54B Pumping Test, February 2006.
- MWH, 2006b. Group 6 Northeastern Portion of Area IV, RCRA Facility Investigation Report, Santa Susana Field Laboratory, Ventura County. September. HDMS00150680, HDMS00151543, HDMS00154507, HDMS00156206, and HDMS00156302.
- MWH, 2007a. Phase 2 Groundwater Site Conceptual Model Work Plan, Santa Susana Field Laboratory, Ventura County, CA. June.
- MWH, 2007b. RCRA Facility Investigation Report, Vapor Migration Modeling Validation Study and VOC Surface Flux and Ambient Air Monitoring at the Former Liquid Oxygen Plant Site. Santa Susana Field Laboratory, Ventura County. July.
- MWH, 2007c. Phase 3 Groundwater Site Conceptual Model Work Plan, Santa Susana Field Laboratory, Ventura County, CA. July.
- MWH, 2007d. Group 4 Southern Portion of Area II, RCRA Facility Investigation Report, Santa Susana Field Laboratory, Ventura County. August.

- MWH, 2007e. Geologic Characterization of the Central Santa Susana Field Laboratory. August.
- MWH, 2007f. Group 8 Western Portion of Area IV, RCRA Facility Investigation Report, Santa Susana Field Laboratory, Ventura County. September.
- MWH, 2007g. Off-Site Data Evaluation Report, Santa Susana Field Laboratory, Ventura County, California. December.
- MWH, 2008a. Work Plan, Site-Wide Groundwater Characterization, Santa Susana Field Laboratory, Ventura County, CA. January.
- MWH, 2008b. Work Plan, Groundwater Interim Measures Addendum, Santa Susana Field Laboratory, Ventura County, CA. February.
- MWH, 2008c. Technical Memorandum, Attachments to Responses to DTSC's Questions on SSFL Vapor Migration Model Validation Study Report. August 27.
- MWH, 2009a. Work Plan (Revision 2), Groundwater Interim Measures Addendum, Santa Susana Field Laboratory, Ventura County, CA. January.
- MWH, 2009b. Group 1A Northeastern Portion of Area I, RCRA Facility Investigation Report, Santa Susana Field Laboratory, Ventura County. February.
- MWH, 2009c. Group 7 Northern Portion of Area IV, RCRA Facility Investigation Report, Santa Susana Field Laboratory, Ventura County. June.
- MWH, 2009d. Feasibility Study Work Plan. Santa Susana Field Laboratory, Ventura County, CA. June.
- MWH, 2009e. Treatability Study Work Plans. Santa Susana Field Laboratory, Ventura County, CA. June.
- NASA, 2008. Draft Group 2 Remedial Investigation Report at the Santa Susana Field Laboratory, Ventura County, California. November.
- NASA, 2009a. Draft Group 3 Remedial Investigation Report at the Santa Susana Field Laboratory, Ventura County, California. April.
- NASA, 2009b. Draft Group 9 Remedial Investigation Report at the Santa Susana Field Laboratory, Ventura County, California. November.
- National Research Council, 1996. Rock Fractures and Fluid Flow: Contemporary Understanding and Applications, National Academy Press, ISBN 0-309-04996-02.
- Nicholson, C., Sorlien, C. C., Atwater, T., Crowell, J. C., and Luyendyk, B. P., 1994. Microplate Capture, Rotation of the Western Transverse Ranges, and Initiation of the San Andreas Transform as a Low-Angle Fault System: *Geology*, v. 22, p. 491-495.
- North American Aviation (NAA), 1963. Internal Letter regarding: Contamination Incident SS Vault, Santa Susana. November 11. HDMSe00024459.
- Ogden Environmental and Energy Services Co., Inc. (Ogden), 1996. RCRA Facility Investigation Work Plan Addendum, Santa Susana Field Laboratory, Ventura County, California. September.

- Ogden, 1998a. Biological Conditions Report, Santa Susana Field Laboratory. April.
- Ogden, 2000a. RCRA Facility Investigation Work Plan Addendum Amendment, Santa Susana Field Laboratory, Ventura County, California. June.
- Ogden, 2000b. Shallow Zone Groundwater Investigation Work Plan, Santa Susana Field Laboratory, Ventura County, CA. December
- Ogilvie, S. R. , Orribo, J. M., Glover, P. W. J., 2001. The Influence of Deformation Bands Upon Fluid Flow Using Profile Permeametry and Positron Emission Tomography. Geophysical Research Letters, Vol. 28, No. 1, pp 61-64.
- Oak Ridge Institute for Science and Education (ORISE), 1993. Verification Survey of the Old Conservation Yard, Building T064 Side Yard, and Building T028, Santa Susana Field Laboratory, Rockwell International, Ventura, California. October. HDMSe00033483.
- ORISE, 1999. Second Addendum to the Verification Survey of the Building T064 Side Yard, Santa Susana Field Laboratory, Ventura County, California (ORISE 1993 and 1995).HDMSe00023043.
- Parker, Beth L, Robert W. Gillham and John A Cherry, 1994. Diffusive Disappearance of Immiscible Phase Liquids in Fractured Geologic Media, Ground Water, Volume 32, Number 5, September-October.
- Parker, Beth L, David B. McWhorter and John A Cherry, 1997. Diffusive Loss of Non-Aqueous Phase Organic Solvents from Idealized Fractured Networks in Geologic Media, Ground Water, Volume 35, Number 6, November-December.
- Parker, B.L. and J. A. Cherry, 2000. Evolution of TCE Source Zones and Plumes in the Chatsworth Formation Groundwater, Appendix E in Technical Memorandum, Conceptual Site Model, Movement of TCE in the Chatsworth Formation, Santa Susana Field Laboratory, Ventura County, CA (Montgomery Watson, 2000a). April.
- Parker, B.L., Cherry, J. and McWhorter, D., 2008. Phase 2 Northeast Area Groundwater Characterization Technical Memorandum. January 30.
- Pierce, A.A. 2005. Isotopic and Hydrogeochemical Investigation of Major Ion Origin and Trichloroethene Degradation in Fractured Sandstone. Master of Science Thesis, Department of Earth Sciences, University of Waterloo.
- Rocketdyne, 1963. Water Supply and Usage for Rocketdyne Propulsion Field Laboratory.
- Rockwell International (Rockwell), 1973. Internal Letter from W.F. Heine to G.W. Meyers regarding Groundwater Sampling at SRE Site. May 7. (HDMSe00024492).
- Rockwell, 1977. SRE Activity Requirement No. 27, D&D of Building 143 Retention Pond and Sanitary Sewer. August 2.
- Rockwell, 1979. S8ER Facilities Decommissioning Final Report. February 28. HDMSP00017217.
- Rockwell, 1982. RMDF Leach Field Decontamination Final Report. September 15. HDMSP00009415.

- Rockwell, 1983. Sodium Reactor Experiment Decommissioning Final Report, ESG-DOE 13403. August 15. HDMS00023450.
- Rockwell, 1985. Interim Storage Facility Decommissioning Final Report. March 15, 1985. HDMSp00017801.
- Rockwell, 1976. Building 003 Decontamination and Disposition Final Report. February 26. HDMS00023398.
- Rockwell, 1990. Final Decontamination and Radiological Survey of the Old Conservation Yard. N704SRR990030. August.
- Rockwell, 1992. Baseline Radiological Survey of the Sodium Disposal Facility (T886). N704SRR990034. August 31. HDMS000437253.
- Rockwell, 1993a. Data Sheets - SREH20 – Summary of Surveillance Well Results (partial) for the SRE and SREPOND – Summary of SRE Pond Water Analyses. July 20 (HDMS00025811).
- Rockwell, 1993b. Final Decontamination and Radiological Survey of the Building T064 Side Yard. September 10.
- Rockwell, 1996. Area IV Radiological Characterization Survey Final Report. August 15. HDMS00030423.
- Regional Water Quality Control Board, Los Angeles Region, 1994. Basin Plan for the Coastal Watersheds of Los Angeles and Ventura Counties. June 13.
- Regional Water Quality Control Board, Central Valley Region, 2008. A Compilation of Water Quality Goals, prepared by Jon D. Marshack, D.Env. July.
- Science Applications International Corporation (SAIC), 1994. Final RCRA Facility Assessment (RFA) Report. Prepared for Rockwell International Corporation, Rocketdyne Division, Santa Susana Field Laboratory, Ventura County, California. May.
- SAIC, 2009. Radionuclides Related to Historical Operations at the Santa Susana Field Laboratory, Area IV. March.
- Sapere Consulting Incorporated (Sapere) and The Boeing Company, 2005. Historical Site Assessment of Area IV, Santa Susana Field Laboratory, Ventura County, California. May. HDMS00032525, HDMS00032615.
- Sternlof, K. R., Karimi-Fard, M., Pollard, D. D., Durlinsky, L. J.; 2006. Flow and Transport Effects of Compaction Bands in Sandstone at Scale Relevant to Aquifer and Reservoir Management. Water Resources Research. Vol. 42 W07425, doi:10.
- Sterling, Sean, 2000. Hydraulic Aperture Determinations from Borehole Information in the Chatsworth Formation, Appendix C in Technical Memorandum, Conceptual Site Model, Movement of TCE in the Chatsworth Formation, Santa Susana Field Laboratory, Ventura County, CA (Montgomery Watson, 2000a). April.
- Sudicky, E., & McLaren, R., 1992. The Laplace Transform Galerkin technique for large-scale simulation of mass transport in discretely fractured porous formations. Water Resources Research, 28(2), 499-514.

- Sudicky, E.A., McLaren, R.G. 2003. FRACTRAN User's Guide: An Efficient Simulator for Two-dimensional, Saturated Groundwater Flow and Solute Transport in Porous or Discretely-fractured Porous Formations. Groundwater Simulations Group, University of Waterloo.
- USGS, 2003. Simulation of Ground-Water/Surface-Water Flow in the Santa Clara-Calleguas Basin, Ventura County, California. Water-Resources Investigations Report 02-4136. A contribution of the Southern California Regional Aquifer-System Analysis Program.
- Vogel, Timothy M. and McCarty, Perry L., 1987. Abiotic and Biotic Transformations of 1,1,1-Trichloroethane under Methanogenic Conditions. Environmental Science Technology, Volume 21, No. 12, pp 1208-1213.
- Washington, John W., 1995 Hydrolysis Rates of Dissolved Volatile Organic Compounds: Principles, Temperature Effects and Literature Review. Ground Water, Volume 33, No. 3, May-June 1995.
- Weidemeier, T.H., H.S. Rifai, C.J. Newell, and J.T. Wilson, 1999. Natural Attenuation of Fuels and Chlorinated Solvents in the Subsurface. John Wiley & Sons Inc. 617 pp.
- Williams, J.H., J.W. Lane Jr., K. Singha and F.P. Haeni, 2000. Application of Advanced Geophysical Logging Methods in the Characterization of a Fractured-Sedimentary Bedrock Aquifer, Ventura County, California. United States Geological Survey, Report WRIR 00-4083. March.
- Williams, J.H. and Knutson K.D., 2009. Integrated Analysis of Flow, Temperature, and Specific-Conductance Logs and Depth-Dependent Water-Quality Samples from Three Deep Wells in a Fractured-Sandstone Aquifer, Ventura, California. USGS open-file report 2009-1023.
- Yerkes, R.F., and Campbell, R.H., 2005. Preliminary Geologic Map of the Los Angeles 30' x 60' Quadrangle, Southern California. USGS open-file report 2005-1019.